REFERENCE ONLY

UNIVERSITY OF LONDON THESIS

Degree PhD Year 2006 Name of Author MEANA L.

This thesis comes within category D.

☑ This copy has been deposited in the Library of UCL

☐ This copy has been deposited in the Senate House Library, Senate House, Malet Street, London WC1E 7HU.

MODULATION OF TRANSFORMING GROWTH FACTOR β (TGF β) AND CONJUNCTIVAL SCARRING AFTER GLAUCOMA FILTRATION SURGERY

Thesis submitted for the degree of Doctor of Philosophy (PhD)

University of London

Anna Louise Mead

MB BChir MRCOphth

Wound Healing Research Unit, Department of Pathology, Institute of Ophthalmology, University College London

ProQuest LLC
789 East Eisenhower Parkway
P.O. Box 1346
Ann Arbor, MI 48106-1346

ABSTRACT

The conjunctival wound healing response remains the major barrier to achieving long term intraocular pressure control after glaucoma filtration surgery (GFS). Current anti-scarring agents improve the outcome of surgery but act by causing widespread cell death and can be associated with potentially blinding complications. In addition, some individuals still fail surgery. A more physiological and targeted approach to wound healing control and scarring prevention is required.

Of all the growth factors, TGF β has been shown to play a pivotal role in wound healing throughout the body, and has been identified as a potent stimulant of the scarring process in the eye. Modulation of TGF β has been highlighted as a possible mechanism by which ocular scarring may be reduced. This thesis has investigated the role of TGF β modulation as a potential anti-scarring strategy in glaucoma surgery.

In vitro, I have demonstrated that the anti- TGF β2 monoclonal antibody, CAT-152, inhibits Tenon's fibroblast collagen production and myofibroblast transformation at physiological concentrations. It appears that these are the key histological changes associated with bleb failure following experimental GFS.

In vivo, subconjunctival administration of CAT-152, given at the time of surgery and in the immediate post-operative period, successfully improves surgical outcome, reduces subconjunctival fibrosis and is safe and well tolerated. Isolated post-operative administration of subconjunctival CAT-152 can prevent late bleb failure and prolonged dosing with CAT-152 appears to modulate the long-term scarring response after GFS. In addition, the anti-scarring effects of CAT-152 have compared favourably to one of the gold standard anti-scarring agents in clinical use. Finally, I have shown that antisense

oligonucleotides directed against TGF β may also have a role in the prevention of conjunctival scarring.

In summary, the work supports the hypothesis that TGF β modulation may represent a novel potential anti-scarring strategy in glaucoma surgery.

LIST OF ABBREVIATIONS

AGIS	Advanced glaucoma intervention trial
ANOVA	Analysis of variance
α SMA	Alpha smooth muscle actin
BAB	Blood Aqueous barrier
β FGF	Basic fibroblast growth factor
CAT	Cambridge Antibody Technology
CAT-152	Anti-TGF β2 antibody
CAT-001	Null 1gG4 antibody
CICP	Collagen I C terminal propeptide
cDNA	Complementary DNA
CTGF	Connective tissue growth factor
DAPI	Diamidino-2- phenylole dilactate
DMEM	Dulbecco's Modified Eagle's Medium
DMSO	Dimethyl Sulphoxide
DNA	Deoxyribonucleic acid
ECM	Extracellular matrix
EGF	Epidermal growth factor
5-FU	5-fluorouracil
FFSS	Fluorouracil filtering surgery study group
HAMA	Human anti-mouse antibody
HRP	Horseradish peroxidase
H and E	Hematoxylin and eosin
IGF	Insulin like growth factor

IOP	Intraocular pressure
LAP	Latency associated peptide
LECs	Lens epithelial cells
LTBP	Latent TGF β binding protein
MMP's	Matrix metalloproteinases
mRNA	Messenger RNA
MMC	Mitomycin C
mAb	Monoclonal antibody
MT MMP's	Membrane type matrix metalloproteinases
NSAIDS	Non-steroidal anti-inflammatory drugs
NZW	New Zealand white
OGN	Antisense oligonucleotides
ONH	Optic nerve head
PBS	Phospahate buffered saline
PCNA	Proliferating cell nuclear antigen
PDGF	Platelet derived growth factor
PEX	Pseudoexfoliation
POAG	Primary open angle glaucoma
SEM	Scanning electron microscopy
TBR I	Type I TGF β receptor
TBR II	Type II TGF β receptor
TBS	Tris buffered saline
TGF β	Transforming growth factor beta
TEM	Transmission electron microscopy

TIMP's	Tissue inhibitors of the matrix metalloproteinases
TMB	5,5'-tertra methylbenzidine
TPA	Tissue plasminogen activator
TSP's	Thromobospondins

TABLE OF CONTENTS

LIST OF TABLES

LIST OF TABLES (CONT)

LIST OF FIGURES

LIST OF FIGURES (CONT)

LIST OF FIGURES (CONT)

LIST OF FIGURES (CONT)

LIST OF FIGURES (CONT)

LIST OF FIGURES (CONT)

LIST OF FIGURES (CONT)

ACKNOWLEDGEMENTS

I would like to express my gratitude to Professor Peng Khaw for his support and advice as my supervisor. He has been a constant source of inspiration. I would also like to thank Dr Ian Anderson for his help in the design and conduct of the studies undertaken in this thesis. Both these individuals have been responsible for developing my interest in basic scientific research and I have benefited greatly from their input. In addition, I would like to thank Tina Wong, Alison Cambrey, Kamiar Mireskandari and Julie Daniels for their invaluable assistance and teaching, without whom, this work would not have been possible.

Finally, I would like to thank my husband, David, for his support and encouragement during the preparation of this thesis.

CHAPTER 1. INTRODUCTION

1.1 GLAUCOMA

1.1.1 Overview

Glaucoma (derived from the Greek word Glaukos describing dull greyish-green or blue colouring) can be defined as a progressive optic neuropathy, which is characterised by a distinct pattern of visual field loss and has elevated intraocular pressure (IOP) as the major risk factor. The glaucomas are not a single disease process but a large group of disorders in which optic nerve head damage is the common pathological process.

Glaucoma is a leading cause of irreversible blindness in the developed and developing world and is estimated to account for 15% of world blindness (Foster et al., 1990; Thylefors et al., 1994). In addition, due to the insidious nature of the disease many cases remain undiagnosed or patients present late with advanced irreversible glaucomatous visual loss (Grant et al., 1982). It is estimated that only 50% of cases are diagnosed in the developing world (Quigley, 1996).

Glaucoma can be broadly classified according to aetiology. In primary glaucoma developmental or intrinsic degenerative processes occurring in the eye give rise to raised pressure and optic nerve damage. In secondary glaucoma, however, the pathological changes are driven by other recognisable ophthalmic or systemic diseases. Glaucoma can be further subdivided into open angle or closed angle glaucoma. These terms relate to the anatomy of the drainage angle of the eye and the mechanism by which the outflow of fluid from the eye is impaired (Figure 1).

Figure 1 Schematic diagram to illustrate the anatomy of the anterior chamber and the normal passage of aqueous humour

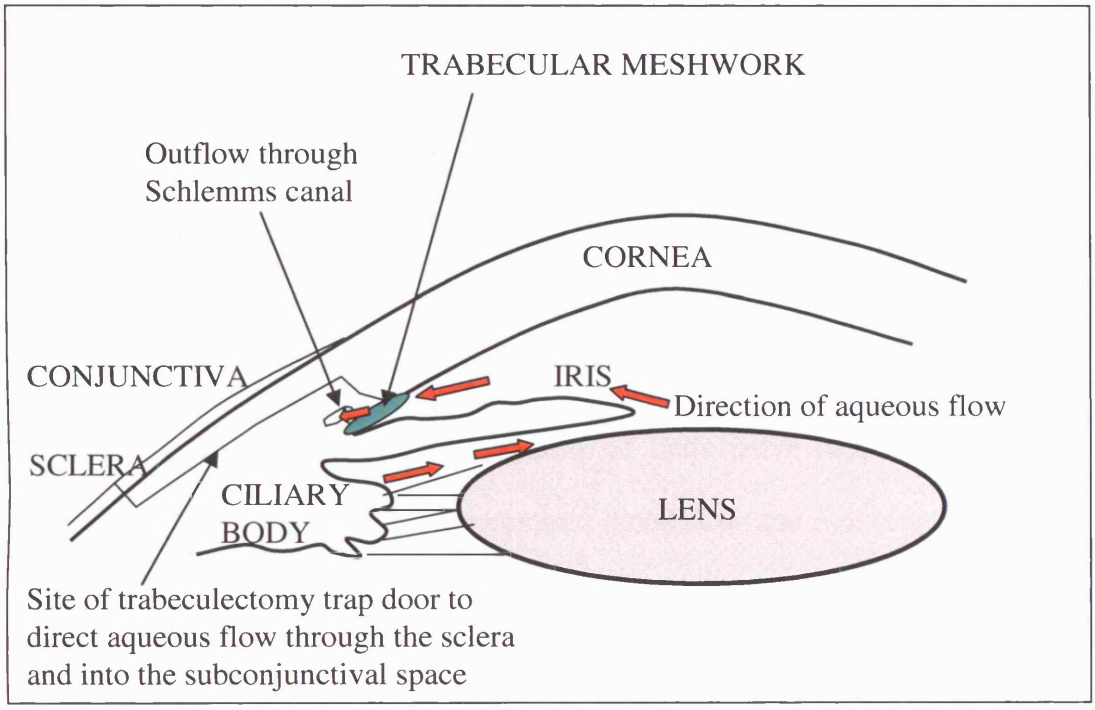

Aqueous is produced by the ciliary body epithelium and flows predominantly anteriorly around the lens into the anterior chamber. When the angle is open aqueous drains from the eye via the trabecular meshwork and is reabsorbed into the circulation through Schlemms canal and the aqueous veins. In angle closure the anterior chamber shallows and the iris becomes opposed to the peripheral inner corneal blocking the ability of fluid to drain into the trabecular meshwork. Following glaucoma filtration surgery an alternate route is created to direct aqueous transconjunctivally under less resistance

Primary open angle glaucoma (POAG) is the commonest form of glaucoma in Britain and the USA affecting approximately 1 in 100 of the general population over 40 years and will be the focus of this discussion.

1.1.2 Intraocular pressure, glaucomatous damage and disease progression

Appreciation of elevated IOP as a risk factor for glaucoma dates back to the middle of the nineteenth century when Von Graefe reported its association with a characteristic type of optic nerve damage leading to blindness. Population based studies have confirmed that increased IOP is associated with increased prevalence and incidence of glaucoma (Armaly et al., 1980; Leske et al., 1995; Sommer et al., 1991). Raised pressure induces compression, stretching and remodelling of optic nerve head which results in direct mechanical axonal damage, compromised blood flow and reduced delivery of nutrients. Progressive loss of retinal nerve fibre axons leads to reduced visual function (Hernandez. M et al., 1997).

It is logical to predict and some evidence shows that reduction of the intraocular pressure will slow the progression of the disease (Grant et al., 1982; Group, 1989; Group, 1996; Mao et al., 1991; Odberg, 1987). More conclusive evidence has been provided recently by large, long term randomised clinical trials that were specifically designed to address this issue. In the advanced glaucoma intervention study (AGIS) individuals in which intraocular pressure was maintained below 18mmHg on all occasions, with an average of 12.3mmHg, showed minimal disease progression, over 8 years of follow up (AGIS Investigators, 2001). The early manifest glaucoma trial was designed to identify risk factors and investigate the effect of treatment on glaucomatous progression. The results showed that each 1 mmHg reduction in IOP was associated with a 10% reduction in disease progression (Leske et al., 2003). Finally the ocular hypertension study showed

that reduction of the IOP was effective in delaying or preventing the onset of optic nerve damage in individuals with raised pressure.

1.1.3 Management of glaucoma

Although other risk factors are recognised to be involved in the development of glaucomatous optic neuropathy, the control of IOP is the principal goal of current glaucoma treatment. IOP can be reduced by either limiting the production, or increasing the outflow, of aqueous humour from the eye. This can be achieved by medical, surgical or laser therapy.

Medical treatment in the form of topical eye drops is the most commonly used method to control IOP. Numerous formularies exist which act via different pathways, and can be used in isolation or as combined therapy. Despite topical administration, medical treatment can cause both local and systemic side effects. For example, the topical beta blockers can be associated with bronchospasm and heart failure (Diggory et al., 1996). Secondly, this mode of treatment is expensive, particularly the newer agents, which precludes use in the developing world. In addition, they require frequent and regular application for prolonged periods. This can lead to problems with administration and compliance particularly in the elderly, who make up a large percentage of the population needing treatment. Finally, studies have shown that long term use of eye drops can limit the success of glaucoma filtration surgery (Broadway et al., 1993a; Broadway et al., 1993b; Broadway et al., 1994a; Broadway et al., 1994b; Lavin et al., 1990).

Laser treatment for primary glaucoma was introduced in the 1980s when the technique of argon laser trabeculectomy (application of laser burns to the trabecular meshwork) was first described. More recently selective laser trabeculectomy using application of Nd

YAG laser has been introduced, which causes less tissue destruction. This treatment modality is effective in the short term, in certain types of secondary glaucoma (Robin et al., 1983), and in individuals of Afro-Caribbean origin (AGIS Investigators, 2001). However, long term IOP control is rarely achieved (Migdal, 1995). It is commonly adopted as a primary treatment in the USA but its use in the UK is normally limited to patients in which a conservative approach to treatment is deemed appropriate.

In cyclodiode laser therapy the ciliary body (site of aqueous production) is ablated. Its use is advocated in cases of severe refractory glaucoma, where other approaches have failed, and is proving to be a very useful tool (Bloom et al., 1997).

1.1.4 Glaucoma filtration surgery

Of all available therapies, surgery has been shown to be the most effective at controlling IOP and preventing visual loss (Hitchings et al., 1994; Jay, 1989; Jay, 1992; Migdal et al., 1994). In addition, glaucoma filtration surgery results in a better quality of life for patients than medical therapy and in the developing world it is the only practical treatment (Sherwood et al., 1998).

The principle of glaucoma surgery is to provide an alternative channel for aqueous to drain out of the eye and thus lower the IOP. Filtration procedures have been performed since the early twentieth century and have evolved from early 'unguarded' techniques, where a full thickness hole in the sclera provided a direct fistula between the anterior chamber and the conjunctival space, to the Cairns 'guarded trabeculectomy' procedure, which is now the operation of choice (Cairns, 1968).

In a trabeculectomy, the conjunctiva is incised along the limbus and blunt dissection of the conjunctival space is performed creating a conjunctival flap. A partial thickness scleral flap is then fashioned as far anteriorly as the corneo-scleral junction. A full

thickness sclerostomy involving either removal of a portion of the anterior trabecular meshwork (as originally described, hence the term trabecul(um) ectomy), or a block of corneo-scleral tissue is then carried out (Watson's modification of Cairn's trabeculectomy (Watson, 1972). A block of peripheral iris tissue is also excised (peripheral iridectomy) and this completes the creation of the new drainage channel. Finally, the scleral flap is sutured down and the conjunctiva is closed. Aqueous flows subconjunctivally forming an elevated bleb, and is then reabsorbed back into the circulatory system via aqueous veins, lymphatic channels and diffusely by the conjunctival tissue (Benedikt. O, 1975) (Figure 2).

Alternative filtration techniques are occasionally performed in severe and refractory cases, where individuals have a poor surgical prognosis or have failed previous surgery. Silicone tubes are inserted into the eye to maintain a permanent drainage channel. The tubes are attached to an external plate that maintains a large potential space between the conjunctiva and the sclera and increases the route of transconjunctival aqueous passage (Molteno et al., 1976).

1.1.5 Outcome of GFS

Trabeculectomy has been show to successfully reduce IOP below 21 mmHg in 85% of cases (Watson et al., 1981). However, some individuals fail surgery. The post-operative wound healing response is the major determinant of surgical outcome after glaucoma filtration surgery (Hitchings et al., 1983). Scarring occurs at the level of the sclera and with in the subconjunctival tissue, thereby creating a barrier to aqueous flow and results in a subsequent rise in IOP following surgery (Doyle et al., 1993a; Khaw et al., 1992b; Miller et al., 1989). Figure 3 shows the appearance of filtration blebs after filtration surgery. Successful surgery is associated with a diffuse elevated bleb with normal

Figure 2 The technique of glaucoma filtration surgery

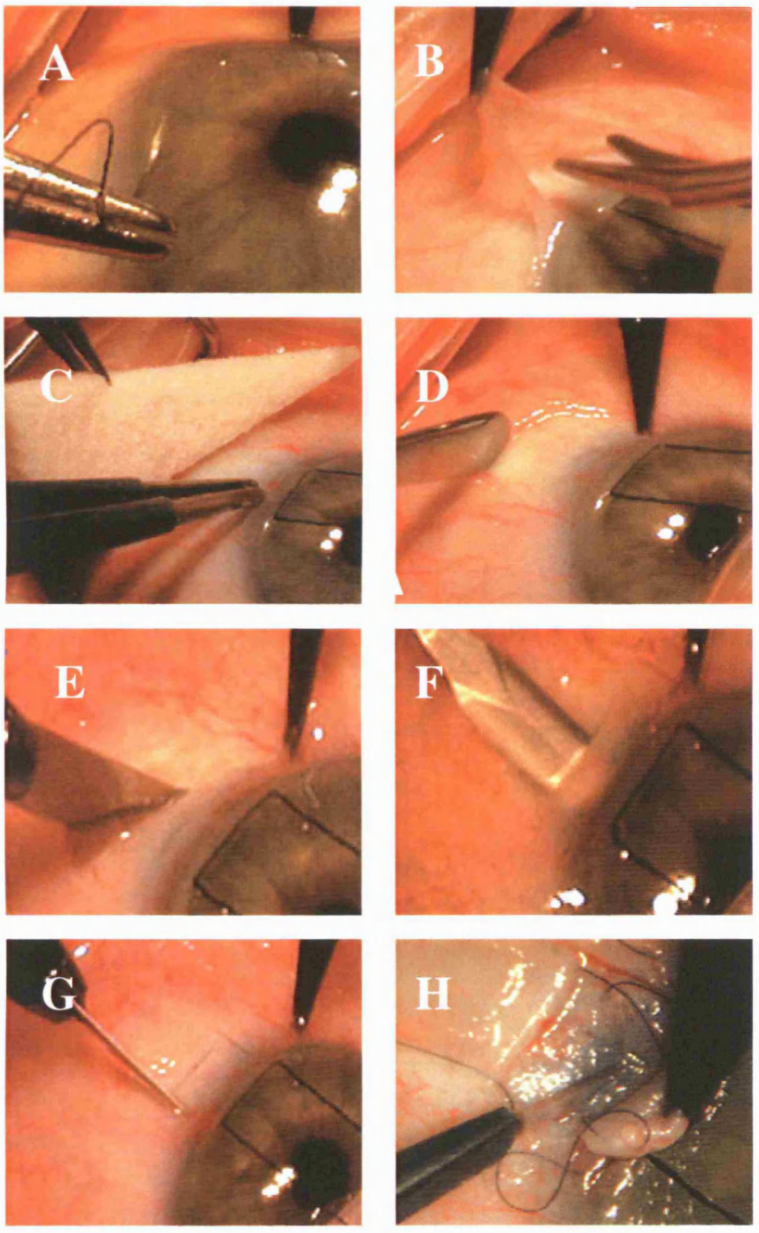

A traction suture is placed in the cornea to provide good exposure to the superior conjunctiva (A). The conjunctiva is incised and undermined (B). Cautery is applied to bleeding scleral vessels to ensure a bloodless field (C). Residual Tenon's and episcleral tissue is cleared. A 45 degree blade is used to make an incision tangential to the limbus to 1/3 to 1/2 scleral thickness (E) and a crescent blade is used to create a partial thickness scleral flap (F). The sides of the flap are cut to convert the partial thickness tunnel into a rectangular flap (G). The eye is entered anterior to the surgical limbus (H) which minimises the risk of complications such as iris plugging of sclerostomy and inadvertant damage to the lens or ciliary body.

Figure 2 The technique of glaucoma filtration surgery (cont)

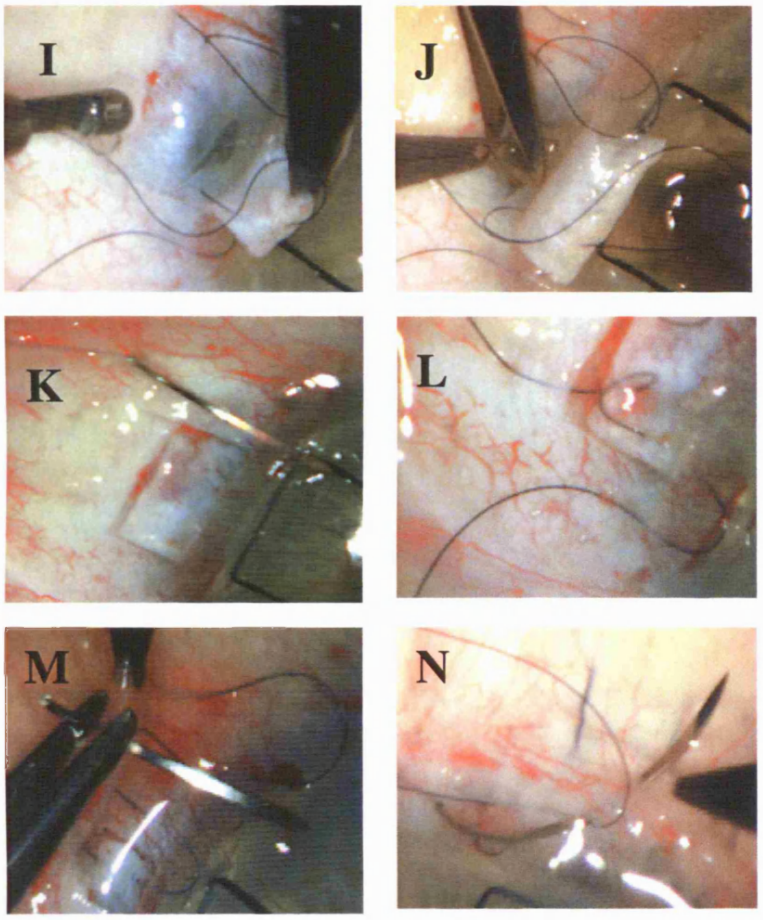

Sclerostomy is made with a scleral punch (I). The removed block of sclera is visible on the shelf of the punch, and the hole left by it is semicircular. A peripheral iridectomy is made to provide a route for aqueous to move from the posterior to the anterior chamber (J). The scleral flap is sutured using a combination of permanent and releasable sutures (L,M). Finally the conunctival is reflected back and a water tight closure is performed (N).

Figure 3 Subconjunctival bleb morphology following glaucoma filtration surgery

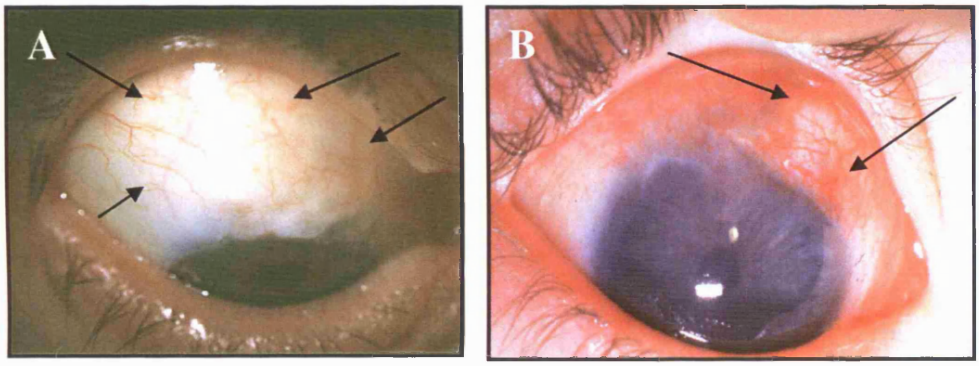

Successful glaucoma filtration surgery produces an elevated diffuse conjunctival bleb (A). Scarring, however, results in contraction and flattening of the bleb with increased vascularisation and reduced fluid flow through the subconjunctival tissues (B).

conjunctival vasculature. Subconjunctival scarring leads to the presence of a flattened contracted bleb reduced drainage at the filtration site.

Increased scar deposition is associated with poor control of postoperative IOP. The subject has become even more important with the realisation that simply lowering the IOP to below 21 is inadequate and that optimal lowering of the IOP should be achieved in all patients undergoing surgery for glaucoma. The healing response varies in each individual patient (Figure 4). Ultimately IOP control and long term preservation of vision can only be achieved if the wound healing response is controlled in all patients.

Figure 4 **Healing profiles after GFS**

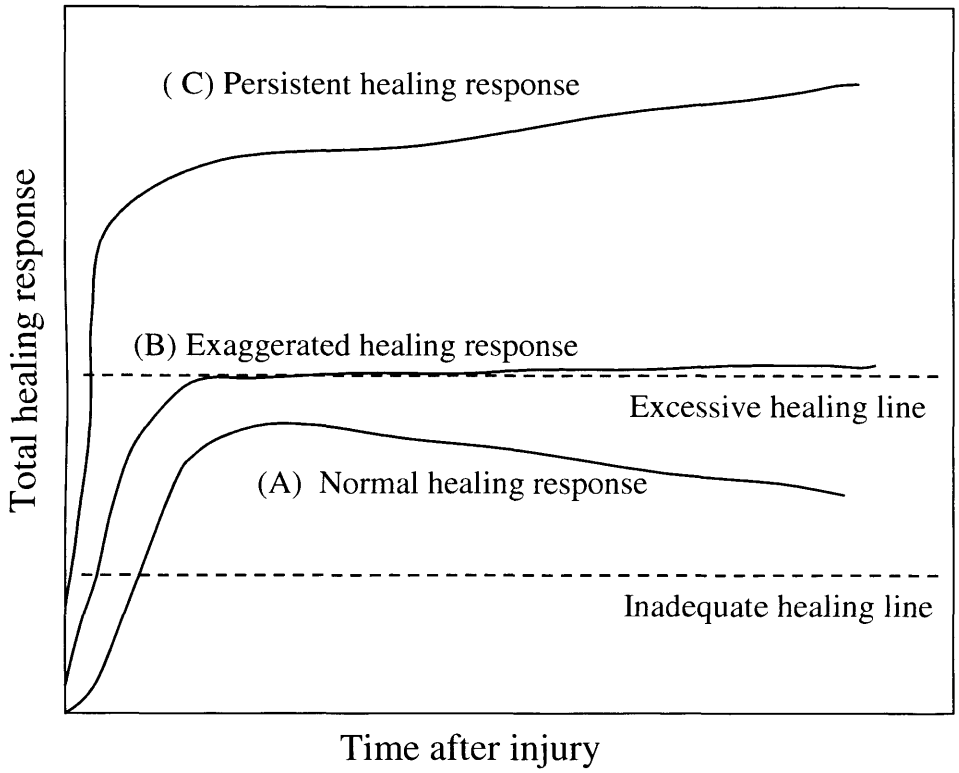

The healing response varies in each individual patient. The two healing lines represent imaginary boundaries; below the inadequate healing line a patient may suffer from complications related to low pressure (hypotony), whilst above the excessive healing line poor IOP control and surgical failure are likely. The normal healing response peaks then quickly plateaus but remains within the two healing boundaries (A). A patient with an exaggerated healing response who for example has received multiple topical treatments starts slightly higher and reaches a greater peak compared with normal (B). Persistent healing can be associated with chronic inflammatory conditions which constantly stimulate the healing response. Healing in this situation is associated with a dramatic initial response which is maintained over time (C). (*Modified from Khaw et al* Khaw, 1994b)

1.2 CONJUNCTIVAL WOUND HEALING

Wound healing is a complex, dynamic process that can be simplified in to three main phases; the inflammatory, the proliferative and the remodelling phase. The sequence of cellular events following glaucoma surgery can be summarised diagrammatically as shown in Figure 5.

1.2.1 Conjunctival insult

Conjunctival, episcleral and scleral incisions result in both connective tissue and blood vessel injury. This stimulates the release of plasma proteins, blood cells and extracellular matrix (ECM) components into the damaged site, which in turn activates the clotting system and a clot forms around the damaged area. Blood loss is initially reduced by the aggregation of platelets forming haemostatic plugs. This process is stimulated by the presence of various factors including thrombin, adenosine phosphate, fibrinogen, collagen, thrombospondin and Von Willebrand factor VIII.

These events are similar to cutaneous wounding; however, the glaucoma filtration surgical wound site is unique in that it is constantly bathed by aqueous humour, which has a significant effect on the healing response. The aqueous contains factors which account for differences in subconjunctival scarring (Radius et al., 1980). Dissected conjunctiva normally scars down rapidly without aqueous, which has led to the suggestion that aqueous contains inhibitory factors (Herschler, 1990). However, aqueous also exhibits stimulatory effects on fibroblasts in vitro and in vivo (Joseph et al., 1987; Joseph et al., 1989). On entering the eye a degree of breakdown of the BAB occurs, with release of stimulatory growth factors into the aqueous and the wound site (Krause et al., 1971; Snaders et al., 1982). Rapid scarring and subsequent surgical failure is often seen in eyes

Figure 5 **The sequence of events in wound healing after GFS**

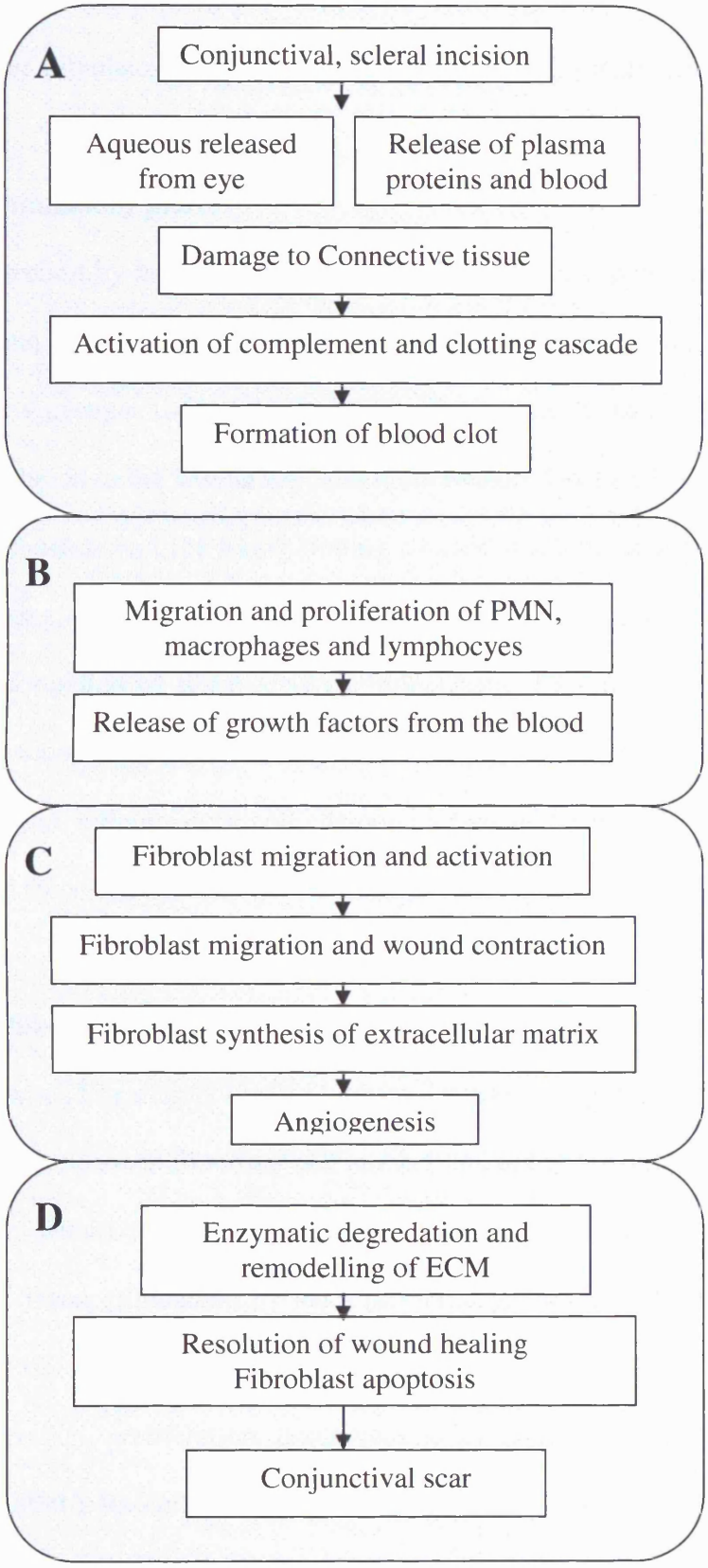

The molecular and cellular events leading to subconjunctival scarring and potential areas of wound modulation after glaucoma filtration surgery. **A-D** represents the wounding, inflammatory, proliferative and remodelling phases of wound healing.

with co-existing inflammatory disease, which is thought to be a result of the high concentration of stimulatory factors in the aqueous of these patients (Reddan et al., 1979).

1.2.2 The inflammatory phase

This is characterised by the influx of polymorphonuclear cells (neutrophils), followed by lymphocytes and macrophages into the damaged area. These cells eliminate infection by phagocytosis, scavenge tissue debris and secrete growth factors which stimulate fibroblasts migration to the wound site. The inflammatory reaction is further enhanced by activation of platelets and the blood clotting cascade resulting in the release of growth factors, proteases, arachidonic acid metabolites, 5-hydroxytryptamine and lectins. In addition, the formation of fibrin, derived from plasma fibrinogen, provides a scaffold bridging the wound edges (Clark et al., 1988). Initiation of the classic complement pathway generates inflammatory cell chemoattractant molecules. As cells migrate they exert tractional forces on the extracellular matrix which causes contraction of the tissue.

1.2.3 The proliferative phase

This stage of wound healing is heralded by the formation of granulation tissue, which is mediated by an increase in fibroblast cell number and activity. Fibroblasts normally exist in low numbers within the subconjunctival tissue as undifferentiated mesenchymal cells, the fibrocytes. Upon stimulation by local factors at the wound site, fibrocytes become **activated** into fibroblasts, which carry out the key cellular functions of wound healing. These are migration, proliferation, tissue contraction and extracellular matrix synthesis (Khaw et al., 1994b). Re-epithelialisation and angiogenesis also occur (Figure 6).

Figure 6 Effect of stimulatory factors at the wound site

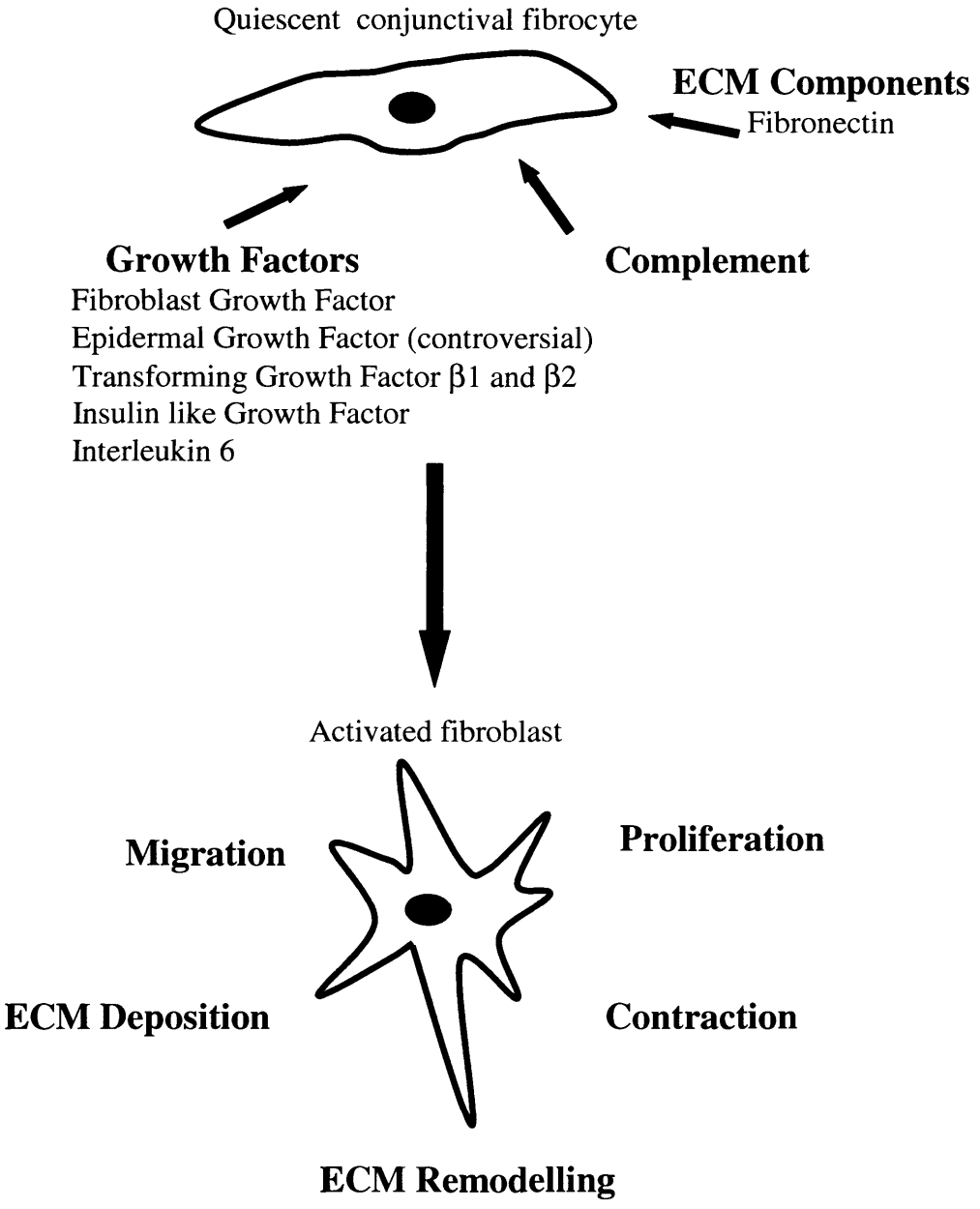

The key cell in mediating the scar formation is the fibroblast. Various factors at the wound site can stimulate fibroblasts to become activated and commence the cellular functions of migration, proliferation, contraction, ECM deposition and remodelling.

1.2.3.1 Fibroblast migration

Environmental factors derived from the locally damaged tissue, blood, inflammatory cells and the aqueous humour stimulate the migration of fibroblasts through the surrounding extracellular matrix towards site of damage. The complement component C5a, leukotriene, extracellular matrix molecules such as fibronectin, collagen fragments, elastin are all implicated in this process (Postlethwaite et al., 1976; Postlethwaite et al., 1981; Postlethwaite et al., 1978; Postlethwaite et al., 1979). Research into the role of growth factors has also shown that transforming growth factor beta (TGF β), basic fibroblast growth factor (β FGF), epidermal growth factor (EGF) and insulin like growth factor (IGF-I) all influence fibroblast migration to the wound site (Postlethwaite et al., 1987); and in corneal fibroblasts TGF β1 has been shown to maximally stimulate this process at much lower concentrations than EGF and β FGF (Khaw et al., 1994a).

1.2.3.2 Fibroblast proliferation

Fibroblasts proliferate to generate sufficient cells to carry out the various wound healing process in a short time. This process peaks at about two weeks after the initial insult and again is regulated by growth factors (Miller et al., 1989; Ross et al., 1968).

TGF β1 has been shown to be a potent stimulator of human Tenon's fibroblast proliferation, stimulating proliferation at much lower concentrations (10-12 M) and to a much greater degree (2-3 times greater) than β FGF, EGF and IGF-1 (Khaw et al., 1994a).

1.2.3.3 Extracellular matrix synthesis

Fibroblasts secrete extracellular matrix components such as fibronectin, glycosaminoglycans and tropocollagen, which are ultimately enzymatically cross linked to form collagen. A fibrin scaffold is formed at the wound site which is initially replaced

by collagen type III and then by collagen type I (Figure 7). Type I collagen is laid down in large parallel bundles perpendicular to the basement membrane providing tensile strength to the mature wound (Thomas et al., 1995). The production of collagen is regulated by growth factors. TGF β has been identified as the most potent stimulator of ocular fibroblast mediated ECM production (Khaw, 1994). Type 1 collagen is the major component of scar tissue and collagen accumulation is a prominent feature in experimental surgical failure in the rabbit and monkey (Desjardins et al., 1986; Miller et al., 1989). Collagen accumulation is also a prominent feature of failing blebs in man (Hitchings et al., 1983). Fibroblasts actively participate in the synthesis of other extracellular components such as fibronectin and tenascin.

1.2.3.4 Wound contraction: Fibroblast and myofibroblast cell phenotypes

The phenomenon of wound contraction is one of the essential steps of subconjunctival wound healing. Excessive or abnormal contraction of granulation tissue leads to pathological scarring.

The contractile force has been shown to reside in the granulation tissue, however, exact mechanisms underlying tissue contraction remain unclear (Grinnell, 1994). Two theories have been put forward to explain the contractile forces in wounds and scars, in which either cell locomotion or cell contraction act as the predominant mechanism. The first theory proposes that fibroblasts exert a tractional force by continual extension and retraction of filipodia as they propel themselves forward. Therefore, as cells migrate they exert tractional forces on their substratum which results in contraction of the tissue. This was elegantly investigated by *Harris et al,* who seeded fibroblasts onto ultra thin polymerised silicon, demonstrated tractional forces and proposed that rearrangement of extracellular matrices was the primary function of fibroblast traction (Harris et al., 1981).

Figure 7 **Scar tissue formation in subconjunctival bleb tissue**

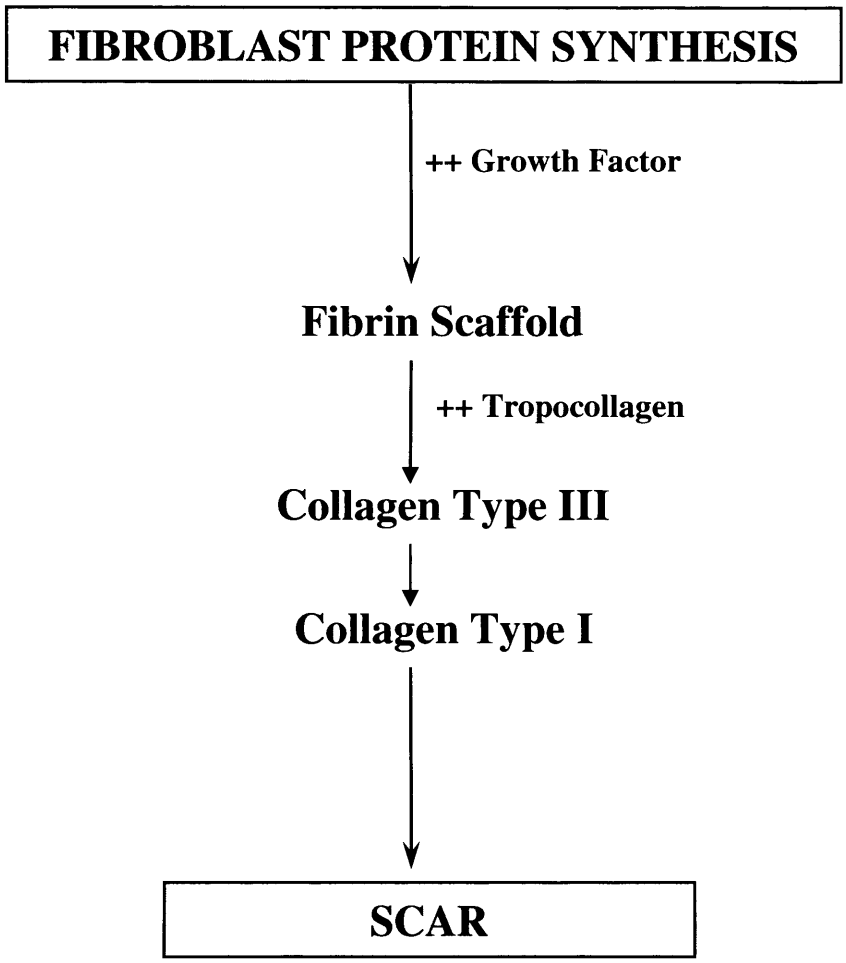

Fibroblasts synthesize tropocollagen, glycosaminoglycans and fibronectin. An initial fibronectin and fibrin scaffold is laid down in the wound. Collagen type III and then type I are sequentially deposited in a highly ordered arrangement of parallel bundles to form the main component of the subconjunctival scar.

Additional information has been generated from extensive in vitro studies of contraction using a model of first described by Bell et al (Bell et al., 1979). Cultured fibroblasts suspended in a rapidly polymerizing collagen matrix produce a fibroblast-populated collagen lattice and with time, this lattice undergoes a reduction in size referred to as lattice contraction. This contractile process has been shown to be dependent on a number of factors including cell number, an intact actin skeleton, collagen concentration, cell-matrix attraction and protein synthesis (Guidry, 1993; Hunt et al., 1994; Nishiyama et al., 1988; Pitaru et al., 1987). The mechanism of collagen fibre movement in 3 dimensional lattices is not fully understood. Meshel et al have recently demonstrated that fibroblast lamellipodia extend along held collagen fibres, bind, and retract them in a 'hand-over-hand' cycle, involving alpha2beta1 integrin. Wild-type fibroblasts move collagen fibres three to four times farther per cycle than fibroblasts lacking myosin II-B (myosin II-B(-/-)).Green fluorescent protein (GFP)-tagged myosin II-B, but not II-A, restores normal function in knockout cells and localizes to cell processes. This data suggests that cyclic myosin II-B assembly and contraction in lamellipodia power 3D fibre movements (Meshel et al., 2005).

Ehrlich et al demonstrated that during lattice contraction two distinct cell populations develop (Ehrlich et al., 1990). At the periphery of the lattice, highly oriented sheets of cells, referred to as myofibroblasts, show cell-to-cell contacts and thick, actin-rich staining cytoplasmic stress fibers. It is proposed that these cells undergoing cell contraction produce a multicellular contractile unit which re-orientates the collagen fibrils associated with them. The cells in the central region, referred to as fibroblasts, are randomly orientated, with few cell to cell contacts and faintly staining actin cytoplasmic filaments. In contrast it is proposed that cells working as single units use cell locomotion forces to re-orientate the collagen fibrils associated with them.

This has lead to the second theory of wound contraction which proposes that a specialised cell the myofibroblast is responsible for generating the contractile force associated with wound closure. **Myofibroblasts** are present transiently during tissue repair and are mesenchymal cells that exhibit morphological and biochemical features of both a fibroblast and a smooth muscle cell (Lorena et al., 2002). They are characterised by the presence of a contractile apparatus, that contains actin microfilaments with associated contractile proteins (non muscle myosin), and a specialised adhesion complex, the fibronexus, where the actin bundles terminate on the cell surface and attach the cell to extracellular fibronectin fibrils. These two elements generate a mechanotransduction system. Another characteristic of myofibroblasts is that they are connected directly to each other through gap junctions, indicating that they might form multicellular contractile units. Finally, myofibroblasts express α smooth muscle actin in the stress fibres, in addition to β and γ cytoplasmic actins found in fibroblasts. Contractile force is exerted on the ECM by stress fibre contraction mediated through cell cell and cell ECM contact.

Fibroblasts respond to signals in the ECM and differentiate into the myofibroblast phenotype. Myofibroblastic differentiation represents an adaptive response to modification of the extracellular matrix environment and is modulated by cytokines. TGF β has been shown to be a direct inducer of the myofibroblast phenotype and is capable of up regulating α SMA both in vivo and in vitro (Kelley et al., 1993; Li et al., 1999, Ronnov-Jessen et al., 1993, Vaughan et al., 2000). TGF β1 stimulates the expression of α SMA in granulation tissue myofibroblasts. Furthermore, the expression of α SMA protein and mRNA by TGF-β1 is induced in both growing and quiescent cultured fibroblastic populations (Desmouliere et al., 1993). Serini and Gabianni have also shown that TGF β2, like TGF β1 induces myofibroblast formation in vitro and in vivo (Serini et al., 1996).

TGF β3 acts as a negative regulator of the myofibroblastic phenotype in vivo but not in vitro. In vitro the three different TGF β isoforms are equally able to induce α SMA mRNA and protein expression in cultured human and rat subcutaneous fibroblasts. However, in vivo, TGF β isoforms may play different but complementary roles in myofibroblast modulation in wound repair.

A two stage model of myofibroblast differentiation has been proposed (Figure 8). In vivo, fibroblasts contain cortical actin but they neither show stress fibres nor do they form adhesion complexes with the ECM. In the presence of mechanical stress, fibroblasts differentiate into proto-myofibroblasts, which form cytoplasmic actin containing stress fibres that terminate in fibronexus adhesion complexes (Dugina et al., 2001, Grinnell et al., 1994, Hinz et al., 2001, Berry et al., 1998). Functionally, these cells can generate contractile force. In the presence of mechanical stress, TGF β and ED- fibronectin promote modulation of the proto-myofibroblasts into fully differentiated myofibroblasts (Serini, 1998). These cells are characterised by the de novo expression of α SMA in stress fibres and by large fibronexus adhesion complexes, and functionally generate greater contractile force.

In summary myofibroblasts represent the main cellular type present in granulation tissue (Gabbiani, 1998) and appear to play an integral role in tissue contraction through generation of a mechanotransduction system. In addition, they are implicated in ECM deposition during tissue repair and actively participate in the synthesis of ECM components such as tenascin, fibronectin and collagens I and III to replace the damaged tissue (Zhang et al., 1994). Myofibroblasts are also responsible for the synthesis of enzymes involved in matrix degradation. The differentiation from fibroblasts in to the myofibroblast phenotype is carefully regulated according to the local environment and an

Figure 8 Myofibroblast transformation

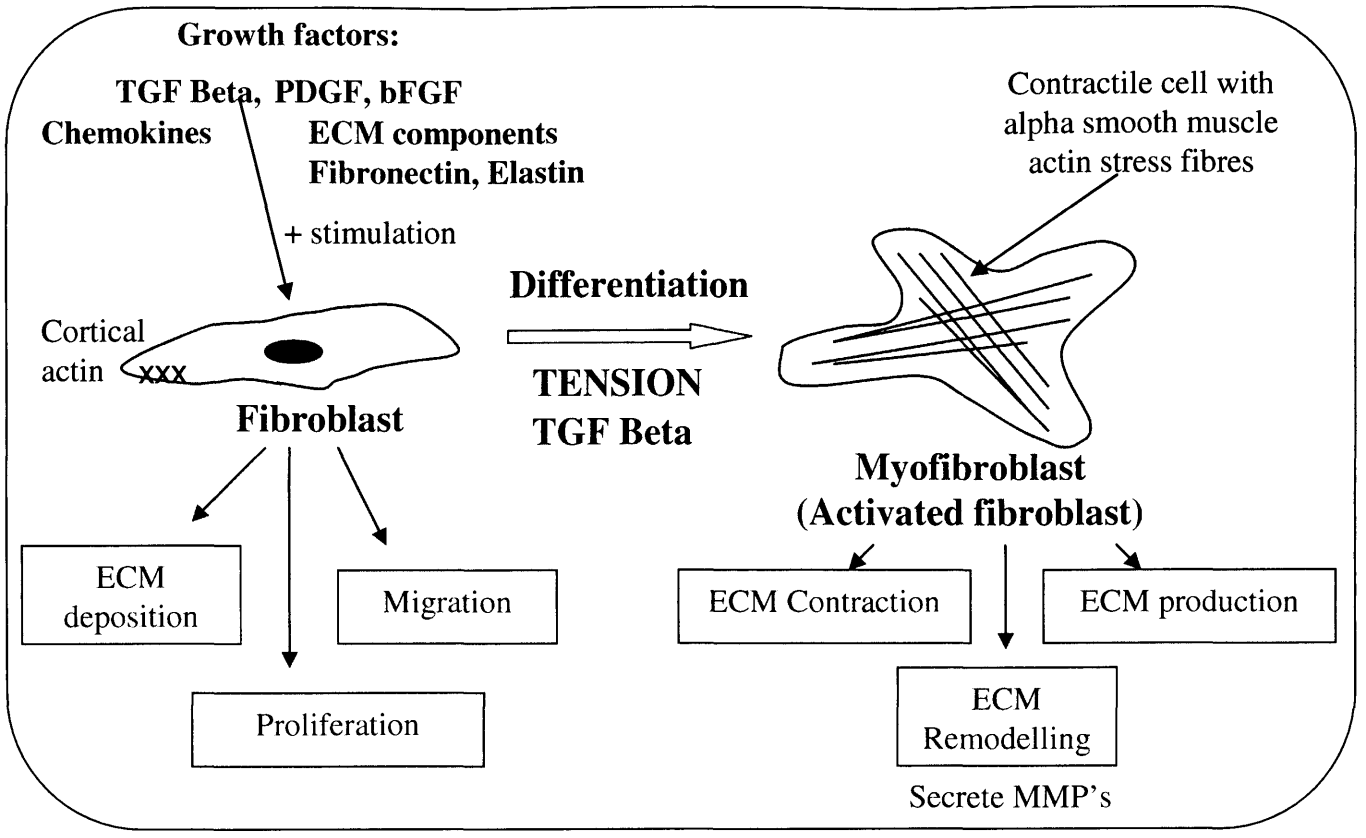

Fibroblasts become activated by growth factors and ECM components inducing proliferation, migration to the wound site and provisional matrix deposition. Fibroblasts adapt to the local environment and in the presence of mechanical tension and TGF β they differentiate into a more contractile phenotype: the myofibroblast which is a key cell in pathological scarring.

abnormal predominance of myofibroblasts results in exaggerated and abnormal wound healing. Figure 9 provides a model of the evolution of contractile forces during wound healing.

1.2.4 Remodelling phase and scar formation

Scar tissue formation requires re-epithelialisation, granulation tissue remodelling with ECM degradation, and decreased tissue cellularity. The newly laid down connective tissue is remodelled continuously over several months (Peacock, 1984). In normal wound healing there is a careful balance between fibroblast and myofibroblasts mediated synthesis and degradation of the ECM which leads to the repair and restoration of normal tissue architecture. During repair of injured tissues, the mass of granulation tissue must be controlled and limited to prevent anarchic remodelling and the development of fibrosis. In aberrant wound healing there is an alteration in the balance and excess connective tissue is deposited which results in a fibrous scar.

The matrix metalloproteinases (MMP's) are a family of over 20 proteolytic enzymes that degrade the extracellular matrix (Wong et al., 2002). They can be divided into four classes on the basis of their preferred substrate: collagenases, gelatinases, stromelysins, and membrane type (MT) MMP's. Collagenases specifically degrade connective tissue collagens, mainly I, II and III by unwinding the helical fibre. This results in a denatured gelatin form which is susceptible to enzymatic cleavage by other MMP's and proteases. Gelatinases, also known as type IV collagenases, degrade the basement membrane and have high enzymatic activity to denatured collagen. Stromelysins have broader substrate specificity, as they are able to degrade ECM components such as fibronectin, proteoglycans, laminin and type IV collagen of the basement membrane (Baramova et al.,1995). The membrane-type MMP's differ in that they have an additional domain and

Figure 9 Contractile forces during wound contraction and scarring

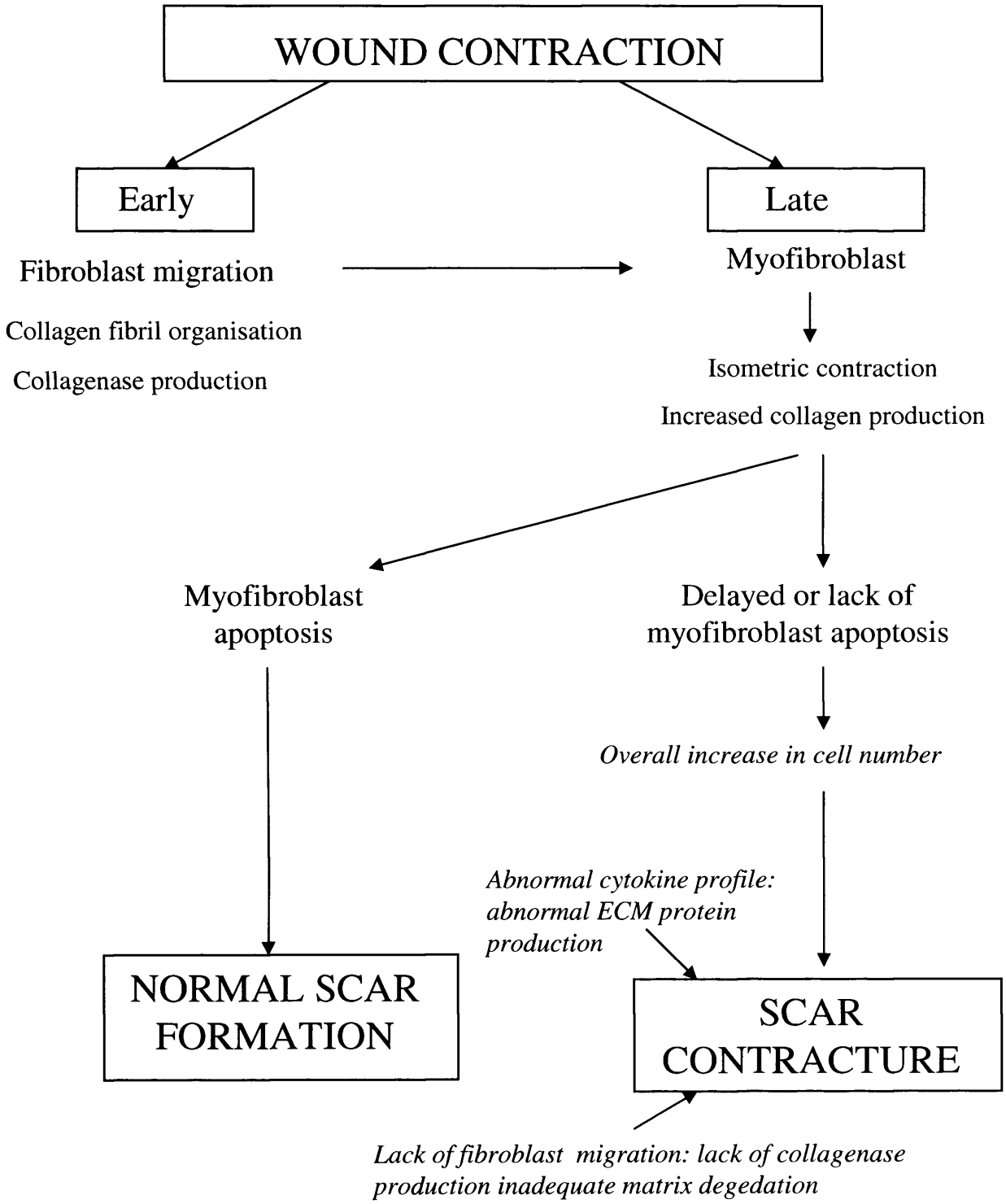

A model to illustrate the evolution of contractile forces during wound healing. One of the pivotal differences between wound that proceed to normal compared to excessive scarring is the lack of myofibroblat cell death.

cytoplasmic tail of 25 amino acids that anchors the enzyme to the extracellular side of the cell membrane. During repair many different MMP's are produced by multiple cell types residing in the wound environment, including myofibroblasts. Proteases may impede wound healing by degrading ECM proteins, but also by degrading peptide growth factors and cell surface receptors. Tissue inhibitors of the metalloproteinases (TIMP's) a gene family of tissue derived metalloproteinase inhibitors, control, at least in part, the catalytic activity of MMP's. The degree of ECM at the wound site is dependent upon the balance between MMP's and TIMP's, which in turn are regulated by several chemical mediators.

The final process in normal wound healing is resolution of the scar. Once the wound is filled with collagenous matrix, angiogenesis ceases, and the fibroblasts and myofibroblasts within the matrix undergo apoptosis (Desmouliere et al., 1995). Persistence of these cells in the wound can lead to abnormal scarring and wound contracture. The induction of fibroblast apoptosis and their clearance by phagocytes is essential for normal wound healing and prevention of scarring. However, little is known about the clearance of apoptotic fibroblasts and whether apoptotic cells are active participants in the recruitment and activation of phagocytes. Evidence suggests that apoptotic fibroblasts may actively release increased amounts of thrombospondin (TSP1) to actively recruit macrophages (Moodley et al., 2003). Thromobospondins (TSPs) 1 and 2 are extracellular modular glycoproteins that are best known for their anti-angiogenic properties and their ability to modulate cell-matrix interactions (Adams et al., 2004). Knowledge is evolving the role of TSP-1 and TSP-2 in wound-healing. Pericellular levels of the matrix metalloproteinase, MMP2, appear to be controlled by TSP2 (and potentially also by TSP1) (Bornstein et al., 2004) and Thrombospondin-1 promotes fibroblast-mediated collagen gel contraction caused by activation of latent transforming growth

factor beta-1 (Sakai et al., 2003). TSP-2 may also play a key role in keratocyte/collagen matrix interactions during corneal stromal repair (Armstrong et al., 2003).

Successful glaucoma surgery is usually associated restoration of the normal conjunctival architecture at surgical site, which allows subconjunctival accumulation of aqueous humour (The bleb). However, in failed filtration surgery a dense scar is formed in the subconjunctival space which prevents aqueous flow and intraocular pressure lowering. Subconjunctival scarring represents the major barrier to achieving long term intraocular pressure control.

1.3 TRANSFORMING GROWTH FACTOR BETA AND CONJUNCTIVAL WOUND HEALING

Wound healing consists of a series of co-ordinated events which are driven by locally released mediators. The growth factor proteins involved in the scarring response are summarised in figure 10.

Transforming growth factor beta (TGF β) is a multifunctional growth factor with diverse effects throughout the body. The term was initially used to describe a protein produced by retro-virally transformed cells, which induced phenotypic changes in normal rat fibroblasts (Roberts et al., 1980; Sporn et al., 1986). TGF β was identified in platelets and subsequently found to be produced by a variety of cells (lymphocytes, monocytes, macrophages) and tissues such as kidney, placenta lung and hepatic (Assoian et al., 1983; Roberts et al., 1981). Its actions depend upon target cell type, the extracellular environment, the cellular state of differentiation and the presence of other growth factors. It therefore displays diverse and opposing effects on many cell processes.

Figure 10 The role of growth factors in wound healing

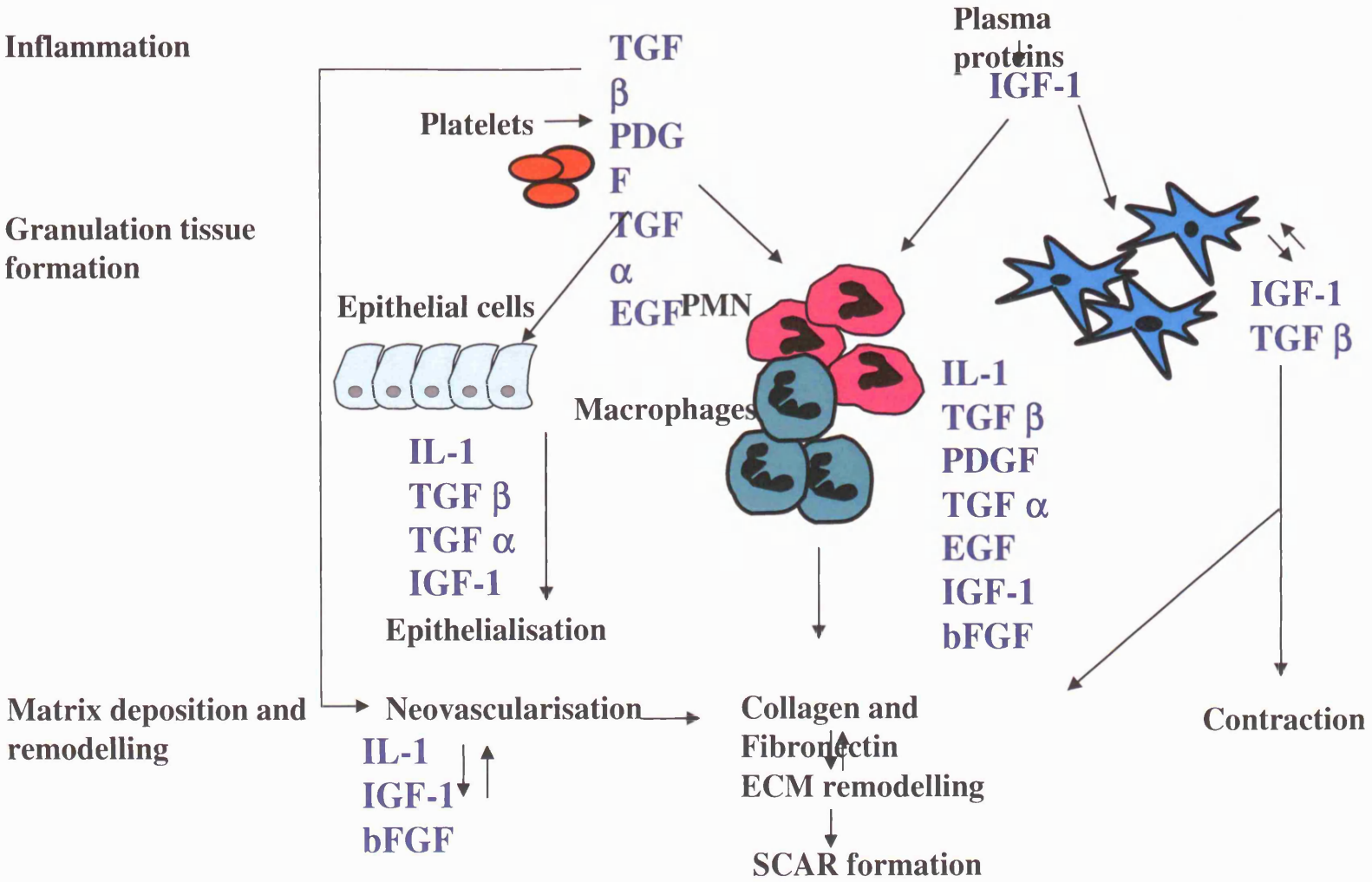

1.3.1 TGF β superfamily

TGF β belongs to large superfamily of polypeptide molecules involved in growth, differentiation and morphogenesis. There are over 30 members which are grouped into four families according to their degree of structural and functional relationship (Kingsey, 1994) (Table 1) .

The TGF β superfamily displays high inter and intra species conservation through evolution. Most of the amino acid sequence similarity is in the C terminal of the precursor molecule. The degree of sequence identity in this domain ranges from 25 to 90% between different family members. At least 7 of the 9 cysteine residues in the C domain are conserved in all members of the superfamily and all 9 are conserved in the TGF β and the inhibin β chain (Roberts et al., 1990).

1.3.2 Molecular Structure

Three different mammalian 25,000 Da isoforms of TGF β have been identified; TGF β1, β2 and β3. TGF β is secreted in a latent form from an inactive precursor, which is then activated to mature form. The TGF β precursor has the characteristics of a secretory propeptide molecule and consists of an N-terminal signal sequence, glycosylated pro region and C-terminal domain bioactive domain. The precursor sequence site consists of four basic amino acids immediately preceding the bioactive domain. The mature 112 amino acid C –terminal domain encodes 9 cysteine residues, which are conserved across the 3 mammalian isoforms. One of these cysteine residues forms an intermolecular bond to form a biologically active dimer molecule (Cheifetz et al., 1988; Schlunegger et al., 1992). The mature C-terminal amino acid sequences display great conservation across the mammalian isoforms. TGF β2 is 70-74% similar to TGF β1, TGF β3 is 78-80% similar to

Table 1 The TGF β superfamily

GROUP	FUNCTION	SUBFAMILY MEMBERS	MEMBERS
TGF β	Embryongenesis Growth and differentiation Inflammation wound healing	TGF β	TGF b1,2,3 mammals TGF b4 chick TGF b5 frog
ACTIVIN	Hormone secretion regulation, growth and development	Activins and inhibins	Activins mammal Inhibin A mammal Inhibin B mammal
DECAPENT APLEGIC	Development of cartilage and bone	Bone morphogenic proteins BMP Decapentaplegic	BMP2 mammal BMP4 mammal DPP Drosophila
60 Å	Development of cartilage and bone	60 Å Bone morphogenic proteins	BMP 5,6,7,8 Mammal 60Å Drosophila
MISC	Growth and differentiation	Growth differentiation factors (GDF) Mullerian inhibiting substance (MIS)	GDF 1,3,9 mammal MIS mammal Dorsalin chick Nodal mice

TGF β1 and 80-82% similar to TGF β2. The precursor sequences are less well conserved with TGF β1 having a G-C rich sequence, β2 A-T rich and β3 displays a combination.

TGF β1 was the first protein to be isolated and acts as the structural prototype for the superfamily. Mature TGF β1 is a dimer of two identical 112 amino acids chains, synthesised from a 390 amino acid precursor (Derynck et al., 1985). The TGF β1 gene is located at 19q13 in the human and chromosome 7 in the mouse (Roberts et al., 1990). The structure of TGF β1 is shown in Figure 11. **TGF β2** is also a homodimer of 112 amino acids cleaved from a 442 or 414 amino acid precursor (Webb et al., 1988). The gene is at chromosome 1q41 in the human and at chromosome 1 in the mouse. **TGF β3** was first identified at the cDNA level and has a 410 amino acid precursor, which forms a homodimeric 112 amino acid mature form (Derynck et al., 1985). The TGF β3 gene is at chromosome14q24 in the human and 2 in the mouse.

There is over 97% identity between the mature TGF β1 sequences from various mammalian and avian species. The same is true for the other two isoforms (Figures 12 and 13)

Knockouts of the three isoforms produce different phenotypes. An auto immune inflammatory reaction is evident in TGF β1 null mice. TGF β2 null mice exhibit perinatal mortality and a wide range of developmental defects for a single gene disruption. These include cardiac, lung, craniofacial, limb, spinal column, eye, inner ear and urogenital defects. The developmental processes most commonly involved in the affected tissues include epithelial-mesenchymal interactions, cell growth, extracellular matrix production and tissue remodelling (Sanford et al., 1997). TGF β3 null mice die with unique and consistent phenotypic features including delayed pulmonary development and defective palatogenesis (Kaartinen et al., 1995)

Figure 11 Precursor latent and bioactive forms of TGF β1

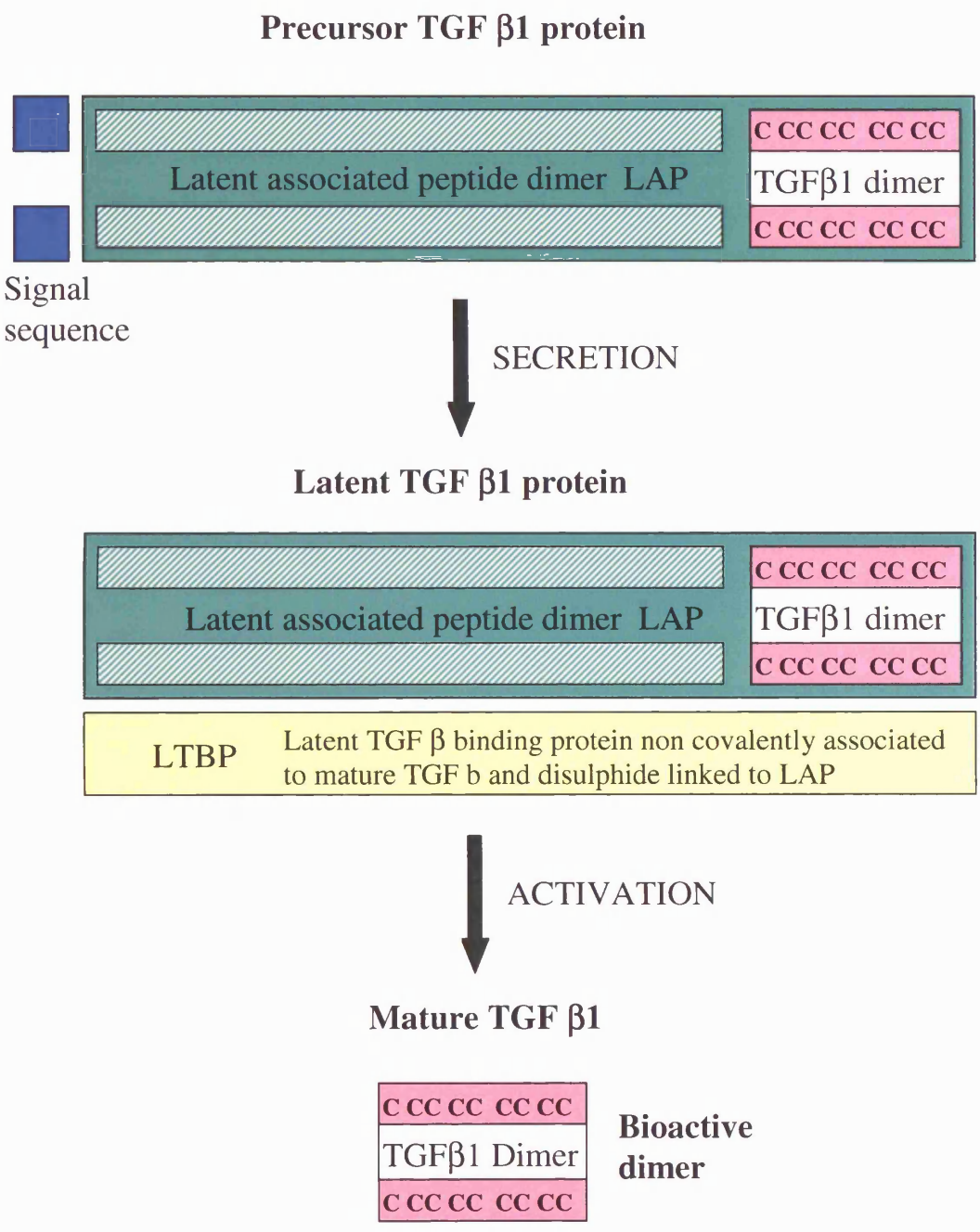

The precursor consists of an N terminal signal sequence, a pro-region and the bioactive domain. After secretion the cleaved pro-region remains associated with the TGF β dimer forming the biologically latent complex. In platelets and certain cell lines the latent complex also contains a 125-190 kd glycoprotein of unknown function. Bioactive TGF β1 is released by disassembly of the complex.

Figure 12 Optimal alignment of TGF-β1 amino acid sequences between species

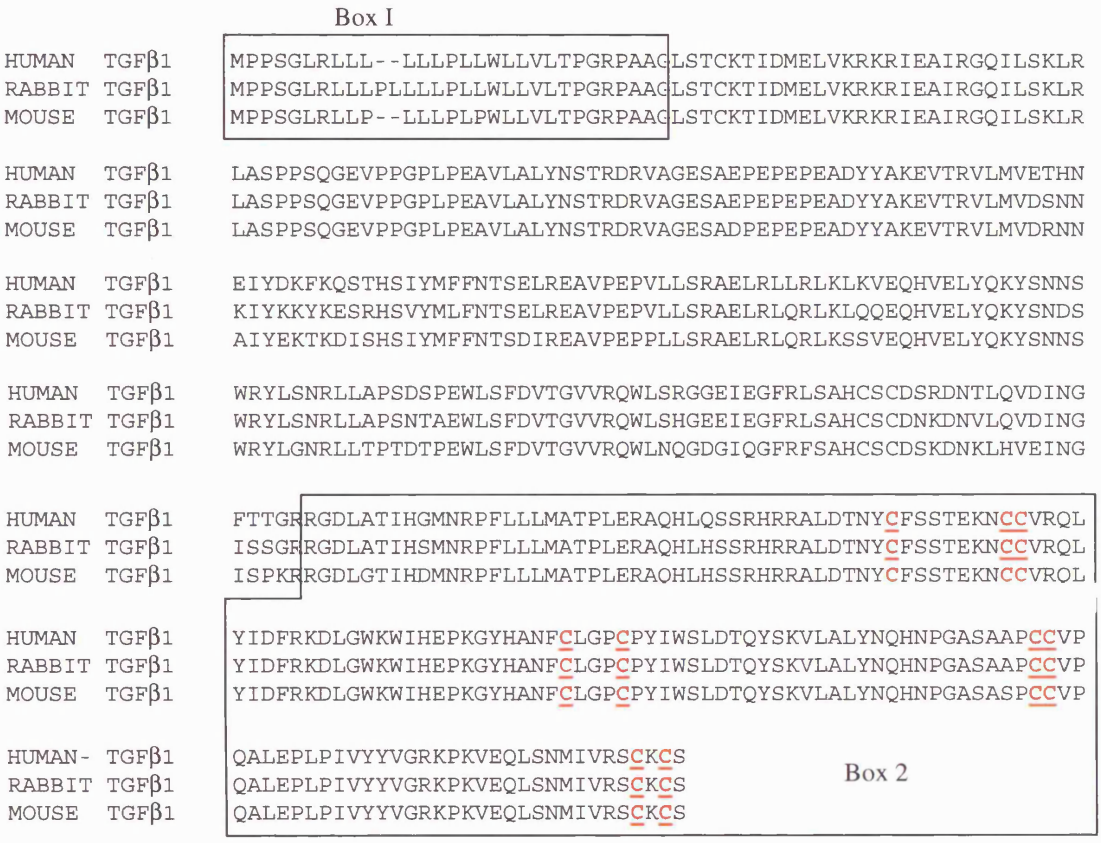

Alignment of amino acid sequences for TGF-β1 precursors translated from human, rat and mouse mRNAs. Box I indicates the signal sequences and Box II indicates the mature protein sequences. The nine cysteine are highlighted in red and show conserved aligment.

Figure 13 Optimal alignment of TGF-β2 amino acid sequences between species

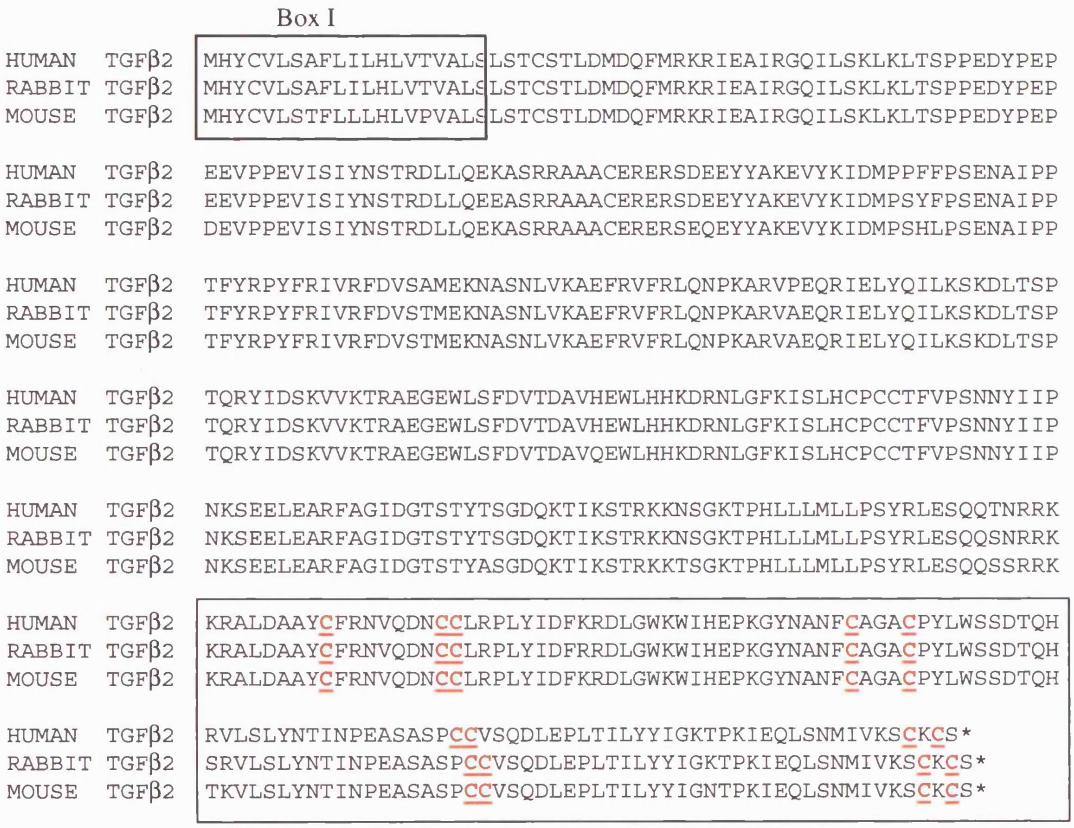

Alignment of amino acid sequences for TGF-β2 precursors translated from human, rat and mouse mRNAs. Box I indicates the signal sequences and Box II indicates the mature protein sequences. The nine cysteine are underlined and show conserved aligment.

1.3.3 Regulation and expression of TGF β

In general, the pattern of TGF β expression varies with each cell type and does not appear to be uniform among cells of the same lineage. Given that most cells types in the body have been shown to produce TGF β, the activity of this growth factor must be carefully regulated to prevent disease. The mechanisms of regulation of TGF β are extensive and complex.

1.3.3.1 Gene transcription regulation Transcription of the TGF β1 gene can be stimulated by phorbol esters via a protein kinase C pathway and by itself (Van Obberghen-Schilling et al., 1988). The 5′ region of the TGF β1 gene contains two transcriptional start sites, one promotor region, 1400 base pairs up from the transcriptional start site, and second located between the two start sites (Kim et al., 1989). Four regions have been identified within the upstream promoter, two negative regulatory regions, an enhancer like element and a positive regulatory region, which contains binding sites for known transcription factors (AP1, Sp1 and NF1). The ability of TGF β1 to positively regulate its own expression is thought to be via the transcriptional enhancer elements in both promoters that respond to induction by the TGF β1 protein as well as AP1 and phorbol ester. Activation via these elements is mediated by binding of the (Jun-Fos) AP-1 complex (Kim et al., 1990). Since the expression and activity of jun and fos genes are modulated by numerous factors including their own products and TGF β1, these mechanisms have the capacity to finely tune TGF β1 expression in response to diverse stimuli.

The three TGF β genes appear to be under differential transcriptional regulation, even thought the protein products are functionally very similar. Each promoter region is different; TGF β1 is rich in G-C with SP1 and AP2-like binding sites but no TATA or

CAAT boxes whilst TGF β2 and TGF β3 both have a TATA box and a functional CRE/ATF binding site. TGF β3 also has a non functional AP2 and several potential Sp1 binding sites. Therefore TGF β1 and β3 both display stimulation by Sp1 transcription factor, whereas TGF β2 does not.

There is evidence that different cells may have different responsive elements in the promoter region of the β1 gene. Sporn and Roberts showed that the retinoblastoma gene product, RB, significantly stimulated the TGF β1 promoter in mink lung epithelial cells but inhibited it in fibroblast cells (Kim et al., 1991). These differences in promoter activity may help to explain the variable TGF β effects seen on different cell lines.

1.3.3.2 Release and activation In most cells TGF β is released as part of a biologically inactive complex which is unable to interact with cell surface receptors. The latent complex consists of a dimer of the N terminal pro region (Latency associated peptide: LAP) non covalently associated with the dimeric C-terminal mature protein. The latent complexes of the three TGF β isoforms significantly differ from one another in that their precursor sequences display variation in glycosylation sites, the number of cysteine residues and the presence or absence of a peptide RGD (Arg-Gly-Asp) sequence.

In some cases the latent complex also contains a latent TGF β binding protein of 125-160 kDa in platelets and 170-190 kDa in fibroblasts (LTBP), which is disulphide linked to LAP and non covalently associated with mature TGF β1 (Kanzaki et al., 1990; Wakefield et al., 1988).The amino acid sequence contains multiple EGF like repeats as the main distinctive feature (Kanzaki et al., 1990). The function of this protein is not fully known in that it does not prevent binding of activated TGF β1 to cells and has no detectable proteolytic activity. However, the LAP lacking LTBP is secreted more slowly from cells

and release of latent TGF β1 from the ECM is as a consequence of proteolytic cleavage of LTBP (McMahon et al., 1996; Taipale et al., 1994).

For TGF β to become biologically active the LAP has to be released from its association with latent TGF β or must undergo a conformational change to expose the binding site. Evidence suggests that proteolytic action of plasmin (Grainger et al., 1995) or Cathepsin D on the pro region, the action of extremes of pH , chaotropic denaturing agents (sodium dodecyl sulfate, urea) or deglycosylation with glycosidases may contribute to the activation of TGF β in vivo (Lyons et al., 1988).In addition, non enzyme catalyst activation can occur with thrombospondin (McMahon et al., 1996). The TGF β1 proregion can bind to mannose-6-phosphate receptors which may also contribute to the activation of the latent molecule (Dennis et al., 1991). Platelets have been shown to contain a furin-like enzyme which is released during platelet degranulation and may act as an alternate means of activating latent TGF β (Blakytny et al., 2004)

1.3.3.3 Sequestration Once released from the latent complex active TGF β1 is bound by various ECM components and serum proteins. Clearance of circulating activated TGF β is extremely rapid (< 3 minutes)(Coffey et al., 1987) and binding α2 macroglobulin maybe involved in this process (Wakefield et al., 1987). High affinity binding to the core protein of proteoglycan and betaglycan or lower affinity interactions with matrix components acts to protect TGF β from degradation, provide a means of sustained release or act as a TGF β clearance system.

1.3.4 Signal transduction

TGF β has diverse effects on cellular function via its binding to specific cell surface protein receptors. Two glycoproteins (Receptors I and II) and a membrane proteoglycan,

designated betaglycan (type III receptor) have been identified as the most widespread high affinity TGF β binding components. Most cell types simultaneously express all three of these receptors simultaneously although each is functionally very different. The receptor characteristics are summarised in Figure 14.

Type I (TBR I) and type II human TGF β receptor (TBR II) are classified as serine/threonin membrane kinase receptors, in which the signal transduction is dependent on phosphorylation of the hydroxyl site of serine or threonin on the target cell. Both receptors have an extracellular ligand domain and an enzymatic region located intracellularly within the cytoplasm. In comparison with TBR II, TBR I is smaller and displays a diminished intracellular domain. The extracellular domain of both receptors share sequence homology and are rich in cysteine residues believed to be important in determination of the correct three dimensional structure needed for specific binding (Ebner et al., 1993).

Both receptors are essential for signal transduction and form a receptor complex. TGF-β binds directly to receptor II, the constitutively active kinase. Bound TGF-β is then recognized by receptor I which is recruited into the complex and becomes phosphorylated by receptor II. Phosphorylation allows receptor I to propagate the signal to downstream substrates. This provides the mechanism by which a cytokine can generate the first step of a signalling cascade (Wrana et al., 1994). A GS-rich region with glycine/serine repeats lies in front of the kinase domain intracellularly and this contains the phosphorylation sites necessary for activation of the TBRI/TBRII complex (Wrana et al., 1994)(Figure 15). The Type III human TGF β receptor, betaglycan, is a proteoglycan that binds to all TGF β isoforms. It forms a stable ternary complex by presenting the TGF β ligand to the type II receptor. The type III receptor is thought to have no role in TGF β signalling

Figure 14 **The molecular structure of TGF β receptors**

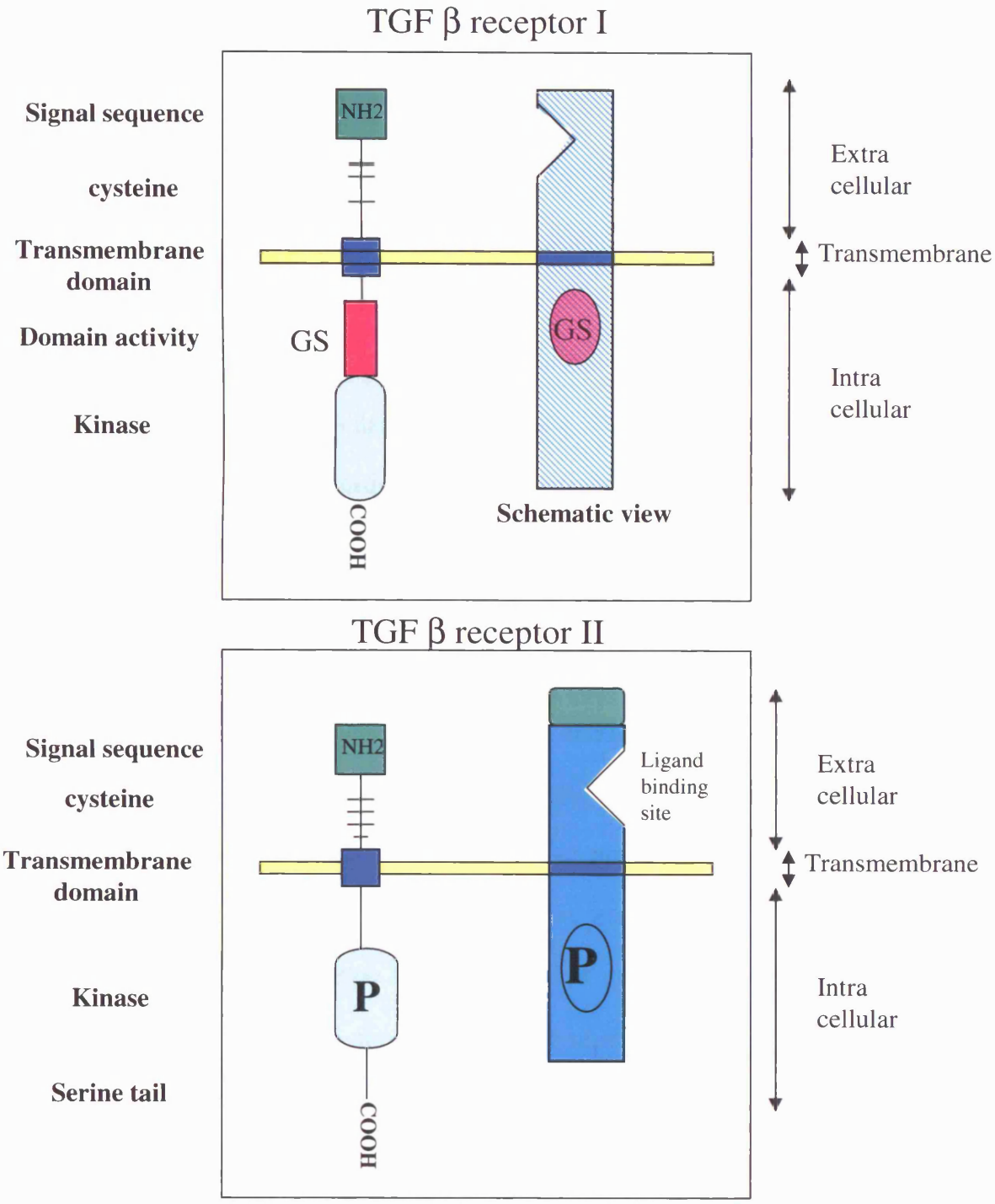

because deletion of the short cytoplasmic domain has no effect on association with the type II receptor, or with the presentation role of the type III receptor. However, Blobe et al have recently demonstrated that the cytoplasmic domains of the type III and type II receptors can interact specifically, in a manner dependent on the kinase activity of the type II receptor and the ability of the type II receptor to autophosphorylate. This indicates that the cytoplasmic domain of the type III receptor may infact play an important functional role in the regulation TGF β signalling (Blobe et al., 2001)

The biological significance of the type IV receptor is unknown. The final TGF β receptor, endoglin, is abundant on endothelial cells. It contains a transmembrane region and cytoplasmic tail homologous to the TBR III receptor. This receptor is mutated in patients suffering from hereditary haemorrhagic telangiectasia (Blobe et al., 2000).

Signal transduction by TGF β1 has been well characterised and is summarised in Figure 15. Briefly TBR I phosphorylation results in activation its kinase, this in turns leads to phosphorylation of transcription factors known as Smads (derived from the Sma and MAD gene homologues in Caenorhabditis elegans and Drosophila melanogaster). These in turn initiate intracellular signalling. Of the 10 smad proteins that have been identified, TBR I receptors specifically phosphorylate smad2 or smad3 which then binds to smad4. The resulting smad complex moves into the nucleus where it interacts in a cell specific manner with various transcription factors to regulate gene transcription. Smad6 and 7 have been shown to block the phosphorylation of smad2, and therefore inhibit TGF β signalling (Massague et al., 2000; Nakao et al., 1997). Although this pathway is inherently simple, interactions in the heteromeric receptor and Smad complexes, receptor-interacting and Smad-interacting proteins, and cooperation with sequence-specific transcription factors allow substantial versatility and diversification of TGF β family

Figure 15 TGF β interaction with its receptors and signal transduction

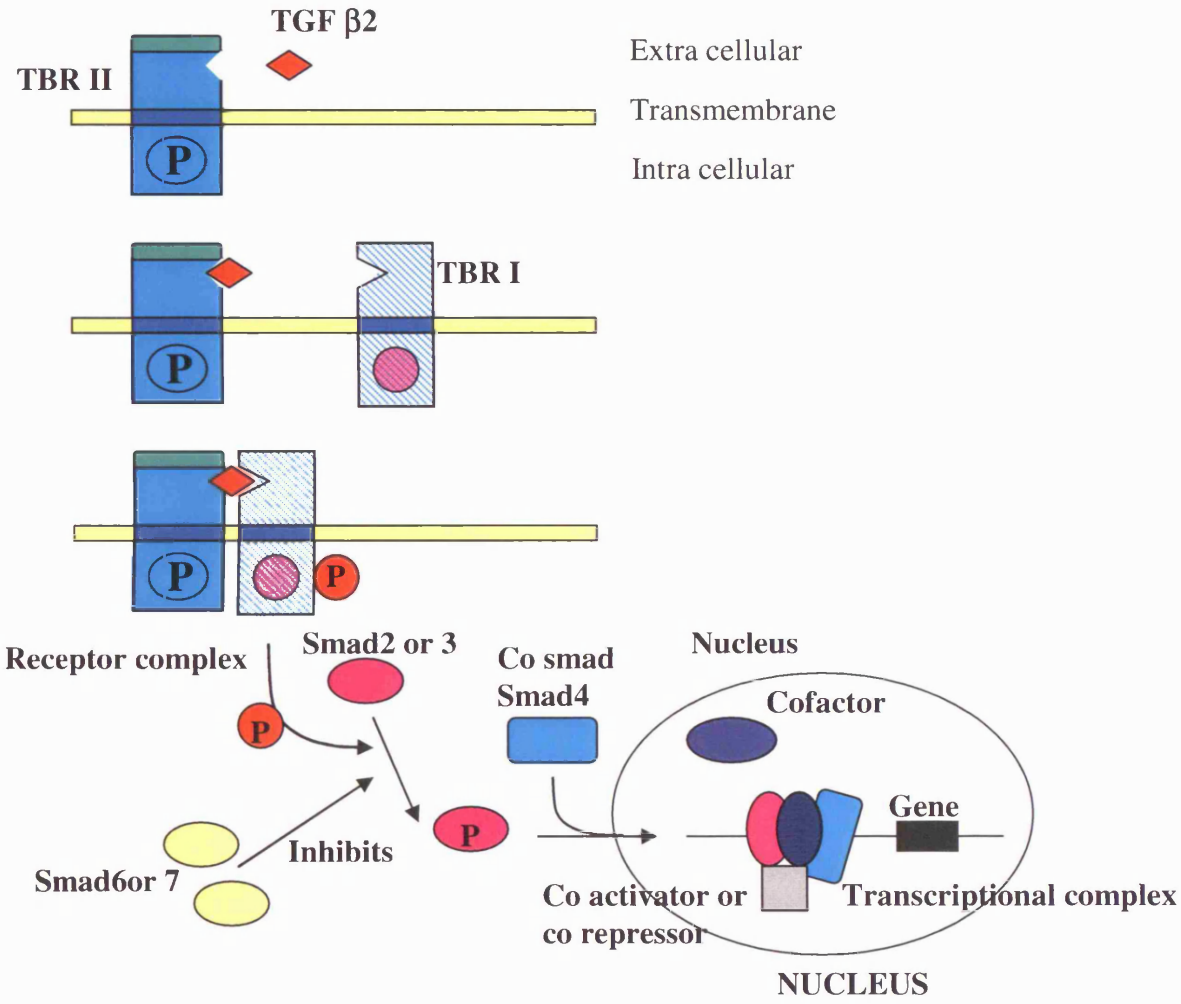

The basic signalling engine: The ligand assembles a receptor complex that phosphorylates Smads, and the Smads assemble a transcriptional complex that regulates target genes. The type II receptors are activators of the type I receptor. Smads are direct substrates of type I receptors. The assembly of receptor-phosphorylated Smads with co-Smads is essential for many transcriptional responses. Smads gain access to target genes by synergistically binding to DNA with cell-specific cofactors, many of which remain unknown. The Smad complex can recruit co-activators or co-repressors that determine the outcome.

responses. Other signalling pathways further regulate Smad activation and function. In addition, TGF-beta receptors activate Smad-independent pathways that not only regulate Smad signalling, but also allow Smad-independent TGF β responses (Derynck et al., 2003).

Receptor binding and activation by the TGF β2 isoform is not as clearly defined. A spliced variant of TBR II named TBRII-B has been identified as a TGF β2 binding receptor which mediates signalling via the smad pathway. The expression of TBRII-B is restricted to cells originating from mesenchymal tissues such as bone where the isoform TGF β2 has a predominant role (Rotzer D, 2001).

1.3.5 Biological effects of TGF β

TGF β has the ability to control the differential potential of many cells and therefore plays an important role in embryogenesis and development. By influencing cell proliferation and activation it is also implicated in the inflammatory and immune response and in tumourgenesis. Finally, it is a potent stimulator of scarring in the body.

The ability of TGF β to elicit multiple and often opposing cellular responses is a subject of great interest. The paradigm of TGF β as a dual factor arose from initial studies in which it was found that depending on the conditions, TGF β can either stimulate or inhibit proliferation (Roberts et al., 1985). The diverse effects on different cell lines has been summarised in Table 2.

Table 2 Effects of TGF β on cell function according to cell type

Cellular function	FIBROBLASTS	EPITHELIUM	ENDOTHELIUM	SMOOTH MUSCLE CELLS	LYMPHOCYTES	MONOCYTES
Proliferation	↑	↓	↓	↑	↓	? ↑
Migration	↑	↑	↓	↑	↑	↑
Collagen contraction	↑	↑	↑	↑	?	↑
ECM deposition	↑	↑	↑	↑	?	? ↑
ECM degradation	↓	↑	↓	↓	↑ ?	↑

↓ Inhibited by TGF β

↑ Stimulated by TGF β

Derived (from Roberts and Sporn, 1990)

1.3.5.1 Effect of TGF β on Cell Proliferation All forms of TGF β display reversible growth inhibitory activity in normal as well as transformed epithelial, endothelial, neuronal and haematopoietic cells (Cheifetz et al., 1987; Roberts et al., 1985; Shipley et al., 1986; Tucker et al., 1984). In certain cell lineages TGF β acts indirectly and reduces proliferation by opposing the action of specific mitogens such as EGF in keratinocytes and IL-1 and IL-2 in lymphocytes. The extent of the growth inhibitory response to TGF β depends on the cell type. TGF β acts by lengthening or arresting the G1 phase of the cell cycle (Heimark RL et al., 1986; Shipley et al., 1985). This is achieved by stimulating production of the cyclin dependent protein kinase inhibitor p15 which thereby inhibits the function or production of essential cell cyle regulators (Ravitz et al., 1997).

TGF β can also stimulate cell proliferation particularly in cells of mesenchymal origin. The mechanism by which this is achieved is not well described although expression of the oncogene c-*fos* appears to be important as does the regulation of the G1 cyclin dependent protein kinases (Ravitz et al., 1997).

1.3.5.2 Effect of TGF β on cell differentiation The differentiative potential of many cell lineages can be affected by TGF β in vitro. TGF β has inhibitory effects on preadipoctye, myoblast, haematopoietic progenitor cell and megakaryocyte differentiation (Ignotz et al., 1986; Massague et al., 1986; Ohta et al., 1987). Induction of differentiation is blocked in the presence of picomolar concentrations of TGF β, however once cells are committed to differentiate, they become refractory to inhibition. Inhibition does not appear to be secondary to the effects of TGF β on cell proliferation, it is reversible once the TGF β is removed, and correlates with a marked alteration in the expression of extracellular matrix proteins and cell adhesion receptors (Ignotz et al., 1985).

TGF β has stimulatory effects on prechondroblasts, osteoblasts and epithelial cell differentiation (Masui et al., 1986). The TGF β isoforms differ in their effects, whilst TGF β1 and TGF β2 are equally potent at inhibiting epithelial cell proliferation and adipogenic differentiation, only TGF β 1 is a potent inhibitor of haematopoietic progenitor cell proliferation (Ohta et al., 1987).

1.3.5.3 TGF β interactions with the ECM The marked and generalised effect of TGF β on the ECM plays a major role in tissue repair processes and the pathogenesis of fibrotic disease

ECM production and remodelling TGF β increases the expression of fibronectin in mesenchymal and epithelial cell types, which can result in up ten fold elevation in fibronectin matrix accumulation (Dean et al., 1988; Ignotz et al., 1986). TGF β also regulates the expression of type 1 collagen α1 and α2 chains, collagen types III, IV and X (Ignotz et al., 1986; Roberts et al., 1986). Other matrix proteins whose synthesis is elevated in response to TGF β include tenasin, thrombospondin, and the chondroitin/dermatan sulphate proteoglycans, biglycan and decorin (Bassols A, 1988; Penttinen et al., 1988). Elevated levels of mRNA for these proteins are seen within 3-5 hours and result from elevated transcription of the corresponding genes combined with increased mRNA stability (Dean et al., 1988, Ignotz et al., 1987).

Not only does TGF β increase the expression of proteoglycan core proteins, it also increases the size of the glycosaminoglycan (GAG) chains attached to them (Bassols A, 1988). Overall TGF β acts to an accumulation and qualitative changes in the composition of ECM.

TGF β simultaneously acts to suppress ECM breakdown. TGF β is intrinsically involved in the balance between the two enzyme systems that control matrix degradation, MMP's

and their inhibitors the TIMP's. It is thought that TGF β down regulates the expression of MMP 1, MMP 3 and plasminogen activators (Overall CM et al., 1988). MMP 3 inhibition has been demonstrated to be at the level of transin/stomelysin gene expression (Kerr LD et al., 1990). TGF β also induces the expression of protease inhibitors such as plasminogen activator inhibitor, TIMP 1and TIMP 2, thereby increasing the deposition of ECM (Edwards et al., 1987; Lund et al., 1987).

Cell matrix and cell cell adhesion Cell migration during tissue repair is guided by a complex set of adhesive interactions between cells and extracellular matrices. The integrin family of cell adhesion receptors have been examined as targets as the mechanism by which TGF β treated cells have a greater ability to bind fibronectin and collagen. Integrins are heterodimeric membrane glycoproteins that consist of a α and β subunit. At least 4 distinct β integrin subunits exist in human cells, each one able to pair with various a subunits, resulting in a αβ integrin complex. Many integrins function as adhesion receptors for ECM components including fibronectin, collagen, laminin, vitreonectin and fibrogen.

TFG β induces marked alterations in repertoire of integrin expression by increasing the mRNA expression of the individual subunits (Ignotz et al., 1987).TGF β has been shown to alter the expression of all the integrin subunits that combine to generate receptors for fibronectin, collagen, laminin and other ECM molecules. The susceptibility of individual integrins to upregulation by TGF β varies depending on the cell type (Heino et al., 1989) . The ability of TGF β to alter cell adhesion receptors influences the ability of cells to interact both with other cells and the ECM, key elements in wound healing.

1.3.6 TGF β and abnormal wound healing

TGF β stored at high levels in platelets or expressed in monocytes can be physiologically delivered to sites of inflammation and wound healing. A localised excess of TGF β activity in tissues can lead to unbalanced ECM deposition and result in fibrotic disease. TGF β has been shown to be intrinsically involved in the formation of scar tissue and the processes of wound healing throughout the body (Ignotz et al., 1986; Khaw et al., 1994a; Khaw et al., 1994b; Postlethwaite et al., 1987; Roberts et al., 1985; Shah et al., 1995).

The initial involvement of TGF β came from important observations of fetal wound healing. Human fetal skin heals via scarless regeneration and this is thought to result from the low levels of TGF β that are present in the foetus (Longaker et al., 1990; Sullivan et al., 1995; Whitby et al., 1991).

TGF β1 and 2 are heavily implicated as potent stimulators of dermal scarring, the organ on which early wound healing research has focused (Gruschwitz et al., 1990; Levine et al., 1993; Roberts et al., 1986; Shah et al., 1995). In addition, cutaneous scarring is also markedly reduced by the application of antibodies to TGF β1 and β2 (Shah et al., 1994). Increased TGF β1 and β2 protein expression in keloids relative to normal human dermal fibroblasts further supports the roles of TGF β1 and β2 as fibrosis inducing cytokines (Lee et al., 1999). Studies of reproductive hormones and wound healing have also indicated that induction of dermal fibroblast TGF β1 secretion in females, may be the mechanism by which oestrogen accelerates wound healing (Ashcroft et al., 1997).

The actions of the third isoform TGF β3 in dermal scarring are less well established, with some evidence indicating that it may inhibit scarring in vivo (Cox, 1995; Shah et al., 1995).

TGF β has a central role in the normal scarring response in number of other organ systems and is particularly abundant in bone lung, kidney and placental tissue (Critchlow et al., 1995). In many diseases excessive TGF β contributes to pathological scarring that can compromise normal organ function. Cicatricial diseases such as systemic sclerosis and rheumatoid arthritis, which are characterised by inflammation and fibrotic destruction result from aberrant growth factor expression (Gruschwitz et al., 1990; Mussener et al., 1997). In the kidney TGF β promotes renal cell hypertrophy and stimulates extracellular matrix accumulation, the two hallmarks of diabetic renal disease (Chen et al., 2003). Pulmonary and hepatic scarring diseases are also associated with increased TGF β activity (Bartram et al., 2004; Sanderson et al., 1995; Sime PJ, 2001)

Growth factors including TGF β play a critical role in the pathogenesis of cardiovascular disease such as atherosclerosis and myocardial remodelling (McCaffrey, 2000). TGF β stimulates fibronectin production by vascular intimal smooth muscle cells, which contributes to atherosclerotic plaque formation (Kaiura et al., 2000).

1.3.7 TGF β production in the eye

TGF β has been detected in the ocular tissues of the anterior and posterior segment, the aqueous and vitreous humour and tear fluid (Kokawa et al., 1996; Lutty et al., 1993, Jampel et al., 1990; Pasquale et al., 1993). Of the three human isoforms TGF β2 is thought to be the most predominant ocular isoform (Connor et al., 1989; Jampel et al., 1990b).

Anterior segment: Immunohistochemical techniques localise TGF β1 to the superficial conjunctival epithelial cells, TGF β2 to the conjunctival stroma, ciliary processes and the ciliary body, and TGF β3 to white blood cells within the anterior segment (Pasquale et al.,

1993). Latent TGF β2 appears to be produced locally by cells found within the iris and ciliary body (Knisely et al., 1991). Latent TGF β2 is also produced by trabecular cells and evidence suggests that it displays an autocrine and/or paracrine action in the trabecular meshwork system. This enables trabecular cells to respond and contribute to the presence of TGF β2 in their microenvironment as well as in aqueous humour (Tripathi et al., 1994a).

The concentration of active TGF β2 in the aqueous of normals is estimated to be 0.73-10.98 x 10^{-11} M compared to a concentration of 12-16 x 10^{-11} M in the serum. 22-66% of the aqueous TGF β2 is estimated to be in the active form. Total TGF β2 concentration in the aqueous decreases with age, shows slight changes with axial length and is elevated in patients with complicated diabetes who have undergone panretinal photocoagulation for diabetic retinopathy (Nakamura et al., 2004). All three isoforms and TBR-I and II receptors have been identified in the cornea (Hayashi et al., 1989; Nishida et al., 1995; Zieske et al., 2001). TGF β1, β2 and TGF β3 mRNA transcripts are expressed in corneal epithelial cells, whilst stromal keratocyte samples express TGF β1 and β2 mRNA but not TGF β3 mRNA. Endothelial cells expressed all three transcripts (Nishida et al., 1995). TGF β1 is implicated as the key molecule responsible for abnormal corneal wound healing. High basal levels of this isoform can be detected pre injury, in contrast, levels of TGF β2 and TGF β3 mRNAs were very low in normal corneas, but increase significantly after injury (Chen et al., 2000).

In quiescent lens epithelial cells (LECs) the expression pattern of TGF β shows regional heterogeneity. Anterior LECs exhibit TGF β immunoreactivity, while equatorial LECs are positive for TGF β1 and β2. Quiescent LECs express TBR-II. Proliferating LECs

express proteins of each TGF β isoform and each TGF β receptor. TGF βs were also localized in the ECM on lens capsules undergoing repair (Saika et al., 1997).

Posterior Segment All isoforms have been detected in the posterior segment with TGF β1 and β2 confined to the rod outer segments, β3 the inner segments and β2 predominantly in the RPE (Anderson et al., 1995)

Overall in the rat eye TGF β2 and β3 were found to be approximately 10 times more potent than TGF β1. All three isoforms were expressed in the eye in spatially distinct but overlapping patterns. TGF β1 and TGF β2 and their mRNA were detected in most ocular tissues, including the lens. Although TGF β3 was immunolocalized in lens epithelium and fibers and in other ocular tissues, its mRNA was detected only in the retina and choroid (Gordon-Thomson et al., 1998). The cornea, ciliary body, iris, lens, retinal cells, RPE and vascular cells all express the receptors for TGF β superfamily at protein level. (Obata et al., 1999)

1.3.8 TGF β and ocular scarring

TGF β is a potent stimulator of scarring in the eye has also been implicated in the pathogenesis of cataract, posterior capsule opacification (PCO: secondary cataract), glaucoma, corneal and retinal disease.

The corneal stromal keratocyte, plays a pivotal role in corneal scarring. TGF β is reported to stimulate ECM production by keratocytes and TGF β isoforms and their receptors are up regulated following corneal injury (Chen et al., 2000; Faktorovich et al., 1999; Kaji et al., 2001; Sakamoto et al., 2000). Studies demonstrate that injury-induced activation and transformation of keratocytes to myofibroblasts results in the deposition of new matrix,

wounds contraction and the development of "haze", which reduces visual acuity. Transformation of keratocytes to myofibroblasts is induced in culture by TGF β and blocked in vivo by antibodies to TGF β (Jester et al., 1999).

Down-regulation of the TGF β signalling system has been employed as a strategy to prevent scarring in the cornea (Jester et al., 1997; Moller-pedersen et al., 1998; Myers et al., 1997; Thom et al., 1997). In addition, Tseng et al have applied amniotic membrane tissue to suppress TGF β1 and β2 protein expression and subsequent myofibroblast differentiation by corneal fibroblasts in the management of ocular surface disease.

In the rodent lens TGF β can induce morphological and molecular changes similar to those associated with cataract formation (Hales et al., 1995; Hales et al., 2000). Human studies have also highlighted the importance of TGF β in cataract formation and in the development of PCO (Lee et al., 2000; Nishi et al., 1995).

In the posterior segment high levels TGF β2 in vitreous aspirates have been found to correlate with the degree of intraocular fibrosis and proliferative vitreoretinopathy (PVR) (Connor et al., 1989; Kon et al., 1999). RPE cells are believed to play an important role in the formation and contraction of epiretinal membranes in PVR and anti TGF β antibodies have be shown to inhibit RPE-mediated contraction (Carrington et al., 2000). Conversely its use as a scarring agent has been advocated and studies have suggest exogenous TGF β2 application as a potential treatment for macular holes and retinal tears. (Glaser et al., 1992; Smiddy et al., 1989)

1.3.9 TGF β and glaucoma

TGF β activity is involved in both the pathogenesis and the treatment of glaucoma. Increased outflow resistance with subsequent elevation of the IOP is an important aetiological factor in POAG, and may be secondary to increased deposition of ECM within the trabecular meshwork. Jampel first highlighted the presence of TGF β in the aqueous humour (Jampel et al., 1990b) and Tripathi identified that the aqueous of glaucomatous eyes contains elevated levels of TGF β2 (1.8×10^{-11} POAG vs. 0.71×10^{-11} Normals) (Tripathi et al., 1994b). These observations have lead to the hypothesis that elevated levels of aqueous TGF β2 may drive the increase in ECM deposition in the trabecular meshwork. In support of this TGF β has been shown to modify the alternative splicing pattern of fibronectin pre-mRNA and enhance the synthesis and secretion of this extracellular matrix molecule by trabecular cells in a dose-dependent fashion (Li et al., 2000). Moreover the up-regulation of fibronectin mRNA by trabecular cells exposed to growth factors present in secondary aqueous humour, augmented by the down-regulation of MMP 3 mRNA, contributes to the accumulation of fibronectin in trabecular cells (Tripathi et al., 2004).

Raised pressure induces compression, stretching and remodelling of optic nerve head which results in direct mechanical axonal damage, compromised blood flow and reduced delivery of nutrients. Fuchshofer et al have demonstrated that TGF β2 is capable of inducing the expression of ECM and basement membrane components in cultured ONH astrocytes via CTGF and upregulated TSP-1, a protein naturally involved in the activation of latent TGF β. This has lead to the hypothesis that TGF β2 could be a factor in the initiation of the modification of ECM in the glaucomatous ONH. In addition, TSP-1

induction may be a mechanism by which TGF β amplifies its own activation (Fuchshofer et al., 2005).

With its widespread involvement in the wound healing processes through out the body, TGF β has also been implicated in subconjunctival scarring and the failure of glaucoma filtration surgery.

1.3.10 TGF β and conjunctival wound healing after glaucoma surgery

Aqueous flow bathes the wound and provides a unique and changeable environment which influences post-operative healing. Latent TGF-β2 is produced by tissues within the eye (ciliary body and trabecular meshwork) prior to activation by plasmin and thrombospondin released from blood components after breakdown of the blood aqueous barrier (Grainger et al., 1995; Knisely et al., 1991; Schultz-Cherry et al., 1995; Tripathi et al., 1994a). After glaucoma surgery elevated levels of activated TGF β2 at the wound site are therefore likely to be related to aqueous concentration, the flow of aqueous and breakdown of the blood aqueous barrier. TGF β is also derived locally from degranulating platelets and inflammatory cells at the wound site. In addition, TGF β also displays the ability to auto induce its own production thereby initiating a perpetuating cascade of activation (Kelley et al., 1993; Li et al., 1999). In general most of the TGF β2 is thought to originate from inside the eye and whilst TGF β1 is produced locally by conjunctival inflammatory cells.

1.3.10.1 Expression of TGF β in conjunctival scarring Reichel et al demonstrated that TGF β1, β2 and β3 are all expressed in a mouse model of conjunctival scarring (Reichel et al., 1998). TGF β2 protein was the predominant isoform, being detected in the basement membrane of conjunctival epithelium, conjunctival stroma,

sclera and corneal stroma. TGF β2 activity in the wounded area was apparent on day 2 and reached a peak on day 7. In situ hybridization highlighted a temporal pattern of TGF β mRNA expression with TGF β2 mRNA, the most predominant type, peaking at day 1 and localizing to granulocytes. TGF β1 and β3 displayed maximal expression on day 2 in lymphocytes and mononuclear cells, with some evident on day 1 in platelets. Only small amounts of TGF β3 mRNA were detected.

TGF β1 and TGF β2 together with their binding protein LTBP-1 have been immuno-localised in failed filtering blebs from patients with POAG and pseudoexfoliation glaucoma. In normal conjunctival specimens, only TGF β2 was present in the conjunctival and subconjunctival stromal fibroblasts, whereas TGF β1 was confined to the basal cells of the conjunctival epithelium. In both POAG and PEX glaucoma, TGF β levels were increased in the subepithelial extracellular matrix of the filtering blebs and co localized with LTBP-1 in the stroma. TGF β immunoreactivity was also increased and localized to epithelial cells and stromal fibroblasts and not to the extracellular matrix. These findings provide further evidence for the role of TGF β in the pathogenesis of the conjunctival wound healing response after glaucoma filtration surgery (Kottler et al., 2003).

1.3.10.2 Effect of TGF β on human Tenon's fibroblast activity in vitro TGF β is the most potent growth factor in the aqueous at stimulating in vitro subconjunctival fibroblast activity. EGF, β FGF, TGF β1 IGF1 all stimulate migration, proliferation and collagen production by human Tenon's fibroblasts. TGF β1, however, stimulates migration and proliferation at much lower concentrations than all the other growth factors and induces greater collagen synthesis than EGF and β FGF (Khaw et al., 1994a) (Denk et al., 2003).

All 3 TGF β isoforms appear to behave in a similar manner in vitro. They each stimulate human Tenon's fibroblast-mediated collagen contraction, proliferation and migration with a characteristic concentration dependent biphasic response, with peak activities at 10^{-9}M (TGF β1), 10^{-12}M (TGF β2), and 10^{-9}M (TGF β3) demonstrating a stimulatory effect on conjunctival scarring (Cordeiro et al., 2000b). This is contrary to Shah et al and others who have showed that TGF β1and β2 promoted scarring in rodent wound healing, whereas TGF β3 inhibited it (Shah et al., 1994; Shah et al., 1995). These somewhat contrasting results may well be attributable to differences between species, wound healing models and the anatomical site studied.

The implications of different peaks of TGF β induced fibroblast functions can be explained physiologically. Following wounding fibroblasts migrate to the area and proliferate. TGF β is initially released from inflammatory cells and platelets at the wound site. At early low concentrations TGF β may stimulate proliferation and act as a week chemoattractant 10^{-13}-10^{-12}M. With time the proliferating fibroblasts secrete growth factors and the concentration of TGF β increases. At concentrations of 10^{-9}M TGF β activity is adapted to stimulate collagen deposition and matrix contraction. The role of TGF β during conjunctival scarring appears to be dependent on its concentration at the wound site.

1.3.10.3 Effect of TGF β on conjunctival scarring in vivo TGF β is a potent modifier of subconjunctival healing response in vivo. Exogenous application of all three TGF β isoforms following conjunctival wounding in the mouse can initiate an exaggerated scarring response compared to controls. TGF β treated eyes displayed an earlier peak in inflammatory cell activity and increased collagen type III production (Cordeiro et al., 1999b).

TGF β2 also has the ability to modify the effects of the anti proliferative agent Mitomycin C, which demonstrates profound pro scarring activity (Cordeiro et al., 1999b; Khaw et al., 1994b). When drainage blebs are injected with TGF β1 a healing response is generated which begins to reverse the effects of mitomycin C. Thick scar formation develops around the bleb which begins to opacify and shrink.

Wimmer et al demonstrated that aqueous TGF β2 levels can become elevated after argon laser treatment to the drainage angle in certain subgroups. Patients in which aqueous TGF β2 levels increased had a higher risk of surgical failure after subsequent trabeculectomy than individuals in which the TGF β2 level remained normal (Wimmer et al., 2003). The technique of microarray has been employed to analyse the changes in gene expression during the failure of filtering blebs in a rat model. TGF β appears to be one of a number of genes upregulated in the conjunctiva (Esson et al., 2004).

1.4 MODULATION OF WOUND HEALING AFTER GFS

1.4.1 General

The processes regulating the wound healing response are both numerous and complex. Strategies to modify scarring can be directed to any stage of the pathway and these principles can also be applied to other surgical procedures (Figure 16). Although some anti-scarring therapies have been in clinical use for some years, an increased understanding of the cellular and molecular biological mechanisms involved in wound healing has lead to advances in their use and to the development of potentially new

Figure 16 Modulation of the wound healing response

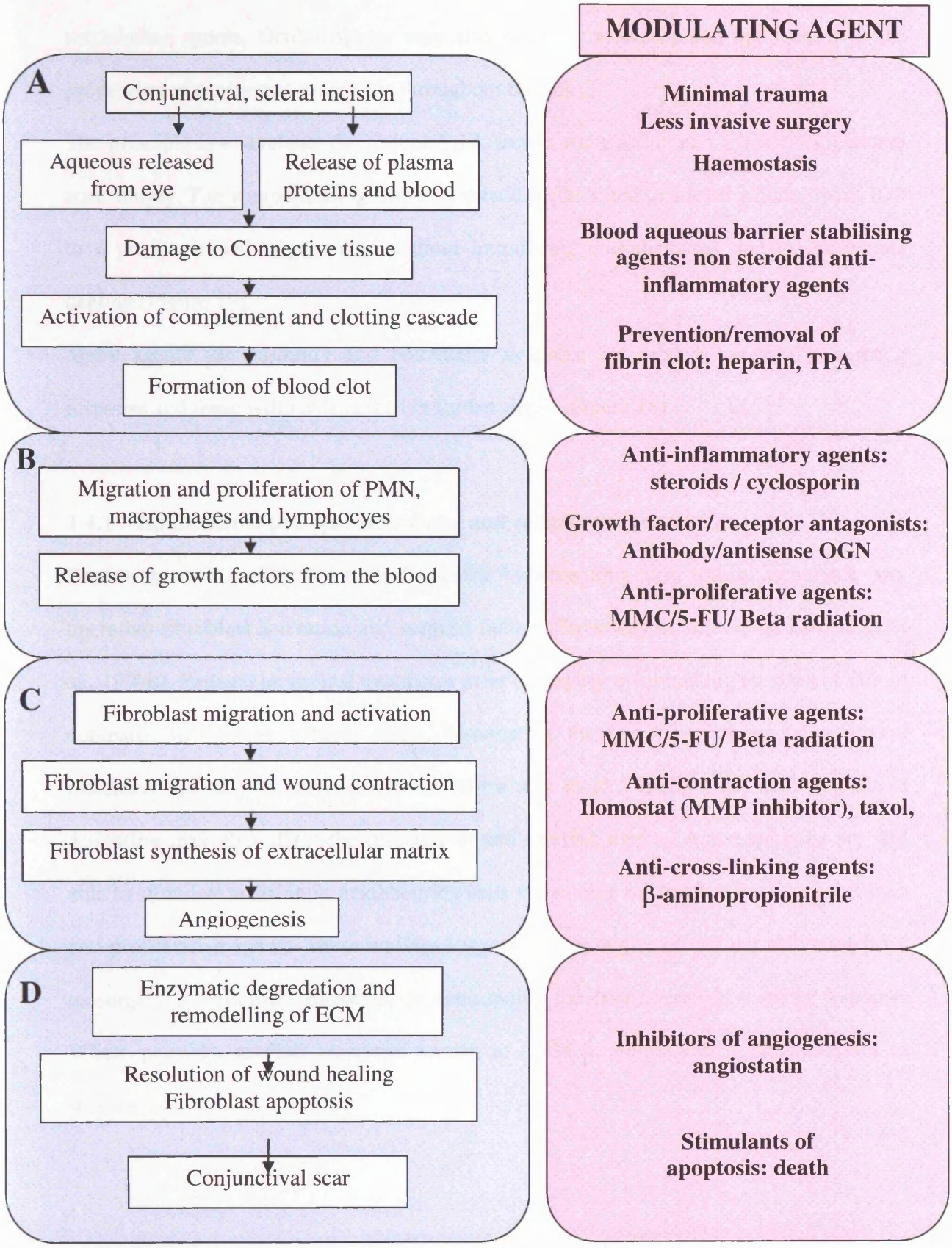

The molecular and cellular events leading to subconjunctival scarring and potential areas of wound modulation after glaucoma filtration surgery. **A-D** represent the wounding, inflammatory, proliferative and remodelling phases of wound healing.

modulating agents. Ocular agents may also have more widespread application in the prevention of scarring at other sites throughout the body.

The principle is to evaluate the patients' risk factors for scarring and adjust the treatment accordingly. The wound healing response should be inhibited to a level which lowers IOP to a predetermined target value without introducing complications due to inadequate healing (Figure 17).

Many agents are currently and potentially available for modulation of the scarring response and these will be described in further detail (Figure 16)

1.4.1 Inhibition of pre-operative tissue and cellular activation

Broadway et al highlighted the relationship between long-term topical treatment, pre-operative fibroblast activation and surgical failure (Broadway et al., 1994a; Broadway et al., 1994b). Patients on topical treatments prior to surgery exhibited higher rates of failure compared to patients without drops. Removal of the pre-operative topical treatment increased the rate of surgical success (Broadway et al., 1996). The state of cellular activation may also affect the response to anti-scarring agents. Activated cells are still able to stimulate scarring in neighbouring cells via soluble mediators after treatment with anti-proliferative agents. These findings suggest that the degree of cellular activation prior to surgery is extremely important in determining the post-operative scarring response. Where possible, medical treatment known to cause inflammation, is stopped prior to surgery.

Figure 17 Aims when modulating the conjunctival wound healing response

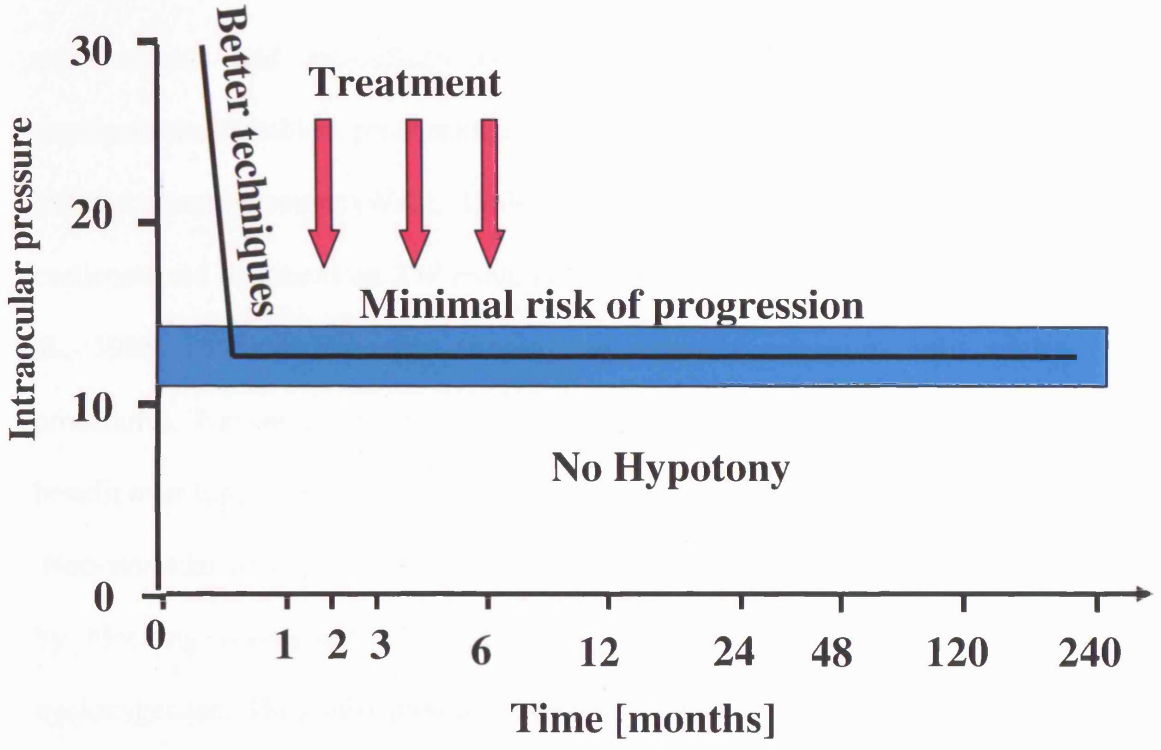

Maintenance of IOP in the low teens delays glaucomatous progression. The use of novel and existing modulating agents combined with improved surgical techniques will ideally enable wound healing to be controlled and low target pressures to be achieved in the long term.

1.4.2 Steroid and Anti-inflammatory agents

Persistent inflammation is associated with enhanced conjunctival scarring. Anterior chamber flare has been shown to be elevated for a prolonged period following phacoemulsification compared to trabeculectomy (Siriwardena et al., 2000). It is also accepted that cataract surgery can reduce co-existing bleb function. These observations highlight the role of the inflammatory response in accelerated wound healing. Treatment with steroids and anti-inflammatory agents inhibit inflammatory cell chemotaxis, angiogenesis, fibroblast proliferation and matrix synthesis, thereby depressing the local inflammatory response (Wahl, 1989). The beneficial effect of post-operative topical corticosteroid treatment on IOP reduction is well established (Roth et al., 1991; Starita et al., 1985) and topical ocular steroids are routinely following most ocular surgical procedures. The use of oral steroids in unselected patients does not confer any additional benefit over topical application after trabeculectomy.

Non-steroidal anti-inflammatory drugs (NSAIDS) suppress the inflammatory response by blocking conversion of arachidonic acid to endoperoxidases via inhibition of cycloxygenase. They also inhibit platelet function and aggregation. Platelets, thrombin and the products of arachidonic acid metabolism are important stimulators of the inflammatory response and hence the wound healing pathway. The beneficial effect of NSAID's as anti-inflammatory agents following glaucoma surgery however, remains unclear (Kent et al., 1998; Migdal et al., 1983). Topical Cyclosporin may also have potential anti-inflammatory role.

Polyvalent dendrimer glucosamine conjugates prevent scar tissue formation (Shaunak et al., 2004). Dendrimers are hyperbranched macromolecules that can be chemically synthesized to have precise structural characteristics. Polyamidoamine dendrimers of D(+)-glucosamine and D(+)-glucosamine 6-sulfate demonstrate immuno-modulatory and

antiangiogenic properties respectively. Dendrimer glucosamine inhibits synthesis of pro-inflammatory chemokines (MIP-1 alpha, MIP-1 beta, IL-8) and cytokines (TNF-alpha, IL-1 beta, IL-6) from human dendritic cells and macrophages but allows upregulation of the costimulatory molecules CD25, CD80, CD83 and CD86. Dendrimer glucosamine 6-sulfate blocks fibroblast growth factor-2 mediated endothelial cell proliferation and neoangiogenesis in human Matrigel and placental angiogenesis assays. A combination of the two dendrimers hyas been shown to increase the long-term success of glaucoma surgery from 30% to 80% in the rabbit model. Engineered macromolecules such as the dendrimers described here can be tailored to have defined immuno-modulatory and antiangiogenic properties, and may represent a novel synergistic approach to prevent scar tissue formation.

1.4.3 Fibrinolytic agents

Fibrin formation can be prevented by heparin. A combined injection of heparin and 5-fluorouracil has been shown to reduce the development of proliferative vitreoretinopathy in high risk patients (Asaria et al., 2001). Once a clot has formed fibrinolysis can be achieved by local administration of tissue plasminogen activator (TPA). Snyder et al developed a quantitative reproducible model for intraocular fibrin deposition and demonstrated the efficacy of human TPA in promoting intraocular fibrinolysis (Snyder et al., 1987). However, the risk of further haemorrhage and the release of pro-scarring breakdown products limit any potential clinical application.

1.4.5 Anti-proliferative agents

The introduction of the anti-proliferative agents 5-fluorouracil (5-FU) and mitomycin C (MMC) represents one of the major advances in glaucoma surgery over the last decade

and these agents are in widespread use. A recent survey performed in university based hospitals in the USA showed that mitomycin C is now used in over 50% of primary trabeculectomies (Chen et al., 1997). An anti-proliferative can be defined as any agent that interferes with cellular division and processing and the mechanisms of action of the anti-proliferative agents used after glaucoma surgery are summarised in Figure 18. 5FU mediates its effect by inhibition of DNA synthesis and its actions ultimately result in cell death. The ribosylphosphate form of 5FU may also be incorporated in to mRNA leading to abnormal ribosymes, altered mRNA translation and abnormal protein synthesis (Falck et al., 1992). MMC is an antibiotic with anti-proliferative activities derived from the soil fungus Streptomyces caespitosus. It can be classified as a cell cycle non specific alkylating agent which x links DNA during all phases of the cell cycle and thereby inhibits DNA replication, mitosis and protein synthesis.

1.4.5.1 Effect of anti-proliferative agents on Tenon's capsule fibroblast activity

The anti-proliferative agents are effective inhibitors of fibroblast function and thereby act to reduce post-operative subconjunctival scarring.

In vitro experiments have identified that short exposures of ocular fibroblasts (5 minutes) to 5FU and MMC can induce long-term fibroblast growth arrest (Khaw et al., 1992c). Given the appropriate concentration and agent effective inhibition of proliferation can be achieved for periods up to 36 days without significant cell death (Khaw et al., 1992c). Long term suppression occurs with both 5-FU and MMC. The inhibitory action of 5FU on thymidylate synthetase should be readily reversible, however the secondary interactions of the drug with RNA synthesis may help to explain its longer term actions. Suppression of proliferation with single short exposures of 5FU and MMC is also able to inhibit other aspects of fibroblast function such as the ability of fibroblasts

Figure 18 Mechanism of action of the anti-proliferative agents

5-Fluorouracil

1° action	Inhibition of thymidylate synthetase prevents DNA synthesis and cell proliferation.
2° action	Incorporation into the RNA abnormal ribosyme formation, altered mRNA translation and abnormal protein synthesis.

MMC

1° action	Alkylating agent which X links the DNA
2° action	Free radicals are generated which cause non-specific damage to DNA, RNA and protein synthesis.

to contract the ECM. Occleston et al demonstrated that ocular fibroblast mediated collagen gel contraction is inhibited by short exposure to both 5-FU and MMC and at high doses MMC induced cytotoxicity (Occleston et al., 1994).

Long term suppression of ocular fibroblast proliferation has also been demonstrated *in vivo* using an experimental model of glaucoma surgery. The treatment appears to be focal (only fibroblasts in the treated area are affected) and titratable in terms of length of action (Doyle et al., 1993a; Khaw et al., 1993b, Khaw et al., 1992b).

Fibroblasts are derived from the local conjunctival population of fibrocytes. To reinitiate the scarring process these cells must either recover from the focal treatment or new untreated fibroblasts must migrate into the area. At the molecular level, it has been shown that suppressed growth arrested fibroblasts are still able to perform several crucial aspects of wound healing, including the expression of growth factors and receptors, migration and ECM production (Occleston et al., 1997). Despite entering growth arrest, fibroblasts still maintain the ability to respond to stimulatory factors in the local environment and can influence the behaviour of other cells by soluble mediators (Figure 19)(Daniels et al., 1999). This may help to explain why some operations still fail due to subconjunctival scarring despite the use of anti-proliferative agents.

At clinical concentrations MMC causes cell death and permanent inhibition of fibroblast function, however there is only temporary inhibition with late recovery after single application of 5-FU (Khaw et al., 1993a; Khaw et al., 1993c; Khaw et al., 1992b). This has important implications in terms of the clinical application and drug selection for each individual patient. In summary, application of 5-FU induces suppression of cellular activity for a number of weeks and this is adequate to modify a normal or exaggerated

Figure 19 **Action of anti-proliferative agents on Tenon's capsule fibroblasts**

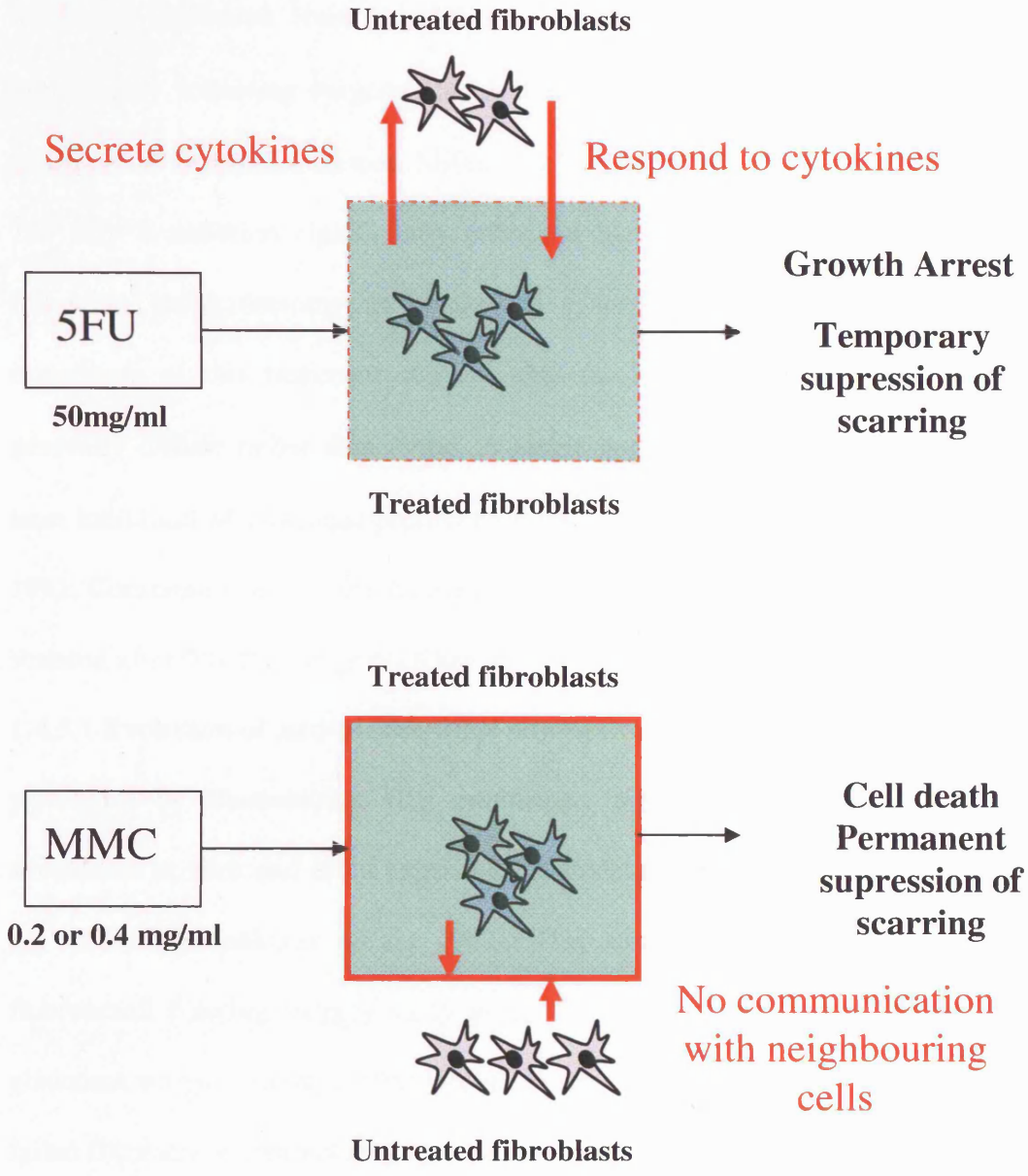

At clinical concentrations MMC causes cell death and permanent inhibition of fibroblast function, however there is only temporary inhibition with late recovery after single application of 5-FU. This has important implications in terms of the clinical application and drug selection for each individual patient

healing response. However persistent healing will only be suppressed by application of mitomycin C (Figure 20).

Application of B irradiation has similar anti-proliferative effects as anti-metabolites. β irradiation delivered from a solid state probe can be focally applied to the bleb immediately following surgery. Rapid attenuation of the β particles makes it ideal for treatment of superficial tissues. Miller and Rice reported that peropertive treatment with 750 cGy b radiation significantly enhanced bleb survival and improved IOP control following trabeculectomy in congenital glaucoma (Miller et al., 1991). Clinical experience of this treatment suggests that the blebs which form after treatment are generally diffuse rather than cystic. A single application of β irradiation leads to long term inhibition of fibroblast proliferation inducing a state of growth arrest (Khaw et al., 1991, Constable et al., 1998). Its use is advocated for patients with an intermediate risk of scarring after filtration surgery (Khaw et al., 2001) .

1.4.5.1 Evolution of anti-proliferative adjunctive therapy Experimental work performed by Blumenkranz first established that 5-FU inhibited the proliferation of fibroblasts in vitro and in an experimental model of epiretinal scarring (Blumenkranz et al., 1984; Blumenkranz et al., 1982). This stimulated the landmark studies of the fluorouracil filtering surgery study group (FFSS) which pioneered the use of 5-FU in glaucoma surgery (Group, 1989; Group, 1996). In this study patients who had previously failed filtration or cataract surgery were randomized to receive a post-operative course of 21 subconjunctival injections of 5-FU (twice a day for one week and once a week for the second week) or no treatment. The trial was stopped early due to the dramatic improvement in surgical success. (73% treated vs. 50% untreated). However corneal

Figure 20 **Healing profiles after GFS**

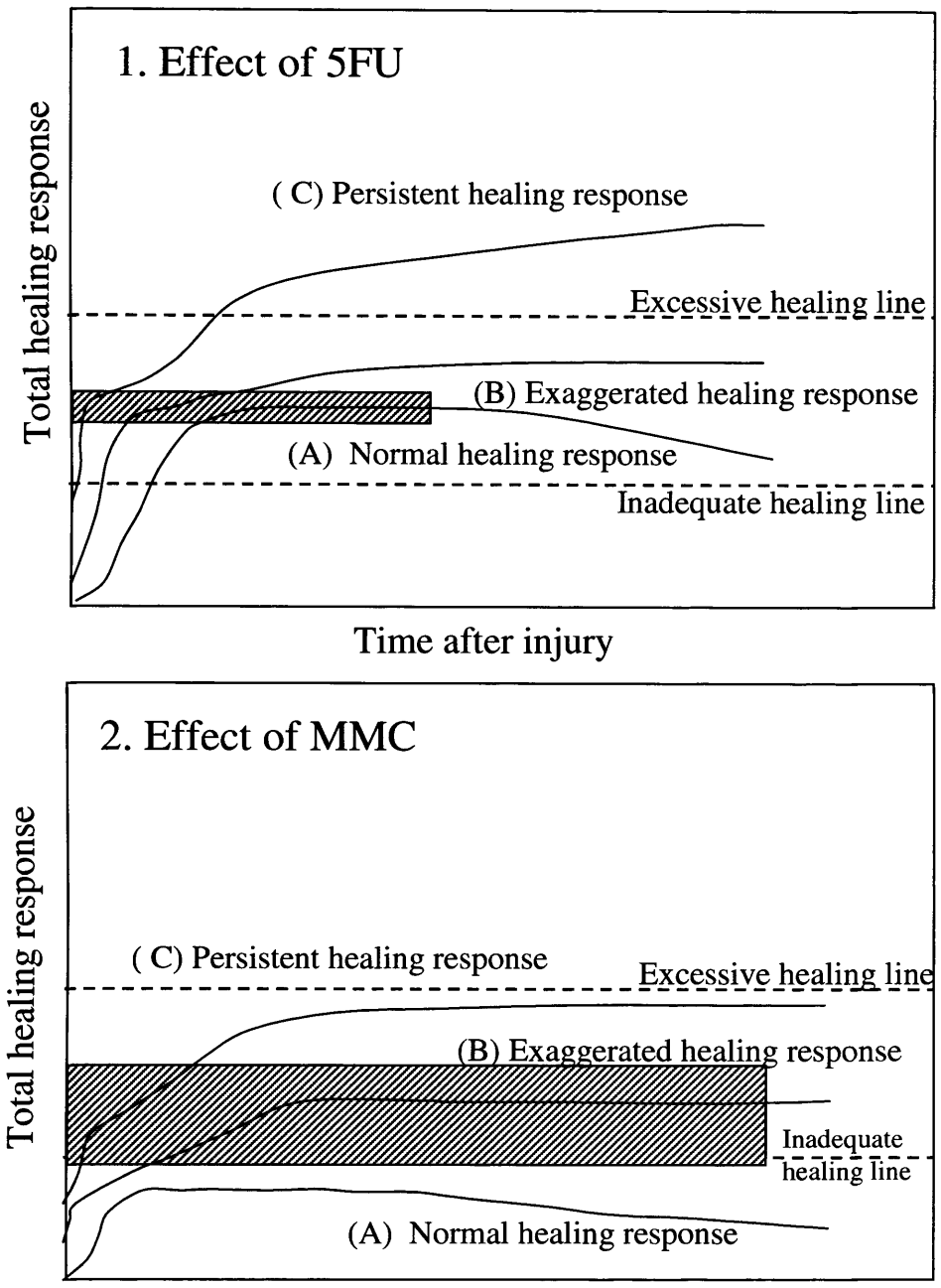

Postulated effect of a single application of 5-FU (1) and MMC (2). 5FU causes temporary suppression which is adequate for normal and an exaggerated response but not for higher risk patients with a persistent healing response who cross the exessive healing line and fail surgery. MMC is able to supress the persistent response but pushes the normal response below the inadequate healing line potentially resulting in hypotony and its related complications. Adapted from Khaw et al (Khaw P.T. et al, 1994b)

epitheliopathy was reported in 50% of patients. Extensive investigation followed looking at the effects of 5-FU and other anti- proliferative agents on ocular fibroblasts in culture in an attempt to find the optimal agent (Blumenkranz et al., 1987; Gillies et al., 1993; Lee et al., 1990a; Lee et al., 1990b; Lee et al., 1991; Schmidt et al., 1982; Senderoff, 1990) and a delivery system that did not require multiple injections (Jampel et al., 1990a; Kay et al., 1986; Lee et al., 1987; Sachdev et al., 1990; Skuta et al., 1987; Winter et al., 1987).

Single applications of intra-operative MMC were first introduced by Chen who had been using this regimen unnoticed for more than a decade (Chen, 1983; Chen et al., 1990). However, this technique did not gain acceptance until sufficient evidence was generated to prove that short term application of these agents could adequately suppress long term fibroblast proliferation (Khaw et al., 1993a; Khaw et al., 1993b; Khaw et al., 1993c; Khaw et al., 1992b; Khaw et al., 1992c; Khaw et al., 1992d, Doyle et al, 1993).

There have been numerous clinical studies demonstrating the efficacy of 5-FU in augmenting the success of glaucoma surgery (Araie et al., 1992; Goldenfeld et al., 1994; Heuer et al., 1986; Mora et al., 1996; Ophir et al., 1992; Rothman et al., 2000; Ruderman et al., 1987; Sidoti et al., 1998; Towler et al., 2000; Tsai et al., 1995). The cumulative data supports a significant benefit in terms of bleb survival and IOP lowering in treated eyes compared to controls. As mentioned the landmark study was performed by the fluorouracil surgery study group. Overall, however, there have been few randomised prospective clinical trials evaluating 5-FU versus no 5-FU. Total dose and mode of administration (injection or sponge) as not been standardised across them, study sizes have been small and considerable variability is demonstrated in patient selection (high risk versus low risk of scarring). The multicentre MRC 5-FU study pioneered by Moorfields Eye Hospital should help to finally answer questions about the optimum use of 5-FU.

The prolonged potent effects of MMC make it suitable as a single-use adjunct in GFS especially in those eyes at high risk of failure. Since 1983 when Chen first used MMC in the treatment of severe refractory glaucoma, numerous studies have investigated the anti-proliferative effects of MMC. Again, most have been retrospective, uncontrolled, non randomised and of relatively short duration. Moreover, the method and duration of application, ocular pathology and patient details have varied significantly. However, despite this MMC has been shown to significantly augment the success of GFS in high risk eyes compared to controls (Cheung et al., 1997; Cohen et al., 1996; Perkins et al., 1998). Several important studies have compared intra-operative 5-FU with MMC and revealed that in high risk patients a single application of MMC provides better long-term pressure control than 5-FU (Katz et al., 1995; Kitazawa et al., 1991; Lamping et al., 1995).

1.4.5.3 Selection of anti-proliferative agent

Intraoperative antimetabolites A number of factors seem to increase the risk of scarring and failure following glaucoma filtration surgery which are summarised in Figure 21. One treatment regimen is not adequate for all patients. A titratable regimen has evolved at Moorfields Eye Hospital called the More Flow (Moorfields/Florida) based on laboratory and clinical data (Khaw et al., 1992c). Both intaoperative MMC and 5-FU are delivered by placement of a drug impregnated cellulose sponge in between the episcleral surface and the undersurface of the conjunctiva for a predetermined time.

Post operative Despite these intra-operative applications bleb failure can occur later in the post-operative period. Injections of 5-FU are used post-operatively on their own or in combination with intraoperative 5-FU or MMC if the pressure is rising and the healing response is still marked (Mastropasqua et al., 1998, Gallenga et al., 1997; Ophir et al., 2000; Shin et al., 1993; Smith et al., 1992, Ophir et al., 1992). Drainage of fluid can

Figure 21 Risk factors for subconjunctival scarring and failure of glaucoma filtration surgery

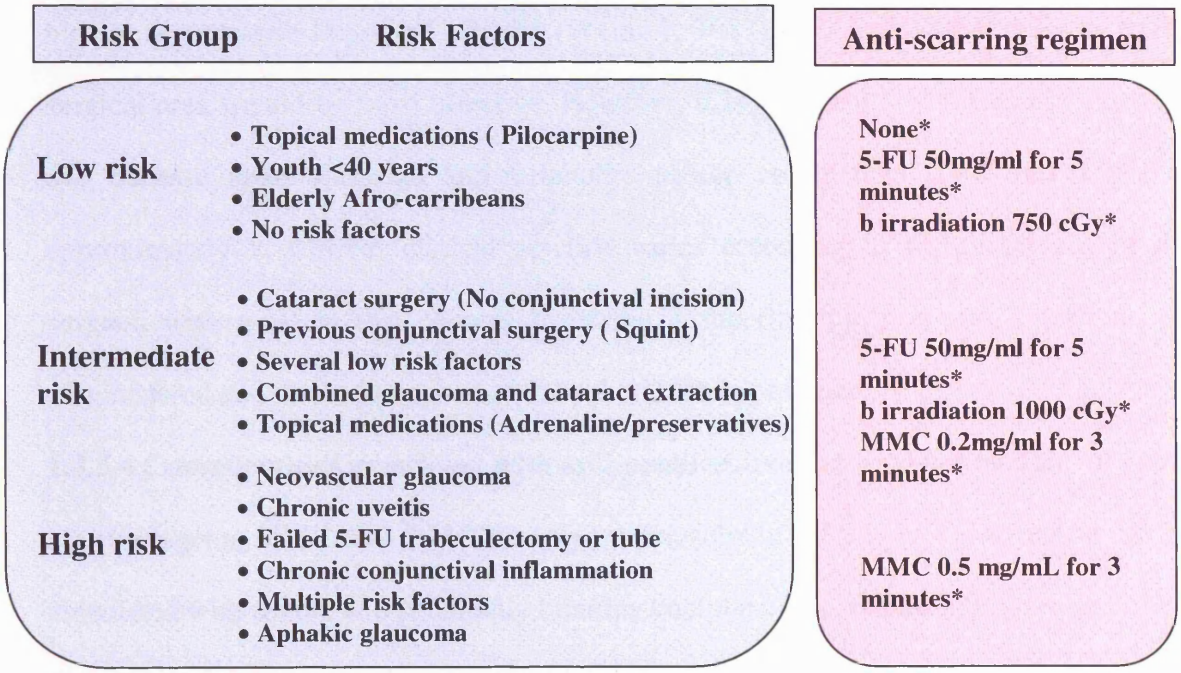

* Post-operative 5-FU injections can be given in addition to intra-operative anti-metabolites

Anti-metabolite regimen currently in use at Moorfields. (Continuously evolving regimen)

become localised with time due to circumferential healing which results in bleb encystment. Subconjunctival injection of 5-FU with physical disruption of the scar tissue provides a useful tool to remodel encysted blebs (Allen et al., 1998).

The technique of injection is important. In the FFSS regimen 5mg of 5-FU was given in a volume of 0.5mg/ml at 180 degrees from the filtration site (Group, 1989). Weinreb subsequently used a higher concentration (5mg in 0.1ml) delivered much closer to the bleb to demonstrate improved efficacy (Weinreb, 1987). It is logical that delivery to the surgical area should be most effective. However, it is vital that 5-FU does not enter the eye because apart form its anti-metabolite action, commercial 5-FU has a pH of approximately 9. Current clinical practice varies according to the preference of the surgeon with most in this country favouring a superior injection site. Injections are administered and titrated as necessary based on bleb appearance.

1.4.5.4 Complications associated with anti-proliferative use Introduction of anti-scarring agents MMC and 5-FU has improved results of GFS however their use can be associated with severe and potentially blinding complications (Figure 22).

Corneal toxicity is the most common complication following application of 5-FU. It decreases the mitotic rate of actively replicating corneal epithelial cells, which can manifest as punctate epitheliopathy, frank epithelial defects or striate melanokeratits. Whilst these complications may resolve without a long term loss of visual acuity, they can be associated with severe discomfort and the development of secondary pathology such as corneal ulceration, melt or even perforation. Concurrent use of topical corticosteroids can potentiate the toxicity. Corneal epitheliopathy was common in the early studies with 5-FU when total doses approached 100mg (Group, 1996) .

Application of both 5-FU and MMC leads to the development of thin avascular blebs, which are associated with enhanced transconjunctival filtration as a result of lowered

Figure 22 Complications associated with antimetabolite use

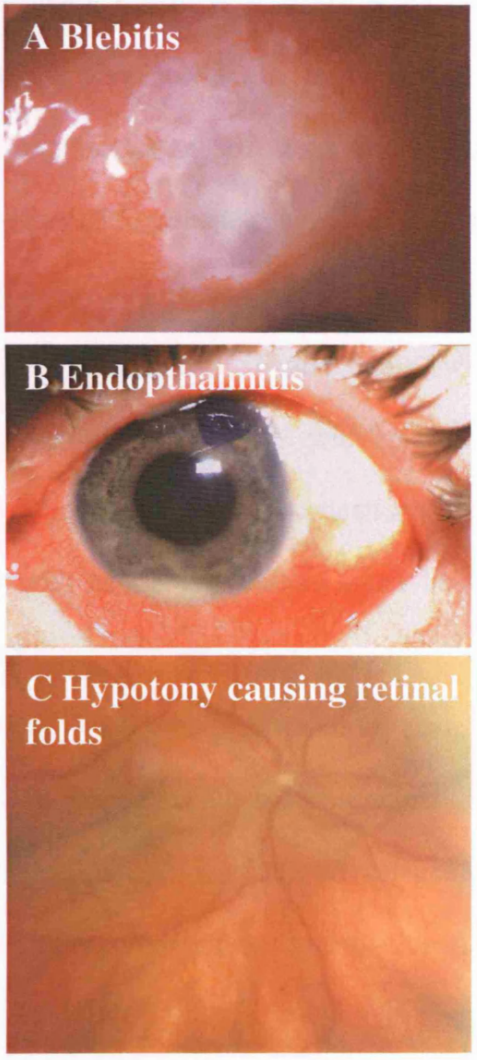

Antimetabolites can be associated with severe and potentially blinding side effects such infection of the eye shown in A and B, and low pressure or hypotony and its associated complications (C).

resistance to flow through the bleb. Whilst this reduces the intraocular pressure it increases the risk of bleb leaks, that can facilitate the passage of bacteria and lead to the potentially blinding complication of endophthalmitis (Soltau et al., 2000, Parrish et al., 1996, Greenfield et al., 1998, Belyea et al., 1997, Kangas et al, 1997).

Low outflow resistance in the bleb can also lead to overfiltration and the development of hypotony and subsequent choriodal effusions and maculopathy (Jampel et al., 1992). Stamper reported a series of 6 patients treated with post-operative 5-FU that developed hypotony with maculopathy and demonstrated that young myopic individuals were more prone to maculopathy with visual loss (Stamper et al., 1992).

As a result of its biological potency, with prolonged cytological toxicity after administration, the risk and severity of complications is more severe when using MMC. Indeed blebs treated with MMC are 3 times more likely to result in focal bleb leaks (Greenfield et al., 1998).

The biological activity of the anti proliferative agents can represent a double edged sword. Whilst the tissue changes enhance transconjunctival flow they can potentiate the risk of blinding complications. To take full advantages of these agents they have to be used appropriately and in combination with adaptations in surgical technique to optimise safety.

1.4.5.6 Advances in anti-proliferative use Strategies to minimise the incidence of complications associated with anti-proliferative use in glaucoma surgery include optimising the choice of agent, method of application and surgical technique.

Anti-metabolite regimen: The selection of the single-application anti-scarring agent and concentration is titrated against patient risk factors. Figure 21 summarises the constantly evolving regimen used by our unit, which is based laboratory and clinical experience.

Exposure time and concentration: Most surgeons now use between 0.2 and 0.5 mg/ml

of MMC, 50mg/ml for intra-operative 5-FU and 5mg (0.1ml of 50mg/ml) for subconjunctival 5-FU. The time of exposure varies amongst centres. We have shown that tissue uptake rises sharply and peaks at 3 minutes. Therefore applications of 3 minutes have the same efficacy as 5 minute exposure but reducing it below 3 minutes can result in suboptimal cellular absorption. Changing the concentration of the agent leads to more reproducible titratable effects than variations in exposure time.

Area of treatment: Experimental work suggested that peripheral growth arrested cells located around the area of anti-proliferative treatment could still form a dense ring of scar tissue ('ring of steel'), which gives rise to encapsulated cystic blebs. In vivo studies have confirmed that increasing the area of anti-proliferative treatment can reduce the incidence of cystic bleb formation. Clinical practice has been changed to adopt this technique which has led to a dramatic fall in the incidence of bleb related complications such as blebitis and endophthalmitis (15% to 0%) (Wells et al., 2003).

Surgical technique: After anti-metabolite use, scleral flap resistance determines the early IOP. The introduction of larger scleral flaps, smaller sclerostomies, and multiple tight adjustable and releasable sutures helps to avoid post-operative hypotony and provides a means of exquisitely controlling early post-operative IOP.

Post-operative injections: The original regimen of 21 injections has been modified and most Ophthalmologists give less than 10 with longer intervals between injections. Injections of 5-FU can be used in conjunction with intra-operative anti-metabolites if the healing response is still marked and the pressure is rising. Technique is also important. Injections are now given closer to the bleb (avoiding intraocular entry as the pH of 5-FU is 9), via a long subconjunctival needle track with the use of small bore needles to improve efficacy and reduce corneal side effects.

Despite high dose anti-metabolites and modifications in their application patients still fail surgery. Development of alternative more physiological anti-scarring agents is needed.

1.4.6 Agents affecting Growth factors

The scarring process is under the control of a number of growth factor proteins as discussed in section 1.2 and illustrated in Figure 10. Consequently, these growth factors and the receptors through which their effects are mediated, present themselves as potential targets for therapeutic intervention. A number of approaches can be employed to antagonise growth factors activity (Figure 23). These include the use of antibodies directed against the growth factor protein or growth factor receptor protein, antisense oligonucleotides and ribozomes. As previous mentioned of all the growth factors involved in the wound healing cascade, TGF β has been shown to be one of the most potent stimulators of scarring in the eye and is involved in the pathogenesis of cataract, proliferative vitreoretinopathy and conjunctival scarring (Connor et al., 1989; Hales et al., 1995). TGF β2, the most predominant of the three mammalian isoforms in the eye, is the most potent growth factor in the aqueous at stimulating conjunctival fibroblast function and elevated levels of this isoform are found in the aqueous of glaucomatous eyes compared to normals (Khaw et al., 1994b; Pasquale et al., 1993; Tripathi et al., 1994b). Shah et al convincingly demonstrated that neutralising antibody to TGF β1 and 2 can reduce cutaneous scarring in adult rats. A reduction was seen in the monocyte and macrophage profile, neovascularisation, fibronectin, collagen III and collagen I deposition in the early stages of wound healing compared to control wounds. To be effective, the neutralising antibody to TGF β needed to be administered at the time of wounding or

Figure 23 Strategies to modify growth factor activity

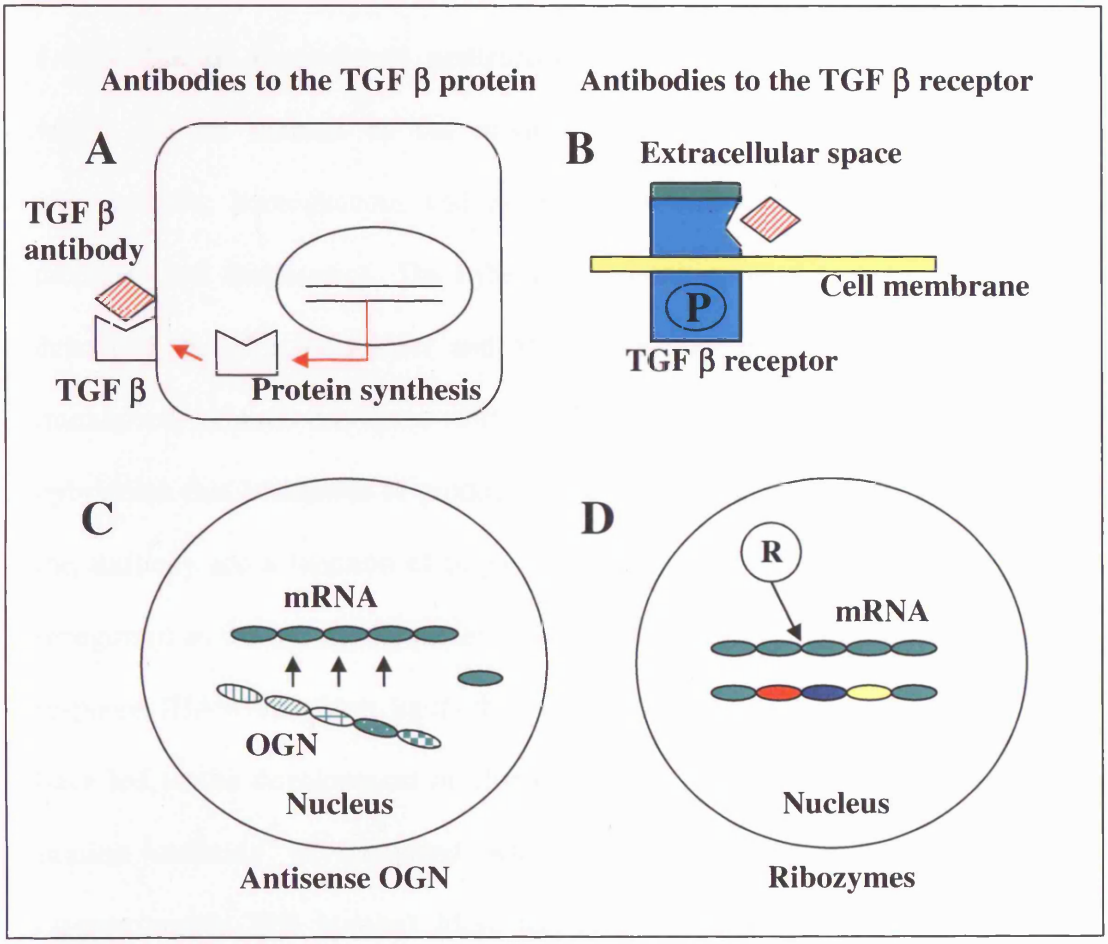

TGF β activity can be inhibited in several ways. Fully human monoclonal antibodies can be directed against TGF β or the TGF β receptor molecule to decrease activity. Alternatively inhibition at the level of gene expression may be possible using antisense oligonucleotides or ribozymes, which act at on the messenger RNA and prevent protein synthesis of TGF β itself or the receptor.

soon thereafter. The antiscarring effects of this neutralising antibody to TGF β were dose dependent (Shah et al., 1992; Shah et al., 1994; Shah et al., 1995).

These findings suggest that neutralising the effects of TGF β isoforms may reduce conjunctival scarring following glaucoma filtration surgery.

1.4.6.1 Human monoclonal neutralising antibodies Monoclonal antibodies (mAB), which can be defined as the product of a single clone of B lymphocytes, are monospecific, homogeneous and are therefore effective tools in the development of therapies and diagnostics. The hybridoma technique used to generate mAB was first described in 1975 by Kohler and Milsten (Kohler et al., 1975). Splenic cells from immunised animals are fused with cells of a cultured myeloma cell line to form a hybridoma that is capable of producing a single antibody. The specificity and affinity of the antibody are a function of original mouse monoclonal. However, murine mAbs are recognised as foreign by the patient and can induce human anti-mouse antibody immune response (HAMA), which limits their therapeutic potential. Attempts to reduce HAMA have led to the development of chimeric antibodies in which the variable region of a murine antibody is combined with the constant region of a human antibody (approximately 70% human). More recently the construction of humanised engineered antibodies, achieved by grafting the murine antigen binding or hypervariable region on to a human antibody, can result in a protein sequence that is 95% human (Figure 24)

The production of fully human monoclonal antibodies has been a major advance in this area. Such antibodies can be engineered by the use of transgenic mice or by phage display technology. Transgenic mice are genetically modified so they express human antibody genes. Endogenous mouse IgG genes are inactivated in embryonic stem cells to block B

Figure 24 Engineering of therapeutic monoclonal antibodies

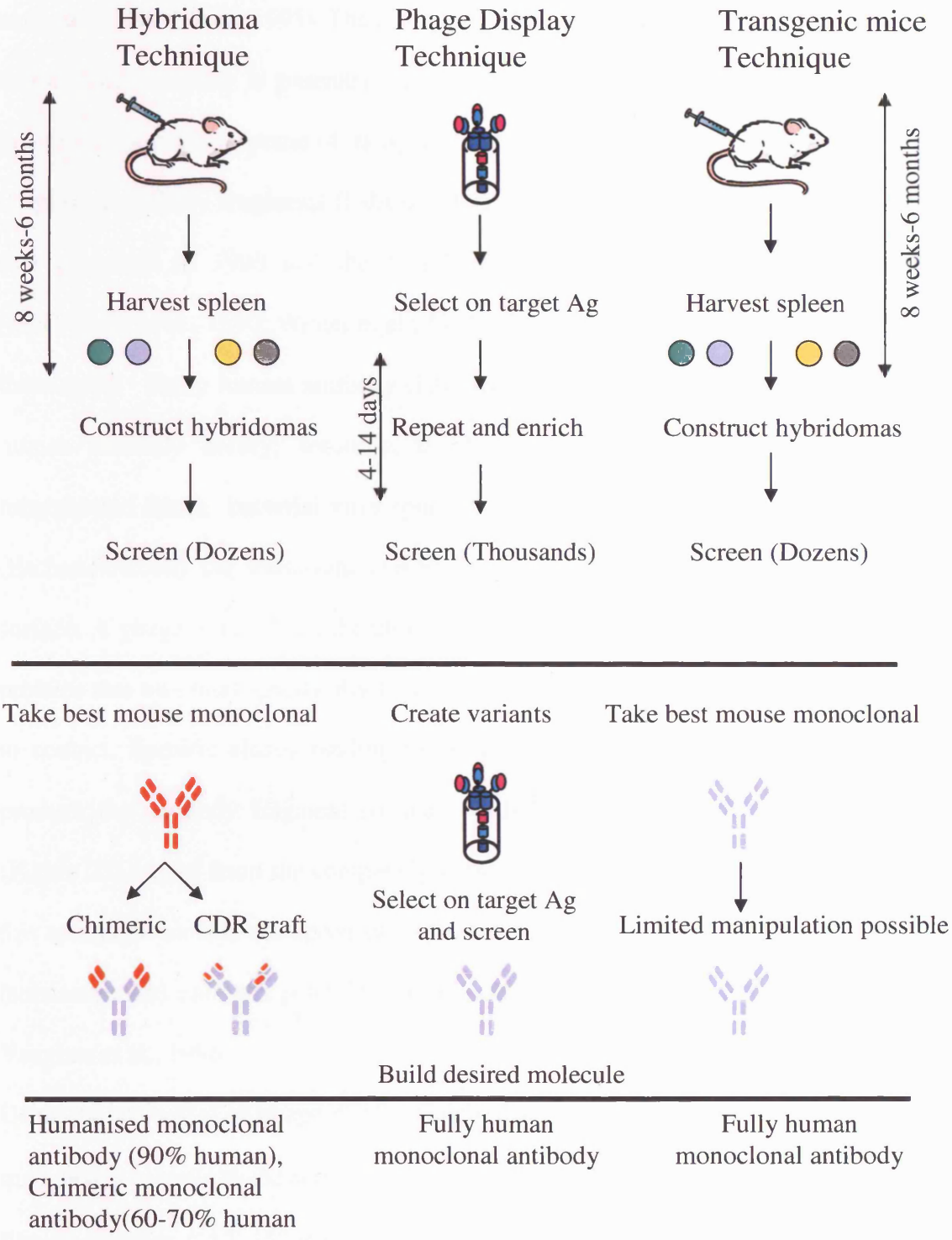

Monoclonal antibodies have been traditionally engineered by the hybridoma technique. Phage display and transgenic mice technologies offer a way of generating fully human highly specific designer antibodies.

cell production followed by subsequent introduction of unrearranged human IgG gene segments. Following immunisation with an antigen these animals produce fully human antibodies (Jakobovits, 1995). The technique, which is still developing, has the advantage that a whole antibody is generated but the specificity and affinity of the mAb remain a function of immune response of transgenic mouse.

Display of antibody fragments (Fabs or scFvs) on the surface of a filamentous phage was first described in 1990 and the first human antibodies were generated soon after (McCafferty et al., 1990; Winter et al., 1994). The technique of phage display consists of three steps: firstly human antibody light and heavy chains are identified from a large human antibody library; secondly, the human genes coding for these chains are incorporated into a bacterial virus (phage); finally when the phage infects a bacterium (Escherichia.coli) the bacterium makes the antibody protein which it displays on its surface. A phage antibody is, therefore, a bacterial virus engineered to display antibody proteins that will bind specifically to a target molecule or antigen with which it comes in to contact. Specific clones binding to the antigen can then be amplified and used to produce the antibody fragment so that a fully human recombinant mAb is produced (Figure 25). Apart from the completely human nature of the antibody the advantages of this technique include the speed of isolation, the ability to generate high affinity mAbs (subnanomolar) and the potential selection of complex antigens (Griffiths et al., 1994; Vaughan et al., 1996).

Using the technique of phage display Cambridge Antibody Technology have designed a mAb that is specific to the active form of TGF β2 (CAT-152) suitable for the treatment of fibrotic diseases. CAT-152 is IgG4 antibody with a high affinity for TGF β2 (dissociation constant of 0.89nM).

Figure 25 **Structure and generation of antibodies using the technique of phage display**

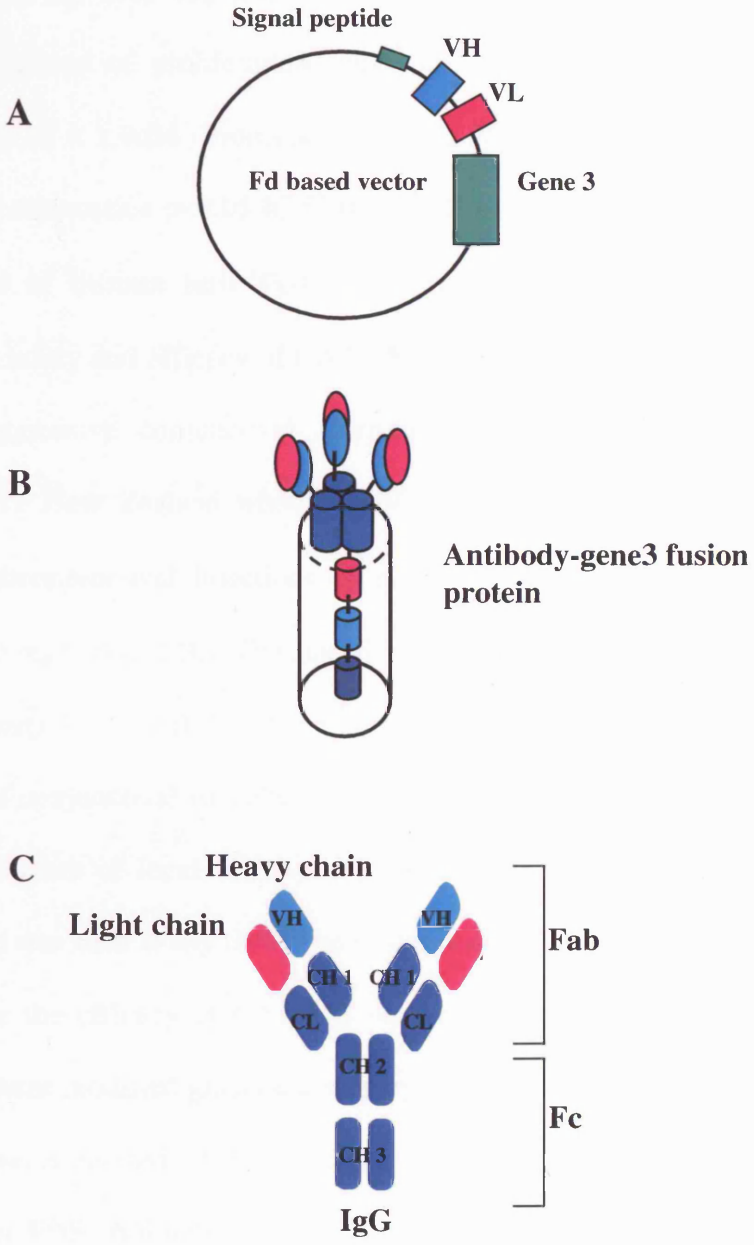

Human antibody light and heavy chains are identified from a large human antibody library. The DNA encoding these genes are then incorporated into a bacterial virus (A). When the phage infects a bacterium (E.coli), the bacterium makes the antibody protein which it displays on its surface (B). Specific clones binding to an target antigen can then be amplified and the whole antibody produced by recombinant methods (C).

It has 9% cross reactivity with TGF β 3 and no displays not detectable binding with TGF β 1 (Thompson et al., 1999).

1.4.6.2 Effect of human anti TGF β 2 antibody (CAT-152) on Tenon's capsule fibroblast activity CAT-152 has been shown to significantly inhibit the conjunctival fibroblast functions of proliferation, migration and collagen gel contraction at IC50 concentrations of < 1.0nM (Proliferation $p<0.05$ IC50 0.885nM, Migration $p<0.05$ IC50 0.627nM and contraction $p<0.05$ IC 50 0.12 0.818nM) (Cordeiro et al., 1999a).

1.4.6.3 Effect of human anti TGF β2 antibody CAT-152 on glaucoma filtration surgery The safety and efficacy of CAT-152 in vivo was initially investigated in a rabbit model of aggressive conjunctival scarring after glaucoma surgery. Tolerance was assessed in 11 New Zealand white (NZW) rabbits which were randomly assigned to receive 7 subconjunctival injections of either 100 μl of CAT-152 (1.0 mg/ml), null antibody (1.0 mg/ml) or PBS. The injections were administered on days 0 (2 injections 1.5 hours apart) 1,2,3, and 7 and the animals were observed for 30 days .The clinical parameters of conjunctival vascularity, anterior chamber activity and intraocular pressure acted as indicators of local toxicity. Injections were well tolerated and no intraocular inflammation was seen at any time. The same subconjunctival injection regimen was used to investigate the efficacy of CAT-152 on the outcome of filtration surgery. 72 NZW rabbit underwent modified glaucoma surgery and were randomly assigned to one of four treatments that consisted of 1.0mg/ml CAT-152, 0.1mg/ml CAT-152, Null antibody (1.0mg/ml) or PBS. Animals were observed until sacrifice on days 3,8,14 and 30. The ocular tissue was processed for histology. CAT-152 significantly prolonged bleb survival, the primary outcome variable, compared to control ($p= 0.0291$), reduced subconjunctival scarring ($p= 0.001$) and improved bleb morphology (Bleb Height $p=0.029$ Area $p=0.059$).

No significant difference was seen between the two doses of CAT-152 (Figure26) (Cordeiro et al., 1999a).

The first clinical trial of CAT-152 was designed to asses the safety and tolerance of CAT-152 in patients undergoing primary trabeculectomy (Randomised prospective placebo controlled phase I/IIa trial). 24 patients were treated with CAT-152 (100mg, n=16) or placebo (n=8). Four subconjunctival injections were given immediately before and after surgery, at one day and one week postoperatively. Assessment consisted of full ophthalmic examination with recordings of LogMAR visual acuities performed at baseline and at set intervals after surgery. No statistical differences in the incidence of complications were seen between the groups after 12 months of follow up and no serious adverse events related to the study drug occurred. There was a trend towards lower IOP and less intervention in those treated with CAT-152. CAT-152 antibody blebs were diffuse, non avascular and non cystic (Siriwardena et al., 2002).

Follow-up was extended to investigate whether these observations were maintained over a longer period of time. Twenty-one patients completed 3 year follow-up with assessments being conducted at approximately six month intervals. A total of 11 patients were defined to be treatment failures by virtue of receiving injection(s) of 5-FU or re-starting topical IOP lowering medications. Six of eight patients in the placebo group (75%) were treatment failures as compared to 5/16 (31.3%) of patients who had been treated with CAT-152 (p=0.082). Survival analysis of the time to treatment failure showed CAT-152 to be superior to placebo at the 10% level (p=0.072). Mean IOP was consistently lower in the CAT-152 treated patients, with a mean IOP at 36 months of 13.2 mmHg. Bleb appearance in both treatment groups was most frequently reported as diffuse, with normal vascularity. Adverse events were infrequent with no longer term adverse consequences of CAT-152 being observed.

Figure 26 Effect of peri-operative CAT-152 on GFS

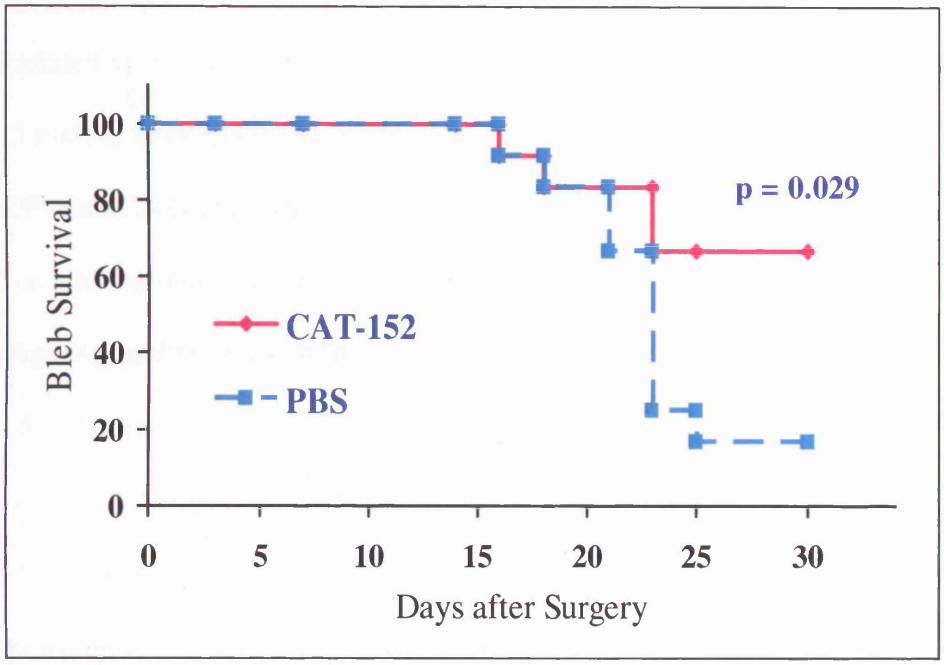

A course of 6 subconjunctival injections of CAT-152 or placebo were administered on day 0,1,2,3,4 up to seven days after surgery. This kaplan meier survival curve shows that CAT-152 significantly improved bleb survival compared to control. In addition, CAT-152 reduced subconjunctival scarring and was safe and well tolerated (Cordeiro et al., 1999a).

The positive results observed at one year were consistently maintained throughout the 3 year post-surgery follow-up (Khaw et al., 2003).

In the second clinical trial the safety and tolerability of CAT-152 was investigated after phacotrabeculectomy. 56 patients were recruited and randomised to receive CAT-152 or placebo. No serious adverse effects occurred. The treatment regimen was the same as for the trabeculectomy study with 4 subconjunctival injections being given in total. CAT-152 was associated with less adverse event and less side effects than placebo. The mean IOP was 14.5 mmHg after CAT-152 compared to 16.6 in the placebo. More patients achieved target IOP after CAT-152 (Broadway et al., 2002).

Two large international confirmatory studies are in progress.

1.4.6.2 Agents against growth factor receptors The antiparasitic drug, suramin (a heparin analogue) specifically inhibits growth factor activity (PDGF, β FGF, TGF β, EGF, IGF-I, IGF-II) (Campochiaro et al., 1994; Chamberlain et al., 1995; Zumkeller et al., 1995). Suramin competitively binds with the growth factor receptors and thereby displaces the growth factor molecule from the target cells. Meitz et al have shown that suramin delays the conjunctival wound healing response in a mouse model. Changes were observed in the expression and time course of growth factors in the forming scar tissue with TGF β1 and TGF β 2 levels persisting longer than in the controls. In addition, Suramin specifically decreased the production of collagen types I and III by ocular fibroblasts in tissue cultures at concentrations that did not affect cell viability (Mietz et al., 1998b).

Furthermore, this group have demonstrated that combined intra-operative and early post-operative application of Suramin significantly delays wound closure after trabeculectomy in the rabbit. At concentrations of 200 mg/ml and 333 mg/ml Suramin increased the mean failure time to 9 and 14 days, respectively, with a p value of 0.001, representing an

evident delay in failure over untreated controls (Mean failure 4.7 days) and MMC treated animals (Mean failure 8.2 days). Histopathological evaluation showed lower degrees of cellularity, fibrosis, collagen III deposition, and CD3 density in the suramin- and mitomycin C-treated eyes compared to control eyes at all time points ($p < 0.05$) (Mietz et al., 1998a).

In this first clinical study using suramin to inhibit fibrosis following trabeculectomy for complicated cases of glaucoma, the use of suramin was associated with fewer cases of severe hypotony, choroidal detachment, and severe visual loss as compared to mitomycin, while the success rates seemed to be similar (Akman et al., 2003). This method of growth factor inhibition may represent a new approach to the surgical treatment of glaucoma, although its application may be limited by the non specific effect on all local growth factor receptors rather that targeting a specific molecule.

1.4.6.3 Modification of gene expression Other methods of neutralizing growth factors include blocking gene expression of the growth factor or the receptor.

Antisense oligonucleotides (OGN) are synthetic molecules that bind to specific intracellular messenger RNA strands. They consist of short DNA/RNA sequences around 20 nucleotides in length, which are designed to be complementary to the mRNA sequence that code for the production of specific proteins. By binding to the mRNA molecules antisense OGN block the synthesis of the target protein. The possible mechanisms by which this occurs include the modulation of protein translation by disruption of ribozome assembly, RNase mediated cleavage of targeted mRNA and pre-translational modification of splicing (Dean et al., 1996) .

Antisense OGN represent a promising therapeutic strategy that has been successfully applied to oncology, inflammatory and viral infective disease. The potential advantage of oligonucleotides as inhibitors of protein expression is the specificity that may be

achieved, as the approach allows the highly selective targeting of particular nuclei acid sequences (Tamm et al., 2001). Antisense technology was first proposed in 1978, but adjustments in their structures and increased understanding of the technology has lead to improvements in pharmacokinetics and pharmacokinetics (Stephenson et al., 1978). Certain criteria need to be met for an antisense OGN to demonstrate optimum biological activity and the search for molecules to reach these requirements had lead to modifications in the nucleobase, sugar and the phosphate backbone of conventional DNA (Altmann et al., 1996, Dean et al., 1997). Firstly, the antisense molecule must be sufficiently resistant to endogenous cellular nucleases to avoid rapid cleavage and breakdown. Incorporation of a sulphur atom for an equatorial oxygen in the phosphate backbone (creating a phosphorothioate backbone) acts to increase resistance to these nucleases and thereby improves OGN stability. Secondly, antisense OGN must have sufficient affinity for the target mRNA to bind with a high degree of specificity and fidelity. Modification of the bases, for example, use of 5-methyl C for C in the synthesised oligonucletide, can increase specificity without interfering with the method of action and is often employed in antisense design. Finally, the antisense molecule must be taken up effectively into the cell and historically this has proved problematic. Combined administration with cationic liposomes such as lipofectin can enhance OGN uptake (Marcusson et al., 1998).

ISIS pharmaceuticals (Carlsbad, CA, USA) have designed a number of phosphorothioate OGN that target the mouse TGF β1 sequence and rabbit TGF β1, β2 and TGF β receptor (typeII TBR II) sequences (Table 3)

The effect of ISIS TGF β 1 antisense OGN has been investigated in a mouse model of conjunctival scarring. Following subconjunctival injection the antisense OGN was localised to the treatment area for 7 days, significantly inhibited the scarring response,

Table 3 Design and selection of TGF β antisense oligonucleotides

RNA target	ISIS number	Sequence
Rabbit TGF β1	105204	GTCACCATTAGCACGGGGG
Rabbit TGF β2	123285	CCGTGACCAGATGCAGGAT
Rabbit TBR II	123787	GGCCAGGGAGCTGCCCAGCT
Universal control	29848	Mix of A,G,C,T

Sequences of selected OGN targeting rabbit TGF β1, β2 and TBR II

reduced the numbers of inflammatory cells in the wound site, and appeared to decrease the expression of conjunctival TGF β1 and β2 (Cordeiro et al., 2000a; Cordeiro et al., 2003).

Ribozymes are RNA molecules that have the ability to enzymatically cleave specific bonds within another RNA molecule (Bartel et al., 1993; Wilson et al., 1995). Transcription and translation of a selected protein can be inhibited if the RNA sequence encoding it is cleaved by ribozyme activity. Ribozymes can be designed to target any message, for example RNA encoding growth factors can provide a targeted approach to the inhibition of wound healing. In addition, they display a number of advantages over antisense OGN in their potential as therapeutic agents. Firstly, they form a more stable intracellular enzyme/substrate within cell that is relatively resistant to intracellular nucleases. Secondly ribozyme activity is not as concentration or time dependent, multiple copies of specific mRNA strands can be cleaved rapidly at a catalytic rate, and each individual molecule is able to re attach and destroy other messages of the same sequence many times.

The use of ribozymes as RNA enzyme directed gene therapies in the management of ocular disease is in its infancy but early studies have shown potential. Ribozymes have been designed that selectively decreased the expression of the insulin like growth factor (IGF-1R) which is associated with abnormal retinal neovascularization. These ribozymes were tested in angiogenesis models and were effective at reducing the expression and function of the IGF-1R in vitro and in vivo. They not only provide an effective method for studying the process of angiogenesis but may also ultimately be effective as gene therapy tools for the reduction of pathologic retinal angiogenesis (Shaw et al., 2003).

Blalock et al investigated the effect of hammerhead ribozymes targeting connective tissue growth factor (CTGF) mRNA on TGF β mediated cell proliferation in cultured human

fibroblasts. TGF β induced cell proliferation was reduced 90% in fibroblasts stably transfected with the ribozyme, CHR 859, compared to control cell groups. This study supports the concept that CTGF mediates TGF β induced cell proliferation, and implies that regulating CTGF expression with ribozymes may be effective in reducing ocular scarring (Blalock et al., 2004).

Ribozymes represent an exciting new mode of specific, focal, titratable treatment.

1.4.7 MMP inhibition: Modulation of cellular migration, wound contraction, matrix synthesis and remodelling

As mentioned in section 1.2.4 matrix metalloproteinases (MMPs) are a group of ubiquitous proteolytic enzymes which degrade the extracellular matrix and play a critical role in the evolution of scar tissue. Dysregulated MMP activity has been implicated in diseases associated with uncontrolled proteolysis of connective tissue matrices such as arthritis and tissue ulceration (Vaalamo et al., 1996). In the eye MMP's are thought to be involved in conjunctival (Di Girolamo et al., 2000), corneal (Daniels et al., 2003b; Mohan et al., 2002; Pflugfelder et al., 2005), lens epithelial cell (Wong et al., 2004) and retinal scarring (Noda et al., 2003; Sheridan et al., 2001; Sivak et al., 2002).

Matrix metalloproteinase gene expression is upregulated in failed filtering blebs in rat (Esson et al., 2004) and rabbit models of glaucoma surgery (Liu et al., 2004) and elevated levels of MMP's are present in the aqueous humour in individuals with glaucoma (Ho et al., 2005).

The use of synthetic MMP inhibitors has been shown to reduce tissue destruction. Recent work in our laboratory has shown that the broad spectrum MMP inhibitor, Ilomastat, can inhibit ocular fibrobroblast mediated collagen contraction, migration and collagen production at concentrations not associated with cellular toxicity (Daniels et al., 2003a).

In vivo Ilomastat can prolong bleb survival, reduce conjunctival scarring and was safe and well tolerated (Wong et al., 2003). More recently we have shown that Ilomastat can maintain long term bleb survival and appears comparable to MMC but without the side effect profile (Wong et al., 2005). Conversely, conjunctival gene transfer of MMP 3 prior to glaucoma surgery appears to prolong bleb survival (Mamiya et al., 2004).

1.4.8 Apoptosis and termination of healing

Wound healing is terminated by apoptosis, although little is know about the physiological signals initiating fibroblast apoptosis. MMC and high dose 5-FU can induce conjunctival fibroblast apoptosis (Crowston et al., 1998). Conversely, Human Tenon's fibroblasts produce interferon beta which prevents T cell apoptosis. These fibroblast/T cell interactions contribute to the persistence of fibroblasts at the wound site and the failure of the immune system to deactivate, which can lead to chronic inflammation and the failure of glaucoma surgery (Chang et al., 2001). Proapoptotic peptides induce death in targeted cells by means of a homing motif and these peptides exhibit anti-proliferative activity in mice. The induction and regulation of apoptotic mechanism offer another potential way to regulate wound healing.

1.5 JUSTIFICATION AND AIMS

The conjunctival wound healing response remains the major barrier to achieving long term intraocular pressure control after glaucoma filtration surgery. Current anti-scarring agents improve the outcome of surgery but act by causing widespread cell death and can be associated with potentially blinding complications. In addition some individuals still

fail surgery. A more physiological and targeted approach to wound healing control and scarring prevention is required.

Of all the growth factors, TGF β has been shown to play a pivotal role in wound healing throughout the body, and has been implicated as a potent stimulant of the scarring process in the eye, where TGF-β2 the second human isoform, is most commonly implicated.

Modulation of TGF β has been highlighted as a possible mechanism by which ocular scarring may be reduced. Initial preclinical studies have identified that neutralisation of TGF β2 reduces conjunctival fibroblast function in vitro and reduces subconjunctival fibrosis in a model of aggressive scarring in vivo.

The main aim of this study was to continue to establish the role of TGF β modulation as a potential anti-scarring strategy in glaucoma surgery. In particular to:

1. Delineate the expression of the TGF β isoforms in the rabbit eye and identify the changes associated with glaucoma surgery and TGF β modulation.

2. Investigate the effect of the human anti-TGF β2 monoclonal antibody (CAT-152) on the outcome of glaucoma surgery using in vitro and in vivo models of conjunctival scarring and move CAT-152 in to the clinical arena.

3. Investigate the role of antisense oligonucleotides directed against TGF β on the conjunctival scarring in vivo.

4. Finally to compare these novel agents with the current gold standard anti-scarring agents to benchmark their future clinical application and benefit.

CHAPTER 2 MATERIALS AND METHODS

2.1 CELL CULTURE TECHNIQUES

The in vitro experiments in this project were based on the cellular activity of human Tenon's fibroblasts, which are the key cell type involved in the subconjunctival scarring response.

2.1.1 Human Tenon's capsule fibroblast explant.

Human Tenon's fibroblasts were propagated from multiple 0.5 cm^3 explants of human tissue (Khaw et al., 1992d). Cadaver eyes were obtained from Moorfields Hospital Eye Bank 1 to 5 days after death. Informed consent and institutional human experimental committee approval were granted and the Tenets of the Declaration of Helsinki were adhered to. Tenon's capsular tissue was identified and carefully dissected from the globe. Up to four 0.5cm^3 explants were placed in a 25cm^3 flask (BD Biosciences, Oxford, UK) and the tissue was left to adhere to the plastic flask for two hours. 5mls of standard culture medium consisting of Dulbecco's Modified Eagle's Medium (DMEM) containing 10% Fetal Calf Serum, 2mM L-glutamine, 100 IU/ml Penicillin and 100µg/ml Streptomycin was carefully added to each flask (All Gibco, Invitrogen Corporation, Scotland, UK). Primary explants were incubated at 37^{0}C in humidified 5% Carbon Dioxide (CO_2) in air and fed once a week with new culture medium. All of the procedures were performed in a laminar flow hood, using aseptic technique, and all the solutions were warmed to 37^{0}C in a water bath prior to use.

2.1.2 Culture and maintenance of fibroblasts.

Human Tenon's fibroblasts were usually observed within two weeks of primary culture and viewed under a phase contrast inverted microscope (Olympus CK4, Japan) at 10x magnification. Epithelial cell growth was occasionally observed in addition, however these cells were unable to survive in the conditions and detached from the flask. The cells reached confluence on average after 4 weeks of culture. At this point the monolayers were passaged in a 1:3 ratio. The culture medium was removed from each flask and the monolayer was washed twice with 5mls of Phosphate Buffered Saline solution (PBS, Gibco: Invitrogen Corporation, Scotland, UK). The cells were detached using a solution of Trypsin (1 in 10 dilution with PBS, Gibco: Invitrogen Corporation, Scotland, UK) of sufficient volume to cover the base of the flask, which was then incubated at 37^0C for approximately 2 minutes. The cells were then observed by phase contrast microscopy and once they had become mobile and adopted a round phenotype, trypsinisation was stopped by adding an equal volume of DMEM culture medium. Explant tissue was removed and the cell suspension was transferred to a Universal container (Sterilin, Staffs, UK) and centrifuged at 1600 rpm for 5 minutes. The resultant cell pellet was resuspended in 12mls culture medium and this volume was placed in a $75cm^3$ flask (1:3 expansion), which was labelled with the cell type, passage number, date of passage, and donor number (cell line). Flasks were kept in a humidified 5% CO_2 incubator at 37^0C and the cells were fed with culture media every 3 days.

Fibroblasts between passage 2 and 6 were used for the following experiments. Cells between these time points have been shown to behave in a similar way with respect to cell proliferation and growth curve characteristics, despite originating from different explant tissue (Khaw, 1994). Experiments were performed on primary cells from at least two

donors to ensure that the trends were reproducible. When monolayers reached over 80% confluence they were passaged using the method described in a 1: 3 ratio.

2.1.3 Storage and recovery of liquid nitrogen frozen cells

Low passage fibroblasts were stored in liquid nitrogen for future use. Confluent monolayers were trypsinised using the method previously described. A sterile solution of 10% Dimethyl Sulphoxide (DMSO, Sigma, Dorset, UK) in standard culture media was prepared and placed at 4^0C for 15 minutes. The resultant cell pellet was resuspended in this solution which was added dropwise with continuous mixing. 1ml of cell suspension was placed in each cryovial at a cell density of 1 x 10^6 cells per ml. The cells were cooled to -70 ^{0}C over a period of 24 hours in propan-2-ol before being transferred into liquid nitrogen (- 160 ^{0}C liquid phase).

The cells were retrieved using the following method. The cells were rapid thawed by immersing the bottom of the cryovial in hot running water (60 ^{0}C). The cell suspension was transferred into a universal container, 5-10ml of culture media was added dropwise with continual mixing and the suspension was centrifuged at 1500rpm for 5 minutes to obtain a cell pellet. The pellet was resuspended in 10 mls of culture media and centrifuged again at 1500rpm for 5 minutes. The process was repeated until the cells had been pelleted 3 times. This was to ensure complete removal of DMSO from the cell suspension. The final cell suspension was seeded into appropriately sized tissue culture flasks and the cells were maintained in 5% humidified CO_2 in air at 37^0C and fed every 3 days with renewed culture media.

2.1.4 Haemocytometry

The fibroblasts in each flask were counted prior to each of the following experiments in order to seed a specific cell density. A Neubauer haematocytomer (Assislent, Germany) was used to obtain a qualitative and quantitative cell count. Confluent tissue culture flask monolayers were trypsinised to obtain a cell pellet. This was resuspended thoroughly in 1ml of culture media and 50µl of this was removed and mixed to 50µl of trypan blue solution (Sigma, Dorset, UK). This solution was transferred to the haematocytometry chamber slide via capillary action. The number of live cells in each chamber A and B (Chamber = grid of 5x5 squares) was counted using a light microscope and an average from both chambers was calculated. Each chamber represents the number of cells in 0.1µl. To obtain the number of cells per ml the average cell count is multiplied by 10000. After allowance for the dilution factor of the original cell suspension, a value for the cell count in the original sample can be made. This method is accurate for cell counts of between 30-300 cells per chamber. Fibroblasts from the original cell suspension were therefore diluted according prior to the mixing with trypan blue to account for this.

2.2 FIBROBLAST MONOLAYERS

2.2.1 Monolayer assays

Monolayer experiments were performed on either 6 well, 24 well or 96 well plates (BD biosciences, Oxford, UK). Cells were seeded at a specific density calculated from pilot studies. Experiments were performed with a minimum of three wells per concentration of treatment (triplicates) and were repeated at least 4 times on primary cells, from at least two different donors.

2.2.2 Stimulation of cells with TGF β

The recombinant TGF β2 used in the following experiments was a generous gift from Cambridge Antibody Technology (Batch number: TG 815). A stock solution of 1.7mg/ml in 12 mM Hydrochloric Acid (HCL) 20% ethanol, pH 2.5 was provided. Single use 20 µl aliquots of a 20 µg /ml solution made up in 4 mM HCl / 1 mg /ml Bovine Serum Albumin (BSA, Sigma, Dorset, UK) were prepared and stored -70 ^{0}C prior to use.

A range of TGF β2 concentrations were selected to investigate the effect of this growth factor on fibroblast functions; 0, 0.01pM, 0.1pM, 1pM, 3pM, 10pM, 30pM 100pM, 300pM and 1000pM which corresponds to 0, 10^{-14}, 10^{-13} ,10^{-12}, $3x10^{-12}$, 10^{-11}, $3x10^{-11}$,10^{-10}, $3x10^{-10}$ and 10^{-9} M and 0.00025, 0.0025, 0.025, 0.075, 0.25, 0.75, 2.5 , 7.5 and 25 ng/ml. These concentrations were selected not only because they covered a large scale to encompass possible biphasic concentration effects of TGF-β, but also on evidence from previous experiments (Cordeiro et al., 2000b). All dilutions were made using serum free cell culture medium with 1% BSA.

2.2.3 Inhibition of TGF β activity with Anti-TGFβ2 antibody (CAT-152)

This recombinant antibody was supplied by Cambridge Antibody Technology (CAT, Cambridge, UK). It is an engineered human monoclonal IgG4 antibody, which is formulated in PBS at pH 7.2, and was stored at a stock concentration of 1 mg/ml at -70 ^{0}C. Working dilutions of the antibody were made in serum free culture medium with 1% BSA prior to use. A range of concentrations were selected to investigate the effects of the antibody on fibroblast function; 0.01nM, 0.1nM, 1nM, 3nm, 10nM, 30nm, 100nM, 1uM which corresponds to 10^{-11} M, 10^{-10} M, 10^{-9}M, $3x10^{-9}$ M, 10^{-8} M, $3x10^{-8}$ M, 10^{-7} M, 10^{-6} M or 0.0015 µg/ml, 0.0015 µg/ml, 0.15 µg/ml, 0.45 µg/ml, 1.5 µg/ml, 4.5 µg/ml, 15 µg/ml

and 150 μg/ml. The control solution CAT-152 was a null 1gG4 antibody, CAT-001 (Cambridge Antibody Technology) used at the same concentrations as the test antibody.

2.2.4 Imaging of Fibroblast Monolayers

Phase contrast microscopy was used to observe the morphology of the cells at set time points throughout the experiments. Images were captured by the use of digital camera with a microscope attachment and stored as JPEG files (Nikon Coolpix 950, Tokyo, Japan)

2.3 EXTRACELLULAR MATRIX PRODUCTION BY HUMAN TENON'S FIBROBLASTS

2.3.1 Acid soluble collagen production (Matrix associated)

2.3.1.1 Effect of TGF β2 on collagen production by human Tenon's fibroblasts This was determined by means of the Sircol Assay (Biocolor, UK) which is a quantitative dye binding method designed for *in vitro* analysis of collagen production (Blease et al., 2002; Huang et al., 2002) (Figure 27) . Cells were seeded into 6 well plates at a cell density of 7 x 10^5 cells per well and allowed to settle overnight. After 12 hours exposure to serum free conditions (DMEM with 1% BSA, 2mM L-glutamine, 100 IU/ml Penicillin and 100μg/ml Streptomycin) the cells were washed and stimulated with increasing concentrations of TGF β2 (0 pM, 0.01pM, 0.1pM, 1pM,10pM, 30pM, 100pM, 300pM and 1000pM). After 48 hours the conditioned media was removed and stored. The cell layer and extracellular matrix was treated with 0.5% acetic acid to release the acid soluble collagen. A sircol dye was mixed to the cell lysate, spun at 13000 RPM for 15 minutes. The pellet was

Figure 27 The molecular structure of sircol dye

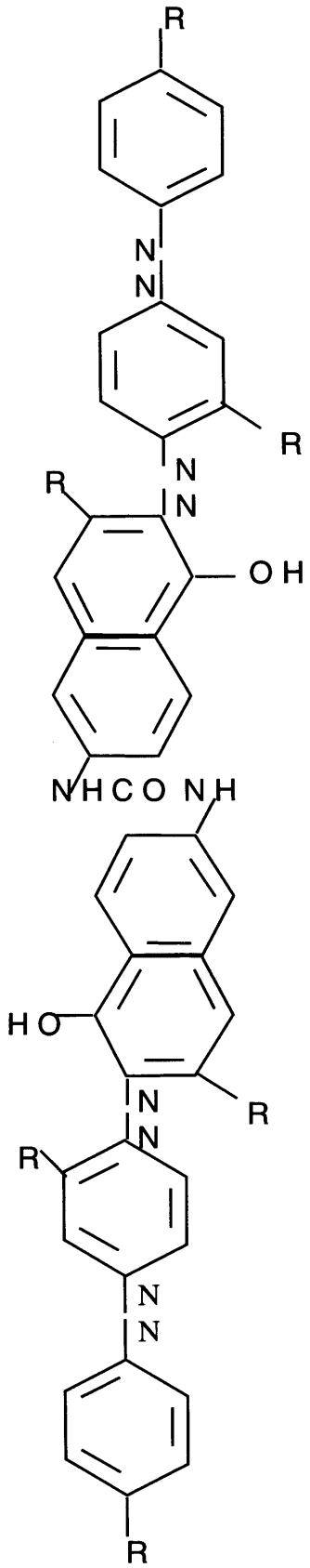

Mode of Action of the Sircol dye with soluble collagens:

The Sircol dye reagent contains sirius red. The colour commission name is Direct Red 80

Mechanism by which the dye reacts with collagen:

Sirius red is an anionic dye with sulphonic acid side chain groups. These groups react with the side chain groups of the basic amino acids present in collagen

The specific affinity of the dye for the collagen, under the assay conditions is due to the elongated dye molecules becoming aligned in parallel with the long rigid structure of native collagens that have intact triple helix organisation.

resuspended in 1ml of 0.5M NaOH and the absorbance was read @ 540 nm. Collagen standards were provided to obtain a standard reference curve.

2.3.1.2 Effect of CAT-152 on TGF β2 mediated collagen production by human Tenon's fibroblasts After the initial experiments had been completed a dose response relationship was generated for TGF-β2 and collagen production. The sircol assay was repeated using a single concentration of TGF β2 (EC 90: 100pM) to stimulate the cells in the presence of increasing concentrations of anti-TGF β2 antibody 0.01nM, 0.1nM, 1nM, 3nm, 10nM, 30nm, 100nM, 1uM and Null antibody.

2.3.2 Type 1 collagen production

Metra CICP (Collagen I C-terminal propeptide) sandwich enzyme linked immuno assay was performed to determine the amount of collagen in the culture supernantant from fibroblast monolayers (Metra CICP EIA kit; Quidel, San Diego, USA). This assay measures the release of collagen propeptides, cleaved from C-terminal of the type 1 collagen molecule prior to the incorporation of collagen into the growing collagen fibril. The release of these peptides thereby provides a stoichiometric representation of the production of newly formed collagen.

2.3.2.1 Effect of TGF β2 on type 1 collagen production by human Tenon's fibroblasts Conditioned media was collected from the cells cultured for the sircol assay after 48 hours of stimulation with increasing concentrations of TGF β2 (2.3.1.1). Briefly, the media was diluted 1 in 64 with assay buffer and then 100µl was added to the wells of a 96 well elisa plate precoated with a monoclonal anti-CICP antibody and incubated at room temperature (RT, 18-25 ^{0}C) for 2 hours. In the sircol assay each concentration of TGF β2 was tested in triplicate providing 3 samples of conditioned

media for the CICP assay. Duplicate aliquots of each of these 3 samples were added to the elisa plate (6 samples per TGF β2 concentration analysed). Collagen standards were provided to generate the standard curve. The strips were manually everted and each well was washed 3 times with wash buffer. 100μl Rabbit anti-CICP antiserum was then added to each well and incubated for 45 minutes at RT after which the cells were washed again. A goat anti-rabbit alkaline phosphatase conjugate was incubated for 45 minutes, followed by a pNitrophenyl Phosphate substrate to quantify the CICP in the media for 30 minutes. The reaction was stopped with 50μl 1N NaOH per well and the optical density was read at a wavelength of 405nm. The assay is summarised in Figure 28.

2.3.2.2 Effect of CAT-152 on TGF β2 mediated type 1 collagen production by human Tenon's fibroblasts Conditioned media was generated in two ways. In the first set of experiments it was collected from the cells in the sircol assay after 48 hours of stimulation with a single concentration of TGF β2 (EC 90: 100pM) in the presence of increasing concentrations of anti-TGF β2 antibody (0.01nM, 0.1nM, 1nM, 3nM, 10nM, 30nM, 100nM, 1uM and Null antibody). In the second set of experiments cells were seeded into 24 well plates at a density of 1 x 10^5 cells per well and allowed to settle overnight. After 12 hours exposure to serum free conditions the cells were washed and stimulated with a single concentration of TGF β2 (100pM) in the presence of increasing concentrations of anti-TGF β2 antibody (0.01nM, 0.1nM, 1nM, 3nM, 10nM, 30nM, 100nM, 1uM and Null antibody). After 48 hours the condition media was removed and analysed. The reason for change in the methodology was primarily to reduce the number of cells need for the assay as explant tissue was unavailable due to temporary closure of Moorfields Eye Bank. In addition, the CICP method provides a more accurate and specific quantification of type 1 collagen production.

Figure 28 Assay of C terminal propeptide of collagen type 1

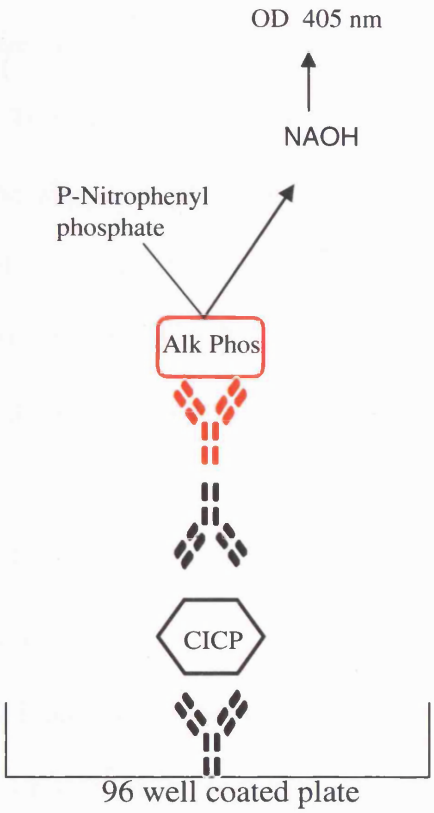

The CICP assay is a sandwich enzyme immunoassay in a mictrotitre plate format utilising a monoclonal anti-cicp antibody coated on the plate, a rabbit anti-cicp antiserum, a goat anti-rabbit alkaline phosphate conjugate and a pNPP substrate to quantify the CICP in the medium.CICP standards were used to generate a standard curve.

2.4 CYTOSKELETON AND CELL MORPHOLOGY

2.4.1 Quantification of alpha smooth muscle actin (α SMA) expression by ELISA

An elisa technique was used to quantify α SMA production in cultured human Tenon's fibroblasts (Richter et al., 2001). Low passage cells were seeded in 96 well plates at a cell density of 7 x 10^3 and allowed to settle for 8 hours. After 16 hours exposure to serum free conditions (culture media with 1% BSA) the cell were treated with increasing concentrations of TGF β2 (0pM, 0.1pM, 1pM, 3pM, 10pM, 30pM 100pM and 1000pM). After 72 hours the elisa was performed. Briefly, the supernatant was removed and the cells were carefully washed three times with PBS. The cells were fixed with methanol for 15 minutes at -20 ^{0}C and then left to air dry for 20 minutes at RT. 100µl of antibody buffer [PBS containing 1% BSA, 1% Ovalbumin and 0.1% Tween-20 (Sigma, Dorset, UK)] to each well and incubated at RT for 30 minutes to block non specific binding sites. After removal of the antibody buffer by blotting the plate the cells were incubated in 100 µl primary anti α SMA antibody (1:2000 dilution in antibody buffer, Clone 1A4; Sigma, Dorset, UK) for 2 hours. The plate was washed three times with 250 µl PBS prior to the addition of 100 µl/well of horseradish peroxidase conjugated anti-mouse secondary antibody (IgG; Dako A/S, Demark). After 1 hour and further washing, TMB one step solution (Promega, Madison, USA) was added 100 µl/ well. The colour reaction was stopped after 15 minutes with 100 µl 1M HCL and the optical density was read at 450nm with a 630nm reference filter.

2.4.1.1 Effect of CAT-152 on alpha smooth muscle actin expression After the initial experiments had been completed a dose response relationship was generated for TGF-β2 and α SMA expression. The elisa was repeated using a single concentration of

TGF β2 (EC 90: 30pM) to stimulate the cells in the presence of increasing concentrations of anti-TGF β2 antibody 0.01nM, 0.1nM, 1nM, 3nm, 10nM, 30nm, 100nM, 1uM and Null antibody.

2.4.2 Immunocytochemical staining of the actin cytoskeleton: α SMA Immunocytochemistry. The presence of α SMA in the cells was demonstrated by fluorescent immunocytochemistry. Low passage fibroblasts were seeded at a density of 1 x 10^5 on glass cover slips in 6 well plates and left to settle for 8 hours. The wells were washed carefully 3 times with PBS and subjected to serum free conditions for 16 hours. The cells were then treated with 0pM, 10 pM or 100pM TGF β2 or a combination of 0pM, 10 pM or 100pM TGF β2 with 100nM or 300nM CAT-152. After 72 hours the cells were washed in PBS, fixed with 4% Paraformaldehyde (Sigma, Dorset, UK) for 30 minutes and left to air dry. The coverslips were removed from the base of the 6 well plate and transferred with forceps to a microscope slide. Briefly the slides were permeablised in 1% Triton x-100 in TBS (Sigma, Dorset, UK) for 15 minutes and blocked with Fetal Calf Serum (1:10 dilution in TBS) for 30 minutes. The primary antibody mouse anti-human α SMA FITC conjugate (1:250 dilution in 1:10 FCS; Sigma, Dorset, UK) was incubated for 3 hours. The slides were counterstained with Diamidino-2- phenylole dilactate (DAPI; Sigma, Dorset, UK) for 1 minute, washed in TBS and air dried. Coverslips were mounted with fluorescent mounting medium. The cells were imaged by confocal microscopy.

2.4.3 Data analysis

Collagen production in response to TGF β2 is presented as the amount of collagen per ml of cell lysate for the Sircol assay, or the amount of CICP per ml of culture medium. The

EC_{50} values for TGFβ2 or IC_{50} values for CAT-152 (geometric mean with 95% confidence intervals) were determined using four-parameter logistic curve fitting (Prism 2, GraphPad Software, San Diego, USA). When a four parameter fit failed, a three or two parameter fit was performed by holding the curve top and/or bottom values constant. All data are tabulated in Appendices. ANOVA and Dunnett's test was used to identify significant changes between treatment groups (Instat, GraphPad Software, San Diego, USA). The level of significance applied to the statistical analysis was $P<0.05$.

2.5 RABBIT MODEL OF GLAUCOMA FILTRATION SURGERY

A number of animal models have been developed in order to study wound healing after glaucoma filtration surgery. The rabbit model is most widely accepted and exhibits an extremely aggressive scarring response compared to human tissue (Miller et al., 1989; Miller et al., 1985; Prince, 1964; Tahery et al., 1989). Histological analysis has shown that scarring after glaucoma surgery occurs at the level of the sclera, conjunctiva and within the subconjunctival Tenon's capsule (Doyle et al., 1993a; Khaw et al., 1992a; Khaw et al., 1992b; Miller et al., 1989). Our group has developed a model of rabbit filtration surgery in which a microtube is inserted into the eye, to maintain a permanent sclera fistula (Cordeiro et al., 1997). This eliminates the effects of scleral wound healing and localises the healing response to the conjunctival tissues (Figure 29). The model has been shown to be consistent, reproducible and to date if efficacy is shown in this model then the treatment has always been shown to be effective in humans (Cordeiro et al., 1999a; Siriwardena et al., 2002). We therefore adopted this model for the purposes of this project, to investigate the effects of novel anti-scarring agents. It is important to note that this is a model of conjunctival scarring rather than elevated pressure and glaucoma.

Figure 29 Model of subconjunctival scarring after experimental glaucoma surgery

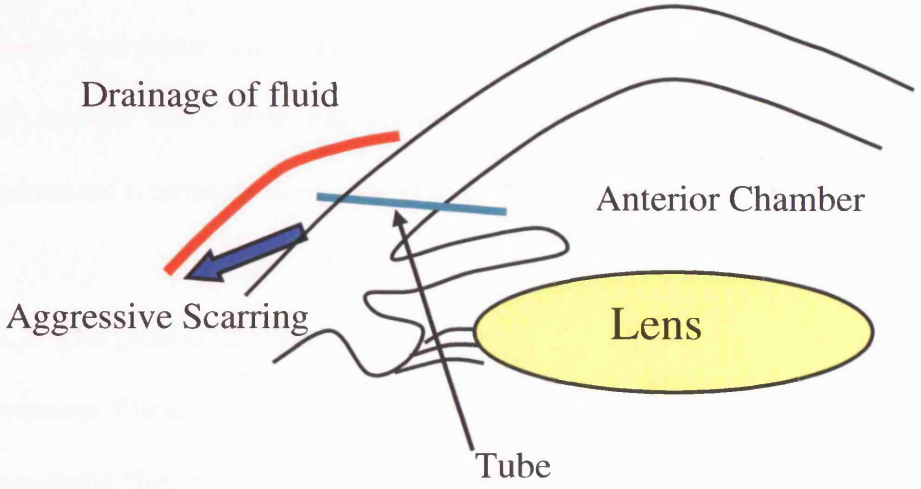

Rabbit model of filtration surgery in which a tube is inserted into the anterior chamber to create a permanent fistula draining fluid into the subconjunctival space. The IOP of the rabbit is normal pre-operatively and it therefore acts as a model of subconjunctival scarring rather one a model of glaucoma. Healing is very exaggerated and a week in this model represents approximately four weeks in humans.

2.5.1 Study design

All experiments were performed as randomised controlled masked observer studies using New Zealand White Rabbits, aged between 12-14 weeks and weighing 1.5-2.0 kg, in accordance with the ARVO Statement for the Use of Animals in Ophthalmic and Vision Research. All animals were housed in the Biological Resources Unit at the Institute of Ophthalmology and were allowed an acclimatisation period of at least 7 days. Surgery was performed in two batches on successive days. Randomisation was performed by a masked individual using the programme available on www.randomisation.com. taking into account the 3 treatment groups and two batches of surgery. Three copies of the randomised treatments were placed in sealed envelopes and stored.

2.5.2 Surgical technique

Glaucoma filtration surgery was performed on the left eye of all rabbits under general anaesthesia [Intramuscular muscular Ketamine (50mg/kg; Fort Dodge Animal Health Ltd, UK) and Xylazine (10mg/kg; Bayer PLC, Suffolk)] as summarised in figure 30. A partial thickness 8-0 silk corneal traction suture (Ethicon; Johnson and Johnson, UK) was placed at 12 O'clock to gain exposure to the superior conjunctiva. A fornix based conjunctival flap was raised and blunt dissection of subconjunctival space was performed to a distance of 15mm behind the limbus. An MVR blade (Vistech; Warwickshire, UK) was used to fashion a partial thickness scleral tunnel starting 4mm behind the limbus and continuing until the blade was just visible in the anterior cornea stroma. A 22 G/25mm Venflon intravenous cannula (BD Biosciences, Oxford, UK) was then passed through the scleral tunnel until the cannula needle was visible in the clear cornea. The cannula needle entered the anterior chamber, the cannula was advanced to the mid pupillary area, and the needle was withdrawn. Finally the cannula was trimmed and bevelled at its scleral end so that it

Figure 30 Model of Rabbit Glaucoma Filtration Surgery

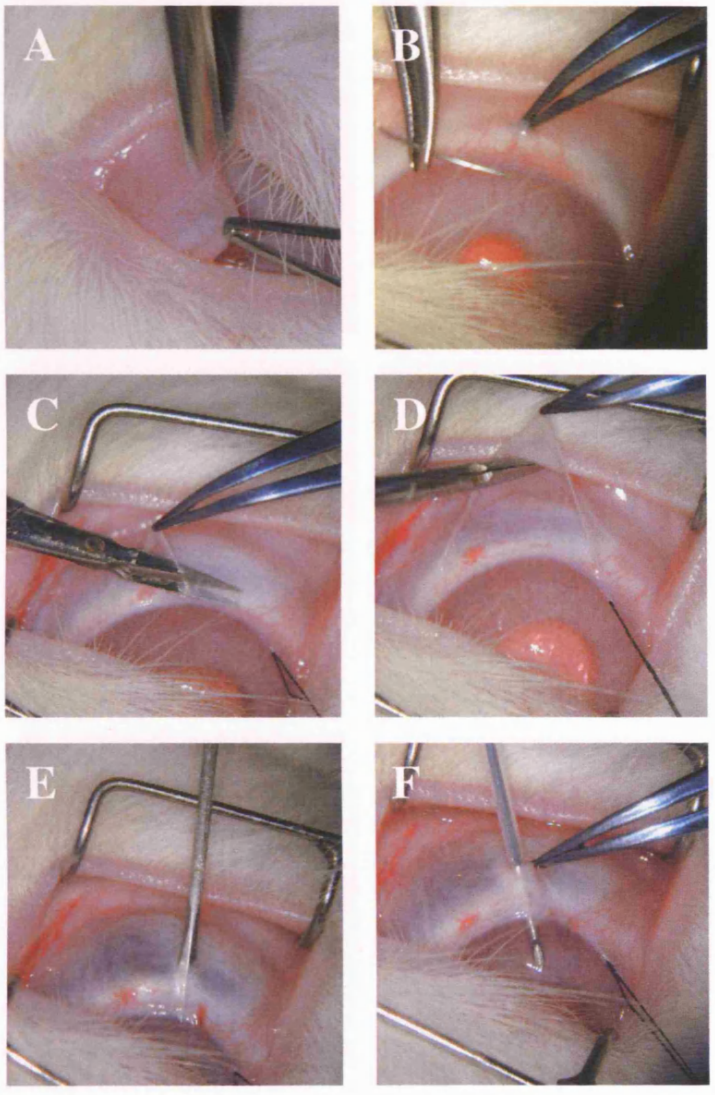

The nyctitating membrane was removed to provide access to the anterior segment (A). A partial thickness 8-0 silk corneal traction suture was placed at 12 O'clock (B) after which a fornix based conjunctival flap was raised and blunt dissection of subconjunctival space was performed (C,D). An MVR blade was used to fashion a partial thickness scleral tunnel starting 4mm behind the limbus and continuing until the blade was just visible in the anterior cornea stroma (E). A 22 G/25mm Venflon intravenous cannula was then passed through the scleral tunnel until the cannula needle was visible in the clear cornea (F).

Figure 32 (Cont) Model of Rabbit Glaucoma Filtration Surgery

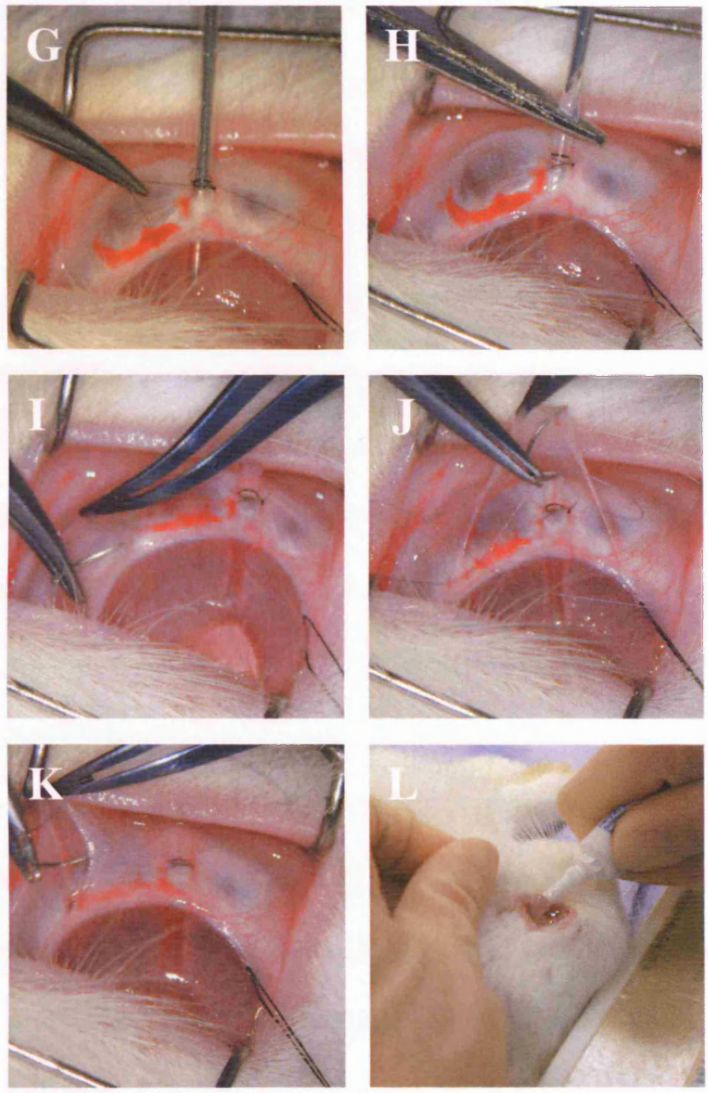

The cannula was trimmed and bevelled at its scleral end so that it protruded 1mm from the insertion point and a 10-0 nylon suture on a B/V 100-4 needle was used to fix the tube to the scleral surface (G,H). The conjunctival incision was closed with two interrupted sutures and a central mattress-type 10-0 nylon suture to give a water-tight closure (I,J,K). One drop of Atropine Sulphate 1% and Betnesol N ointment was instilled at the end of surgery (L).

protruded 1mm from the insertion point and a 10-0 nylon suture on a B/V 100-4 needle (Ethicon, Johnson and Johnson, UK) was used to fix the tube to the scleral surface. The conjunctival incision was closed with two interrupted sutures and a central mattress-type 10-0 nylon suture on a B/V 100-4 needle to give a water-tight closure. One drop of Atropine Sulphate 1% (Martindale Pharmaceuticals, Romford, UK) and Betnesol N ointment was instilled at the end of surgery.

2.5.3 Clinical assessment of the rabbit model

Baseline observations were performed prior to glaucoma filtration surgery. The contralateral unoperated eye acted as a control. Measurement of IOP in both eyes was made using the Mentor Tonopen (Mentor, Norwall, MA, USA) after topical instillation of 0.5% Proxymetacaine HCL eye drops (Chauvin Pharmaceuticals, Romford, Essex) 1 drop per eye, with a mean reading of three recordings being documented per time point. The conjunctival appearance and the drainage area were observed. All animals were examined by a masked observer at set times after surgery. Assessment of both eyes was made daily from day 0 to day 4 and there after at regular periods, at least twice weekly, until sacrifice. Bleb characteristics including length, width and height were measured using calipers, and IOP were recorded. Previous experience with this surgical model has identified a small area of avascularity (<3mm) that appears in the nasal conjunctiva. This is a transient clinical observation and appears to develop independently of any treatment given. The incidence of avascularity was noted (normal vascularisation, 0; avascular region, 1). The drainage bleb vascularity characteristics were assessed independently from this area and were graded by dividing the conjunctival areas into quadrants (superior, nasal and temporal) and scoring the appearance (0, avascular; +1 normal vascularity; +2 hyperaemic; +3 very hyperaemic). Slit lamp examination was performed

to identify both anterior chamber activity (0 quiet; 1 cells; 2 fibrin; 3 hypopyon) and anterior chamber depth which was recorded as either deep (+2), shallow (+1), or flat (0).

An assessment of the presence and duration of corneal epitheliopathy was made after topical installation of 0.5% Proxymetacaine 0.25% Fluorescein (Chavin Pharmaceticals, Romford, Essex) into the left eye and was graded according to the area of the cornea affected (0 = nil, 1 = < 25%, 2 = < 50%, 3 = < 75%, 4 = < 90%, 5 = up to 100%). To minimise discomfort in the case of worsening corneal epitheliopathy, defined as deterioration or an increasing corneal epithelial defect as recorded on two consecutive examinations, affected animals would stop receiving subconjunctival injections until the defect healed. The conjunctival was observed for the presence of a chemotic response (localised swelling and injection) which was graded as mild, moderate or severe (grade 1=mild, grade 2=moderate and grade 3=severe).

Any other clinical findings were noted including the presence of blood in the anterior chamber (hyphaema), lid swelling or subconjunctival haemorrage. All observations were recorded on an observation data sheet.

2.5.4 Photography and image storage

Images of the operative wound site were taken weekly after surgery. At the start of the study a 35mm fundus camera was used (Genesis, Kowa Company Ltd, Japan). This method was superseeded by use of a digital camera in terms of image quality, acquisition and storage (Nikon Coolpix 950, Tokyo, Japan). Digital images were stored as JPEG files.

2.5.5 Technique of drug administration

In the following experiments anti-scarring agents or control vehicle were administered by subconjunctival injection at set time points on the day of surgery or in the post-operative period. The subconjunctival injections were administered under topical anaesthesia (Proxymetacaine hydrochloride 0.5% eye drops, 1 drop per eye), using a 30 G needle (Myjector 100u; Terumo, Japan). 100µl of agent was injected 5mm behind the limbus at the nasal margin of the superior rectus muscle, such that a visible bleb was formed on the supranasal quadrant of each eye (Figure 31). This volume was selected to be the maximum deliverable by the subconjunctival route in this model. Subconjunctival 5-FU was administered 180 degrees from the site of surgery. The rationale for this injection site selection was in keeping with the method used in the original studies of subconjunctival 5-fluorouracil in glaucoma filtration surgery and widespread clinical practice (Group, 1989; Group, 1996). 5-FU has a pH of 9 and the risk of intraocular penetration must be reduced to a minimum. No other agents were administered at the time of injection. All injections were given in a masked fashion to ensure that the operator (ALM) was unaware of the treatment being given. When 5-FU was given the injections were given by an independent clinician as the different injection sites for each treatment precluded masking.

Treatment was either given at the time of surgery or in the post-operative period. Intra operative CAT-152 and control vehicles was given as two subconjunctival injections The first dose was administered 0.5 hour prior to surgery and the second dose was given immediately post-operatively. Inter-operative 5-FU was the only treatment administered by a different technique. It was given by application of a sponge soaked in 5-FU which was positioned under the conjunctival flap for 5 minutes. This is the accepted route of administration of inter-operative 5-FU in clinical practice. Extreme care was taken to

Figure 31 Technique of subconjunctival injection in the rabbit

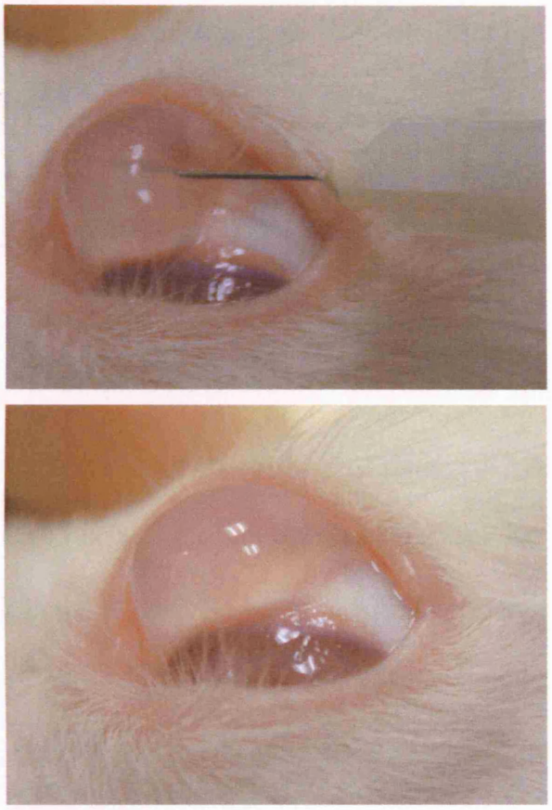

The subconjunctival injections were administered under topical anaesthesia using a 30 G needle.100µl of agent was injected 5mm behind the limbus at the nasal margin of the superior rectus muscle, such that a visible bleb was formed.

avoid exposure of the free conjunctival edge to the anti-metabolite. All post-operative treatments were given by subconjunctival injection. (Table 4)

CAT-152 was prepared as a sterile colourless solution at a concentration of 1mg/ml, which was stored at 4 ^{0}C. Previous studies by our group had determined that 100μg was the optimum dose per treatment, so 100μl of drug was administered with each subconjunctival injection (Cordeiro et al., 1999a). 100ml of 1mg/ml CAT 001 was given as the control antibody.

2.5.6 Blood Sampling

Pre dosing venous blood was sampled from the ear vein of each rabbit 3 days before the start of the study. A small area of the ear was shaved and the topical local anaesthetic Ametop (Smith and Nephew Healthcare Ltd, Hull, UK) was applied to the area, which was warmed by application of a hot sponge to dilate the vessels. 4 mls of blood was collected using a 25 gauge butterfly cannula (BD Biosciences, Oxford, UK) attached to a 5 ml syringe. The blood was transferred to a clotted sample blood bottle with serum filter (BD Biosciences, Oxford, UK) and centrifuged at 4000 rpm for 20 minutes to separate the serum from the cellular components. The serum was placed in a labelled eppendorf (BD Biosciences, Oxford, UK) and stored at -70 ^{0}C. 2mls of blood was also sampled from each animal once a week until day 45. A terminal sample of blood (30mls) was collected by cardiac puncture under general anaesthesia just prior to sacrifice of the animal on day 70.

2.5.7 Measurement of CAT-152 or CAT-001 in rabbit serum

Detection of CAT-152 and CAT-001 concentrations in the rabbit serum were based on an anti-Fc capture ELISA developed at CAT (SOP number 06/07/044). Briefly, 96-well

Table 4 Drug administration in the rabbit model of glaucoma surgery

Drug	Dose	Intra-operative treatment	Post-operative treatment	Site of injection
CAT -152	1mg/ml 100µg	2 x 100 µl subconjunctival injections (First dose 30 mins before surgery, second dose immediately after)	100 µl subconjunctival injection	Superior
5FU	50mg/ml 5mg	Pre soaked sponge positioned under the conjunctival flap for 5 mins	100 µl subconjunctival injection	Inferior
PBS	100 µl	2 x 100 µl subconjunctival injections	100 µl subconjunctival injection	Superior or inferior
CAT-001 Null antibody	1mg/ml 100µg	2 x 100 µl subconjunctival injections	100 µl subconjunctival injection	Superior
Antisense Oligonucleotides TGFβ1 TGFβ2 TBRII Misense	25mg/ml 50mg/ml 1mg/ml 25µg 50µg 100µg	2 x 100 µl subconjunctival injections		Superior

maxisorb plates (Nunc) were coated (100 µl per well) with goat anti-human Fc (1:400 in Dulbecco's PBS Sigma [D-PBS]) and incubated at +4°C overnight. Thereafter, the plates were washed three times with PBS/T (PBS + 0.1% Tween 20) and non-specific sites blocked for one hour at +25°C with 150 µl of M-PBS (PBS + 2% [w/v] Marvel dried skimmed milk). Eleven point CAT-152 or CAT-001 standard curves in M-PBS (1 : 2 serial dilution; top concentration 2 µg/ml) and rabbit serum samples (1 : 4 start dilution or 1 : 2 serial dilution, respectively) were incubated on the plates at +25°C for one hour. CAT-152 or CAT-001 were detected by incubating the plate with a detection antibody (sheep anti-human λ-HRP conjugate; diluted 1 : 2,500 in M-PBS) and after washing 3,3', 5,5'-tertra methylbenzidine (TMB) substrate (Sigma) was added and the absorbance measured at 450 nm.

2.5.8 Measurement of Anti-CAT-152 and Anti-CAT-001 in rabbit serum

Rabbit anti-CAT-152 and anti-CAT-001 were measured using a procedure based on CAT SOP number 06/07. Maxisorb plates (Nunc) were coated (100 µl per well) with 0.1 µg/ml in D-PBS, of either CAT-152 or CAT-001 and incubated at +4°C overnight. Plates were washed with PBS/T and blocked with M-PBS for one hour at +25°C. Rabbit anti-human IgG standards (eleven point curve, 1:3 serial dilution; top concentration 200 µg/ml) and rabbit serum samples (1:500 start dilution, 1: 3 serial dilution) were incubated at +25°C for one hour. Anti-CAT-152 or Anti-CAT-001 were detected by incubating the plate with a detection antibody (goat anti-rabbit Ig-HRP; dilution, 1: 5000 with M-PBS) and after washing TMB substrate was added and the absorbance measured at 450 nm.

2.5.9 Tissue collection

All animals were sacrificed at 30 days using a lethal injection of pentobarbitone intravenously under a general anaesthetic. Both eyes were enucleated. The upper lid was left intact, attached to the globe in order to preserve the architecture of the superior fornix and conjunctival tissues around the drainage site. All of the eyes were fixed in 10% buffered formal saline for 24 hours and then stored in 70% alcohol. The site of the conjunctival injections in the left eye was marked post-mortem, but pre-exenteration with 10-0 nylon suture. Tissue was stored until the efficacy data had been analysed when a decision was made to process it.

2.5.10 Data analysis

Bleb survival was taken as the primary efficacy end point in the analysis of a treatment on subconjunctival scarring in rabbit filtration surgery. Bleb failure was defined as the appearance of a flat, vascularised and scarred bleb in the presence of a deep anterior chamber. Kaplan Meier and log rank statistics were used to compare treatment groups in bleb and intraocular pressure failure (defined as the return of the intraocular pressure in the surgical eye to baseline level). Bleb area and height, anterior chamber depth and activity, and conjunctival vascularity per quadrant were all analysed using repeated measures procedure and the generalised linear model (SPSS, SPSS Inc. Chicago, USA). This allowed comparison of treatment groups over the whole study period, using between subject tests. Duration corneal epitheliopathy and avascularity were analysed using Kruskal-Wallis test and Dunn's test. Finally intraocular pressure was analysed using the multivariate analysis of variance, with Bonferroni's modification to compare differences between treatments and the effects of time and treatment. The level of significance applied to the statistical analysis was $P<0.05$.

2.6 TEMPORAL AND SPATIAL EXPRESSION OF TGF β AND ECM MOLECULES IN SUBCONJUNCTIVAL RABBIT TISSUE AFTER GLAUCOMA FILTRATION SURGERY

Three isoforms of TGF β are expressed in the eye. Previous studies have identified that TGF β2 is the most predominant ocular isoform (Pasquale et al., 1993; Tripathi et al., 1994a; Tripathi et al., 1994b). We set out to investigate which intraocular and extraocular tissues express TGF β RNA and protein in unoperated eyes and in eyes in which glaucoma filtration surgery has been performed. Only once the temporal and spatial expression of the TGF β isoforms has been fully identified will it be possible to fully delineate how modulation of this growth factor can reduce conjunctival scarring in vivo.

2.6.1 Experimental details

The model of glaucoma filtration surgery described in section was adopted and the experimental protocol is summarised in Table 5.

2.6.2 Tissue retrieval

Tissue samples from the Conjunctiva (tube drainage area), Sclera, Cornea, Iris, Ciliary body, Lens and Vitreous Humour, from right and left eyes, were collected under general anaesthesia on days 1, 3, 8 and 14 after surgery (Day 0). The tissue was then divided in half. One part was placed in an eppendorf containing a solution of RNA later (10ul reagent per 1 mg tissue; Qiagen, UK). The thickness of the tissue did not exceed 5mm to allow the solution to fully penetrate the tissue and prevent RNA degradation. The samples were stored at 4^{o} C prior to processing. The other half of the tissue was placed in a

Table 5 Expression of TGF β in ocular tissue after rabbit glaucoma surgery: Experimental details

Study	No of NZW rabbits	Treatment groups	Treatment regimen Day of surgery = 0	Day of Sacrifice	Tissue collection
	8	CAT-152 n=4 No treatment n=4	Inter-operative treatment only (Pre-operative and immediate post-operative doses only)	1	Samples of conjunctiva, sclera, cornea, iris, ciliary body, lens, and aqueous humour were collected from the operated (i.e. left) eyes at each time point. Unoperated right eyes were sampled on day 1 (8 eyes in total) to provide control tissues for evaluation of TGFβ levels
	8	CAT-152 n=4 No treatment n=4	Inter and post-operative treatment Days 0,1,2	3	
	8	CAT-152 n=4 No treatment n=4	Inter and post-operative treatment Days 0,1,2,3,4,7	8	
	8	CAT-152 n=4 No treatment n=4	Inter and post-operative treatment Days 0,1,2,3,4,7,9,11	14	

cryotube and snap frozen in liquid nitrogen. The cryotubes were stored at -70 ^{0}C before processing. 0.1ml of aqueous humour was also sampled and snap frozen. Injections due to be given on the day of sacrifice were omitted (i.e. animals sacrificed on day 1 had two doses of treatment before the tissue was retrieved.) After the tissues had been sampled the animals were sacrificed using lethal injection of pentobarbitone (Rhone Merieux, Essex, UK)

2.6.3 Tissue analysis: mRNA Detection: Quantitative Competitive Reverse Transcriptase Polymerase Chain Reaction (QCRT-PCR / TaqMan)

2.6.3.1 Primer And Probe Design

For mRNA quantification, TaqMan primers and probes were designed to the target genes TGFβ1 and TGFβ2. All primers and probes were designed using Primer Express software (Applied Biosystems, California, USA). Probes were designed to span two exons to ensure assay specificity for cDNA rather than any contaminating genomic DNA. BLAST N searches were performed against the nr (non redundant set of Genbank, EMBL, DDBJ and PDB) database sequences to confirm the gene specificity of the selected primer and probe nucleotide sequences. The sequences of the primers and probes used are shown in Table 6.

2.6.3.2 RNA extraction from tissue samples

Control tissue samples for each ocular structure were pooled and homogenised together before total RNA extraction. Left eye samples from both untreated and CAT-152 treated groups were homogenised and extracted individually. Total RNA was extracted from each sample with RNAeasy 96 using a Biorobot 8000 (Qiagen, UK).

Table 6 Primers and probes used for quantitative PCR

Primers

Gene	Sequence in 5'-3' direction
TGFβ1 (forward)	CGGGCTCAACATCTACACAGTTC
TGFβ1 (reverse)	GTCCTTGCGGAAGTCAATGTACA
TGFβ2 (forward)	CTACAAGATAGACATGCCGTCCTACT
TGFβ2 (reverse)	CATCAAATCGGACAATTCTGAAGT
18S ribosomal RNA (forward)	CGGCTACCACATCCAAGGA
18S ribosomal RNA (reverse)	CAATTACAGGGCCTCGAAAGAG

Probes

Gene	Sequence in 5'-3' direction	5' reporter	3' quencher
TGFB1	ACCAACTACTGCTTCAGCTCCACAGA GAAGAACT	FAM	TAMRA
TGFB2	CCCCTCCGAAAATGCCATCCCA	FAM	TAMRA
18S ribosomal RNA	CAGCAGGCGCGCAAATTACCCA	TET	TAMRA

2.6.3.3 cDNA synthesis Reverse transcription of RNA was performed in a final volume of 30μL in the presence of 1x RT-PCR buffer (Applied Biosystems) containing 50mM KCl, 10mM Tris-HCl (pH 8.3), 5.5mM $MgCl_2$, 500μM each deoxynucleotide triphosphate, 2.5μM random hexamer primer, 12 units of RNase inhibitor and 37.5 units MultiScribe RT (Applied Biosystems). Samples were incubated at 25°C for 10min then 48°C for 30min before inactivation of reverse transcriptase by heating at 95°C for 5min.

2.6.3.4 PCR Amplification Real-time semi-quantitative TaqMan PCR and data analysis was performed using the ABI Prism 7700 Sequence Detection System (Applied Biosystems). For each PCR reaction, 2μL cDNA was added to 23μL of master mix containing: 5 mM $MgCl_2$, 200μM dATP, dCTP, and dGTP, 400μM dUTP, 300nM each primer and 1.25 units of AmpliTaq Gold DNA polymerase (Applied Biosystems) in TaqMan buffer. Each reaction contained 100nM specific TaqMan probe carrying the reporter dye FAM (6-carboxy-fluorescein) at the 5' end and the quencher TAMRA (6-carboxy-tetramethyl-rhodamine) at the 3' end. Thermocycler conditions were as follows: 95°C for 10min, 40 cycles at 95°C for 15s and 60°C for 1min. Experiments were performed in duplicate for each data point and included a no-template control. RNA input was normalised to 18S ribosomal RNA as a housekeeping gene control. Amplification of 18S ribosomal RNA was performed with the TaqMan ribosomal RNA control reagents kit (Applied Biosystems).

The readout of the PCR amplification reaction is the parameter Ct, defined as the fractional cycle number at which the increase in fluorescence crosses a threshold above baseline. The threshold is set as ten times the standard deviation of the baseline signal before amplification is detectable. The methodology used in this study does not provide an absolute quantification of RNA levels in each sample, but rather a measure of relative

mRNA expression in a given sample group. An explanation of the way that relative mRNA expression is calculated is outlined in Figure 32.

2.6.4 Tissue analysis: Protein detection

2.6.4.1 TGF β2 content of aqueous humour samples Total (i.e. latent and active) and active TGF β2 concentration was measured in each aqueous humour sample using a human TGF β2 ELISA kit (Quantikine; R&D Systems). The Quantikine kit enables quantitative analysis of total TGF β2 after conversion of latent TGF β2 to the active form by acidification. Assays were carried out according to the manufacturer's instructions except that 20μL 1M HCl was used for sample acidification, 20μL 1.2N NaOH/0.5M HEPES was used for subsequent sample neutralisation, followed by addition of 640μL of the supplied calibrator diluent (RD51). A sample dilution of 1:10 in calibrator diluent was used for measurement of active TGF β2 and a dilution of 1:7.8 (including all reagents used for activation) was used for measurement of total TGF β2.

2.6.4.1 TGF β2 content of conjunctival samples

Total TGF β2 content of conjunctival bleb tissue was determined using pooled samples from each group for a given time point. Pooled tissue was cut up in 0.3mL ice-cold PBS before centrifugation at 9300 rcf (10min, 4°C). The supernatant was removed for measurement of active TGF β2 concentration using a human TGF β2 ELISA kit (Quantikine; R&D Systems) according to the manufacturer's instructions. Samples were assayed at a dilution of 1:10 in the supplied calibrator diluent (RD51).

Figure 32 Quantification of gene expression Comparative Ct Method

The **Ct value** is defined as the PCR cycle at which a given sample passes through a predetermined fluorescence threshold.

Delta Ct (ΔCt) is a measure of the relative expression of one target to another, as illustrated in the example below:

target A/target B= 2-DCt

If the difference in Ct (ΔCt) between mRNA species A and B = 5 cycles (i.e it took 5 more cycles to see amplification of A) then there is: 2^{-5}=1/32 as much A as B. In order to control for sample input, the relative amount of a chosen target is normalised to an endogenous control using the formula

$$2^{-\Delta\Delta Ct}$$

For the this calculation to be valid, the efficiency of the target amplification and the efficiency of the reference amplification must be approximately equal. For amplicons designed and optimized according to Applied Biosystems guidelines (amplicon size <150 bp), the efficiency is close to one.

Example calculation

The table below shows the average Ct results for the human brain, kidney, liver and lung samples and how these Cts are manipulated to determine ΔCt, ΔΔCt, and the relative amount of c-myc mRNA.

Relative Quantitation Using the Comparative Ct Method

Tissue	**c-myc Average Ct**	**GAPDH Average Ct**	**DCt** c-myc – GAPDH	**DDCt** ΔCt –ΔCt Brain	**c-myc Rel to Brain** $2^{-\Delta\Delta Ct}$
Brain	30.49	23.63	6.86	0.00	1.0
Kidney	27.03	22.66	4.37	–2.50	5.6
Liver	26.	24.60	1.65	–5.21	37.0

2.6.5 Data analysis

Statistical comparison between sample groups was performed as outlined below. In all cases a probability (P) value of <0.05 was considered significant.

In order to calculate relative mRNA expression levels in each tissue following experimental GFS, data were normalised to the level of mRNA detected in control tissues obtained from unoperated eyes. Therefore, the relative level of gene expression in control tissue was 1 in all cases. Changes in mRNA expression after GFS were analysed by comparing mean relative mRNA expression in no-treatment group tissues to mean control mRNA expression (i.e. 1) using ANOVA followed by Bonferroni's post-hoc test. The same statistical test was also applied for comparison of the relative mRNA expression between CAT-152 treated and no-treatment groups at each time point.

The effect of experimental GFS on TGF β protein expression was analysed by comparing mean protein values in no-treatment group tissues to mean control protein values using ANOVA followed by Bonferroni's post-hoc test. Comparison of mean protein values between CAT-152 treated and untreated groups at each time point was performed by ANOVA followed by Bonferroni's test.

2.7 MODULATION OF THE WOUND HEALING RESPONSE IN VIVO: NEUTRALISATION OF TGF β WITH AN ANTI-TGF β2 ANTIBODY (CAT-152) IN THE RABBIT MODEL OF GLAUCOMA SURGERY

Four experiments were performed in this project to investigate the potential role of this novel anti-TGF β2 antibody in glaucoma surgery. Experiments were designed to

specifically address issues that related to the application and development of the antibody for clinical use and the methodology used in these studies is summarised in Table 7.

2.7.1 Investigation of the effect of intra-operative application of CAT-152 on experimental glaucoma surgery (Intra-operative study)

Treatment at the time of surgery would be the optimum method of drug delivery of a new anti-scarring agent in terms of ease of application and surgeon acceptance. We therefore performed a randomised masked observer study to investigate the efficacy of intra-operative application of CAT-152 in experimental glaucoma surgery.

2.7.2 Comparison of prolonged post-operative application of CAT-152 with 5-Fluorouracil after experimental glaucoma filtration surgery (Prolonged post-operative study)

Current anti-scarring agents are used in the post-operative period to maintain long-term bleb function. Using the same model of glaucoma filtration surgery, this present study was designed to determine:

(a) if post-operative application alone of CAT-152 could improve bleb survival and

(b) to compare the effectiveness of CAT-152 to one of the gold standard post-operative anti-scarring agent 5-FU.

2.7.3 Investigation of the long term effects of combining intra-operative and prolonged post-operative CAT-152 treatment on experimental glaucoma surgery (Maximum dosing study)

The ongoing healing response remains the major barrier to a maintaining long-term bleb function. In this study we used the model of glaucoma surgery to investigate:

(a) How long blebs can survive when treated with a combined intra-operative and extended long-term post-operative regimen and

(b) Compared CAT-152 with the anti-scarring agent 5-FU.

By combining the previously tested intra-operative and post-operative treatments, we anticipated that we may be able to determine the optimal dosing of CAT-152 required to prevent long-term failure of experimental glaucoma surgery.

2.7.4. Investigation of the effects of a combined course of intra-operative and prolonged treatment with the CAT-152 on the immune response in the rabbit (Chemosis Study)

The DNA encoding rabbit TGF β2 shares over 96% homology with human TGF β2 with conserved alignment of the nine cysteine residues as shown in figure 13 (Cordeiro et al., 2003). Therefore treatment of the rabbit with a human antibody anti-TGF β2 antibody, CAT-152, should still show efficacy in neutralising TGF β2, as we have shown in previous studies (Cordeiro et al., 1999a). However, we were suspicious that prolonged dosing with a human antibody may induce a systemic immune response in the rabbit. In order to investigate this further we repeated the experiment described in 2.7.3 using combined intra-operative and prolonged post-operative course of treatment. Blood samples were collected for to look for the presence of antibody (CAT-152) and anti-product (anti-CAT-152) antibodies.

Table 7 Neutralisation of TGF β with an anti TGF β2 antibody in the rabbit glaucoma surgery: Experimental details

Study	No of NZW rabbits	Treatment groups	Treatment regimen Day of surgery = 0	Day of Sacrifice	Histology	Blood sampling
Intra - operative study	30	CAT-152 n=10 (Batch 150427) PBS n=10 No treatment n=10	Intra-operative treatment only 2x subconjunctival injections	30	No	No
Prolonged post-operative study	48 24 Efficacy	CAT-152 n=8 (Batch 150427) 5FU n=8 NT n=8	Post-operative treatment Days 2,3,4,7,9,11 and 14	30	No	No
	24 Histology	CAT-152 n=8 5FU n=8 NT n=8	As above	10 n=12 21 n=12	Yes	No
Maximum dose study	27	CAT-152 n=9 (Batch 8086) 5FU n=9 PBS n=9	Inter and post-operative treatment Days 2,3,4,7,9,11, 14, 21, 24, 28, 31, 35, 38 and 42 (PBS 5 inferior injection, 4 superior injection)	45	No	No
Chemosis Study	18	CAT-152 n=6 (Batch P020821) Null n=6 PBS n=6	As for maximum dose study	70	No	Yes

2.8 MODULATION OF THE WOUND HEALING RESPONSE IN VIVO: INHIBITION OF TGF β WITH ANTISENSE OLIGONUCLEOTIDES IN THE RABBIT MODEL OF GLAUCOMA SURGERY

2.8.1 Assessment of tolerance to TGF β antisense oligonucleotides in the rabbit eye.

The aim of this experiment was to determine whether the selected doses of antisense oligonucleotide to TGF β, administered by the subconjunctival route, were tolerated and safe to administer in vivo, using the rabbit model.

2.8.2 Assessment of efficacy of TGF β antisense oligonucleotides after experimental glaucoma surgery.

The aim of this experiment was to determine whether single application of antisense oligonucleotides to either: TGF β1, TGF β2, TBR II were able to reduce conjunctival scarring in vivo following experimental glaucoma filtration surgery. The methodology is summarised in Table 8.

2.9 HISTOLOGICAL ANALYSIS OF THE RABBIT MODEL

2.9.1 Histological preparation

All of the eyes were fixed in 10% buffered formal saline for 24 hours, stored in 70% alcohol. A ballot of tissue was removed from each globe to access the area of interest (Figure 33) and the specimens were then transferred to processing cassettes and subjected to conventional overnight processing including dehydration, clearing and infiltration

Table 8 Inhibition of TGF β with antisense oligonucleotides in rabbit glaucoma surgery: Experimental details

Study	No of NZW rabbits	Treatment groups	Treatment regimen Day of surgery = 0	Day of Sacrifice	Histology	Blood sampling
Intra – operative tolerance study	9	25μg TGF-β1 OGN 50μg TGF-β1 OGN 100μg TGF-β1 OGN	2x subconjunctival injections only: no surgery performed	30	No	No
Intra – operative efficacy study	60 48 Efficacy	100μg of TGFβ1, TGFβ2, TGFβ Type II Receptor, misense OGN or 100μl PBS	2x subconjunctival injections only As above	15 n=18 30 n=30	Yes	No
	12 Histology			21 n=12	Yes	No

Figure 33 Preparation of rabbit eye prior for histological sectioning

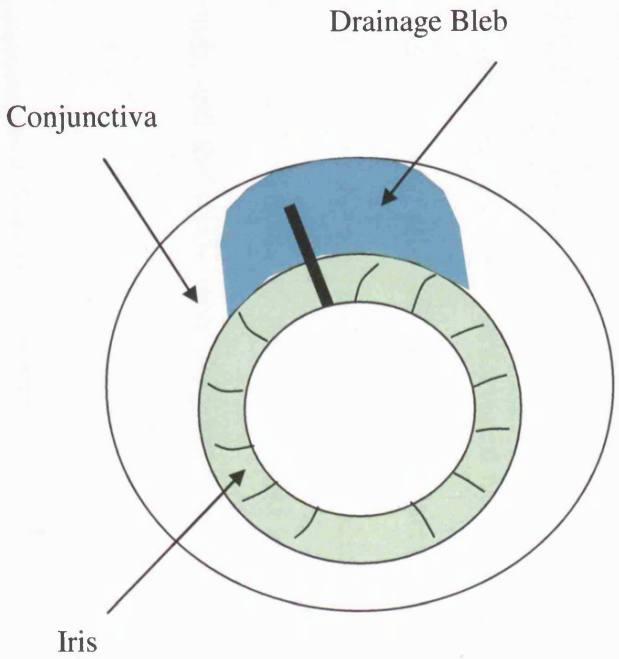

Rabbit Eye

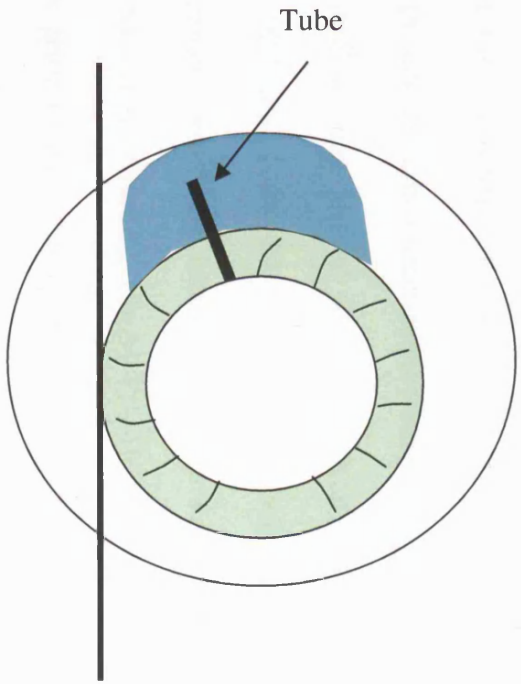

Section of tissue removed from globe prior to embedding

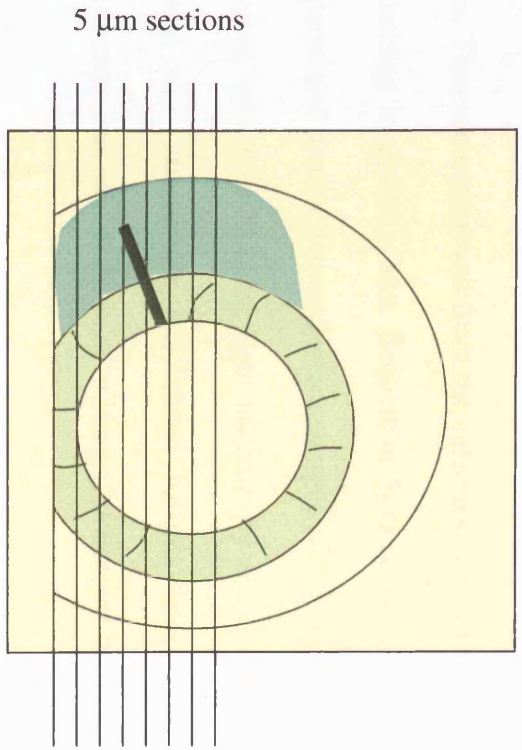

Wax embedded tissue block from which 5µm sections of the operative wound site were cut

steps. They were removed from the cassettes, and carefully orientated in moulds prior to embedding in paraffin wax. Sequential 5μm sections of the operative wound site were prepared and mounted on superfrost charged slides (Merck Eurolab, Leicester, UK).

Sections were viewed using light microscopy and images were captured using a digital camera with microscope attachment. Images were stored as JPEG files. Confocal microscopy was also performed to image fluorescent immunohistochemical sections.

2.9.2 Cellular analysis

Sections were stained with hematoxylin and eosin (H and E) to demonstrate cellular nuclei for assessment of total cellularity. For more specific cellular identification α smooth muscle actin immunohistochemistry was performed to identify the presence of myofibroblast transformed fibroblasts. Briefly, sections were dewaxed through xylene, 70%, 90% and 100% Methylated Spirit, washed in 70% alcohol and then placed in endogenous peroxidase blocking solution for 20 minutes. Tris buffered saline (TBS: 150mM sodium chloride, 10mM Tris-HCl, pH 7.6) was prepared and used to wash the slides prior to blocking non specific binding sites with normal rabbit serum for 20 minutes (NRS, 1:10 dilution in TBS; DAKO A/S Denmark). The sections were incubated in the primary antibody, Mouse anti-human α SMA (1:150 dilution in 1:100 NRS, IgG2A, Clone1A4 DAKO, A/S, Denmark) for 1 hour, washed in TBS and then incubated in the secondary antibody, biotinylated rabbit anti-mouse (1:300 in TBS, DAKO) for 45 minutes. A streptavidin AB complex / horseradish peroxidase kit was used (DAKO A/S, Demark) and finally a solution of 3,3- Diaminobenzadine (DAB, Sigma, Dorset, UK) was placed on the slides for 10 minutes. Nuclei were stained in Meyer's haemotoxylin for 30 seconds, and the slides were dehydrated through alcohol and mounted. Positive control

was in built in the iris and ciliary body of the eye. For negative control slides a mouse anti- human negative control primary antibody was used (IgG2a, DAKO A/S, Demark). α SMA fluorescent labelled antibody staining was also performed using the method described in section 2.4.2.

Proliferating cell nuclear antigen (PCNA) immunohistochemistry was used as a marker of recent cell division. Before incubation with the antibodies, citrate buffer was added to the sections, which were then placed under microwave power for 2 x 5 minutes, for antigen retrieval purposes. Mouse anti-rat proliferating cell nuclear antigen (1:8000 in 1:100 NRS, IgG2a, DAKO A/S, Denmark) was used as the primary antibody. A section of tonsillar tissue was used as a positive control. The primary antibody stage was omitted on tonsillar sections to act as a negative control.

2.9.3 Extracellular matrix demonstration

Extracellular matrix collagen deposition was identified using several stains; Picrosirius red for total collagen and Gamori's trichrome for scar formation, collagen density and orientation (Juinquera et al., 1978; Lillie et al., 1980; Shah et al., 1994). Aldehyde fuschin staining was performed to identify members of the elastic fibre family of connective tissues. Oxytalan fibres, a member of this family, are characteristic of the early stages of elastogenesis indicating early local extracellular matrix production and deposition. Oxytalan fibres were demonstrated by oxidised aldehyde fuschin staining (Jefferies et al., 1995; Montes, 1996).

2.9.4 Histological grading system

2.9.4.1 Light microscopy The parameters of cellularity and extracellualr matrix deposition were graded by two masked observers using a modified scoring system based

on that described by Shah (Shah et al., 1994). Each parameter was graded on a scale: 0 to 4; 0 = same as control eye; 1 = 1%-25% of control; 2 = 26%-50% of control; 3= 51%-75% of control; 4 = >75% of control. We identified visual reference standards for each grade and incorporated these into the system. All operated eyes were compared to contralateral non surgical eyes. Mean scores of histological parameters for each treatment group per time point were calculated and this semi quantitative data was analysed using analysis of variance statistics (SPSS).

2.9.4.2 Confocal microscopy Quantification of the fluorescent α SMA staining in the histological tissue sections was performed using a binary image analysis system, originally described by Wormstone et al (Wormstone et al., 2002). Confocal images slices were converted from colour into binary format with black pixels representing the FITC fluorescent label, using Adobe Photoshop software (Adobe systems software, Middlesex, UK). A threshold for intensity of pixel detection was selected and applied to all images (central point of the intensity range of all the images in data set). All images were the same dimensions (i.e. total number of pixels per image was constant) and were stored as TIFF files. The images were analysed using Scion Image (Scioncorp, Maryland, USA) and the total number of black pixels was recorded for each image. The central image slice from each confocal stack and two further slices, one 2 slices above and one 2 slices below, were analysed per section of rabbit tissue. (Image stack n=10, central slice =5, slices 3 and 7 also analysed). 3 tissue sections per treatment group were included. Finally, the pixel data was analysed using analysis of variance statistics (SPSS) to compare the effect of treatment on α SMA expression.

2.9.5 Electron Microscopy

We also compared the electron micrograph characteristics of 2 rabbit eyes treated with CAT-152 and 2 untreated eyes. The methodology from experiment 2.7.2 was repeated in terms of surgical technique and post-operative injection regimen. Animals were sacrificed on day 10 and the operative wound site was processed for both scanning and transmission electron microscopy. This time point was selected to provide maximum information on the comparative bleb appearances between treated and untreated animals prior to the onset of bleb failure.

Tissue preparation for Electron Microscopy

Rabbit eyes were immersion fixed in 3%glutaraldehyde and 1% to pH 7.4 with 0.07M sodium cacod-HylateCl. After 1 -12h, cells were washed three times with PBS, and dissected to remove the anterior segment and lens from the posterior segment. Specimens were then osmicated for 2h with a 1% aqueous solution of osmium tetroxide and dehydrated through ascending alcohols (50 - 100%, 10 min per step).

2.9.5.1 Transmission EM After 3 changes of 10% ethanol specimens for TEM examination were passed through propylene oxide (2 x 20 minutes). Specimens were then osmicated for 2h with a 1% and left overnight in a 50:50 mixture of popylene oxide and araldite. Following a single change to fresh araldite (5h with rotation) specimens were embedded and cured overnight at 60'C. Semithin and ultrathin sections were cut using a Leica ultracut S microtome fitted with the appropriate type of diamond knife. Following sequential contrasting with 1% uranyl acetate and lead citrate thin sections were viewed and photographed using a JEOL 1010 TEM operating at 80kV.

2.9.5.2 Scanning EM Specimens for SEM examination were critical point the third change of absolute alcohol, mounted on stubs and sputter coated dried after with gold prior to examination in a JEOL 6100 SEM operating at 15kV.

CHAPTER 3 RESULTS

3.1 EFFECT OF TGF-β ON CELLULAR EVENTS OF WOUND HEALING

3.1.1 ECM production in Human Tenon's Fibroblasts

3.1.1.1 Effect of TGF β2 on acid soluble collagen production by human Tenon's fibroblasts Stimulation with TGF β2 resulted in a dose dependent increase in soluble collagen production as shown in Figure 34. At a concentration of 1000pM TGF β2 increased collagen production by 148 % over serum free (basal) levels. The concentration at which TGF β2 displayed 50% of maximal stimulation (Effective Concentration 50, EC 50 was 41.7 (95% CI 14.6-118.9) pM. From these results a concentration of 100 pM TGF β2 (EC 90) was selected to investigate the effect of CAT-152 on TGF β2 stimulated soluble collagen production by human Tenon's fibroblasts. At a concentration of 100pM and above, TGF β2 stimulation significantly increased collagen production over basal levels ($p<0.05$).

3.1.1.2 Effect of TGF β2 on Type 1 Collagen production by human Tenon's fibroblasts Collagen type 1 C terminal peptide (CICP) released into the conditioned media from fibroblast monolayers during the soluble collagen assay (3.1.1.1) was quantified by ELISA. The results are displayed in Figure 35. A dose dependent increase in Type 1 collagen production was demonstrated in response to TGF β2 stimulation, which correlated closely to the effect of TGF β2 on soluble collagen production. Maximal stimulation was seen at a concentration of 1000pM TGF β2, which resulted in a 265.5% increase over basal levels. The EC 50 was calculated to be 12.3 (95% CI 1.3-121.4) pM. Analysis of variance statistics revealed that the effect of TGF β2 was significant ($p<$

0.0045; multiple comparisons: $p< 0.05$ 100pM and 300pM TGF β2, $p< 0.001$ 1000pM TGF β2).

3.1.2 Cytoskeleton and cell morphology

3.1.2.1 Effect of TGF β2 on α smooth muscle actin expression by human Tenon's fibroblasts To investigate the effect of TGF β2 on myofibroblast differentiation, an ELISA procedure was used to quantify α SMA expression by human Tenon's fibroblasts. Figure 36 shows that a proportional increase in α SMA expression was seen in the presence of TGF β2 ($p< 0.001$). Maximal stimulation was seen at a concentration of 1000pM TGF β2, which increased α SMA production by 200.8 % over serum free conditions. EC 50 was calculated to be 7.3 (95% CI 3.1-17.3) .The data was also analysed according to cell passage number at the time of seeding, where low passage experiments used cells at $p \leq 4$, and higher passage experiments used cells at $p > 4$. Figure 37 illustrates that cells at higher passage have increased expression of α SMA under serum free conditions. TGF β2 still upregulates α SMA production, however this additional effect of is not as pronounced. On the basis of these results low passage cells were stimulated with 30pM (EC 90) TGF β2 when investigating the effect of CAT-152 on myofibroblast differentiation.

3.1.2.2 Effect of TGF β2 on cell morphology and α smooth muscle actin stress fibre formation in human Tenon's fibroblasts The morphology of TGF β2 treated cells was observed by phase contrast microscopy at $t = 0$ and $t = 72$ hours. The cells appeared larger, less spindle shaped and adopted a contractile phenotype with intracellular stress fibres. These changes appeared to be related to the concentration of TGF β2 as shown in

Figure 38. Induction of α SMA and the assembly into stress fibres following TGF β2 treatment was confirmed using confocal immunofluorescence microscopy (Figure 39).

Figure 34 Effect of TGF β2 on acid soluble collagen production by human Tenon's fibroblasts.

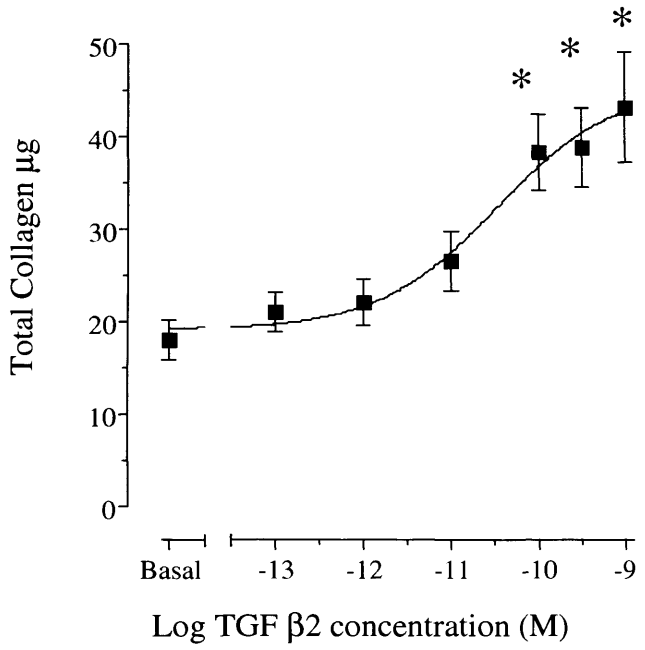

Mean soluble collagen production with respect to stimulation by TGF β2 at different concentrations at 48 hours. TGF β2 resulted in a dose dependent increase in soluble collagen deposition. Peak activity was seen at a concentration of 1000 pM TGF β2 with an associated 148 % increase in collagen production. * Significantly different to serum free conditions $p<0.05$. (Error bars represent standard error of the mean, n=7)

Figure 35 Effect of TGF β2 on collagen 1 production by human Tenon's fibroblasts.

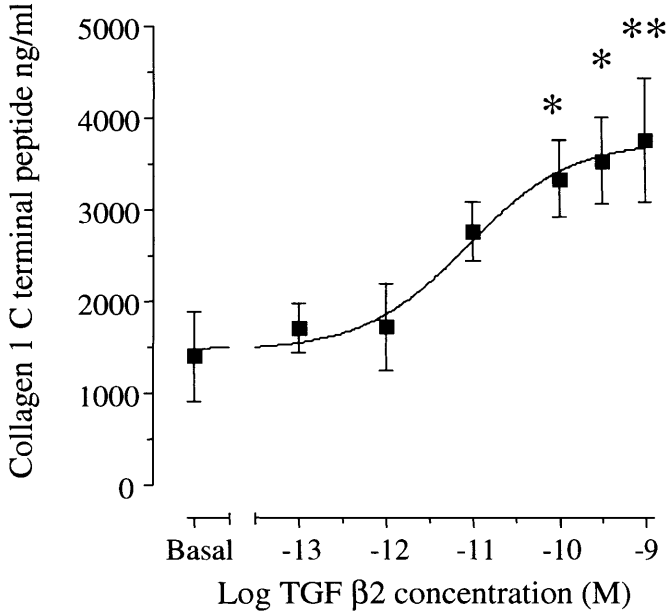

Mean type 1 collagen production with respect to stimulation by TGF β2 at different concentrations at 48 hours. TGF β2 resulted in a dose dependent increase in soluble collagen deposition. Peak activity was seen at a concentration of 1000 pM TGF β2 with an associated 265% increase over basal levels. Significantly different to serum free conditions * $p<0.05$, ** $p<0.01$ (Error bars represent standard error of the mean, n=4)

Figure 36 Effect of TGF β2 on α smooth muscle actin expression by human Tenon's fibroblasts.

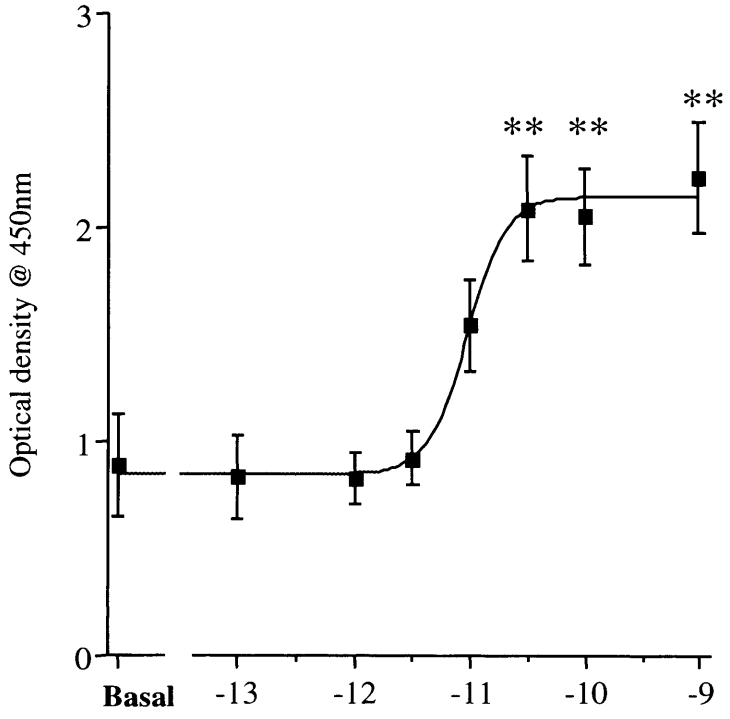

The α SMA content of cells was measured using an ELISA technique. TGF β2 induced a dose dependent upregulation of α SMA, which was significant over basal levels at concentrations of 30pM, 100pM and 100pM. **P< 0.001. Data are means +/- standard error of 5 experiments.

Figure 37 **Effect of cell passage number on α smooth muscle actin production in human Tenon's fibroblasts**

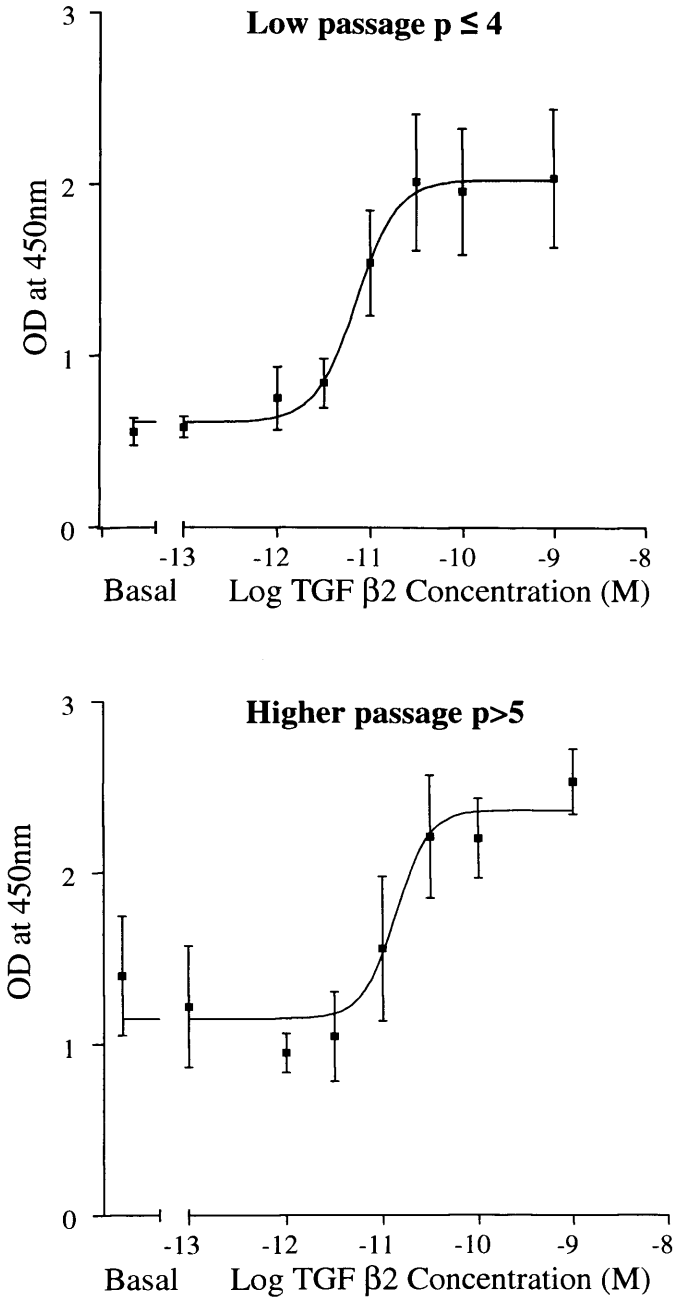

Basal α SMA expression was increased in cells of higher passage. TGF β2 still resulted in an increase in α SMA production, however this was less marked than in low passage cells. Maximal stimulation was seen at 1000pM and this was associated with a 374.9% and 190% increase over basal levels with low passage and higher passage cells, respectively.

Figure 38 Effect of TGF β2 on cell morphology

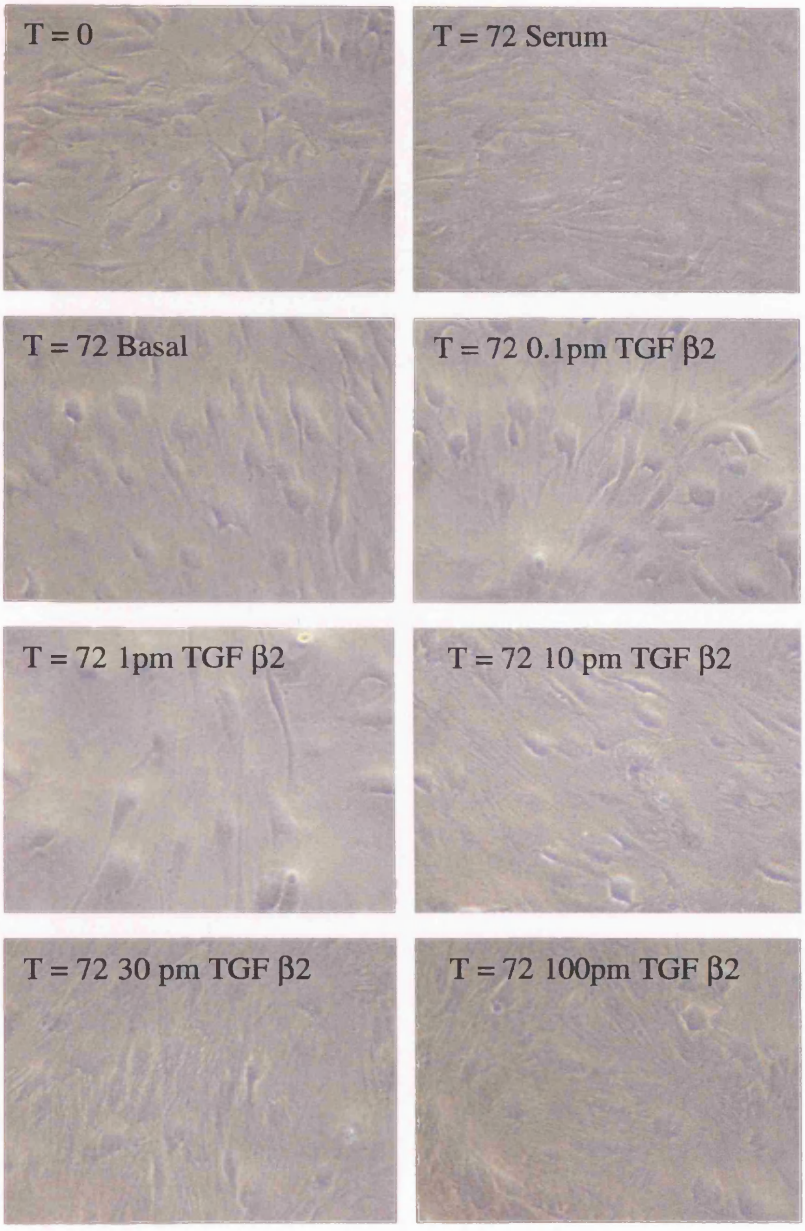

At concentrations of 10pM and above stimulation with TGF β2 was associated with intracellular fibre formation. Cells became less spindle shaped and there appeared to be a greater degree of cell/cell overlap

Figure 39 **Effect of TGF β2 on α smooth muscle actin stress fibre formation in human Tenon's fibroblasts.**

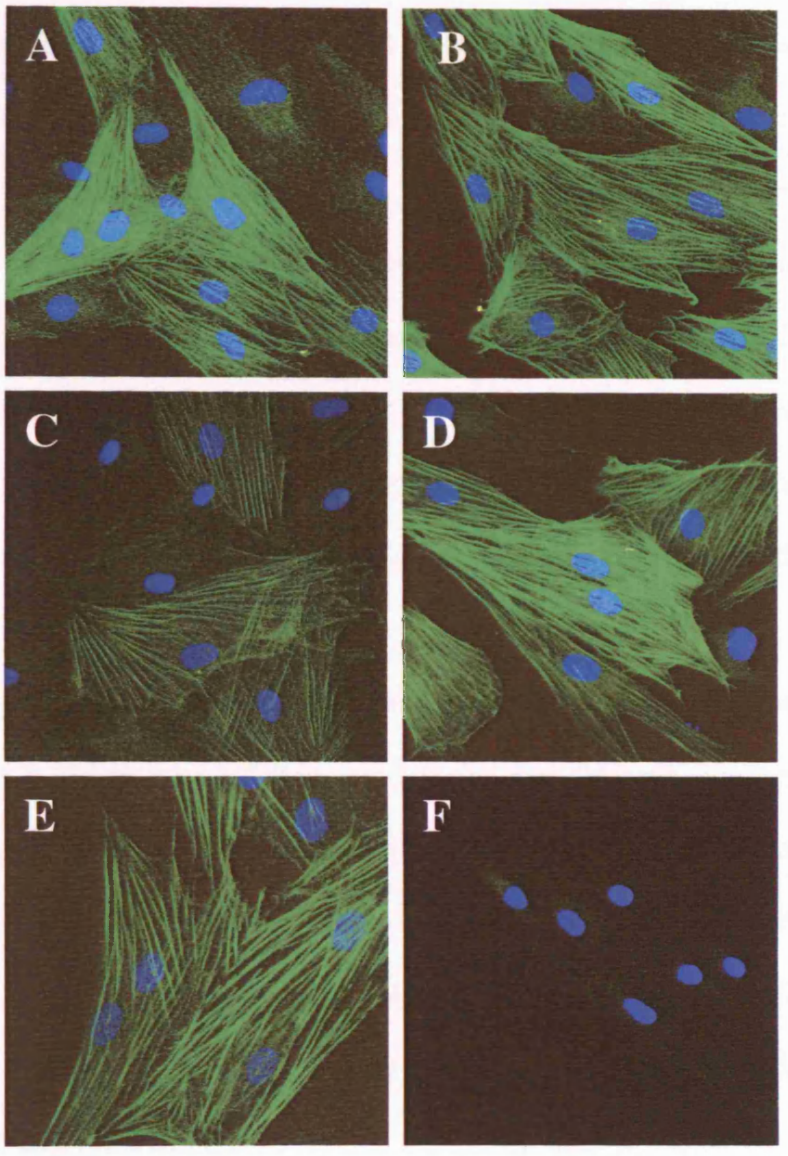

Confocal images of human Tenon's fibroblasts after stimulation with 10pM TGFβ2 (A and B) or 100 pM TGF β2 (C-E). F represents untreated control. A SMA is labelled with FITC (green) and the nuclei labelled with DAPI (blue). Images A-D and F are taken at a magnification of x 40. Images C-E are at x 60. TGF β2 induces the formation of intracellular αSMA stress fibres.

3.2 EFFECT OF CAT-152 ON TGF β MEDIATED CELLULAR EVENTS OF WOUND HEALING

3.2.1 ECM production in human Tenon's fibroblasts

3.2.1.1 Effect of CAT-152 on TGF-β2 mediated acid soluble collagen production The sircol assay for acid soluble collagen production was used to investigate the effect of CAT-152 on human Tenon's fibroblasts. The results are shown in Figure 40. CAT-152 resulted in a dose dependent inhibition of soluble collagen production. Complete inhibition of the TGF β2 response was achieved at concentrations of 10nM, 30nM and 100nM. However, because of the high seeding density for this assay and difficulty obtaining primary tissue from Moorfields Eye Bank it was only performed once. In addition the type I collagen ELISA was judged to be a more specific and accurate method of determining collagen production.

3.2.2.1 Effect of CAT-152 on TGF-β2 mediated Type 1 Collagen production The effect of CAT-152 on type 1 collagen production was determined using two methods. In the first experiment the conditioned media that had been generated from the sircol assay 3.2.1.1 was analysed (Figure 40). CAT-152 resulted in a dose dependent inhibition of soluble collagen production with complete inhibition of the TGF β2 response being achieved at concentrations of 10nM, 30nM and 100nM. Null antibody (CAT-001) had no effect on collagen production.

In the second set of experiments an independent CICP assay was performed, in which cells were seeded into 24 well plates at a density of 1 x 10^5 cells per well. Stimulation with 30 pM TGF β2 resulted in a mean increase in collagen production of 34 % over basal levels, which was lower than had been detected when the type I collagen had been

analysed from the conditioned media from the sircol assay (3.1.1.2). Application of CAT-152 achieved full inhibition of this TGF-β2 induced response. At concentrations of 10 nM and above CAT-152 reduced collagen production to below serum free levels and significantly inhibited the TGF β2 response compared to control antibody ($p<0.05$) (Figure 41). The concentration of CAT-152 to produce 50% inhibition of the TGF β2 response (Inhibitory Concentration 50, IC 50) was calculated to be 1.31 (CI 95% 0.36-4.86) nM.

3.2.2 Cytoskeleton and cell morphology

3.2.2.1 Effect of CAT-152 on TGF β2 mediated α smooth muscle actin expression by human Tenon's fibroblasts The increased expression of αSMA in response to TGFβ2 (30pM) was inhibited by CAT-152. This inhibition was related to the concentration of CAT-152 and attained statistical significance (Figure 42). CAT-152 30nM fully inhibited the response to TGFβ2 and CAT-152 had an IC_{50} of 1.54 (0.56-4.25) nM. CAT-001 (100nM) did not significantly affect the response to TGFβ2.

3.2.2.2 Effect of CAT-152 on cell morphology and α smooth muscle actin stress fibre formation in human Tenon's fibroblasts The morphology of TGF β2 stimulated cells after treatment with CAT-152 was observed by phase contrast microscopy at t = 0 and t = 72 hours. CAT-152 appeared to prevent the cells from adopting the morphological changes seen with isolated TGF β2 stimulation. At concentrations of 10nm and above the cells remained spindle shaped and minimal intracellular fibre formation was detected (Figure 43). Confocal immunofluorescence microscopy confirmed that CAT-152 prevented the assembly of α SMA into stress fibres (Figure 44).

Figure 40 **Effect of CAT-152 on acid soluble collagen production in human Tenon's fibroblasts**

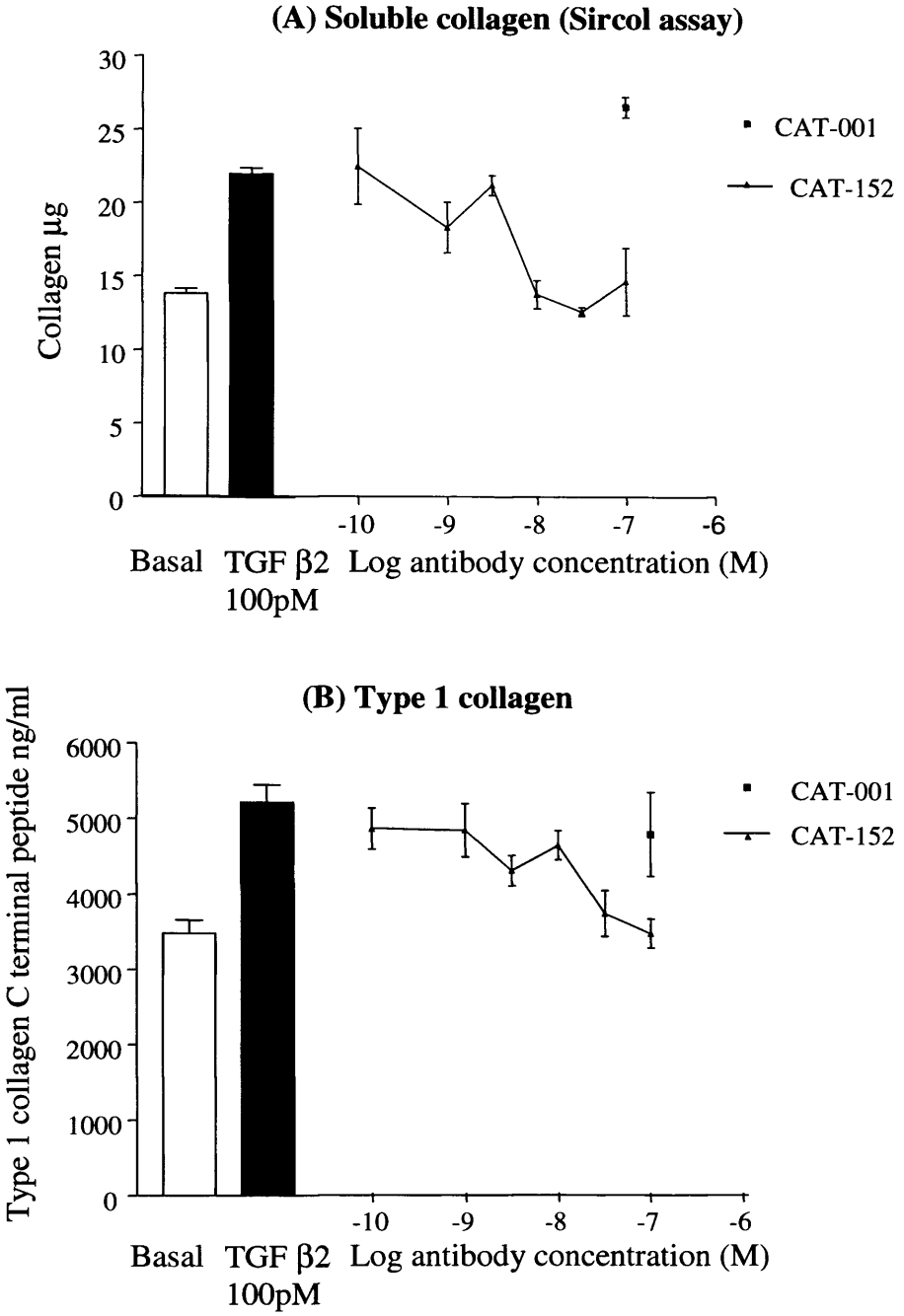

The effect of CAT-152 on TGF-β2 stimulated soluble collagen production was investigated using the sircol assay (Chart A, n=1). At concentrations of 10nM, 30nM and 100nM CAT-152 reduced collagen production to basal levels. The data in chart B represents the type 1 collagen production from the supernatant of the same experiment (n=1). A similar effect of CAT-152 was shown. Null antibody (CAT-001) did not reduce collagen production. Error bars represent the standard error of the triplicate samples per time point in N=1 experiment.

Figure 41 **Effect of CAT-152 on Type 1 Collagen production by human Tenon's fibroblasts.**

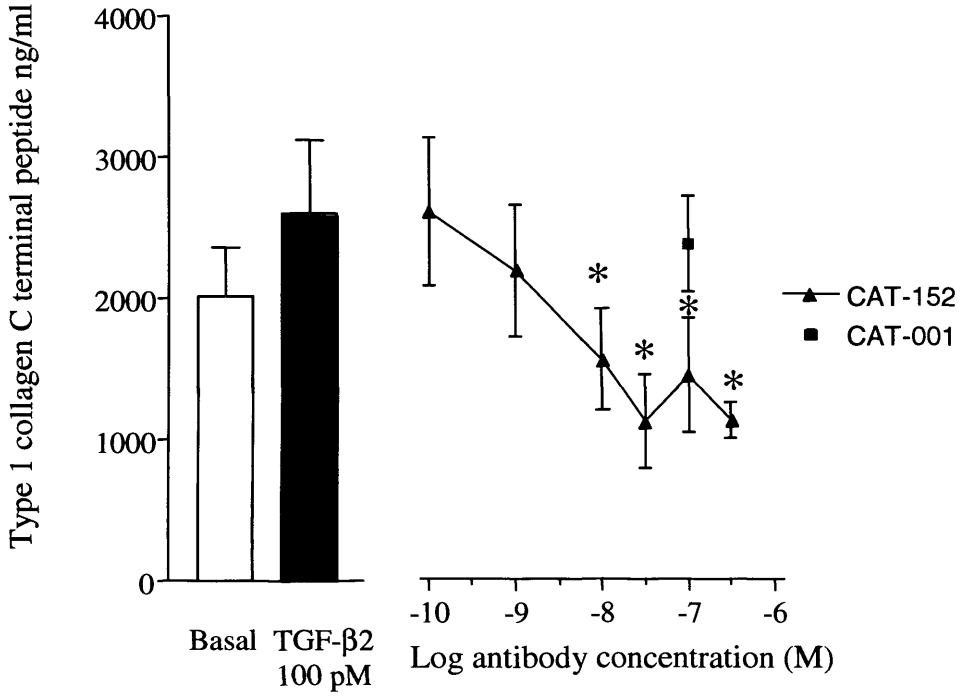

The effect of CAT-152 on Type 1 collagen production was assessed using the C terminal peptide ELISA. 30pM TGF β2 generated a 34% increase in collagen production that was completely inhibited by CAT-152. * significant reduction in TGF β2 response $p<0.05$ (Mean and Standard error plotted, n=4)

Figure 42 Effect of CAT-152 on α smooth muscle actin expression

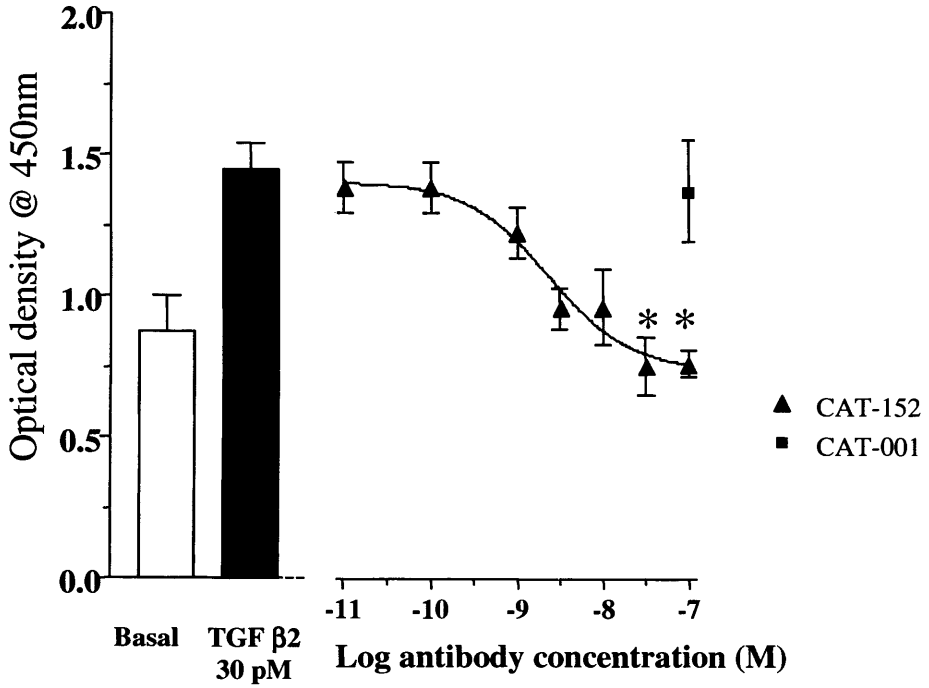

30 pM TGF β2 induced a mean increase of 75% over basal levels. CAT-152 application resulted in a dose dependent inhibition of α SMA production. The concentration of CAT-152 to produce 50% inhibition of the TGF β2 response (Inhibitory Concentration 50, IC 50) was calculated to be 2.079 nM +/- 0.776 nM. At a concentration of 30nM and 100nm CAT-152 significantly inhibited the TGF β2 response compared to control antibody ($p<0.05$).

Figure 43 **Effect of CAT-152 on the cell morphology of TGF β2 stimulated human Tenon's fibroblasts**

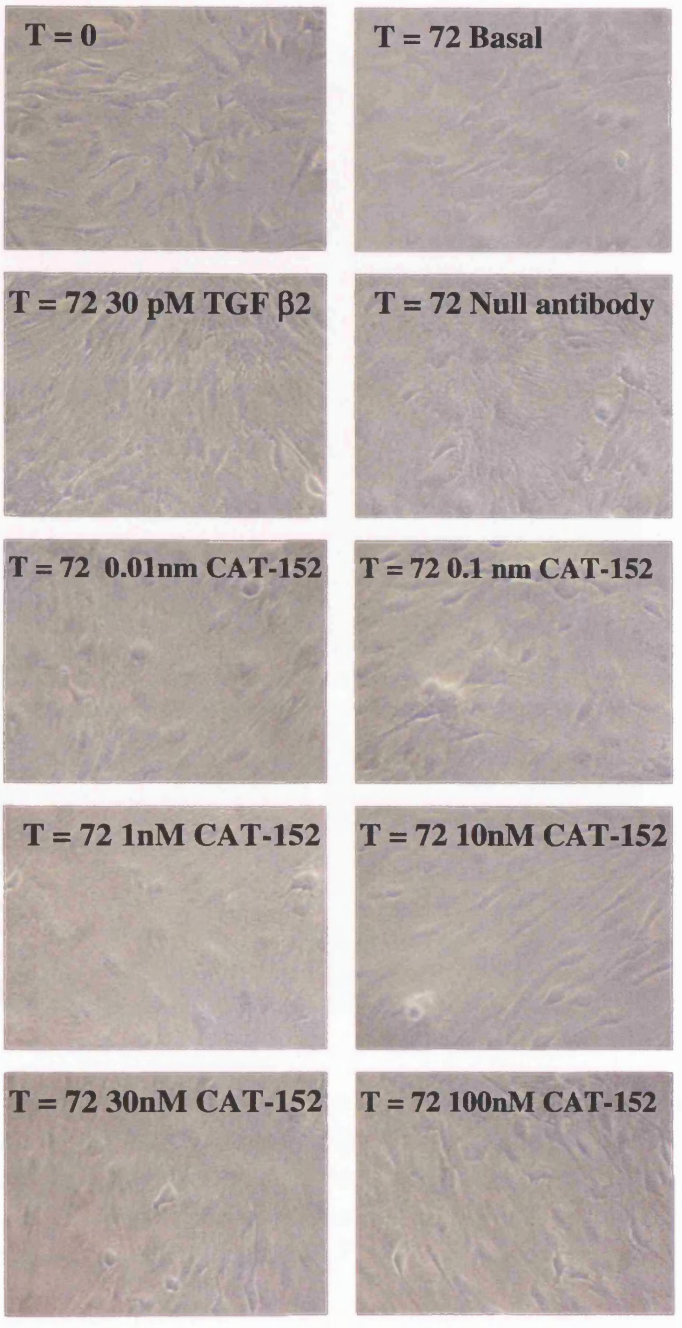

CAT-152 appeared to prevent the cells from adopting the morphological changes seen with isolated TGF β2 stimulation. At concentrations of 10nm and above the cells remained spindle shaped and minimal intacellular fibre formation was detected.

Figure 44 **Effect of CAT-152 on α SMA stress fibre formation in human Tenon's fibroblasts.**

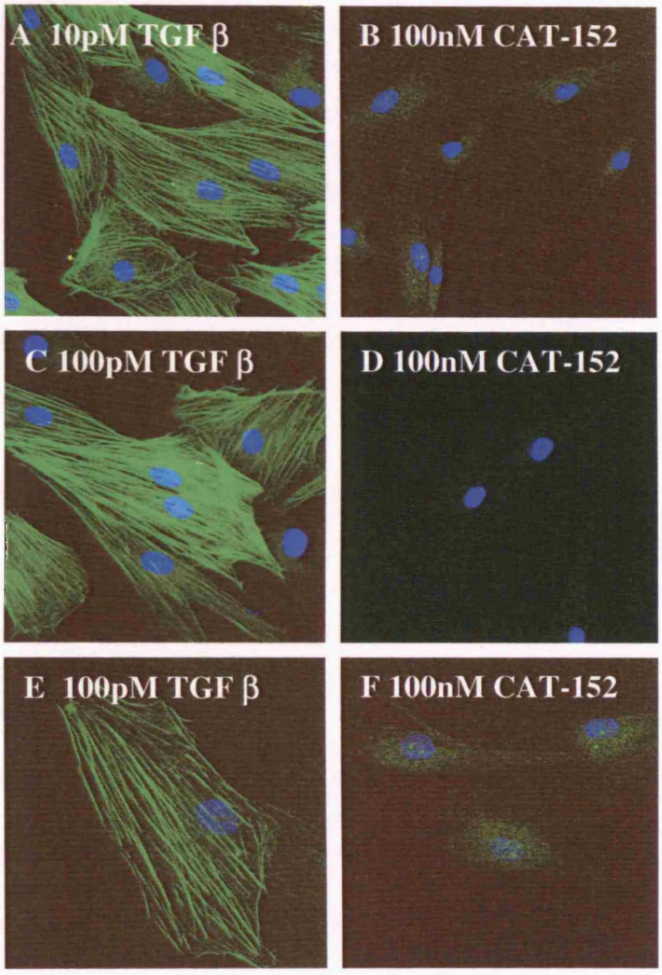

Confocal images of low passage human Tenon's fibroblasts stimulated with TGF-β2 labelled with FITC to demonstrate the presence of α SMA (green). The cells in B,D and F have also been treated with 15mg/ml (100nM) CAT-152. Neutralisation of TGF-β2 prevents the assembly of α SMA stress fibres. Magnification: Images A-D x 40, E and F x 60.

3.3 TEMPORAL AND SPATIAL EXPRESSION OF TGF β AND EXTRACELLULAR MOLECULES IN OCULAR RABBIT TISSUE AFTER GLAUCOMA FILTRATION SURGERY

3.3.1 mRNA expression in control eye tissue

The relative expression of mRNA encoding TGFβ1 and TGFβ2, collagen I, collagen III and α SMA was determined in tissues sampled from control (right) eyes that had not undergone experimental GFS. Data for each gene of interest were normalised relative to the expression level observed for the conjunctiva. Variation in TGF β1 mRNA expression across the tissues analysed was small, with greatest expression observed in the iris (rank order of expression; iris > ciliary body > conjunctiva > cornea > sclera). In contrast, the ciliary body appeared to express considerably greater levels of TGF β2 mRNA than all other tissues (rank order of expression; ciliary body >> iris > cornea > conjunctiva > sclera) (Figure 45).

Expression of collagen Types I and III was greatest in the conjunctiva. Small variation in Collagen I was demonstrated between tissues. Negligible levels of Collagen I and III were detected in the lens. α SMA was expressed most highly in the iris and ciliary body (approx 700-fold and 100-fold higher than conjunctiva respectively). Sclera showed similar α SMA levels to the conjunctiva while lower levels of α SMA mRNA were detected in the cornea and lens (Figure 46).

3.3.2 TGF β mRNA expression following experimental GFS

Relative expression of TGF β1 and TGF β2 mRNA was determined in tissues taken from CAT-152 treated, or untreated, rabbits that had undergone experimental GFS. For each

gene, data were normalised to the level of mRNA detected in control tissues obtained from unoperated eyes.

Conjunctival TGF β1 mRNA in samples from untreated animals was significantly increased at day 3 post-GFS ($P<0.05$ c.f. unoperated control conjunctiva). Although TGF β1 mRNA expression appeared to remain elevated at day 8 this was not significant ($P>0.05$) when compared with control tissues. Similarly, whilst there was a trend for a small increase in TGF β2 mRNA expression in conjunctiva at day 3 post-GFS, this was not statistically significant ($P>0.05$) (Figure 47).

As observed in conjunctival tissue, scleral TGF β1 mRNA expression was also significantly increased at day 3 post-GFS in samples from untreated animals ($P<0.001$ c.f. unoperated control sclera). There was no significant change in scleral TGF β2 mRNA expression at any other time point (all $P>0.05$ cf unoperated control sclera).

TGF β1 mRNA expression in the cornea was unchanged at all time points studied (all $P>0.05$). However, TGF β2 mRNA levels were significantly raised in corneal samples from untreated eyes at day 14 post-GFS ($P<0.05$ c.f. unoperated control cornea), but not at any other time point (Figure 47).

Expression of TGF β1 mRNA in post-GFS iris tissue was unchanged at most time points compared with control iris expression levels. However, a small but significant increase (i.e. 1.6-fold over control iris; $P<0.05$) in TGF β1 mRNA expression in samples from untreated animals was observed at day 1 post-GFS (Figure 47). At day 3 post-GFS, there was a small but significant ($P<0.01$) increase in TGF β2 mRNA expression in iris samples taken from untreated animals. Furthermore, at day 3 post-GFS CAT-152 TGF β2 mRNA expression levels were significantly lower than those observed in the untreated group. Thus, TGF β2 mRNA expression in the untreated and CAT-152 treated samples

was 1.83±0.26 –fold and 1.25±0.24 –fold that seen in control samples, respectively (both n=4; P<0.05) (Figure 47).

Ciliary body samples from untreated animals displayed significantly raised TGF β1 mRNA levels at day 3 post-GFS, compared to control samples (P<0.001). TGF β1 mRNA levels in samples taken at the same time point from CAT-152 treated animals were significantly lower. Thus, TGF β1 mRNA expression in untreated and CAT-152 treated samples at day 3 post-GFS was 1.87±0.05 –fold and 1.34±0.23 –fold that seen in control samples, respectively (both n=4; P<0.05). There was a small but significant increase in TGF β2 mRNA expression relative to control ciliary body samples in the untreated group samples at days 3 and 14 post-GFS (P<0.001 and P<0.05, respectively) (Figure 47).

Finally mRNA of collagen types I and III and α SMA was negligible in the lens both before and after experimental glaucoma surgery therefore accurate data on changes in expression could not be obtained.

Overall, the expression of TGF β1 and β2 in most of the tissues appears to follow the same temporal pattern. Levels rise to a peak on day 3 following surgery and then follow a step wise reduction back towards pre operative levels by day 14. This is clearly demonstrated in the conjunctiva (Figure 47).

3.3.3 ECM molecule mRNA expression following experimental GFS

Strong up regulation of α SMA was seen in conjunctiva following glaucoma surgery, over 100-fold increase compared to controls. Lower level of mRNA induction was also seen for collagen type III, collagen type I. However, on day 3 conjunctival collagen I mRNA expression was significantly increased compared to the control unoperated eyes (p<0.05). Increased levels of mRNA of α SMA and collagen III were seen in sclera

following glaucoma surgery, over 30-fold higher for α SMA (Day 3, $p< 0.001$) and over 10-fold for collagen III compared to controls (Day 3 $p<0.01$; day 8 $p<0.05$). No up regulation was seen in mRNA levels of collagen I. In the cornea strong up regulation of α SMA and collagen III was seen up to a maximum of around 100-fold increase on day 14. At this time point expression of collagen I ($p<0.01$) and collagen III ($p<0.001$) reached significance over controls. Weak up regulation of collagen type III mRNA was seen in the iris following glaucoma surgery. A 2-fold increase was seen compared to controls and this was significant on days 3, 8 and 14 ($p<0.01$). No evidence of up regulation was seen for collagen type I or α SMA. In the ciliary body samples GFS resulted in a 3-fold increase in collagen type III mRNA on day 3 ($p<0.001$) and day 14 ($p<0.01$). No evidence of up regulation was seen for collagen type I. A small but significant increase in α SMA expression was detected on day 1 (Figure 48).

As for TGF β, mRNA expression of collagen types I and III and α SMA was negligible in the lens both before and after experimental glaucoma surgery, therefore, accurate data on changes in expression could not be obtained.

Again, a temporal expression pattern was demonstrated across the tissues. This was most clearly demonstrated in the conjunctiva, where collagen I, III and α SMA expression peaked on day 3 and then followed a stepwise reduction by day 14 (Figure 48).

Treatment with CAT-152 significantly reduced corneal collagen III mRNA expression on day 3 ($p<0.01$). However, it does not appear to have had any other significant effects on the mRNA level of any of the genes tested in the other ocular tissues (Figure 48).

3.3.4 TGF β2 protein expression in aqueous humour

TGF β2 protein levels were determined in samples of aqueous humour taken from unoperated rabbit eyes at day 1 post-GFS (control), and from operated eyes at days 1, 3, 8, and 14 post-GFS. Separate determinations were made for levels of active TGF β2 and total TGF β2 (i.e. active plus latent) in the samples.

Total TGF β2 protein content of control rabbit aqueous humour samples in this study was 2363.9±289.4 pg/mL (n=6). There were significantly greater levels of total TGF β2 protein in samples taken from untreated animals at day 1 post-GFS (i.e. 4344.0±341.1 pg/mL, n=4; $P<0.01$ c.f. control) (Figure 49). Total TGF β2 levels were highest on day 1 and gradually returned to control levels by day 14, demonstrating a similar temporal pattern to mRNA expression. CAT-152 treatment was associated with a reduction in TGF β2 aqueous protein on days 1, 3 and 8, however, this did not reach significance. The level of active TGFβ2 protein in control samples of rabbit aqueous humour in this study was 1623.9±183.8 pg/mL (n=6). Active TGFβ2 protein levels were significantly lower in aqueous humour samples taken from untreated animals at days 1, 3 and 14 post-GFS (i.e. $P<0.01$, $P<0.05$ and $P<0.01$, respectively) (Figure 49). Statistical comparison of the day 8 post-GFS measurement could not be made because only a single sample was available for analysis. Treatment with CAT-152 reduced TGF β2 aqueous levels compared to untreated controls on days 1, 3 and 8. However, pair wise comparison of results between treatment groups did not highlight any significant effect of CAT-152 treatment.

3.3.5 Total TGF β2 protein expression in conjunctival bleb tissue after GFS

Conjunctival tissue samples were pooled for each treatment / sampling time point and assayed for total TGF β2 protein content only. Thus, expression of total TGFβ2 protein in control conjunctival tissue sampled from seven unoperated right eyes at day 1 post GFS was 5.60 pg/mg tissue. Statistical comparison of post-surgical TGF β2 expression in bleb tissues was not possible because data was obtained from pooled tissues (each containing 2-3 samples per treatment /time point). However, the results did highlight an apparent 16-fold increase in total TGF β2 protein content of conjunctival blebs taken from untreated animals (Figure 50).

Figure 45 Relative expression of TGF β in rabbit ocular tissue

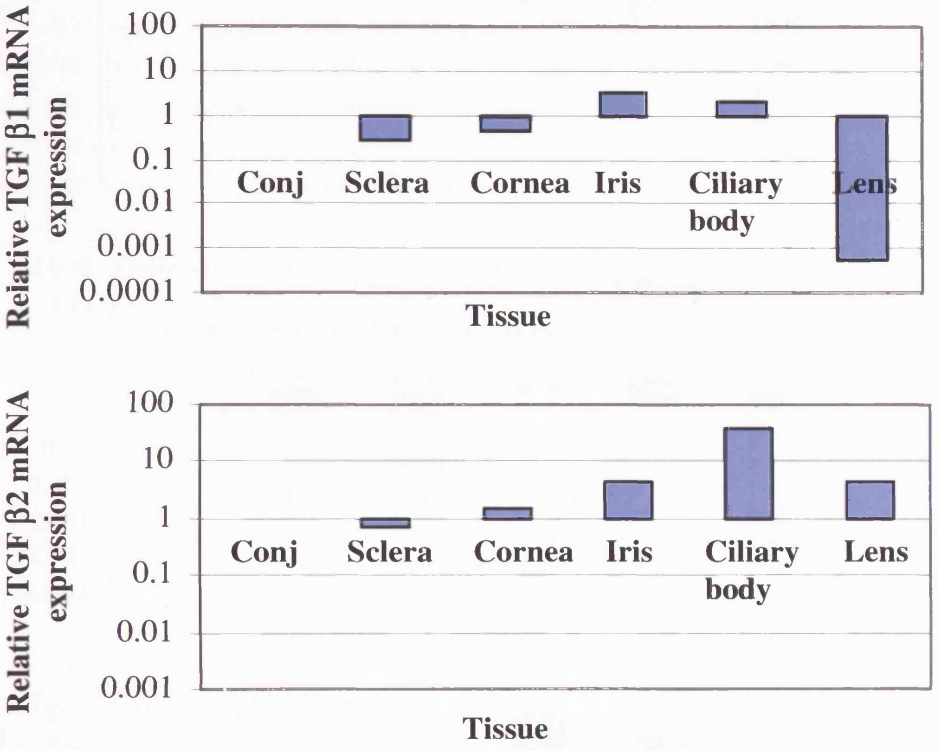

Data indicate mean relative mRNA expression calculated from 5 separate determinations. Each determination was performed using the RNA extracted from pooled samples of eight control tissues for each structure, taken from unoperated right eyes one day after experimental glaucoma filtration surgery. Samples were normalised to the expression in the conjunctiva. TGF β2 expression was greatest in the iris and ciliary body. Greater variation was seen in TGF β2 expression across the sampled tissues

Figure 46 Relative expression of ECM molecules in rabbit ocular tissue

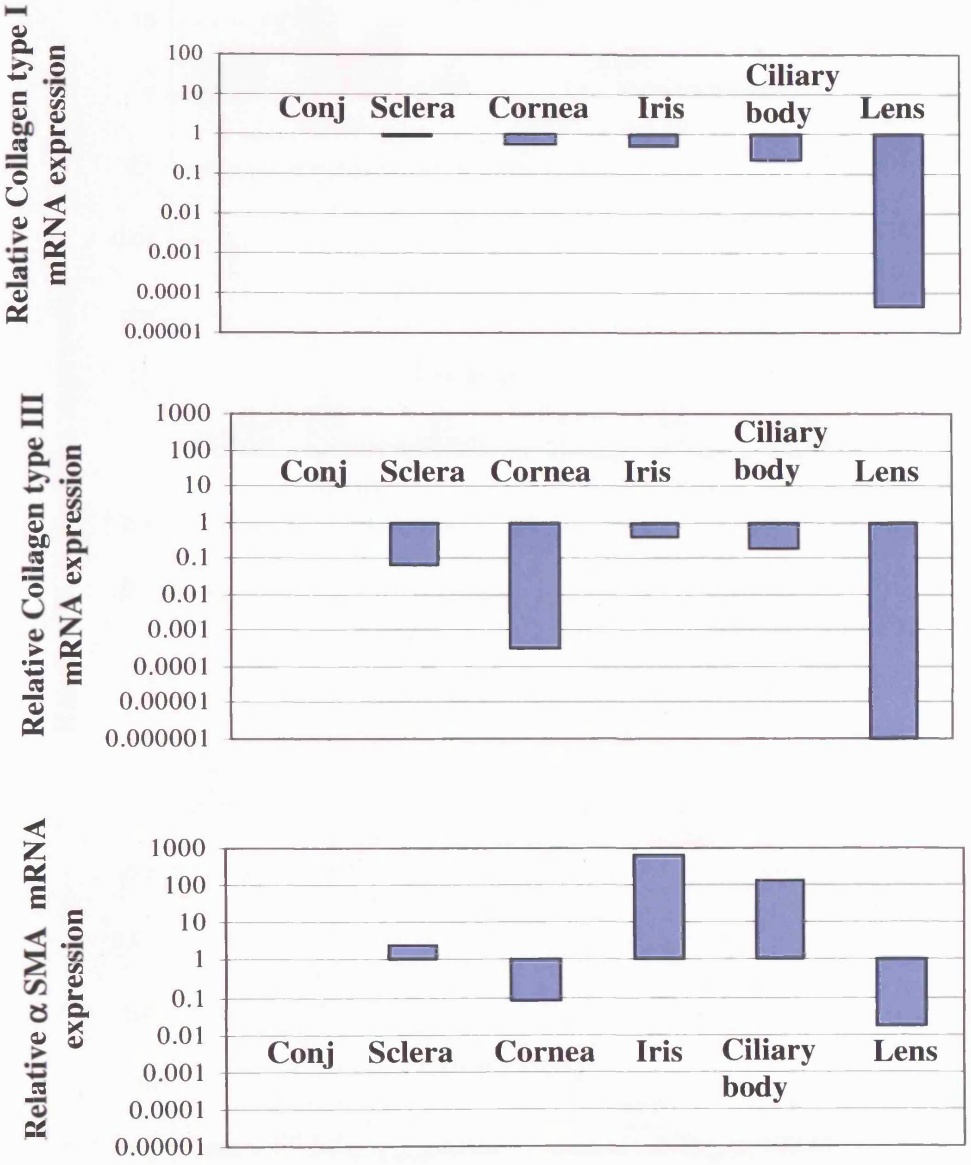

In order to evaluate relative expression of each gene within the different tissue of the control unoperated eye, samples were first normalised to expression in the conjunctiva. Expression of collagen Types I and III was shown to be greatest in the conjunctiva. Small variation in Collagen I was demonstrated between tissues. α SMA was expressed most highly in the iris and ciliary body.

Figure 47 TGF β mRNA expression in ocular tissues after GFS

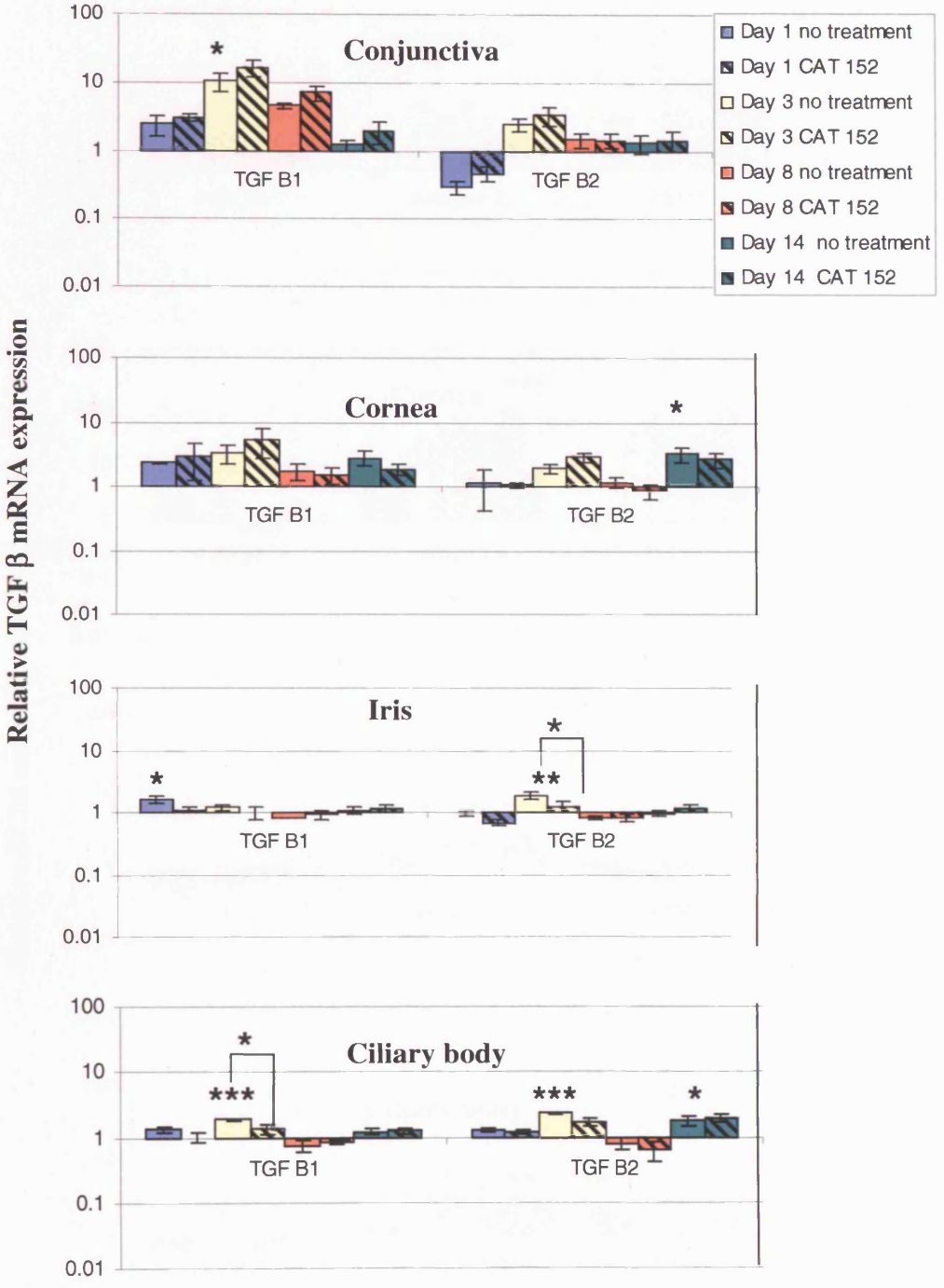

For each gene, data were normalised to the level of mRNA detected in control tissues obtained from unoperated eyes. Overall TGF β1 and β2 expression appeared to be increased following surgery. CAT-152 significantly reduced TGF β2 expression in iris tissue on day 3 and TGF β1 expression in the ciliary body on day 3. * $p<0.05$, ** $p<0.01$, *** $p<0.001$

Figure 48 ECM mRNA expression in ocular tissues after GFS

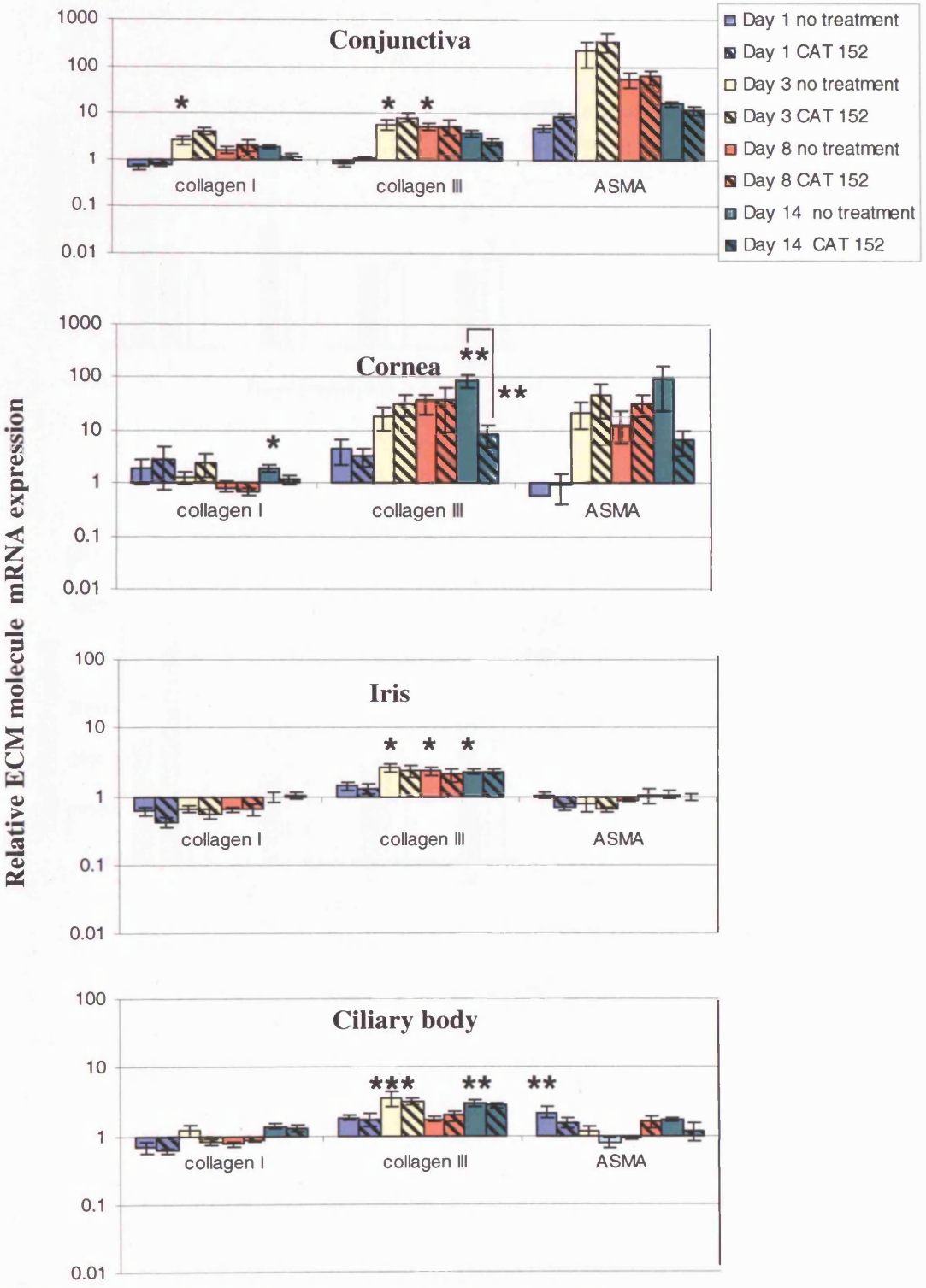

For each gene, data were normalised to the level of mRNA detected in control tissues obtained from unoperated eyes * $p<0.05$, ** $p<0.01$, *** $p<0.001$. ASMA represents alpha smooth muscle actin expression which acts as a marker of myofibroblast transformation.

Figure 49 TGF β2 protein levels in the aqueous humour following experimental glaucoma filtration surgery

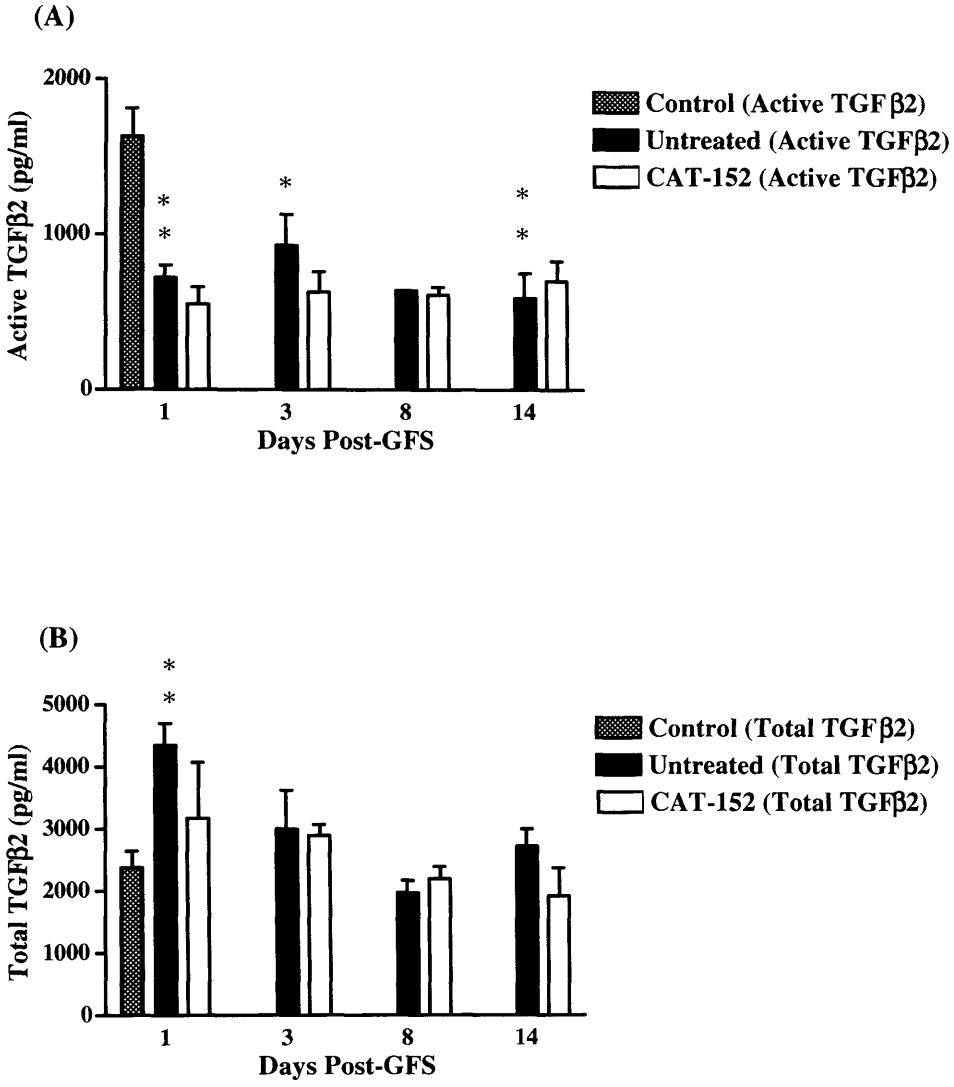

Figure 50 **TGFβ2 protein levels in conjunctival bleb tissue following experimental glaucoma filtration surgery**

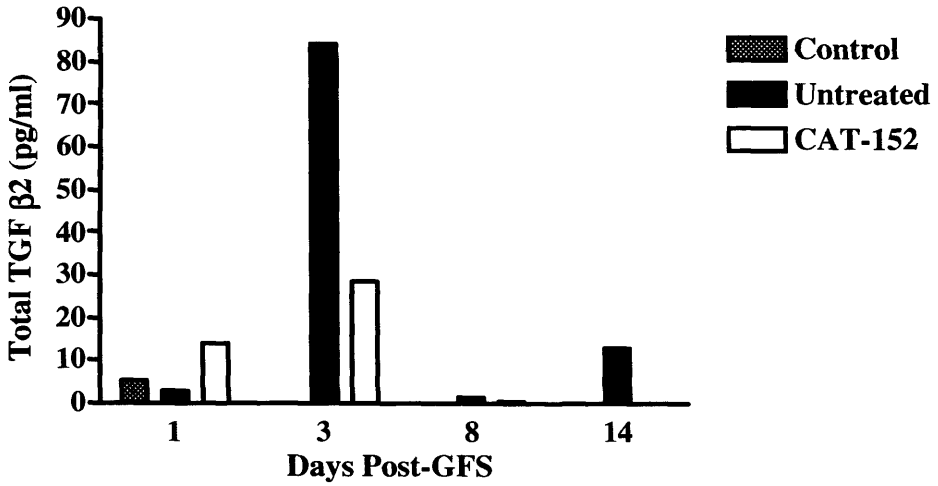

3.4 MODULATION OF THE WOUND HEALING RESPONSE IN VIVO: EFFECT OF ANTI TGF β2 ANTIBODY (CAT-152)

3.4.1 Effect of intra-operative CAT-152 on the outcome of Experimental Glaucoma Filtration Surgery

3.4.1.1 Bleb survival Using the single dose treatment regime CAT-152 was not found to significantly improve surgical outcome in this aggressive model of subconjunctival scarring. No significant advantage in bleb survival was shown with CAT-152 compared to control treatments as illustrated in the Kaplan-Meier curve in Figure 51. All blebs failed by day 21. Median bleb failure was 14 days after treatment with CAT-152, PBS and with no treatment (Table 9). These findings were consistent with previous studies using this model, in which untreated control animals most commonly fail around day 14.

3.4.1.2 Bleb Morphology All blebs were associated with normal conjunctival appearance and morphology (Figure 52). Subconjunctival scarring occurring at the filtration site causes flattening and a decrease in surface area of the bleb, important indicators of effective filtration surgery therefore include the bleb area and bleb height. Analysis of these variables using the repeated measures procedure by the generalized linear model did not reveal any statistically significant differences between the three groups (Bleb area p= 0.838, bleb height p= 0.598; Figure 51). These findings correspond to and are consistent with the absence of any effect of treatment on bleb failure across the groups.

3.4.1.3 Intraocular Pressure There was an initial rise in the IOP within the first 24 hours in most cases followed by a fall between days 2 to day 4. IOP failure, defined as the return of the IOP in the operated eye to the baseline level, was seen in 28 of the 30 rabbits by 10 days after the surgery. In the 2 remaining cases, both treated with CAT-152, the

IOP did not fail; this result however, did not reach statistical significance (p= 0.368). Analysis of mean intraocular pressure, in the surgical eyes during the entire study period, showed no significant differences between treatment groups over the entire study period ($p > 0.05$, Figure 53).

3.4.1.4 Side effects of treatment No drug related side effects were detected. Cytotoxic anti-scarring regimes use can result in non perfused, avascular areas in the locally treated tissues. These areas of avascularity are associated with thin walled, cystic blebs and the attendant risks of leakage and infection. All the rabbit eyes were studied for the presence of avascularity. In all the rabbits a small region of avascularity (< 3mm) was noted on the nasal side of the bleb, within the first 7 days. This was a transient finding and no significant increase in this variable was seen after treatment with CAT-152 compared to controls.

3.4.1.5 Tolerance Local reaction to CAT-152 injections was assessed by the degree of anterior chamber activity and conjunctival vascularity. No treatment was found to adversely influence either of these indicators of the inflammatory response. All treatments were safe and well tolerated (Figure 54).

Figure 51 Effect of intra-operative CAT-152 on bleb survival

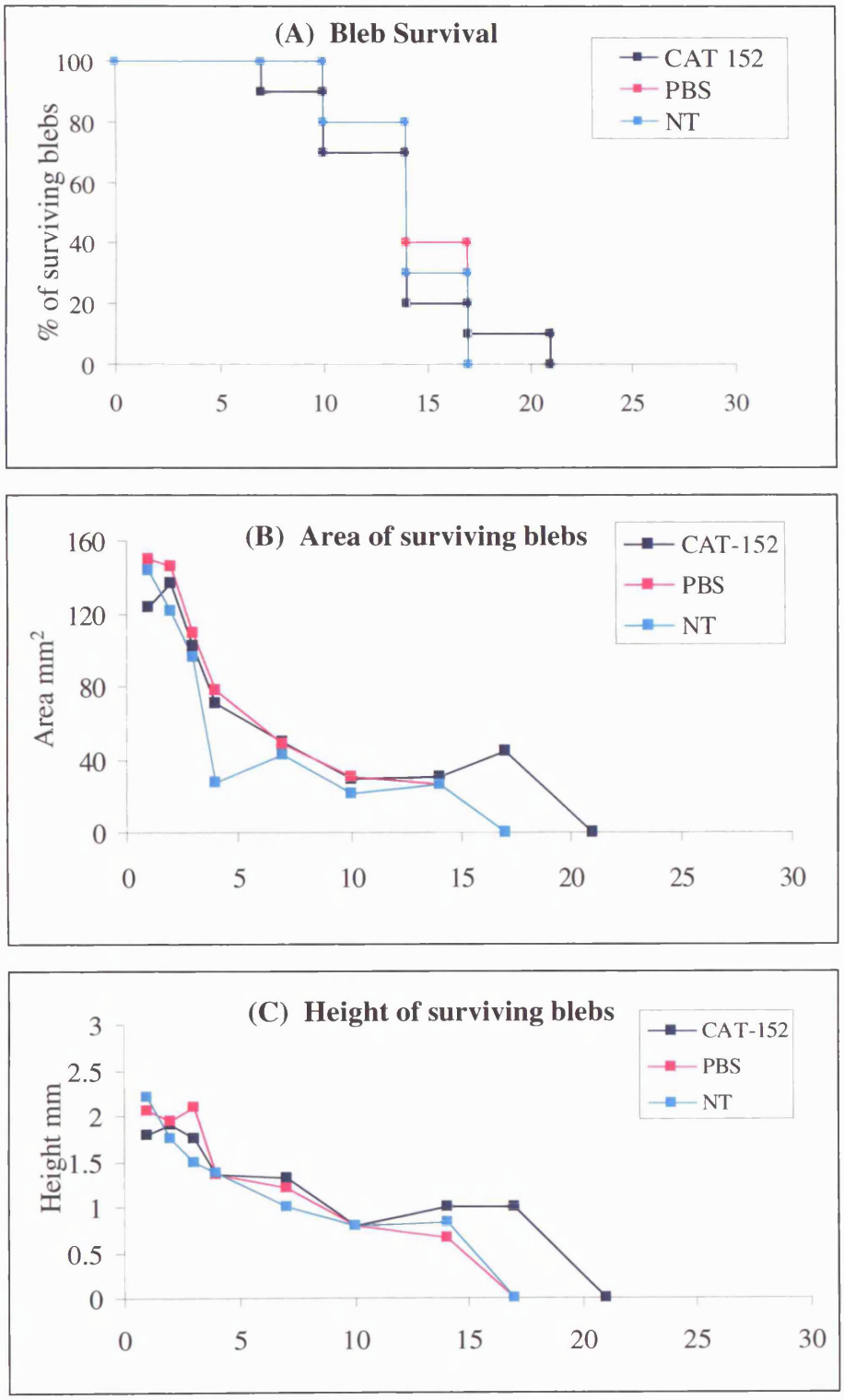

All blebs had failed by day 21 (A). Median bleb survival was 14 days after CAT-152, PBS or no treatment. No statistically significant differences were shown between the treatment groups for bleb survival (A; p= 0.8570), bleb area (B; p= 0.838) or bleb height (C; p=0.598).

Figure 52 Effect of intra-operative CAT-152 treatment on bleb morphology

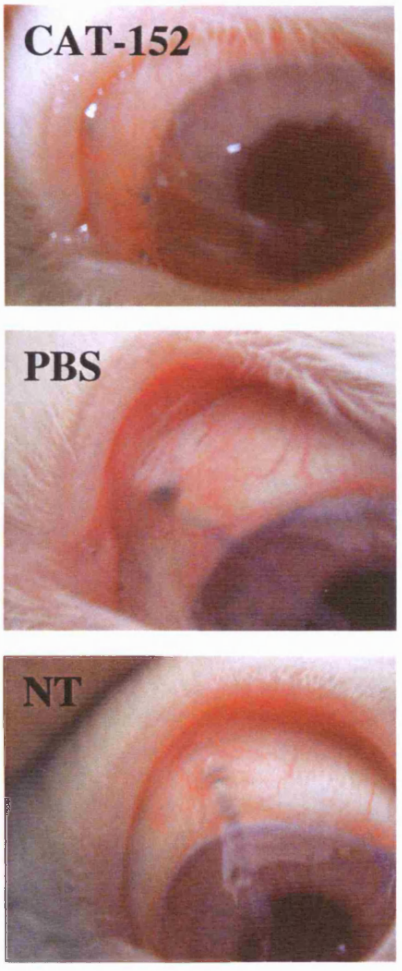

Bleb morphology on day 10 after surgery. CAT-152 treatment was well tolerated and normal conjunctival vascularity was preserved.

Figure 53 Effect of intra-operative CAT-152 treatment on intraocular pressure

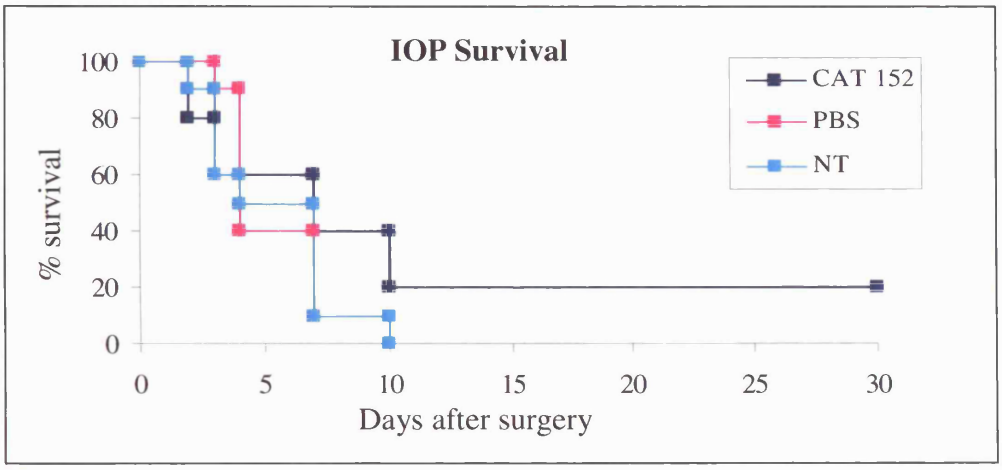

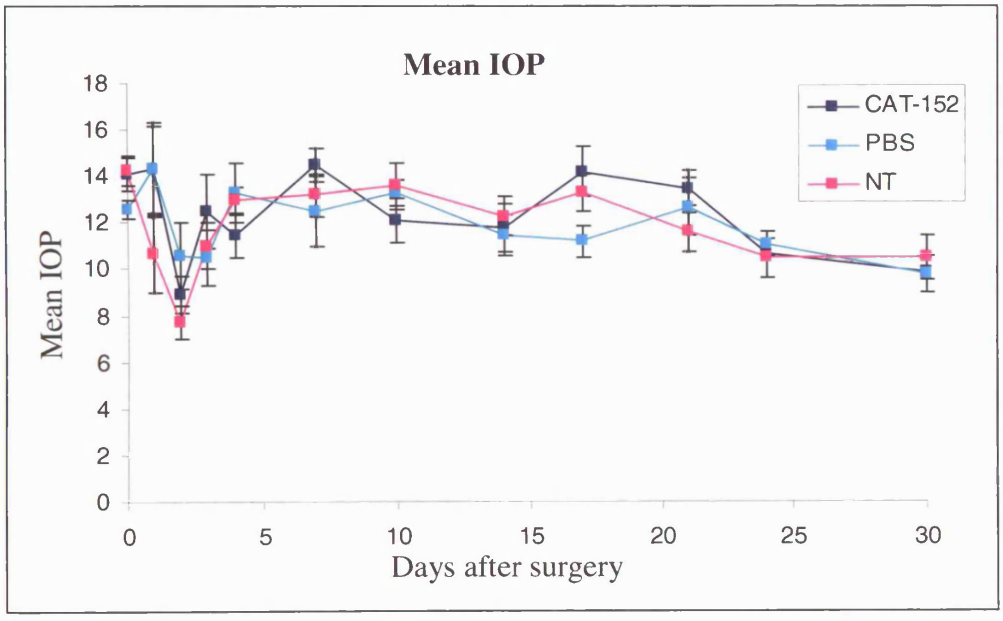

IOP failure was defined as return of the IOP to the pre-operative level. In two animals both treated with CAT-152, the IOP did not fail during the 30 day period ($p = 0.368$). However, no significant differences were seen in mean IOP at any time point ($p < 0.05$)

Table 9 Incidence of bleb failure and the percentage bleb survival in rabbits undergoing glaucoma filtration surgery with intra-operative CAT-152

Treatment	Days after Surgery							Survival 30 days
	0	7	10	14	17	21	30	/ n
CAT-152	**0**	**1**	**2**	**5**	**1**	**1**	**0**	**0 / 10**
% survival	*100*	*90*	*70*	*20*	*10*	*0*	*0*	
PBS	**0**	**0**	**2**	**4**	**4**	**0**	**0**	**0 / 10**
% survival	*100*	*100*	*80*	*40*	*0*	*0*	*0*	
No Treatment	**0**	**0**	**2**	**5**	**3**	**0**	**0**	**0 / 10**
% survival	*100*	*100*	*80*	*30*	*0*	*0*	*0*	

Bleb survival: Log rank Statistics and (significance)

Treatment	**CAT-152**	**PBS**
PBS	0.24 (0.6235)	
NT	0.05 (0.8198)	0.13 (0.7162)

Figure 54 **Effect of intra-operative CAT-152 on conjunctival vascularity after glaucoma filtration surgery**

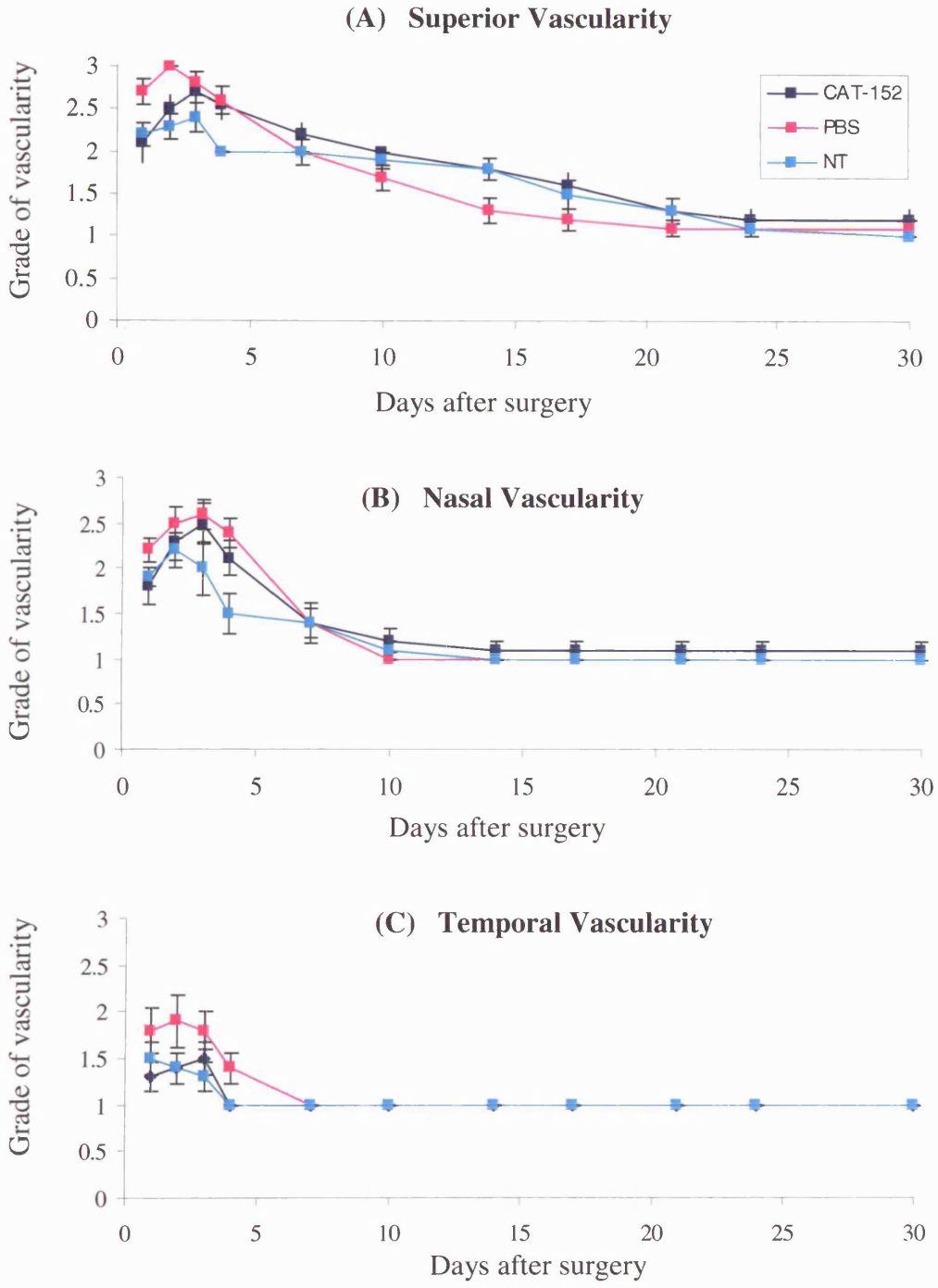

All treatments were well tolerated. Conjunctival injection was graded according to severity (Grade 1= normal vascularity, grade 2= hyperaemic, grade 3= very hyperaemic). No significant differences in this variable were detected between treatment groups during the 30 day study period (Nasal conjunctival p= 0.453, superior conjunctiva p= 0.524, temporal conjunctiva p= 0.07)

3.4.2 Effect of prolonged post-operative application of CAT-152 on subconjunctival scarring after experimental glaucoma filtration surgery: Comparison with 5-Fluorouracil.

3.4.2.1 Experimental details Of the 24 rabbits observed for the duration of the 30 day experimental period, 23 completed the experimental protocol. One animal was observed to be developing signs of severe intraocular infection 3 days after surgery. The rabbit was sacrificed and an independent observer (to preserve masking) identified that the animal was in the control group. Observational analysis was therefore performed on 8 animals that received CAT-152, 8 animals that received 5-FU and 7 untreated control animals.

3.4.2.1 Bleb survival CAT-152 was found to significantly improve glaucoma filtration surgery outcome in this animal model of aggressive post-surgical scarring. CAT-152 significantly prolonged bleb survival compared to the 5-FU group and the untreated control group as shown in the Kaplan Meier survival curve in Figure 55 (Log rank statistics P = 0.0009). The rate of bleb failure and percentage survival in each treatment group is shown in Table 10. Interesting, subgroup analysis of the log rank statistic showed CAT-152 significantly improved surgical survival compared to both 5FU and NT, however 5FU did not have a significant effect over the NT group (Table 10). All the blebs in the control and 5-FU groups had failed by day 22, however 62.5% of the CAT-152 treatment group had functioning blebs. By day 30 all but one of the operations had failed; the only animal with a functioning bleb had received CAT-152. The median (range) survival rates were 23.5 (20-30), 20 (16-22) and 16 (14-21) days in the CAT-152, 5-FU and control groups, respectively (Figure 56).

3.4.2.2 Bleb morphology The presence of a well formed bleb is an important indicator of effective filtration. Subconjunctival scarring causes contraction and flattening of the bleb. Figure 57 shows the typical appearances of the filtration blebs on days 10, 21, 30. Treatment with CAT-152 was associated with elevated, diffuse, fleshy looking blebs compared to the flat scarred blebs in the other groups. Analysis of both bleb area and bleb height using the repeated measures of the generalized linear model, revealed significant difference in both these variables after treatment with CAT-152 compared to 5-FU or no treatment regimens (Figure 55 $P<0.005$ Area; $P<0.001$ Height: Figure B and C).

3.4.2.3 Intraocular Pressure Analysis of IOP survival or mean intraocular pressure in the surgical eyes showed no significant differences between treatment groups over the entire study period ($P>0.05$). (Figure 58)

3.4.2.4 Side effects of treatment Corneal epitheliopathy is a recognized adverse effect associated with the clinical use of 5-FU and is associated with both ocular discomfort and the risk of infection. Given this, a grading system was included in the methods to assess the severity of this variable. In this experiment only mild punctuate staining of the cornea (superficial punctuate keratitis, grade 1) was detected in all treatment groups and this was a transient finding. Observations for corneal epitheliopathy were started on day 1 after surgery. During the procedure a superior corneal traction suture is used to position the globe. This results in a transient epithelial defect which would be present in all animals and heals over 24 hours. The duration of the staining however, was significantly longer in the 5-FU treated group ($P<0.01$). The duration of staining in the CAT-152 group was similar to that observed in the no treatment control group (Table 11, Figure 59).

One of the features of existing cytotoxic anti-scarring regimes is their production of non perfused, avascular areas in locally treated tissues. These areas of avascularity are associated with thin walled, cystic blebs and the attendant risks of leakage and infection. In all the rabbit eyes a small region of avascularity was noted in the nasal side of the bleb (<3mm), within the first 7 days. This was transient finding. The duration of the avascular segment tended to be longer in the 5-FU treated animals but this did not reach statistical significance (P=0.159). The duration of avascularity in the CAT-152 group was similar to that observed in the no treatment control group (Table 11).

3.4.2.5 Tolerance Local reaction to treatment was assessed by the degree of anterior chamber inflammation and conjunctival vascularity. No significant difference was found between treatment groups for either of these indicators of the inflammatory response (GLM: vascularity, superior P=0.402, temporal P=0.434, nasal P=0.668; anterior chamber inflammation P=0.430: Figure 60)

3.4.2.6 Anterior Chamber Observations The depth of the anterior chamber was assessed as an indirect indicator of drainage. On day 1 after surgery the anterior chamber was flat in most of the animals. Over the next 7 days the anterior chamber gradually deepened. No significant difference was found between the treatment groups in the time taken for the anterior chamber to deepen (P=0.302).

3.4.2.7 Histological effects

The histological grading system was used to identify changes in cellularity (H and E), total scar tissue deposition (Picrosirius Red), collagen fibre density and orientation (Gamoris Trichrome), elastic fibre deposition (oxidative aldehyde fuschin) and myofibroblast transformation (α SMA expression) between the treatment groups over the study period.

CAT-152 treatment reduced scarring at a microscopic level. The greatest histological difference between treatment groups was seen on day 10 (Figure 61). At this time point total scar formation, as judged by the staining characteristics of picrosirius red, was significantly reduced by CAT-152 treatment (P=0.01, Figures 61 and 62). In addition CAT-152 significantly reduced the population of cells expressing α smooth muscle actin, indicating less fibroblast differentiation into the myofibroblast phenotype. α SMA staining was performed by two different methods, using a DAB detection method and also with a fluorescent labelled antibody. Both these methods detected similar trends in the expression of α SMA in the post-operative wound site (Figures 63 and 64). No other significant differences were found between treatment groups in total cellularity, elastic fibre deposition or PCNA at day 10 (Figure 61 and 65).

The number of proliferating and total cell population was maximal in the early stages and reduced over time (Figure 66 A, B and F). Collagen fibre deposition peaked at day 10, whilst differences in collagen fibre orientation were most apparent by day 21 (Figure 66 C and D). High levels of elastic fibres were seen at all time points with maximum deposition by day 21 (Figure 66 E).

By day 30 subconjunctival scarring at the wound site consisted characteristically of densely packed collagen and fibroblasts. In contrast, the only surviving CAT-152 treated bleb showed much looser architecture with visible conjunctival bleb formation (Figure 67). Clinical observation of bleb failure correlated well with the degree of conjunctival scarring as shown in Figure 68 with higher levels of scar tissue were found in failed blebs.

3.4.2.8 Electron Microscopy We compared electron microscopic (EM) characteristics of CAT-152 treated animals and untreated controls. Morphologically

scanning EM demonstrated looser subconjunctival bleb architecture with CAT-152 treatment (Figure 69 A, C, E). At a cellular level, transmission EM showed a corresponding reduction in inflammatory cell infiltrate and collagen fibril formation within the blebs of CAT-152 treated animals (Figure 69 : compare E and F).

Figure 55 Effect of post operative treatment on bleb survival and bleb morphology

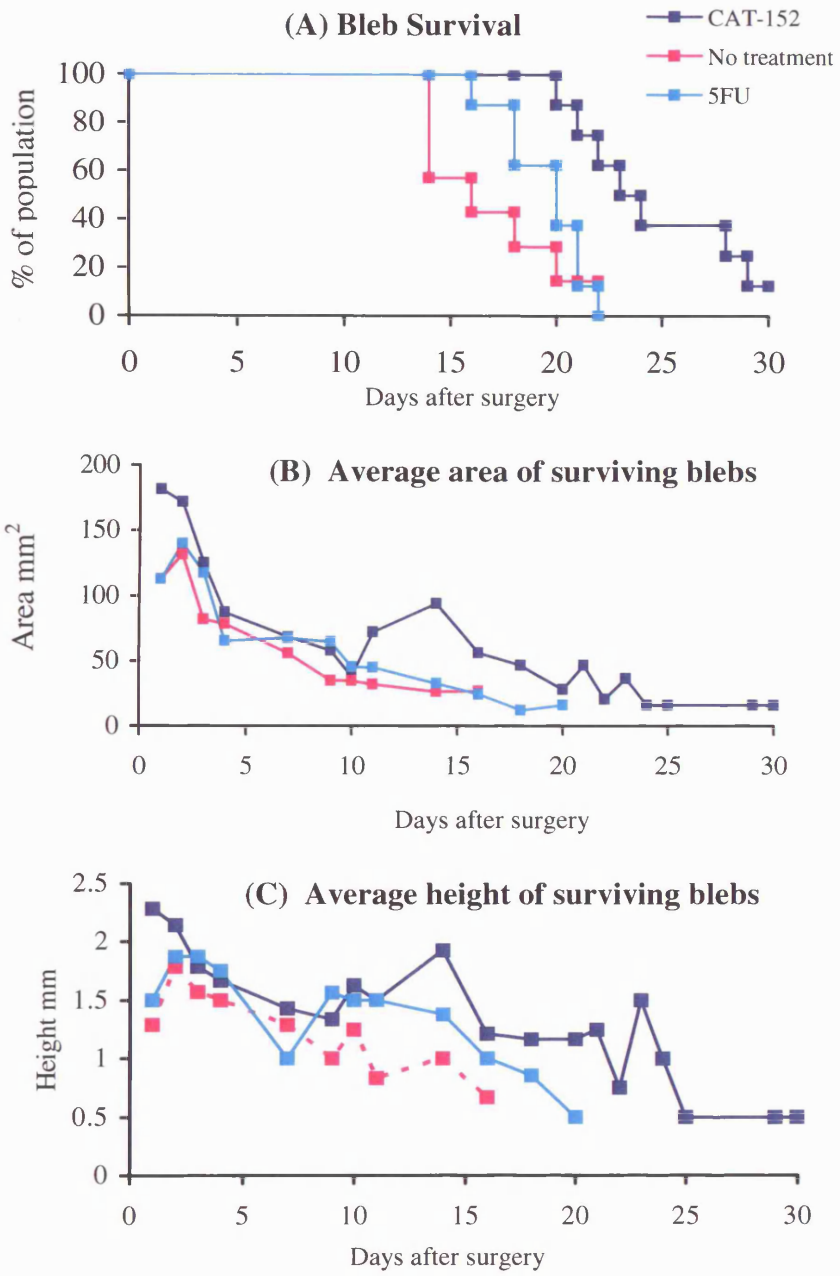

The effect of CAT-152 (n=8), 5-FU (n=8) or no treatment (n=7) on A) bleb survival, B) bleb area and C) bleb height. CAT-152 significantly prolonged bleb survival compared to 5-FU and the untreated control group as shown in the Kaplan Meier survival curve (P=0.0009 Log rank statistics). CAT-152 treated eyes had significantly larger blebs (area and height, $P<0.05$).

Table 10 Incidence of bleb failure and the percentage bleb survival in rabbits undergoing glaucoma filtration surgery: Effect of CAT-152 and 5-FU treatment compared to control.

Treatment	Days after Surgery												Survival 30 days
	0	14	16	18	20	21	22	23	24	28	29	30	/ n
CAT-152	0	0	0	0	1	1	1	1	1	1	1	0	1 / 8
% survival	*100*	*100*	*100*	*100*	*87.5*	*75*	*62.5*	*50*	*37.5*	*25*	*12.5*	*12.5*	
5-FU	0	0	1	2	2	2	1	0	0	0	0	0	0 / 8
% survival	*100*	*100*	*87.5*	*62.5*	*37.5*	*12.5*	*0*	*0*	*0*	*0*	*0*	*0*	
No Treatment	0	3	1	1	1	1	0	0	0	0	0	0	0 / 7
% survival	*100*	*57.1*	*42.9*	*28.6*	*14.3*	*0*	*0*	*0*	*0*	*0*	*0*	*0*	

Bleb survival: Log rank Statistics and (significance)

Treatment	**CAT-152**	**NT**
NT	10.55 (0.0012)	
5FU	8.94 (0.0028)	1.28 (0.2576)

Figure 56 The effect of post-operative treatment on Bleb survival

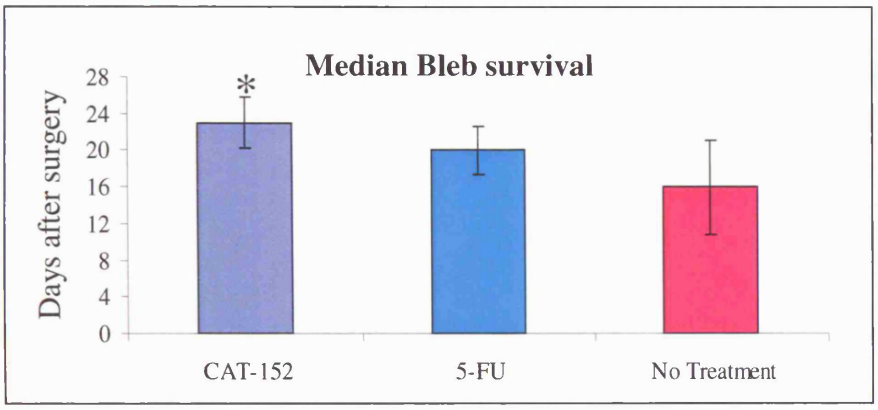

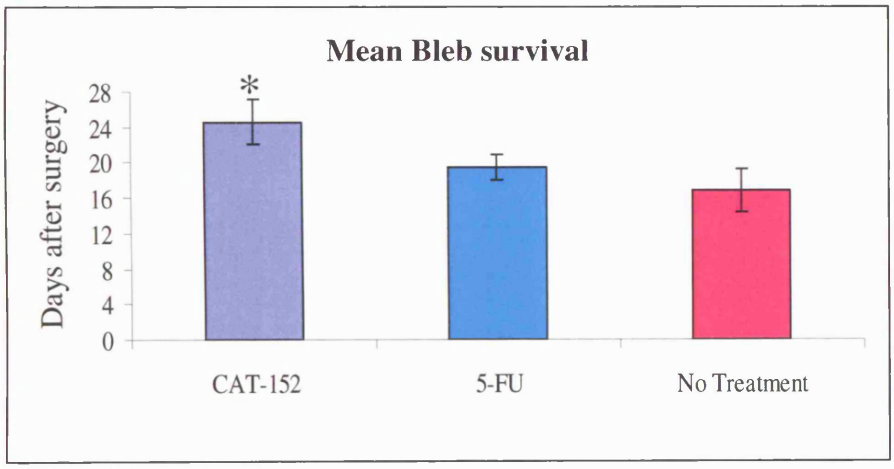

Median bleb survival in the CAT-152 treated group was 23 days compared to 16 in the untreated group and 20 after 5-FU application. On average CAT-152 prolonged mean bleb survival by 5.1 and 7.7 days compared to treatment with 5-FU or no treatment, respectively. (* $P < 0.05$)

Figure 57 Effect of Post-operative treatment on bleb morphology

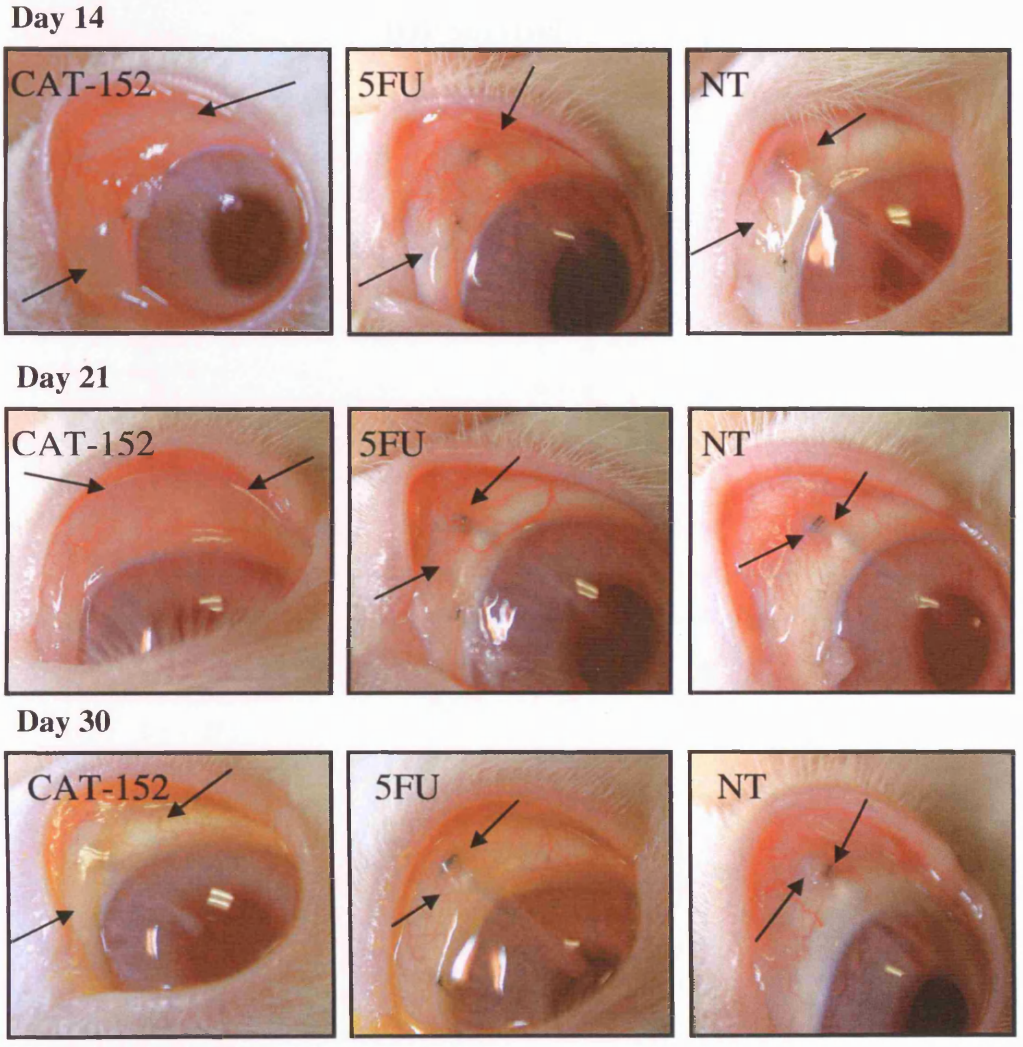

Bleb morphology on days 10, 21 and day 30 after glaucoma filtration surgery. One representative animal is shown per group. Animals were treated with either CAT-152 or 5-FU or received no treatment. Treatment with CAT-152 was associated with elevated, diffuse, fleshy looking blebs compared to the flat, scarred blebs in the 5-FU and control groups. (Black arrows demarcate the bleb border and the white arrow shows the cannula.)

Figure 58 Effect of post-operative treatment on intraocular pressure after glaucoma filtration surgery

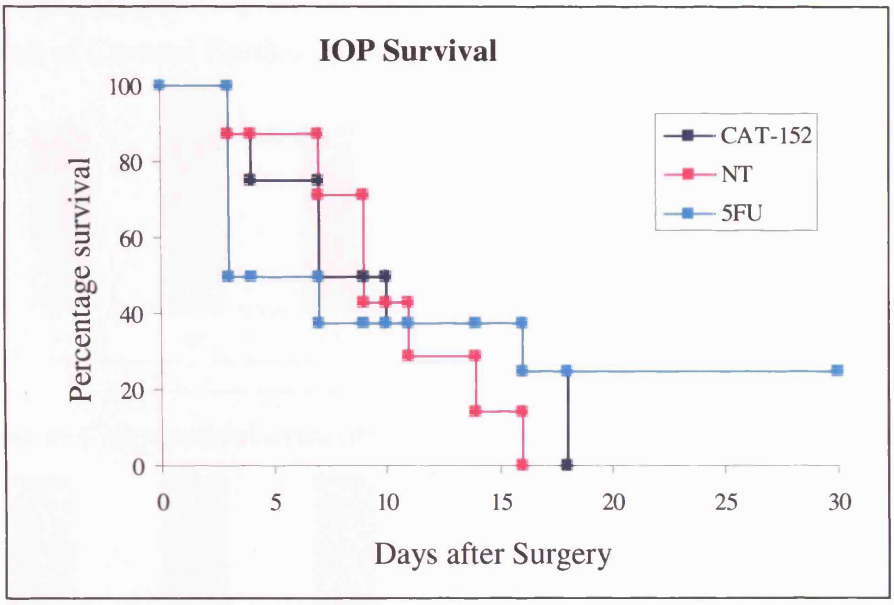

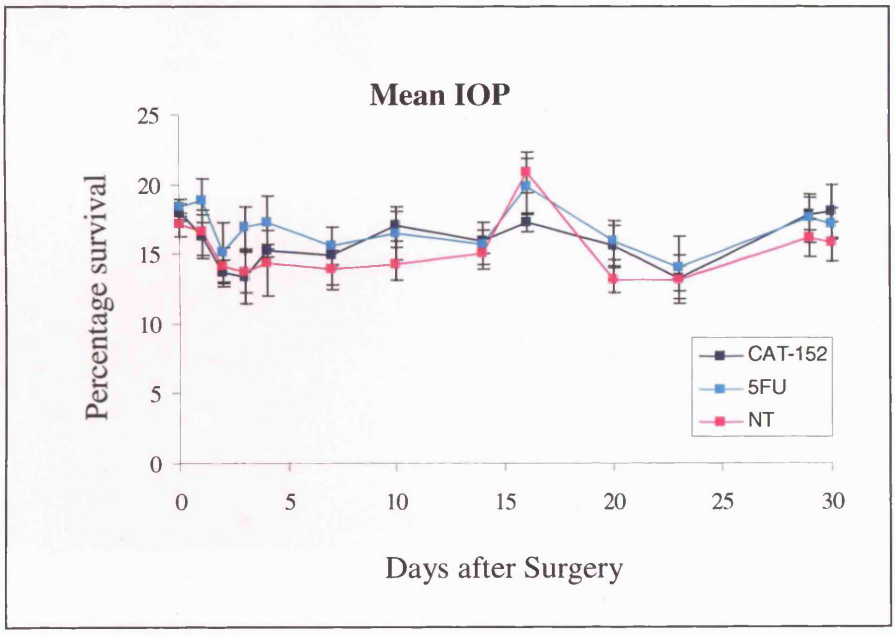

No significant differences in intraocular pressure were found between treatment groups in terms of IOP Survival (Return of IOP to pre-operative baseline) or mean IOP. (Error bars represent standard error of the mean)

Figure 59 Side effects associated with post-operative treatment

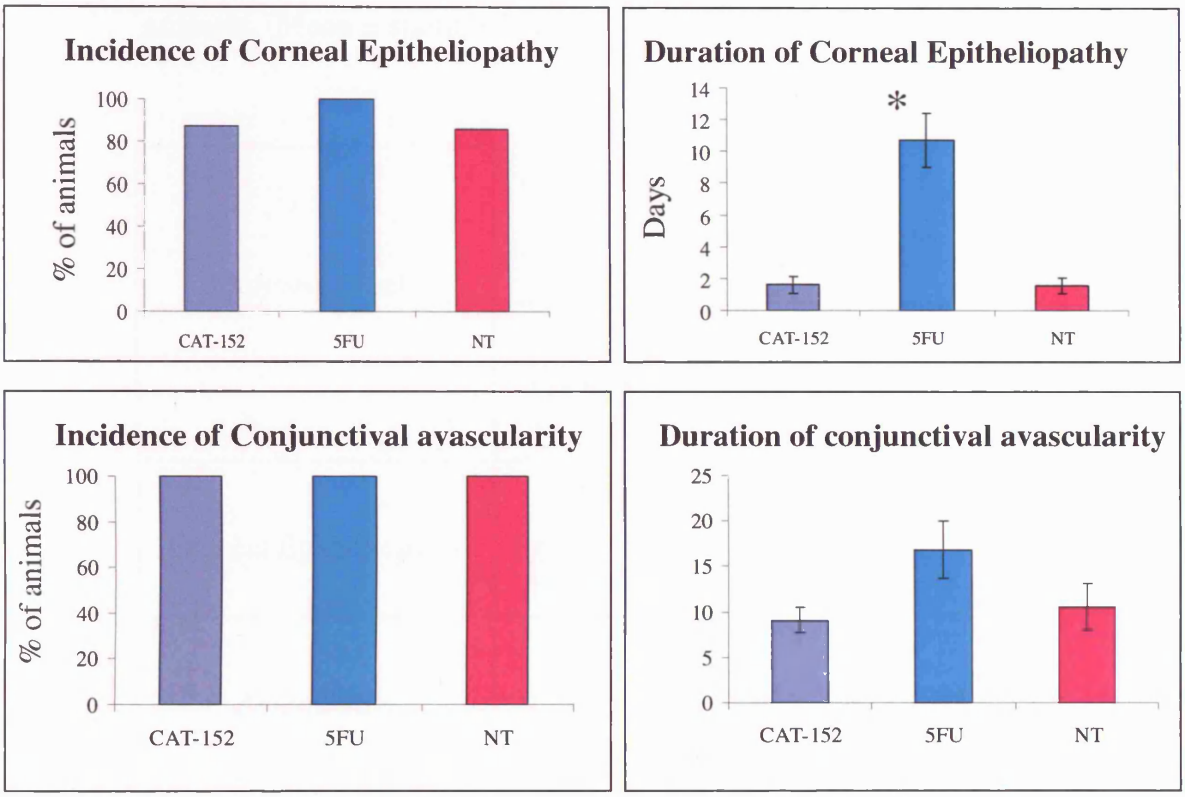

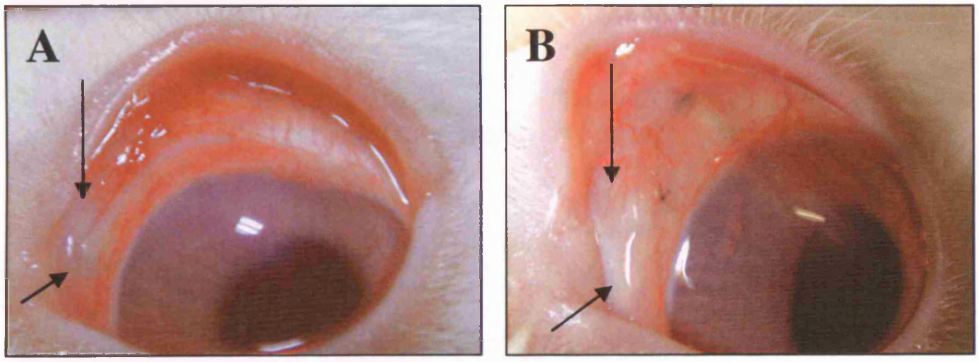

In all the rabbit eyes a small region of avascularity was noted in the nasal side of the bleb (<3mm), within the first 7 days as shown in image A. This was a transient finding. The duration of the avascular segment tended to be longer in the 5-FU treated animals but this did not reach statistical significance (P=0.159). The black arrows demarcate area of nasal conjunctival avascularity

Table 11 Duration of low grade corneal epitheliopathy or avascularity following treatment with CAT-152 or 5-FU compared to the no treatment control animals. (Mean ± standard error)

Adverse event	Duration of effect (days)		
	CAT-152	5FU	NT
Corneal Epitheliopathy	1.63 ± 0.53	10.71 ± 1.71*	1.57 ± 0.48
Avascularity	9.13 ± 1.33	16.88 ± 3.2	10.57 ± 2.5

* $P < 0.01$ comparing CAT-152 or 5-FU treatment groups to the no treatment group using Kruskal-Wallis test and Dunn's test. NT = no treatment group.

Figure 60 **Effect of Post operative treatment on conjunctival vascularity after glaucoma filtration surgery**

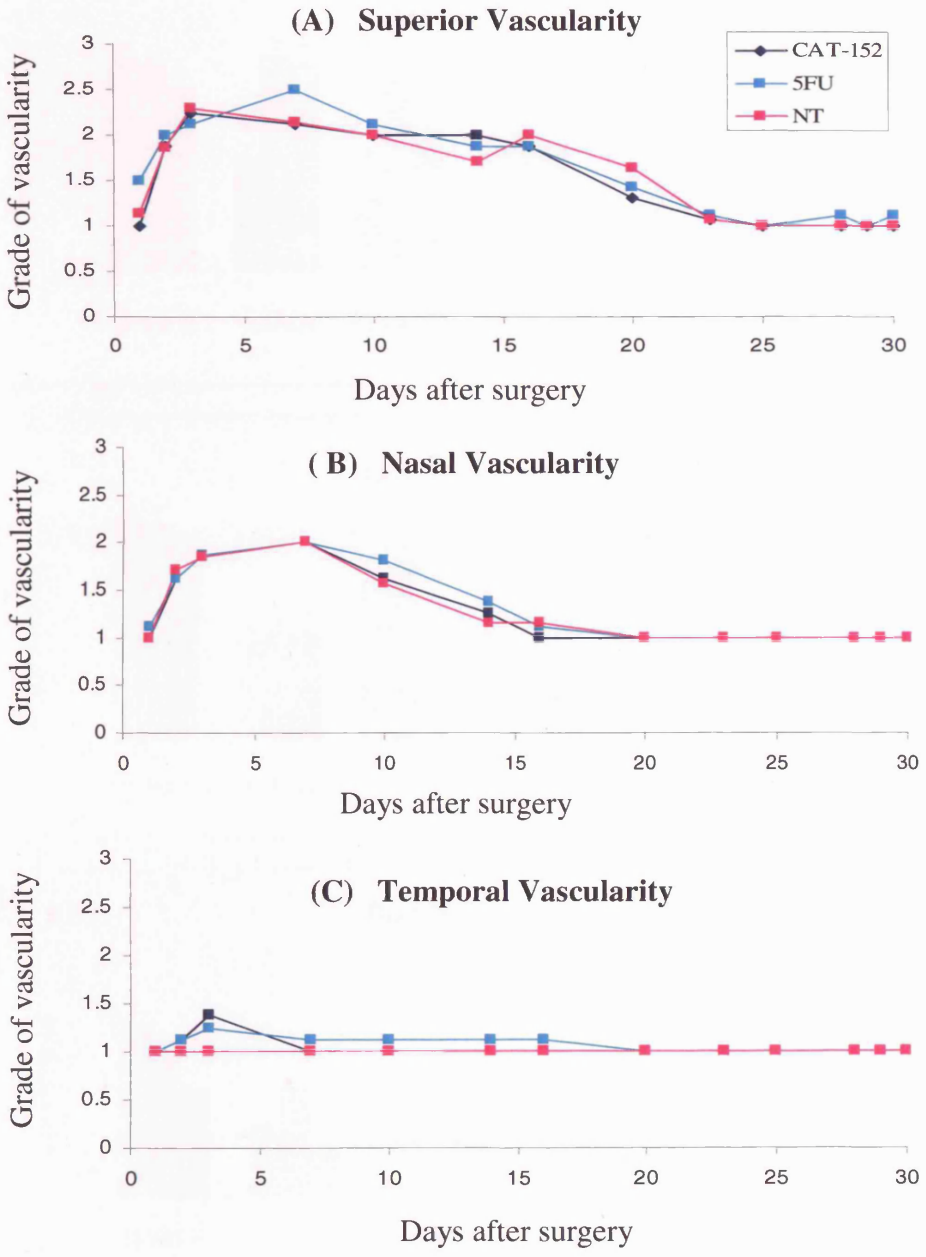

Analysis of the mean grade of vascularity is shown in charts A-C. No significant differences were detected between the three treatments in terms of conjunctival vascularity. Superior P=0.402, temporal P=0.434, nasal P=0.668; Grade 1 Normal, Grade 2 hyperaemic, Grade 3 extensive hyperaemia.

Figure 61 **Effect of post-operative treatment on the different elements of the scarring response after glaucoma filtration surgery**

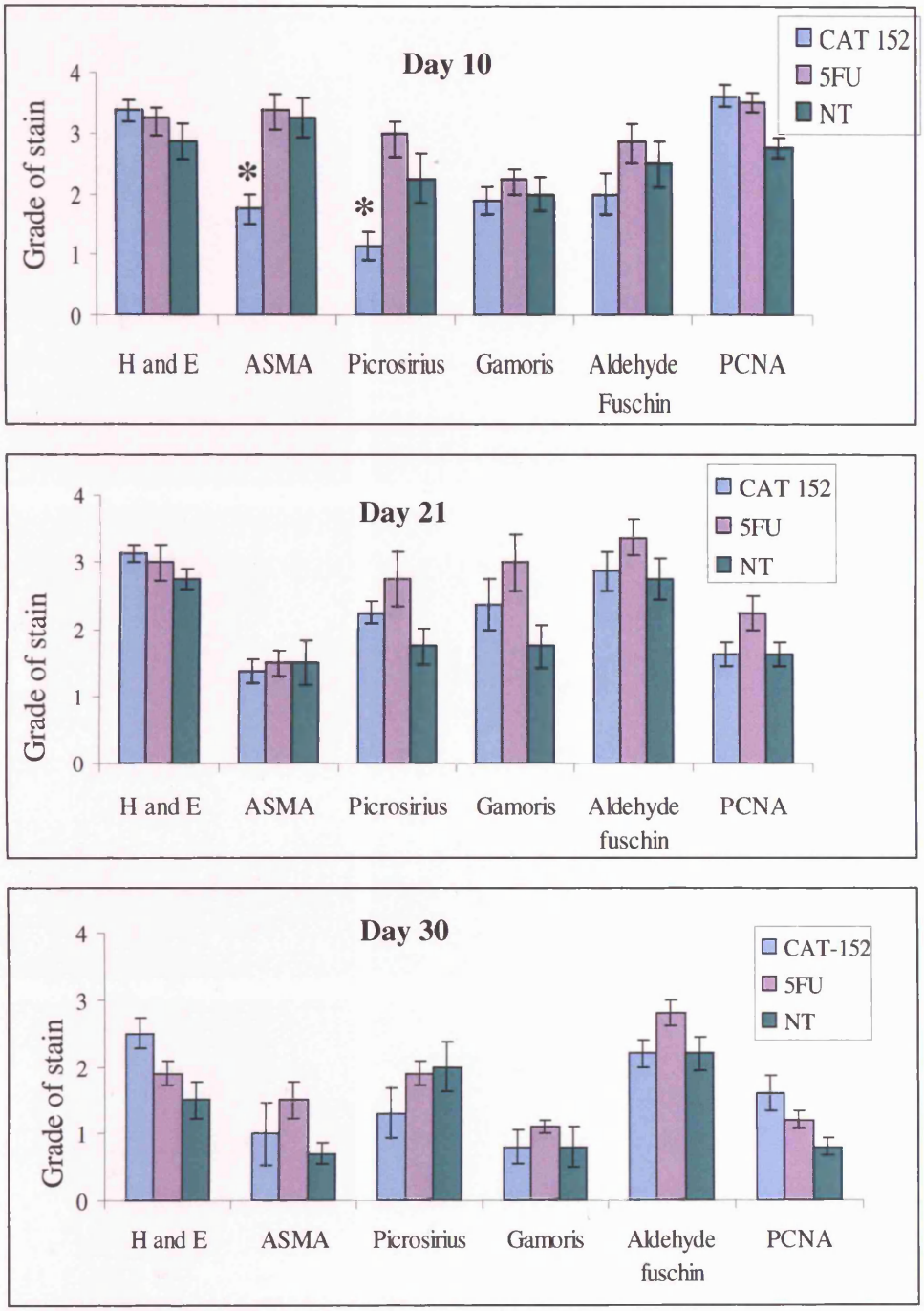

On day 10 CAT-152 significantly reduced collagen production as graded by picrosirius red staining and the expression of α smooth muscle actin (* p=0.01). At other time points trends were demonstrated in which CAT-152 reduced collagen deposition (picrosirius red), elastic fibre formation (Oxytalan staining) and collagen orientation (Gamoris trichrome) although these did not reach significance.

Figure 62 Effect of post-operative treatment on subconjunctival scarring on day 10 after glaucoma filtration surgery

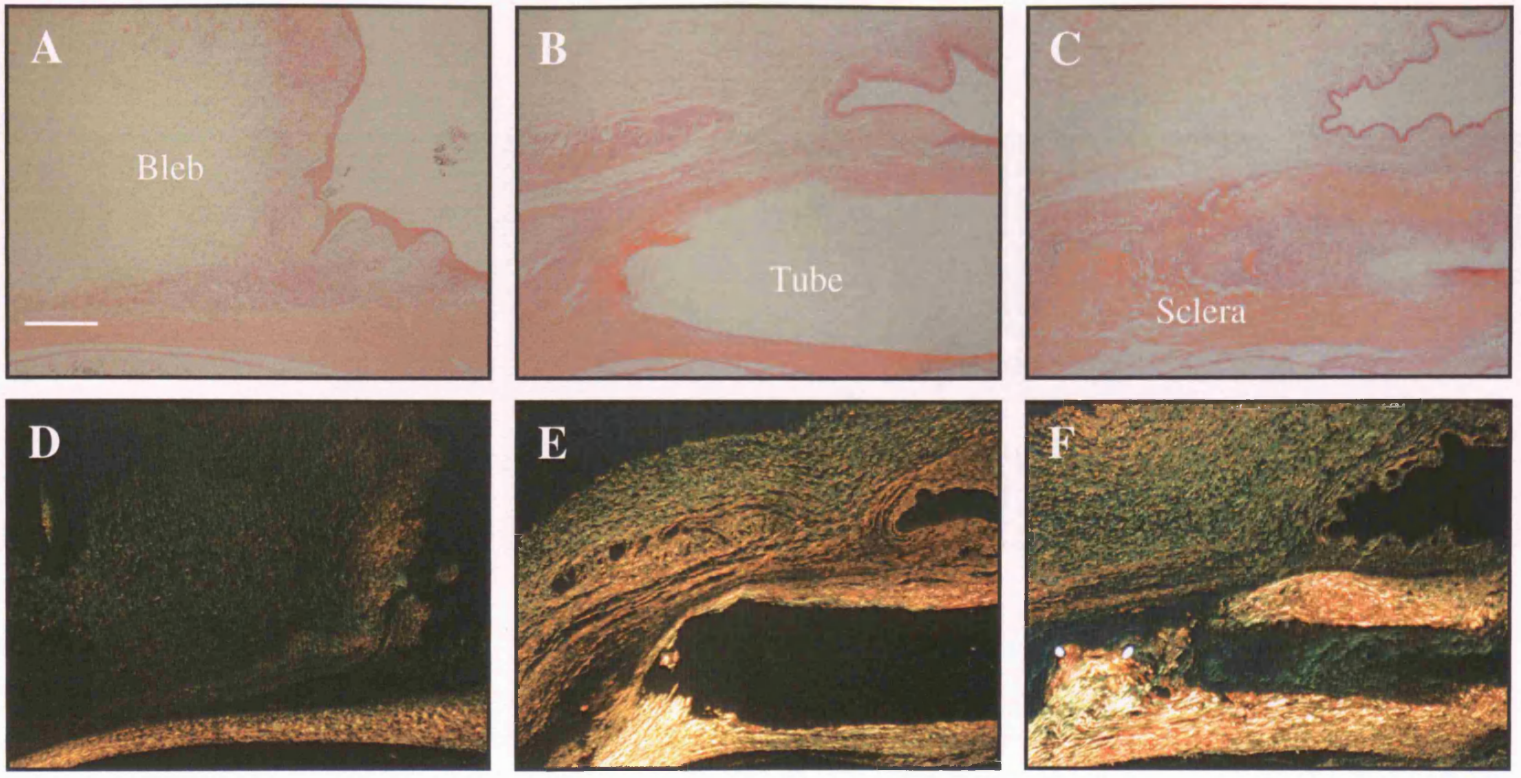

Histological characteristics of filtration blebs on day 10. Hematoxylin and eosin (A-C) and picrosirius red (D-F) stained sections are shown of one representative animal per group: CAT-152 treated (A,D), 5-FU treated (B,E) and control group (C,F). CAT-152 treatment reduced subconjunctival scarring at the microscopic level. The picrosirius red staining demonstrates a reduction in the density of subconjunctival collagen deposition (green and yellow) in CAT-152 treated animals. Bar represents 500µm

Figure 63 Effect of post-operative treatment on myofibroblast transformation on day 10 after glaucoma filtration surgery

Fibroblast differentiation to the myofibroblast phenotype is characterised by the expression and assembly of a smooth muscle actin into stress fibres. Immunohistochemical staining of the filtration blebs on day 10 , using a DAB detection system, demonstrates a reduction in the number of α smooth muscle actin expressing cells after CAT-152 treatment (A) compared to 5-FU (B) and controls (C). Bar represents 500μm

Figure 64 Quantification of alpha smooth muscle actin expression in subconjunctival tissue after glaucoma filtration surgery

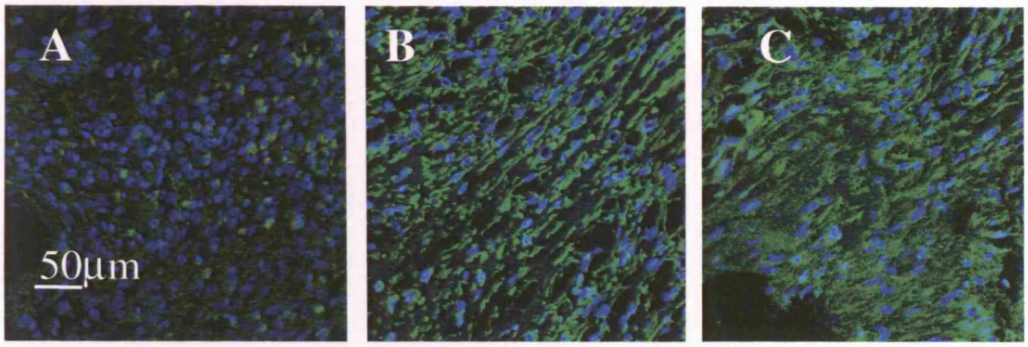

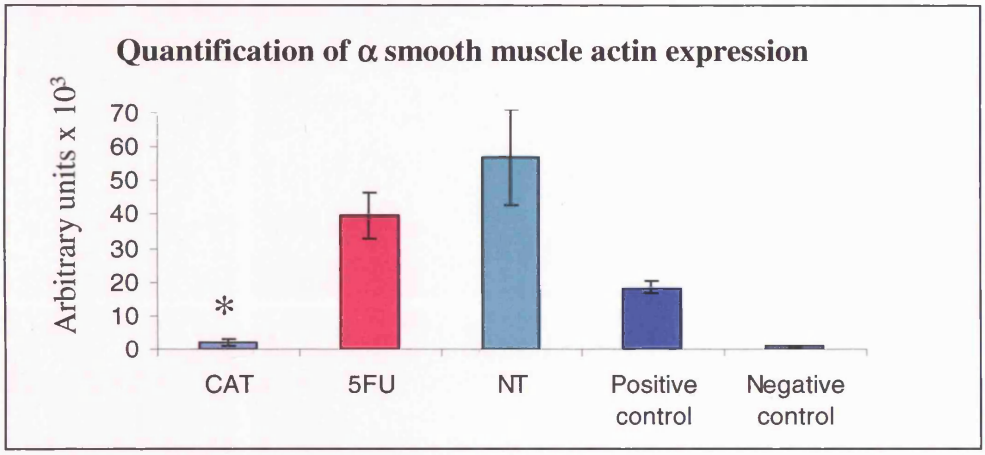

Fluorescent immunohistochemical staining for α smooth muscle actin was perfomed on 3 animals per treatment group (Day 10, N=3, A= CAT-152, B= 5FU and C= NT). These images were quantified using a binary image analysis system. CAT-152 significantly reduced α smooth muscle actin expression compared to 5-FU and control treatments ($p< 0.05$). The α sma was labelled with FITC shown in green and the nuclei were counterstained with DAPI (blue). A negative control primary antibody was used and an internal positive control was located within the ciliary body of the eye. Bar represents 50 µm

Figure 65 Effect of post-operative treatment on the subconjunctival scarring response

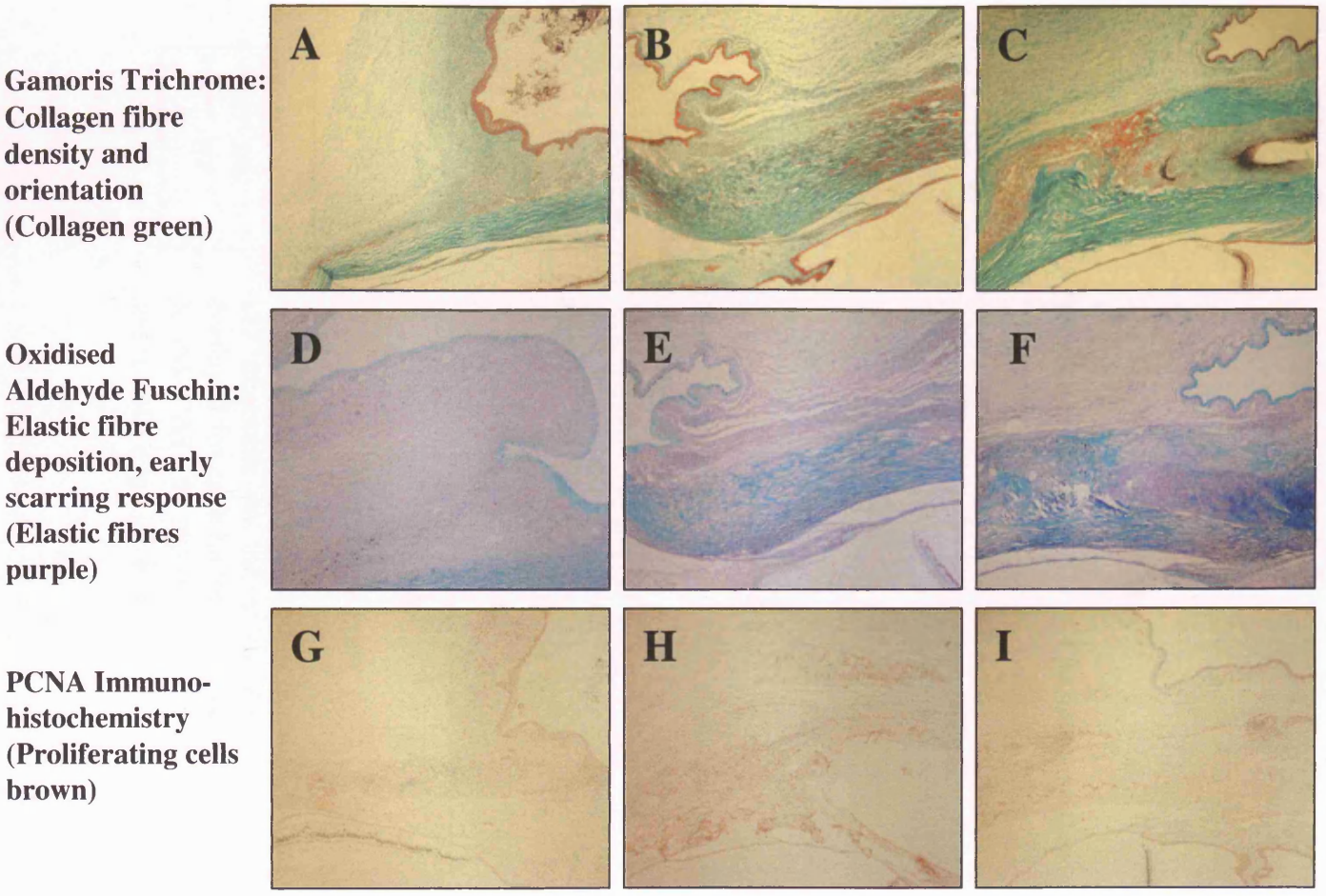

Histological characteristics of filtration blebs on day 10. One representative animal per group: CAT-152 treated (A,D, G), 5-FU treated (B,E,H) and control group (C,F,I). No significant differences seen between groups.

Figure 66 Effect of post-operative treatment on subconjunctival scarring over the 30 day study period

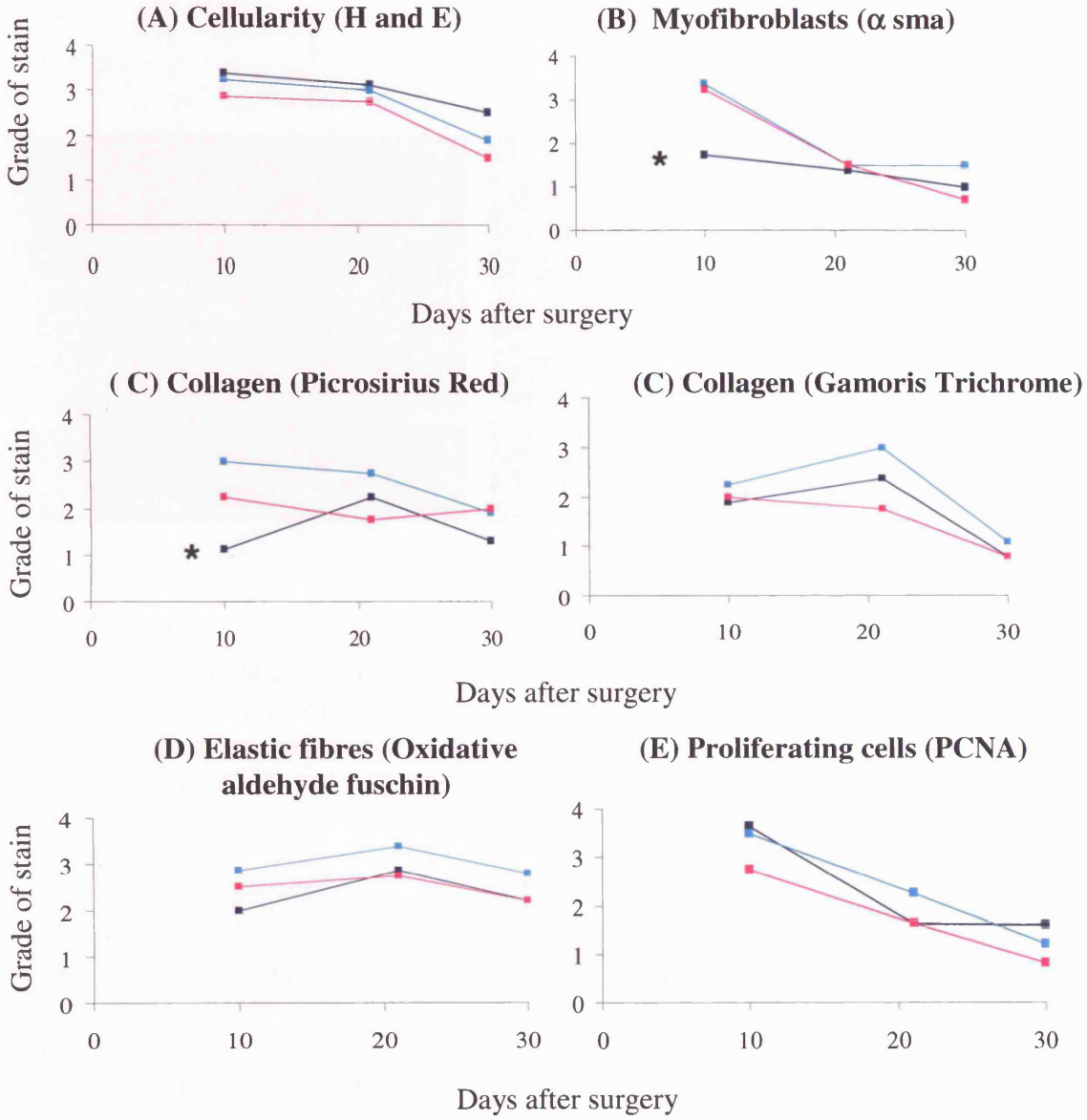

A grading system was used to quantify the effect of CAT-152 treatment on the extracellular matrix. The data is displayed for each histological stain over the 30 day study period. CAT-152 significantly reduced collagen deposition and α SMA expression on day 10. * $p<0.05$

Figure 67 Subconjunctival architecture on day 30 after glaucoma filtration surgery

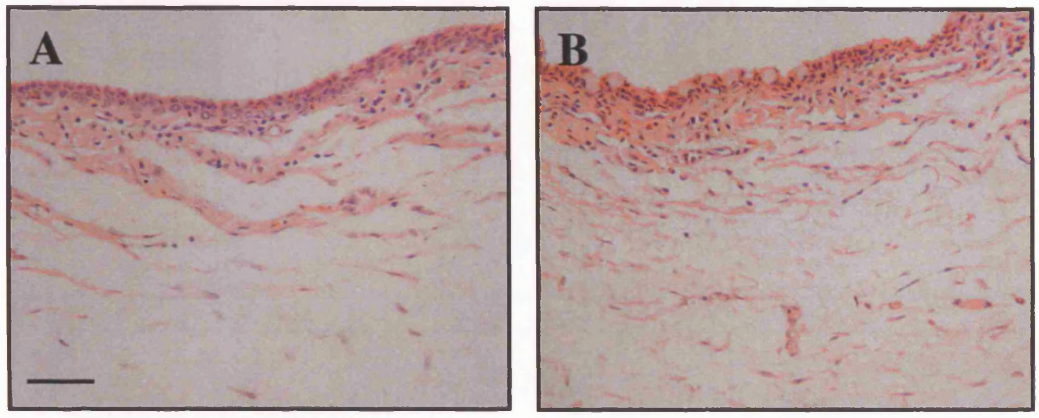

By day 30 only one bleb (CAT-152 treated) was still functioning. In failed blebs subconjunctival scarring consisted of dense collagen fibres and fibroblasts (B). In constrast the surviving bleb showed much looser architecture and visible evidence of bleb formation (A). Bar represents 100mm

Figure 68 Comparison of subconjunctival scarring indices in failed versus surviving blebs

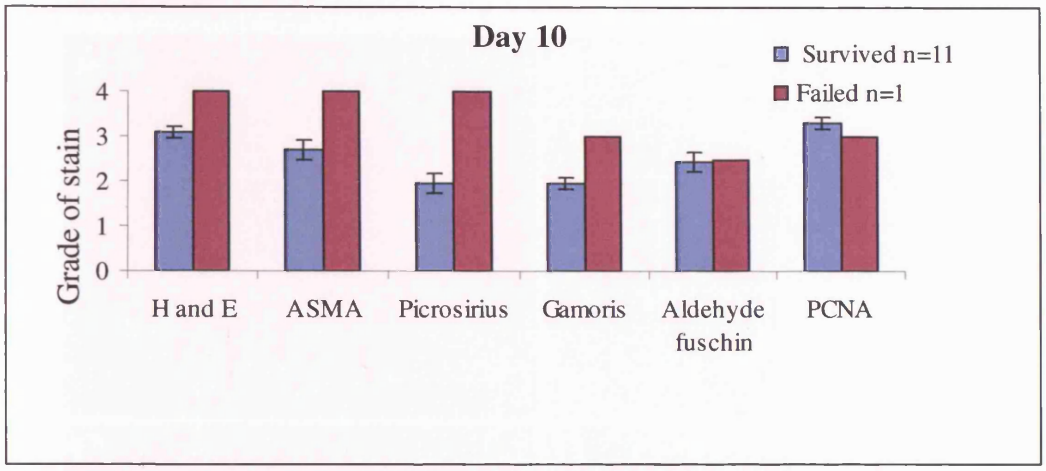

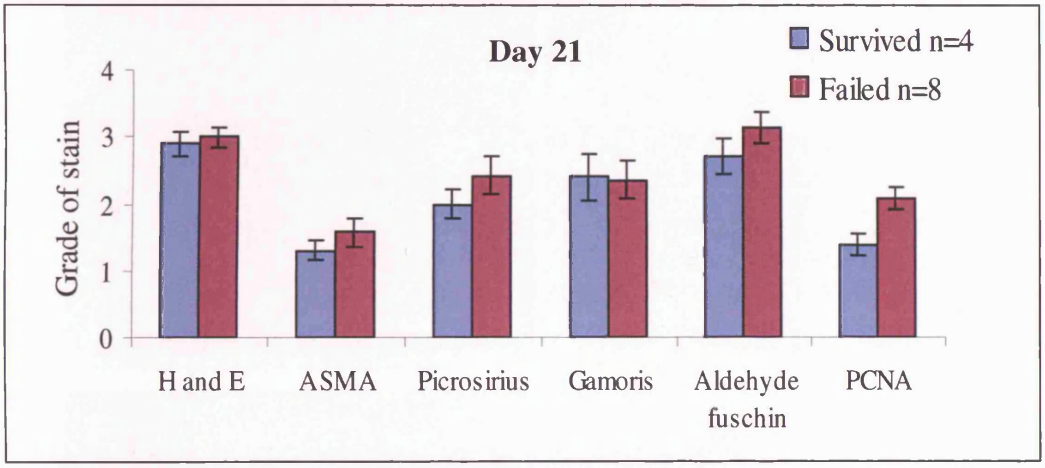

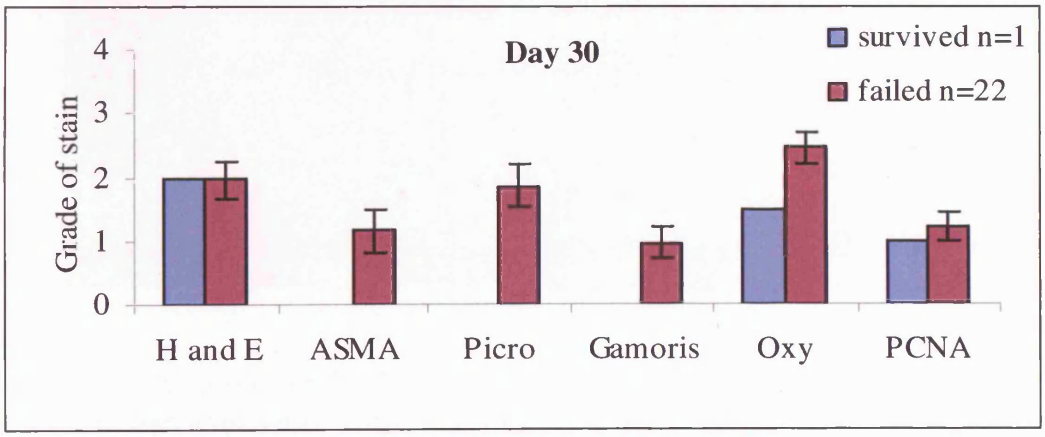

The animals were observed to identify the time of bleb failure. The histology grading data has been analysed to compared failed versus surviving blebs for each time point.

Figure 69 Bleb and subconjunctival architecture after experimental glaucoma surgery

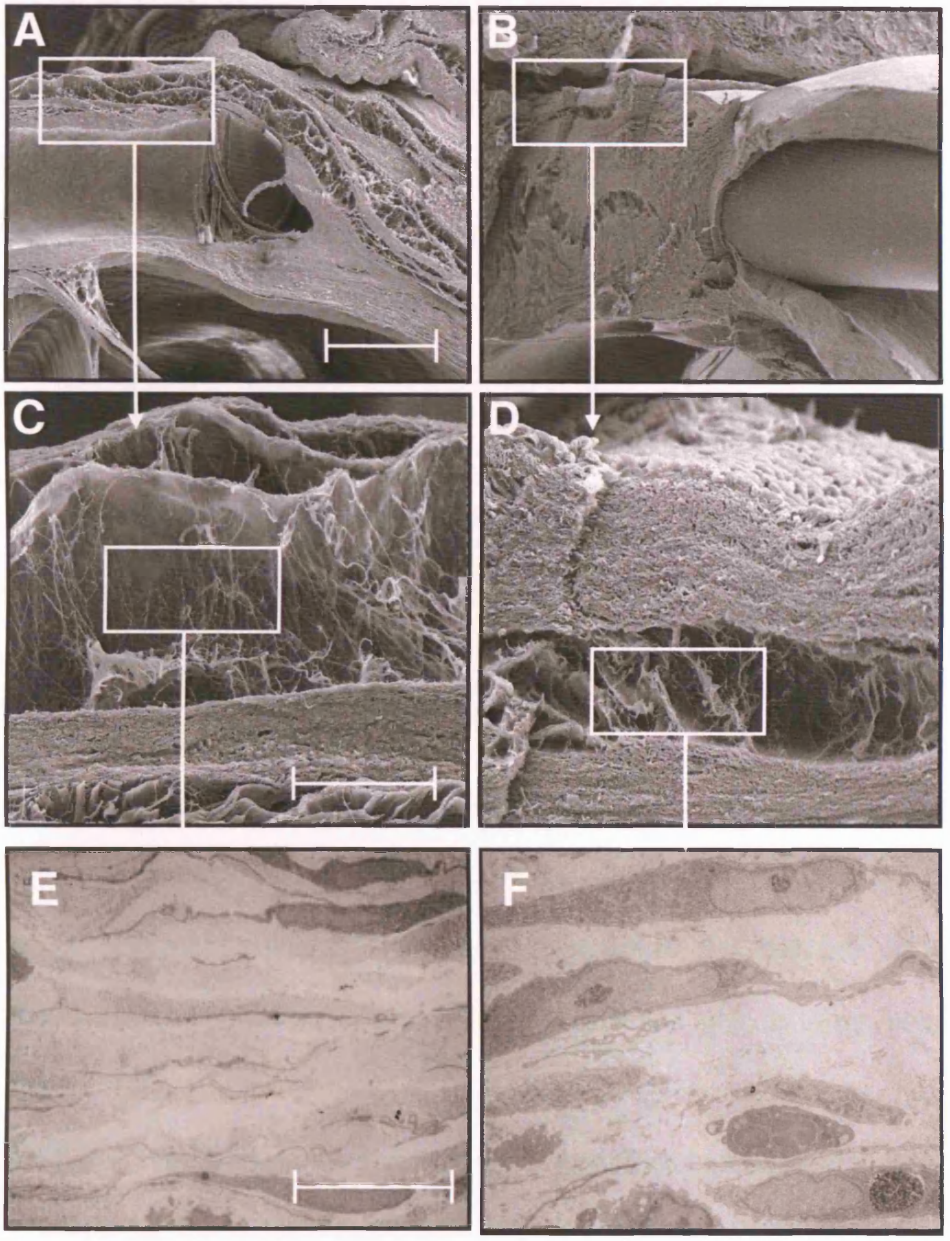

Electron microscopy (EM) was performed on CAT-152 treated animals (A,C,E) and untreated controls (B,D,F). Morphologically scanning EM (A-D) demonstrates looser subconjunctival bleb architecture with CAT-152 treatment. At a cellular level, transmission EM shows the associated reduction in inflammatory cell infiltrate and collagen fibre deposition in the CAT-152 treated animals. Bars A-B 1mm, C-D 100mm E-F 10

3.4.3 Long term effects of combining intra-operative and prolonged post-operative CAT-152 treatment on the outcome of experimental glaucoma surgery.

3.4.3.1 Bleb survival All 27 animals completed the study. The main outcome variable was the effect of CAT-152, 5-FU or PBS treatment on bleb survival. CAT-152 significantly prolonged the bleb survival compared to 5-FU and PBS as shown in the Kaplan Meier curve in Figure 70 A (Log rank statistics $P < 0.0001$). Median bleb survival was 41, 27 and 17 days with CAT-152, 5-FU and PBS treatment, respectively (Figure 70 C). Animals treated with CAT-152 started to fail after day 24. 3 animals failed in week 4, 3 failed in week 6 and in the remaining 1/3 of the CAT-152 animals surgical success was maintained throughout the 45 day experiment (Table 12). 5-FU treatment significantly prolonged bleb survival compared to PBS (Figure 70 A and table 13, $P=0.0024$). All the animals in the PBS control group failed by the end of week 3.

In half the control animals the PBS treatment was given by superior subconjunctival injection and in the remaining ones it was given by inferior subconjunctival injection. This was to identify if the site of injection influences bleb survival in this model. Subgroup analysis of the PBS animals by injection site did not demonstrate any significant differences in bleb survival (Figure 70 B and table 13; Log rank survival, $p= 0.97350$).

3.4.3.2 Bleb Morphology The presence of a diffuse, elevated drainage bleb is an indicator of scleral patency and trans-conjunctival drainage. Treatment with CAT-152 was associated with larger more diffuse areas of drainage compared to 5-FU and PBS. Analysis of bleb area and bleb height by the generalized linear model revealed significant differences in these variables with CAT-152 treatment (Figure 71 $p<0.001$). Bleb morphology was recorded by digital imaging at regular intervals to enable comparison of treatment effect. Figure 72 shows bleb morphology after 14, 21 and 42 days. As

subconjunctival scar tissue is laid down and the bleb fails the tube becomes more prominent as seen in the PBS treated animals. CAT-152 appeared to prevent this observation and an elevated bleb appearance was maintained.

3.4.3.3 Intraocular Pressure IOP survival was not shown to be significantly different between treatment groups as shown in Figure 73 A (Log rank p=0.385). However, a trend for higher mean post-operative pressure was seen in the 5-FU treated group (Figure 73 B). Multiple comparisons between groups highlighted significantly higher pressures in the 5-FU animals compared to CAT-152 on day 14 (p=0.069), day 28 (p=0.096) and day 31 p=0.068) and also compared to PBS on day 28 (p=0.075). Mean IOP with CAT-152 was similar to control.

3.4.3.4 Side effects of treatment

Conjunctival chemosis Transient chemosis has been noted in this model in the immediate post-operative period in some animals and resolves spontaneously over 48 hours (Early chemosis). Transient chemosis was seen in 4 animals, 1 treated with CAT-152, 1 with 5-FU and 2 treated with PBS on day 1 after surgery (Figure 74). However, using this prolonged injection regimen 3 CAT-152 treated animals were also noted to develop chemosis after 2-3 weeks of treatment on a mean of 2.7 occasions, which appeared to be related to the injections and had not been previously associated with this model. This was termed late chemosis. The conjunctiva became injected and swollen (Figure 74 A). These appearances resolved but residual conjunctival hyperaemia persisted (Figure 74 B).

Corneal epitheliopathy Self limiting corneal staining is seen in some animals after the surgical procedure and results from placement of the corneal traction suture. Corneal epitheliopathy is associated with the clinical use of 5-FU. Combined intra-operative and

prolonged post-operative application of 5-FU significantly increased the duration of low grade epithelial changes with a mean duration of 14.6 days ($p< 0.01$ using Kruskal-Wallis test and Dunn's test). This compared to a mean duration of 10.7 days seen with isolated post-operative use. Treatment with CAT-152 was similar to control (Figure 75).

Corneal oedema and vascularision Additional corneal side effects were observed in animals treated with combined intra-operative and combined post-operative 5-FU. The duration of corneal oedema and vascularisation was significantly prolonged by 5-FU, compared to CAT-152 or control (Kruskal Wallis: vascularity $p= 0.02$, oedema $p= 0.007$, Dunn's Test $p<0.05$). These findings tended to occur together rather then in isolation. Similar observations have been previous noted in this model. It is likely that reduced flow of aqueous through the bleb leads to back pressure and a build up of fluid in the cornea, which presents as corneal cloudiness and oedema. This can be aggravated by co-existing epitheliopathy. Chronic corneal changes induce secondary vascularisation (Figure 76)

Conjunctival avascularity was observed in conjunctival bleb tissue after treatment with 5-FU. This was more extensive than the changes observed after isolated post-operative subconjunctival injections of 5-FU and extended across the superior conjunctival in the region where the subconjunctival sponge had been applied intra-operatively (Figure 77 A). Repeated post-operative injection of 5-FU also resulted in an area of inferior conjunctival avascularity at the injection site (Figure 77 B).

3.4.3.5 Tolerance Intensity of conjunctival vascularity and the degree of intraocular inflammation indicate if a treatment is well tolerated. Analysis of the mean grade of vascularity is shown in Figure 78 A-C. Treatment with CAT-152 increased superior conjunctival vascularity. (GLM $p=0.003$). Using multiple analysis of variance superior conjunctival vascularity was significantly increased by CAT-152 on days 21 and 38

compared to control (Bonferroni correction: Day 21 p=0.052, day 38 p=0.029). These time points correspond to the presentation of conjunctival chemosis in 3 CAT-152 treated animals. Mean grading of nasal and temporal conjunctival vascularity did not significantly differ between the three groups (GLM: nasal vascularity p=0.98, temporal vascularity p=0.237)

No significant differences in anterior chamber inflammation were detected between treatment groups (GLM: p= 0.179)

Figure 70 Effect of combined intra and post-operative treatment on bleb survival after glaucoma filtration surgery

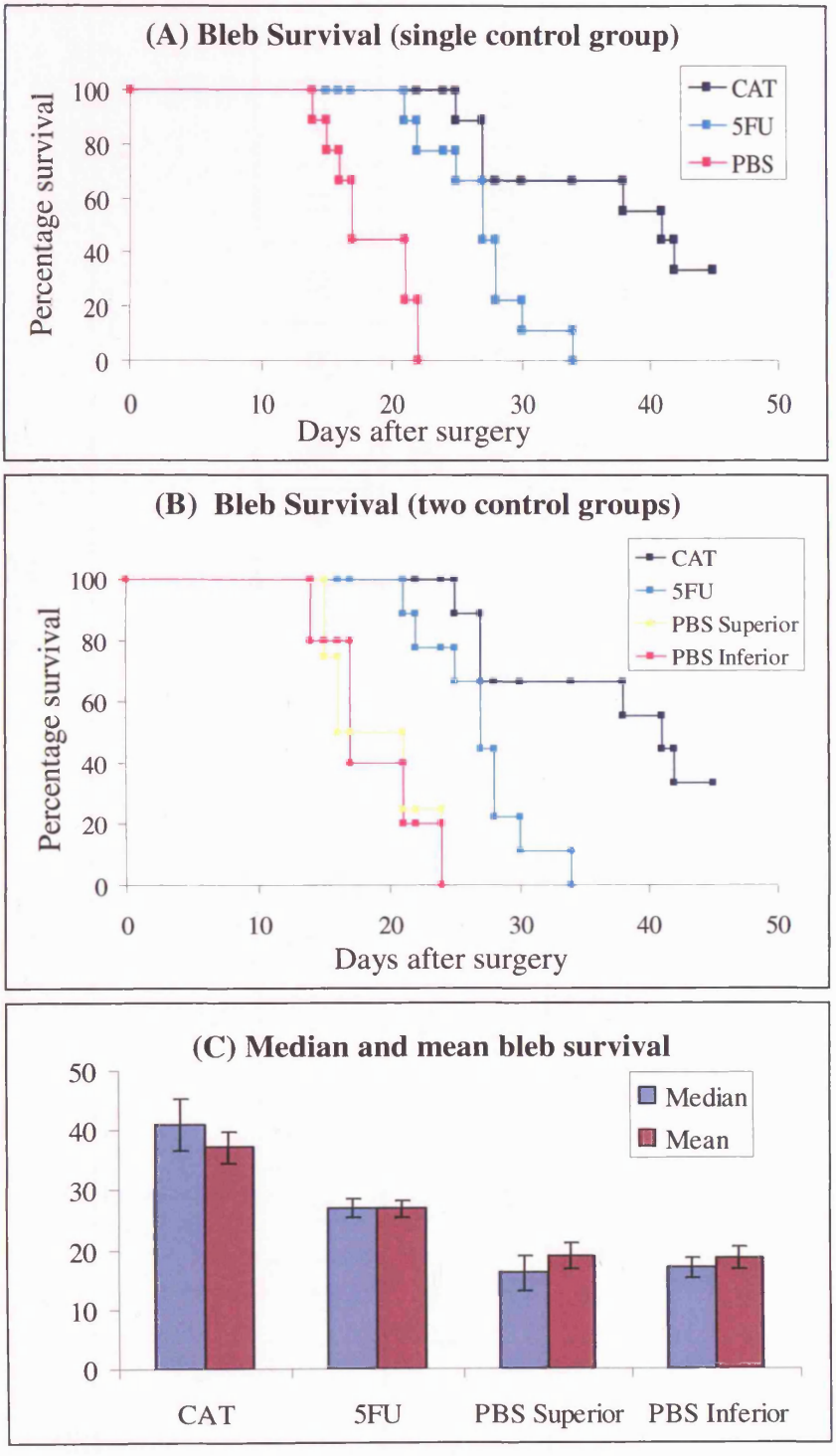

Treatment with CAT-152 significantly prolonged bleb survival compared to both 5FU and PBS (A:log rank statistics $P<0.0001$). Subgroup analysis of the PBS group showed that the site of injection does not influence bleb survival in this model (B).

Table 12 Incidence of bleb failure and the percentage bleb survival in rabbits undergoing glaucoma filtration surgery: Effect of CAT-152 and 5-FU treatment compared to control.

Treatment	Days after Surgery																	No of surviving blebs
	0	14	15	16	17	21	22	24	25	27	28	30	34	38	41	42	45	/ n
CAT-152	0	0	0	0	0	0	0	0	1	2	0	0	0	1	1	1	0	3 / 9
% survival	*100*	*100*	*100*	*100*	*100*	*100*	*100*	*100*	*88.89*	*66.67*	*55.56*	*55.56*	*55.56*	*44.44*	*33.33*	*33.33*	*33.33*	
5-FU	0	0	0	0	0	1	1	0	1	2	2	1	1	0	0	0	0	0 / 9
% survival	*100*	*100*	*100*	*100*	*100*	*88.89*	*77.78*	*77.78*	*66.67*	*44.44*	*22.22*	*11.11*	*0*	*0*	*0*	*0*	*0*	
PBS	0	1	1	1	2	2	0	2	0	0	0	0	0	0	0	0	0	0 / 9
% survival	*100*	*88.89*	*77.78*	*66.67*	*44.44*	*22.22*	*22.22*	*0*	*0*	*0*	*0*	*0*	*0*	*0*	*0*	*0*	*0*	

Table 13 Bleb survival: Log rank Statistics and (significance)

	CAT-152	5FU	PBS Superior
5FU	7.37 (0.0066)		
PBS Superior	15.62 (0.0001)	9.22 (0.0024)	
PBS Inferior	16.34 (0.0001)	10.72 (0.0022)	0 (0.9735)

Figure 71 Effect of combined intra and post-operative treatment on bleb morphology after glaucoma filtration surgery

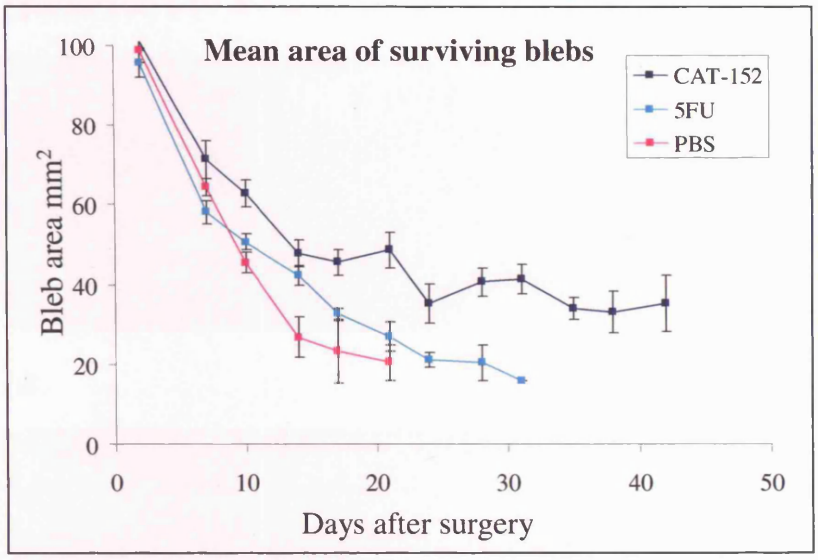

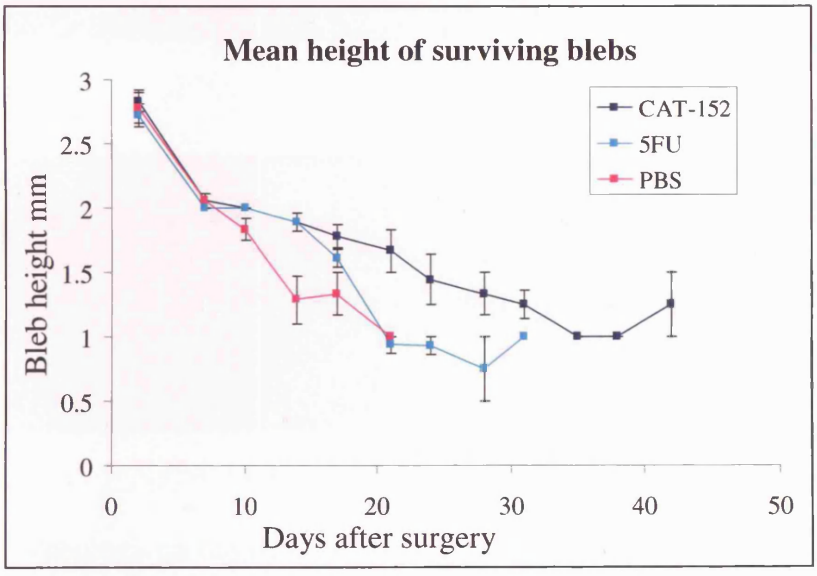

Bleb morphology is an important indicator of effective filtration. Treatment with CAT-152 was associated with larger more diffuse areas of drainage. Bleb area and height $P<0.001$. (Mean and Standard error plotted)

Figure 72 Effect of combined intra and prolonged post-operative treatment on bleb morphology

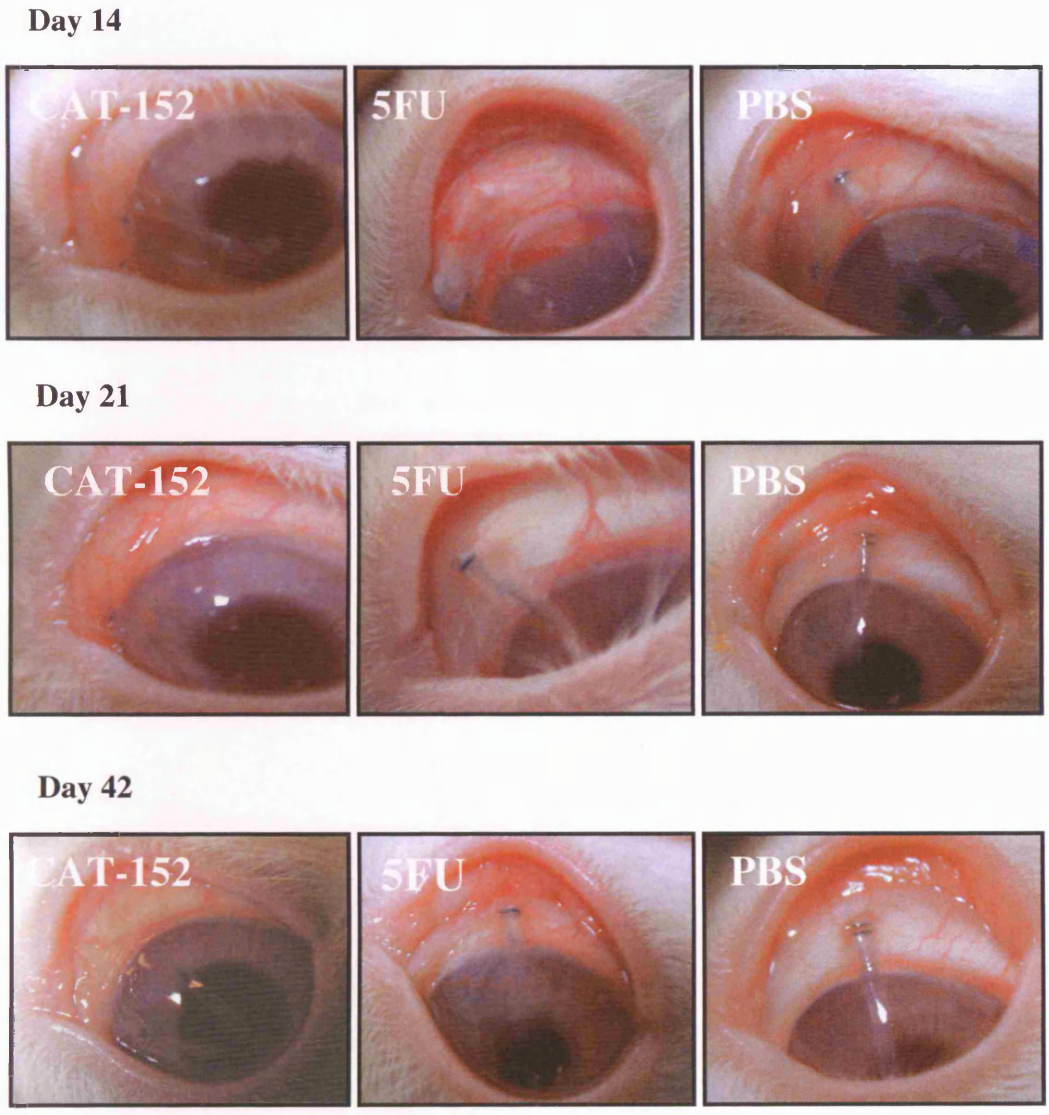

Bleb morphology on days 14, 21 and day 42 after glaucoma filtration surgery. One representative animal is shown per group. Animals were treated with either CAT-152 or 5-FU or received PBS. Treatment with CAT-152 was associated with elevated, diffuse, fleshy looking blebs compared to the flat, scarred blebs in the 5-FU and control groups. (Black arrows demarcate the bleb border and the white arrow shows the cannula.)

Figure 73 Effect of combined intra and prolonged post-operative treatment intraocular pressure

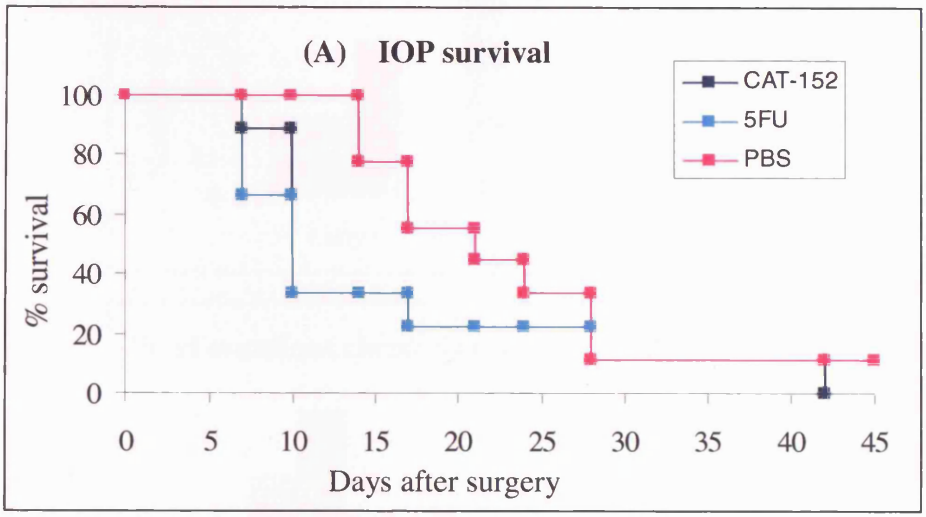

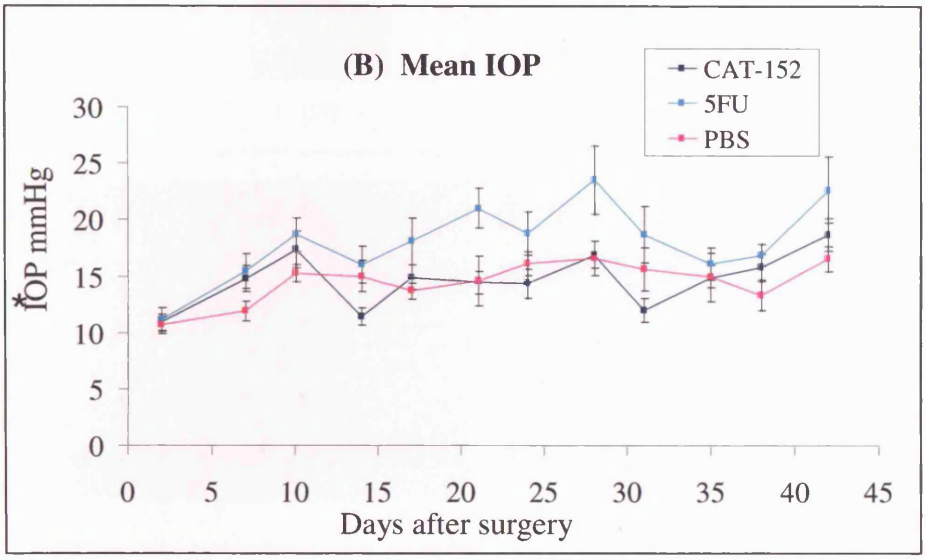

IOP survival was not shown to be significantly different between treatment groups (Log rank P=0.385). However, a trend for higher mean post-operative pressure was seen in the 5FU treated group. ANOVA (multiple comparisons after bonferroni correction): Day 14 p=0.069 (5FUvs CAT-152), day 28 p=0.096 (5FUvs CAT-152), p=0.075 (PBS vs 5FU) and day 31 p=0.068 (5FUvs CAT-152). Mean IOP with CAT-152 was similar to control.

Figure 74 Effect of combined intra and prolonged post-operative CAT-152 on the conjunctival appearance after glaucoma filtration surgery

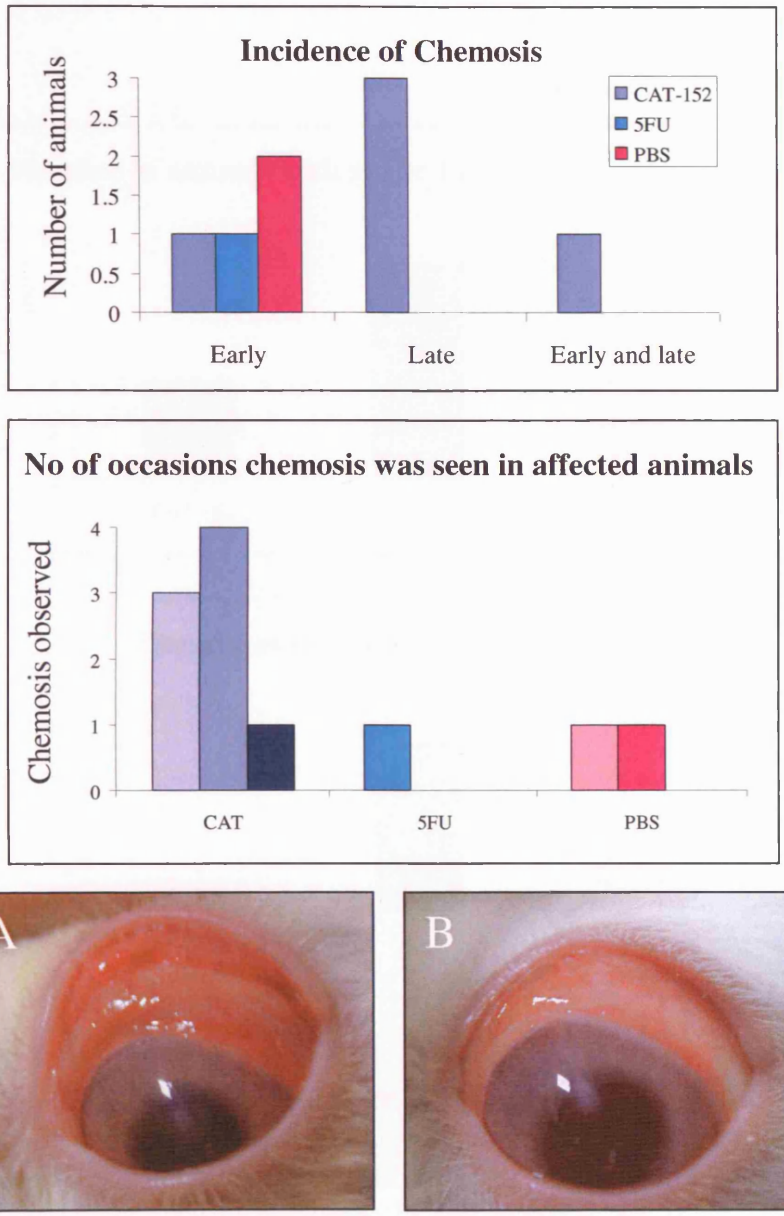

Transient chemosis has been noted in this model in the immediate post-operative period in some animals and resolves spontaneously over 48 hours (Early chemosis) However, using this prolonged injection regimen 3 CAT-152 treated animals were noted to develop chemosis after 2-3 weeks of treatment on a mean of 2.7 occasions, which appeared to be related to the injections and had not been previously associated with this model (Late chemosis). The conjunctival became injected and swollen (A). These appearances resolved but residual conjunctival hyperaemia persisted (B).

Figure 75 Effect of combined intra-operative and prolonged post-operative treatment on the corneal epithelium after glaucoma filtration surgery

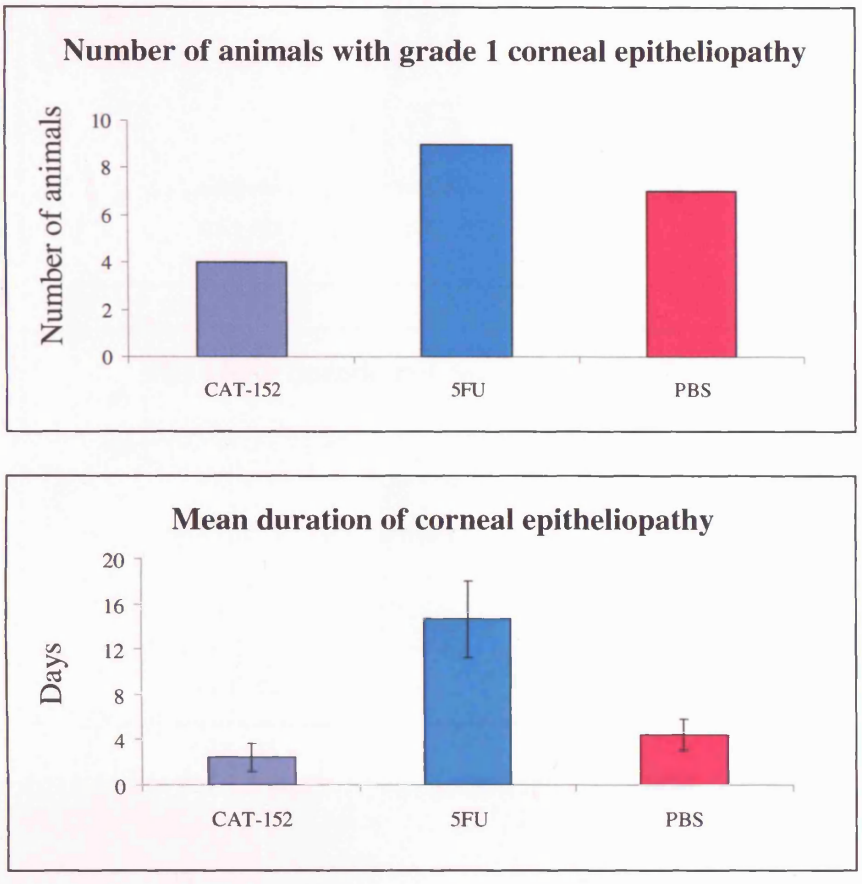

Corneal epitheliopathy is associated with the clinical use of 5-FU. Combined intra-operative and prolonged post-operative application of 5-FU significantly increased the duration of low grade epithelial changes with a mean duration of 14.6 days ($P<0.01$ Kruskal wallis and Dunn's Test). This compared to a mean duration of 10.7 days seen with isolated post-operative use. Treatment with CAT-152 was similar to control. Mean and standard error plotted.

Figure76 Additional corneal side effects associated with combined intra-operative and prolonged post-operative application of 5-FU after GFS

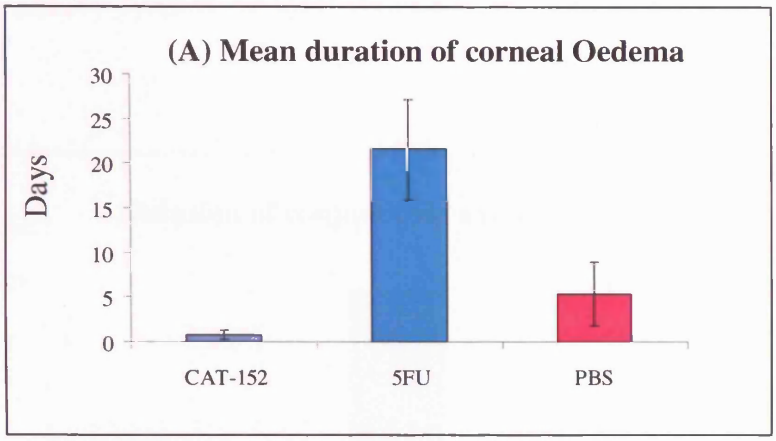

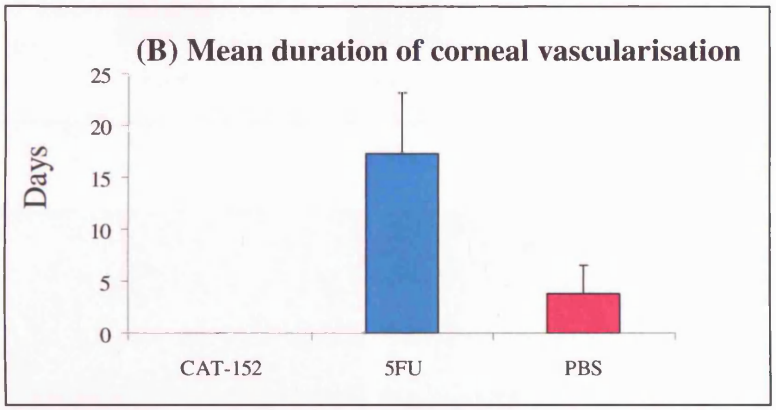

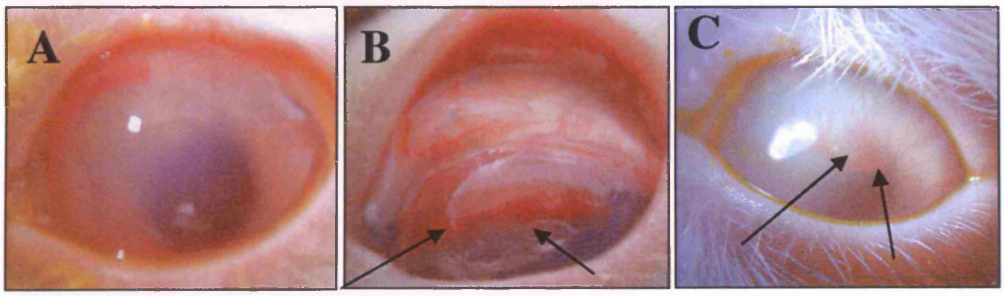

Corneal oedema (A) and vascularisation (B-C) were observed in animals treated with combined intra-operative and combined post-operative 5-FU. The duration of these findings was significantly prolonged by 5-FU, compared to CAT-152 or control. (vascularity p= 0.02, oedema p= 0.007). These findings tended to occur together rather then in isolation. Similar observations have been previous noted in this model. (Black arrows demarcate corneal vessels). Mean and standard error plotted.

Figure 77 Effect of combined intra and prolonged post-operative application of 5-FU on conjunctival avascularity

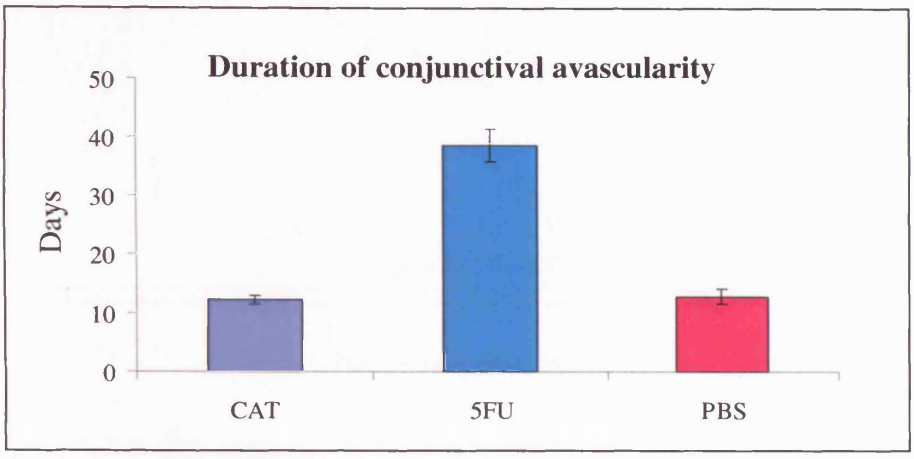

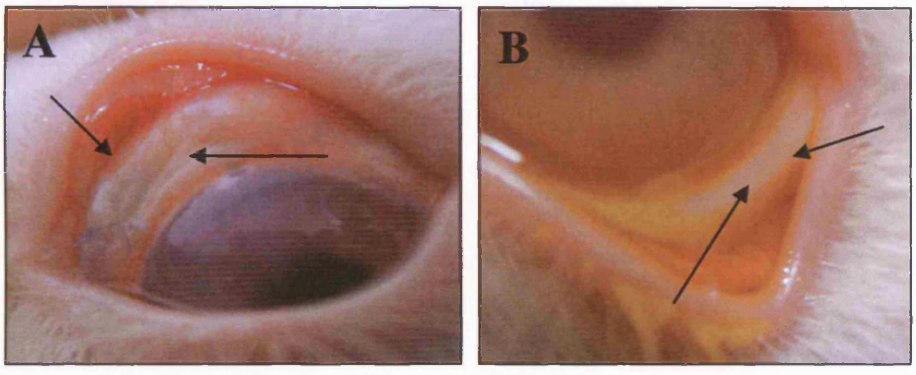

Conjunctival avascularity was observed in conjunctival bleb tissue after treatment with 5-FU. This was more extensive than the changes observed after isolated post-operative subconjunctival injections of 5-FU and extended across the superior conjunctival in the region where the subconjunctival sponge had been applied intra-operatively (A). Repeated post-operative injection of 5-FU also resulted in an area of inferior conjunctival avascularity at the injection site (B).

Figure 78 Effect of combined intraoperative and prolonged post-operative treatment on conjunctival vascularity

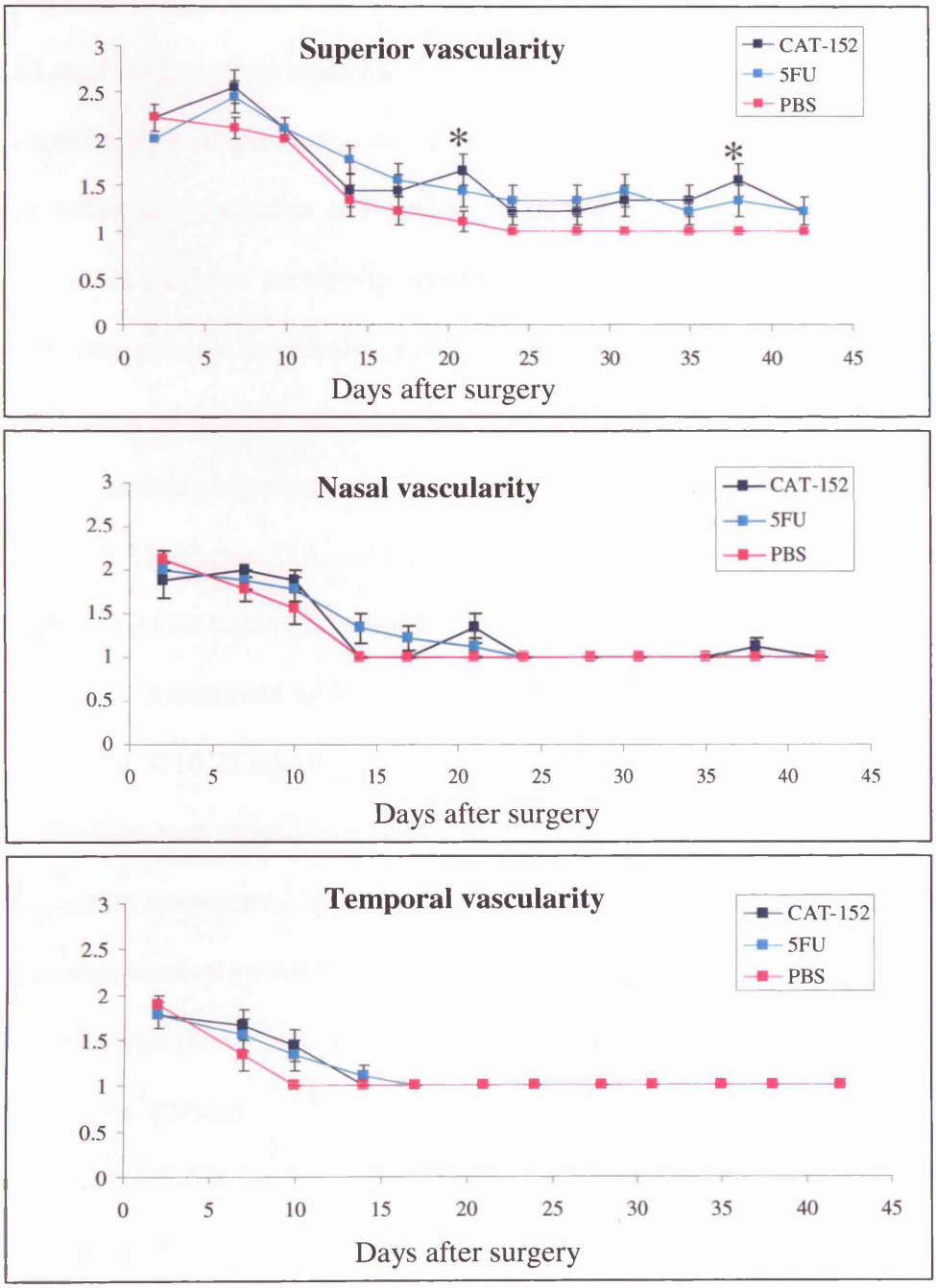

Analysis of the mean grade of vascularity is shown in charts A-C. Multiple comparisons showed significantly increased superior conjunctival vascularity after treatment with CAT-152 compared to control (ANOVA Bonferroni correction: Day 21 p=0.052, day 38 P=0.029).These time points correspond to the presentation of conjunctival chemosis in 3 CAT-152 treated animals. Mean grading of nasal and temporal conjunctival vascularity did not significantly differ between the three groups.

3.4.4 Effects of a combined course of intra-operative and prolonged treatment with the CAT-152 on the immune response in the rabbit

3.4.4.1 Local conjunctival reaction

This experiment was performed to investigate why conjunctival chemosis had been detected with intra-operative and prolonged treatment of CAT-152 (3.4.3). Transient early chemosis has been previously noted in this model in the immediate post-operative period in some animals and resolves spontaneously over 48 hours with no residual effects. This does not appear to be related to the treatment given. In this experiment 7 animals developed transient early chemosis, 2 treated with CAT-152, 4 with Null antibody and 1 treated with PBS (Figure 79A). The clinical finding of late chemosis was again detected using this combined treatment regimen. 4 animals showed signs of chemosis later in the experiment (Null treatment n=3, CAT-152 n=1), the onset of which was during weeks 3-4, after a mean of 10.25 injections had been given (Figure 79 B). Late chemosis increased in severity with each episode, reached a maximum intensity after 13 injections and was associated with conjunctival hyperaemia (Figure 80). Chemosis appeared to be a response to the subconjunctival treatment and when present was always detected in the 24 hours after a subconjunctival injection had been given (Figure 79 C). The time course of each response to the injection varied, but was maximal after 24 hours and resolved after 48 hours leaving residual superior conjunctival hyperaemia. Once the reaction had been detected in a bleb it occurred with all subsequent injections but to a lesser degree with time.

3.4.4.2 Systemic detection of CAT-152 and Null antibody in rabbit serum CAT-152 was detected in the serum of all CAT-152 treated rabbits 4 days after initiation of subconjunctival dosing and GFS. On day 4 (after 6 injections of CAT-152 100μg) the

serum concentration for CAT-152 was 1095ng/ml (n=6, Table 14). In 4 of 6 rabbits the concentration of CAT-152 decreased over time and was not detected at the 70 day time point. CAT-152 was detected in the serum of 2 rabbits 70 days after GFS.

Similarly, CAT-001 was detected in the serum of all CAT-001 treated rabbits 4 days after initiation of subconjunctival dosing and GFS. On day 4 (after 6 injections of CAT-001 100μg) the serum concentration for CAT-001 was 999ng/ml (n=6, Table 15). In all rabbits the concentration of CAT-001 decreased over time and was not detected at the 70 day time point

3.4.4.3 Detection of rabbit serum antibodies to CAT-152 and CAT-001

Antibodies were raised against CAT-152 and CAT-001 in a subset of the animals treated with these human antibodies. Anti-CAT-152 and anti-CAT-001 antibodies were detected in the serum of treated rabbits 70 days after GFS (4 of 6, and 5 of 6 rabbits respectively; Table 16). All the animals that displayed late chemosis were found to have either anti-CAT-152 or anti-CAT-001 antibodies in the serum.

Figure 79 Effect of combined intra-operative and combined post-operative treatment on conjunctival chemosis

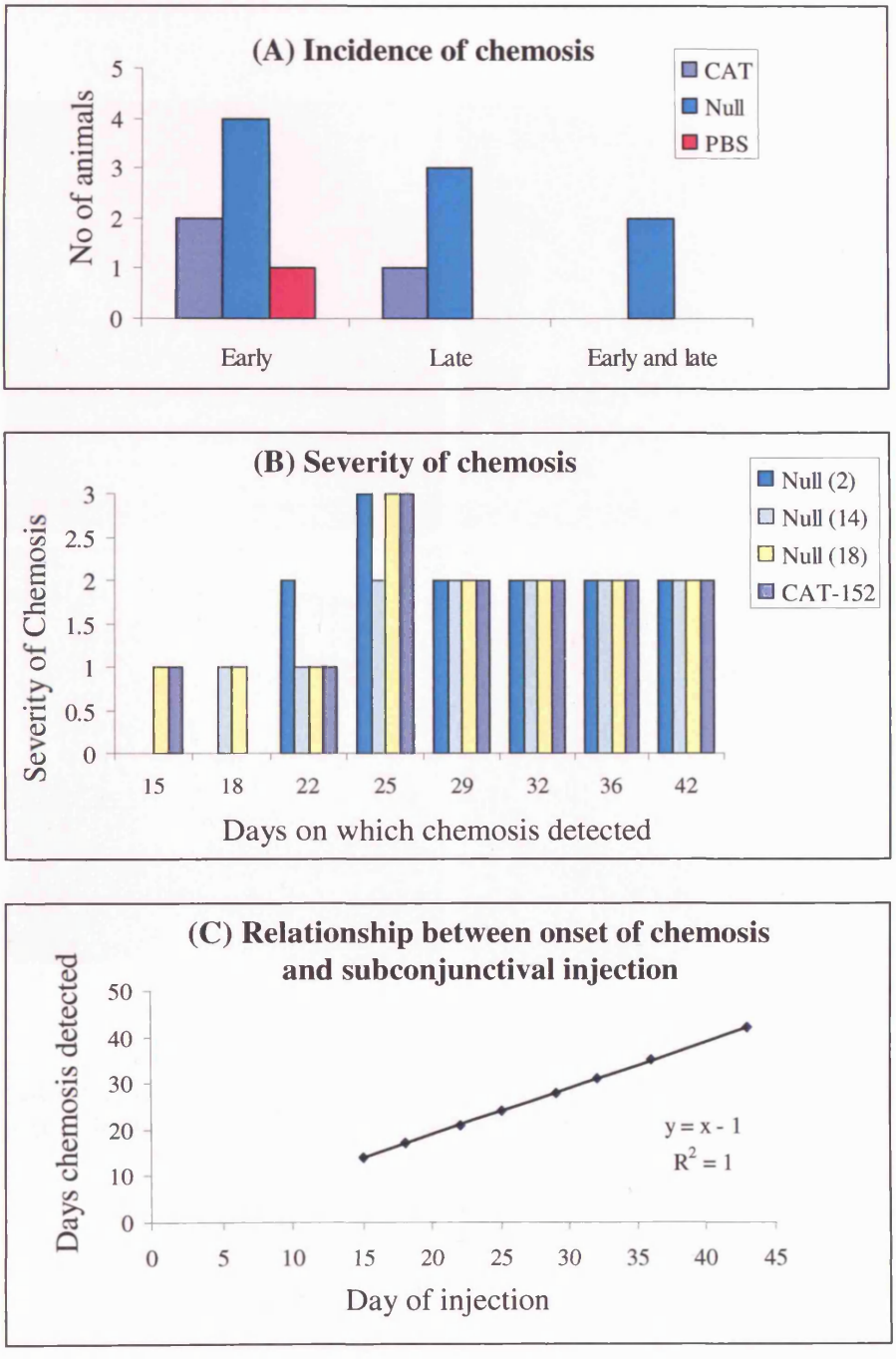

Conjunctival chemosis was seen in 7 animals on day 1. This was a transient finding and resolved within 24 hours. Chemosis was also detected in week 3-4 after 10 injections had been given (Null treatment n=3, CAT-152 n=1) (A). Late chemosis increased in severity with each episode, reached a maximum intensity in week 4 (13 injections) and then persisted (B). Chemosis appeared to be a response to the subconjunctival treatment (C)

Figure 80 Appearance of chemotic blebs on day 25

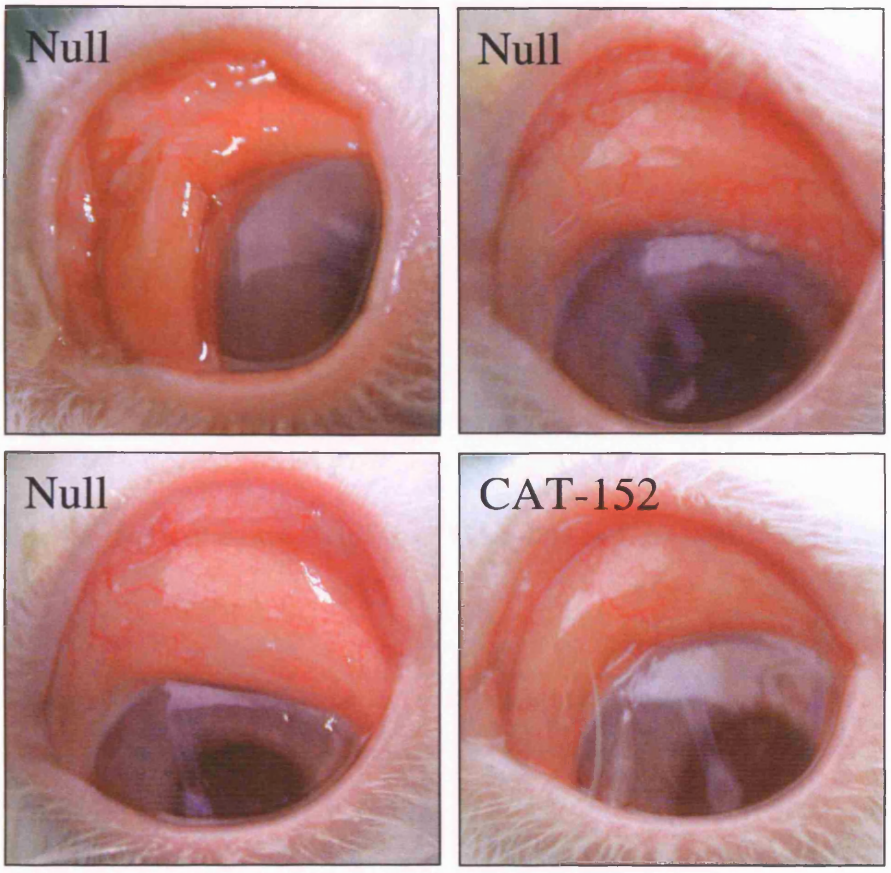

4 animals developed conjunctival chemosis which was at maximum severity after 13 injections (Null n=3, CAT-152 n=1)

Table 14 Serum concentration of CAT-152 in CAT-152 treated rabbits

ID No.	Treatment	CAT-152 serum concentration ng/ml (days after GFS)							
		Predose	4	11	17	24	32	44	70
5	CAT-152	ND	1260	ND	ND	63	112	1014	65
6	CAT-152	ND	872	404	432	922	1571	1895	368
7	CAT-152	ND	1379	753	ND	ND	ND	ND	ND
8	CAT-152	ND	1098	535	ND	ND	ND	ND	ND
15	CAT-152	ND	1290	43	ND	ND	ND	31	ND
17	CAT-152	ND	802	97	71	32	80	66	ND
Geometric mean			1095						

ND, not detected

Table 15 Serum concentration of CAT-001 in CAT-001 treated rabbits

ID No.	Treatment	CAT-001 serum concentration ng/ml (days after GFS)							
		Predose	4	11	17	24	32	44	70
2	CAT-001	ND	1161	ND	ND	ND	ND	ND	ND
4	CAT-001	ND	813	527	33	16	73	169	ND
9	CAT-001	ND	660	77	ND	ND	ND	ND	ND
12	CAT-001	ND	580	>2000	710	332	344	57	ND
14	CAT-001	ND	>2000	59	ND	ND	18	31	ND
18	CAT-001	ND	1374	140	74	ND	ND	ND	ND
Geometric mean			999						

ND, not detected; >2000, above the standard curve maximum concentration (2000ng/ml)

Table 16 Serum concentration of rabbit anti-CAT-152 or anti-CAT-001 antibodies 70 days after GFS.

CAT-152 treatment				CAT-001 treatment			
Rabbit ID.	Anti-CAT-152 μg/ml	Serum CAT-152 ng/ml	Late Chemosis	Rabbit ID.	Anti-CAT-001 μg/ml	Serum CAT-001 ng/ml	Late Chemosis
5	302	65	Yes	2	123	ND	Yes
6	34	368	No	4	6	ND	No
7	25	ND	No	9	44	ND	No
8	ND	ND	No	12	ND	ND	No
15	14	ND	No	14	43	ND	Yes
17	ND	ND	No	18	30	ND	Yes

Serum level of CAT-152 or CAT-001 and incidence of chemosis are also shown.
(ND = not detected)

3.5 MODULATION OF THE WOUND HEALING RESPONSE IN VIVO: EFFECT OF ANTISENSE OLIGONUCLEOTIDES TARGETING TGF β

3.5.1 In vivo tolerance to TGF β antisense oligonucleotides in experimental glaucoma surgery

To assess tolerability of the TGF β antisense in vivo, we investigated the effects of single 100μl subconjunctival injections of rabbit TGF β1 antisense OGN at doses of 25 μg, 50 μg and 100 μg. All injections were well tolerated in NZW rabbits with no evidence of intraocular inflammation being seen in any rabbit at any time in the study, or at any concentration of the drug. Conjunctival vascularity remained normal throughout the study period in all animals.

3.5.2 Efficacy of TGF β antisense oligonucleotides in experimental glaucoma surgery

3.5.2.1 Experimental details One anaesthetic death occurred in the first batch of surgery. The animal had received Misense OGN and was in the group of rabbits that would have been sacrificed after 15 days.

3.5.2.2 Bleb survival All animals failed surgery by day 23. However, TGF β2 antisense OGN significantly prolonged bleb survival in this model of aggressive scarring (p=0.0059, Figure 81 A). Mean bleb survival was increased by 5.68 days compared to PBS control. Kaplan Meier survival analysis also demonstrated enhanced bleb survival in the BRII treated animals but this did not reach significance (p= 0.0729, Table 17). TGF β1 antisense did not affect the surgical outcome. The incidence of bleb failure is shown in Table 18.

3.5.2.3 Bleb morphology All blebs became flat and scarred during the study period. Mean bleb area and bleb height were not significantly increased by any of the treatments (Bleb area p= 0.407, bleb height p= 0.405, Figure 81 B and 81 C). Figure 82 shows the appearances of successful and failed filtration blebs on day 17 of the study. TGF β2 antisense was associated with diffuse conjunctival drainage compared to flat scarred blebs in the other treatment groups.

3.5.2.4 Anterior chamber depth Anterior chamber (AC) depth reflects the drainage of fluid through the microtube into the subconjunctival space. Flat or very shallow anterior chambers are seen in the early post-operative period, where the drainage of fluid exceeds aqueous production. The anterior chamber deepens with time and is usually of equal depth to the control eye by day 14, as the bleb starts to fail and transconjunctival drainage is reduced. Bleb failure is, therefore, defined as the presence of a flat scarred bleb with a deep anterior chamber. TGF β2 antisense prolonged the duration of a shallow AC and this result approached significance (GLM p= 0.065, Duration; Kruskal Wallis p= 0.065, Figure 83).

2.5.2.5 Intraocular pressure Analysis of mean IOP and IOP survival in the operated eyes showed no significant difference between treatment groups at any time point.

2.5.2.6 Tolerance Although an assessment of tolerability had been made for TGF β1 antisense OGN in the rabbit, additional oligonucleotides were studied in this efficacy experiment, the tolerance of which had not been previously assessed. Therefore, conjunctival vascularity and intraocular inflammation were observed throughout the study period. No significant differences in these indices were detected between the groups

(superior p= 0.3, nasal p= 0.739 and temporal vascularity p= 0.201; Figure 84). All treatments were safe and well tolerated.

3.5.2.7 Histological effects Ocular tissue from the animals sacrificed on days 15 (n=17) and 21 (n=15) was processed and analysed. By day 30 all the blebs had failed. The tissue from animals sacrificed on day 30 was not analysed. Previous experience with in this model has shown that once all the blebs have failed, only limited information can be gained on the effect of treatment on subconjunctival scarring.

The histological grading system was used to identify changes in cellularity (H and E), total scar tissue deposition (Picrosirius Red), collagen fibre density and orientation (Gamoris Trichrome), elastic fibre deposition (Oxidative Aldehyde Fuschin) and myofibroblast transformation (α SMA expression) between the treatment groups over the study period. It must be noted that tissue was analysed from a maximum of 3 animals in each group. This must be taken into account when interpreting the data.

TGF β2 antisense OGN treatment reduced collagen deposition and improved fibre orientation as judged by Gamoris Trichrome staining (p=0.036, Figure 85 and 86). In addition TGF β2 antisense OGN significantly reduced the deposition of elastic fibres (p= 0.019). There was a trend for TGF β2 antisense OGN to reduce cellularity (H / E) and collagen production (Picrosirius) compared to PBS control (p> 0.05 Figure 85 and 87). No other significant differences were found between treatment at day 21 or day 15 (Figure 85).

Figure 81 **Effect of intra-operative antisense oligonucleotides on the outcome of glaucoma surgery**

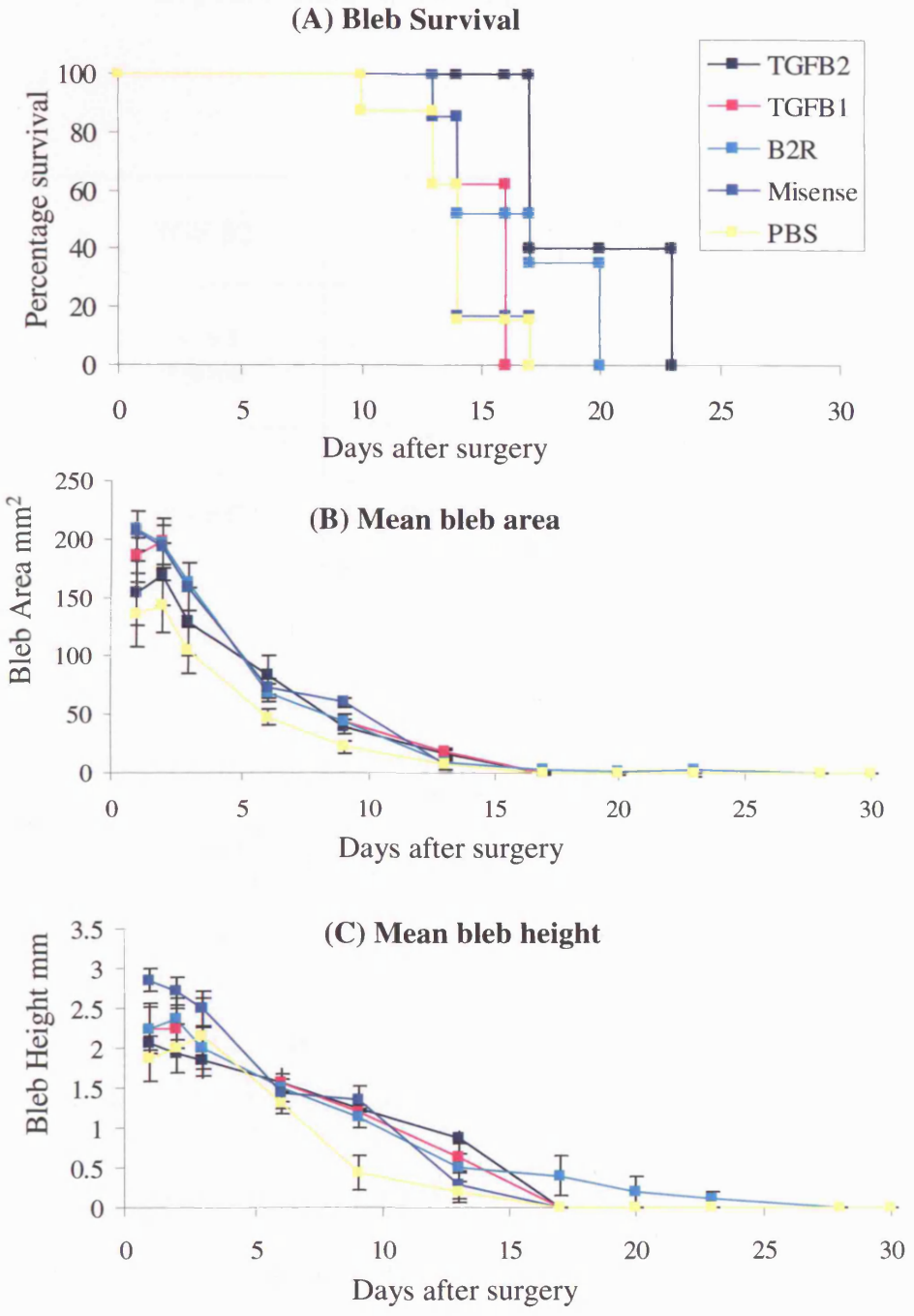

Antisense OGN directed against TGF β2 significantly prolonged bleb survival in this model of aggressive scarring (Kaplan meier Survival analysis p= 0.0059).TGF β1 antisense did not effect outcome. Interestingly, mean bleb area and bleb height were not significantly increased by any of the treatments (Bleb area p= 0.407, bleb height p= 0.405). Charts B and C: Mean and SE plotted. Legend codes for charts A,B and C

Table 17 Effect of antisense oligonucleotides on bleb survival

Log rank Statistics and (significance):

	TGF β2	TGF β1	BRII	Misense
TGF β1	10.93 0.0009			
BRII	2.56 0.1097	1.94 0.1642		
Misense	7.22 0.0072	0.01 0.9291	1.78 0.1821	
PBS	8.54 0.0035	0.41 0.5223	3.22 0.0729	0.56 0.4557

Table 18 **Incidence of bleb failure after treatment with antisense OGN against TGF β**

Treatment	Days after Surgery									Survival 30 days
	0	**10**	**13**	**14**	**16**	**17**	**20**	**23**	**30**	/ n
TGF β2	0	0	0	0	0	2	0	3	0	0 / 5
% survival	*100*	*100*	*100*	*100*	*100*	*40*	*40*	*0*	*0*	
TGF β1	0	0	1	0	4	0	0	0	0	0 / 5
% survival	*100*	*100*	*80*	*80*	*0*	*0*	*0*	*0*	*0*	
BRII	0	0	0	2	0	1	2	0	0	0 / 5
% survival	*100*	*100*	*100*	*60*	*60*	*40*	*0*	*0*	*0*	
Misense	0	0	0	4	0	1	0	0	0	0 / 5
% survival	*100*	*100*	*100*	*80*	*80*	*0*	*0*	*0*	*0*	
PSB	0	1	0	3	0	1	0	0	0	0 / 5
% survival	*100*	*80*	*80*	*20*	*20*	*0*	*0*	*0*	*0*	

Treatment	Days after Surgery			Survival 15 days
	0	**13**	**15**	/ n
TGF b2	0	1	0	3 / 3
% survival	*100*	*100*	*100*	
TGF b1	0	2	0	1 / 3
% survival	*100*	*33.33*	*33.33*	
BRII	0	1	0	1 / 3
% survival	*100*	*66.67*	*66.67*	
Misense	100	1	0	1 / 2
% survival	*100*	*50*	*50*	
PSB	0	2	0	0 / 3
% survival	*100*	*33.33*	*33.33*	

Figure 82 Bleb appearance on day 17 after intra-operative treatment with antisense OGN directed against TGF β

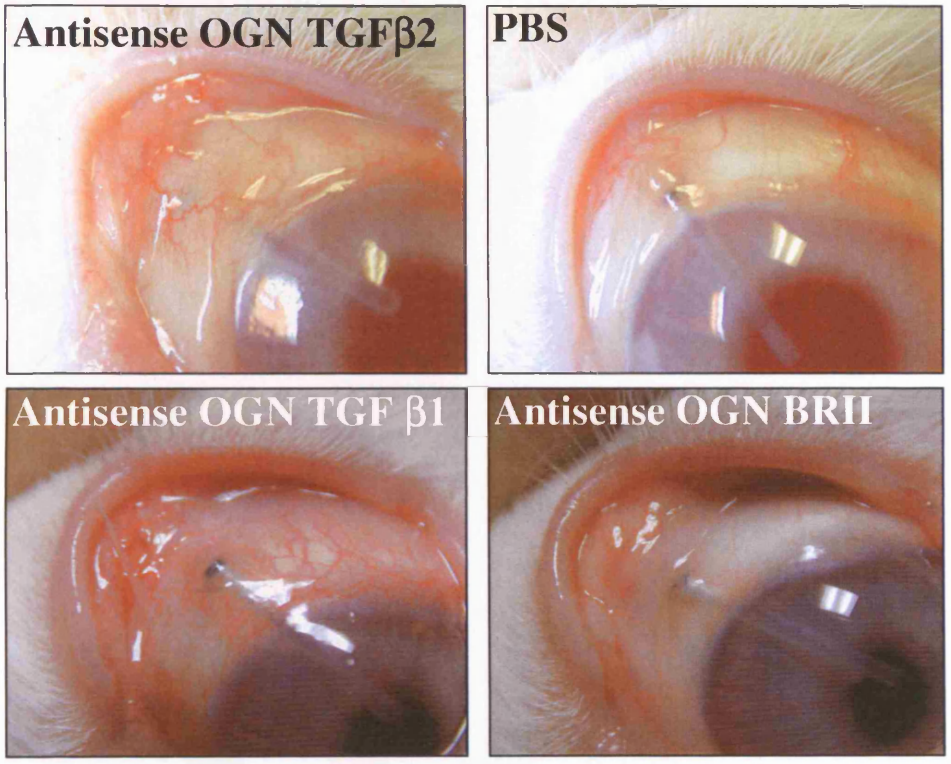

Typical appearances of filtration blebs on day 17. TGF-β2 antisense OGN was associated with diffuse drainage and normal conjunctival vascularity.

Figure 83 Effect of intra-operative antisense OGN on anterior chamber depth after glaucoma filtration surgery

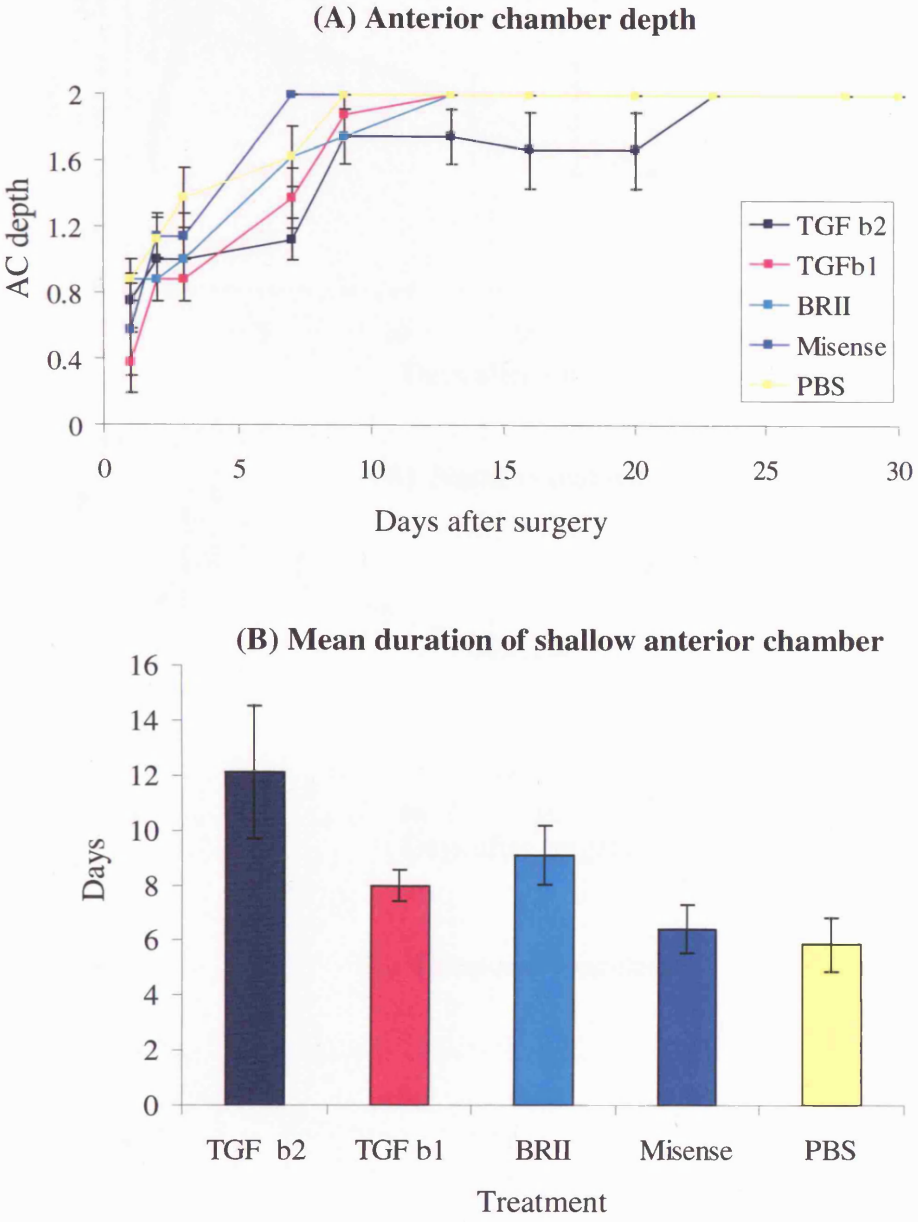

Anterior chamber (AC) depth reflects the drainage of fluid through the microtube into the subconjunctival space. Flat or very shallow anterior chambers are seen in the early post-operative period, where the drainage of fluid exceeds aqueous production. Bleb failure is defined as the presence of a flat scarred bleb with a deep anterior chamber. TGF β2 antisense prolonged the duration of a shallow AC and this result approached significance (GLM p= 0.065, Duration; Kruskal wallis p= 0.065).

Figure 84 Effect of intra-operative antisense OGN on conjunctival vascularity

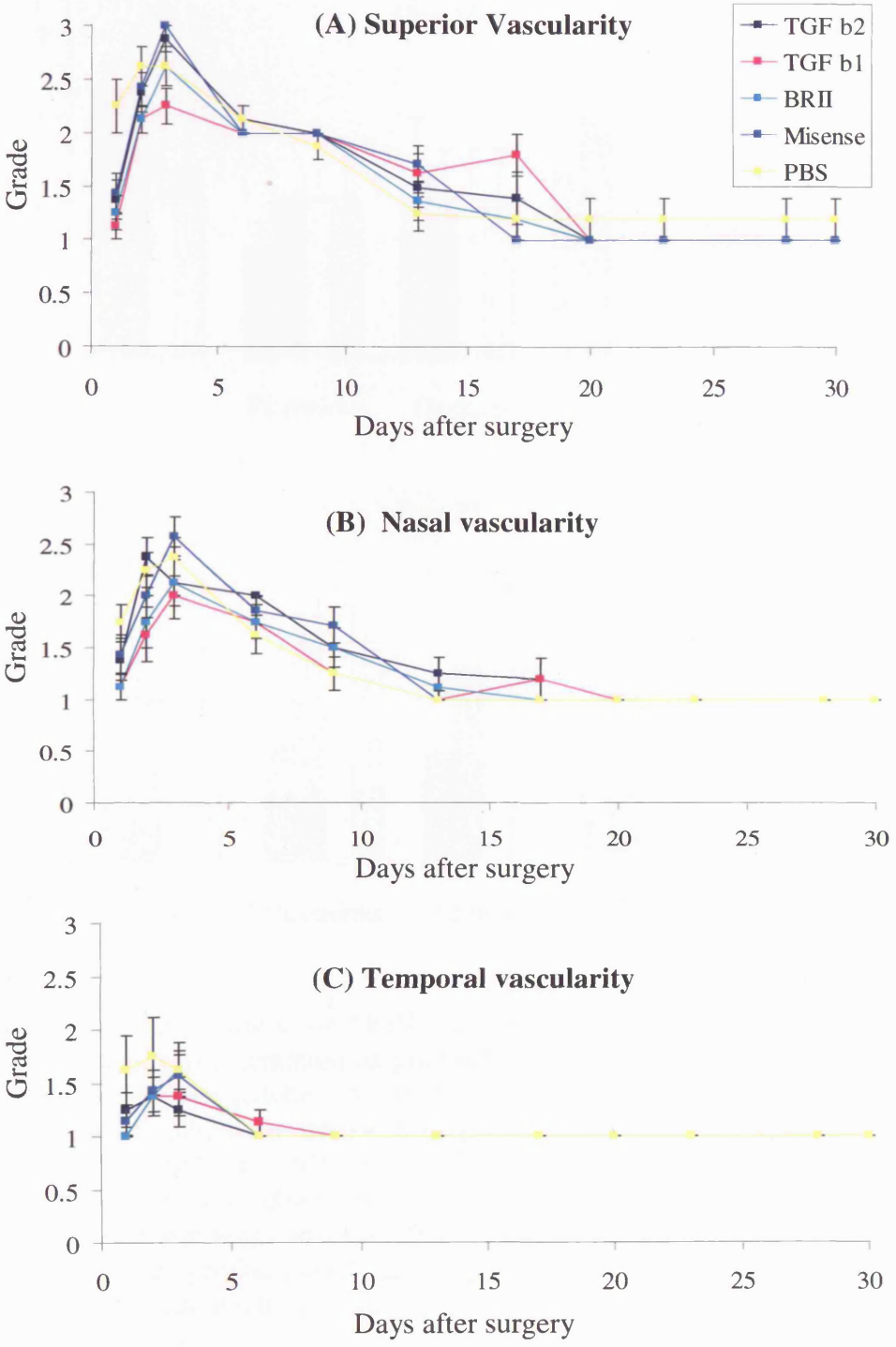

All treatments were well tolerated with no increase seen in conjunctival vascularity (Superior p= 0.3 , nasal p= 0.739 and temporal vascularity p= 0.201)

Figure 85 Effect of intra-operative treatment with antisense OGN on the different elements of the scarring response after glaucoma filtration surgery

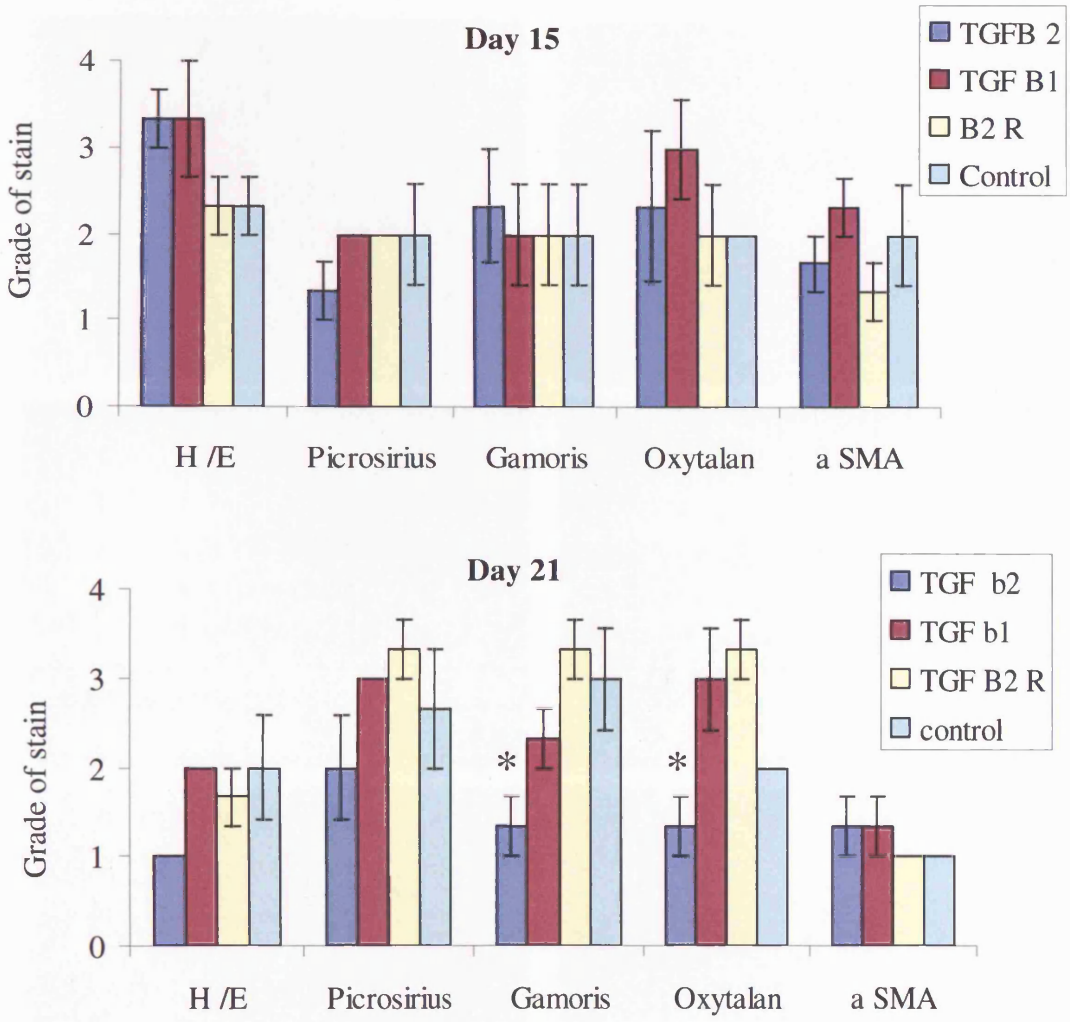

On day 21 TGF β2 antisense OGN a significantly reduced collagen density and improved collagen orientation as graded by gamoris trichrome staining. TGF β2 antisense OGN also reduced the deposition of elastic fibres (* p=0.05). At other time points trends were demonstrated in which CAT-152 reduced collagen deposition (picrosirius red), elastic fibre formation (Oxytalan staining) and collagen orientation (Gamoris trichrome) although these did not reach significance. There was a trend for TGF b2 antisense OGN to reduce cellularity (H / E) and collagen production (Picrosirius) compared to PBS control although these parameters did not reach statistical significance.

Figure 86 Effect of intra-operative antisense OGN treatment on subconjunctival scarring on day 21 after glaucoma filtration surgery

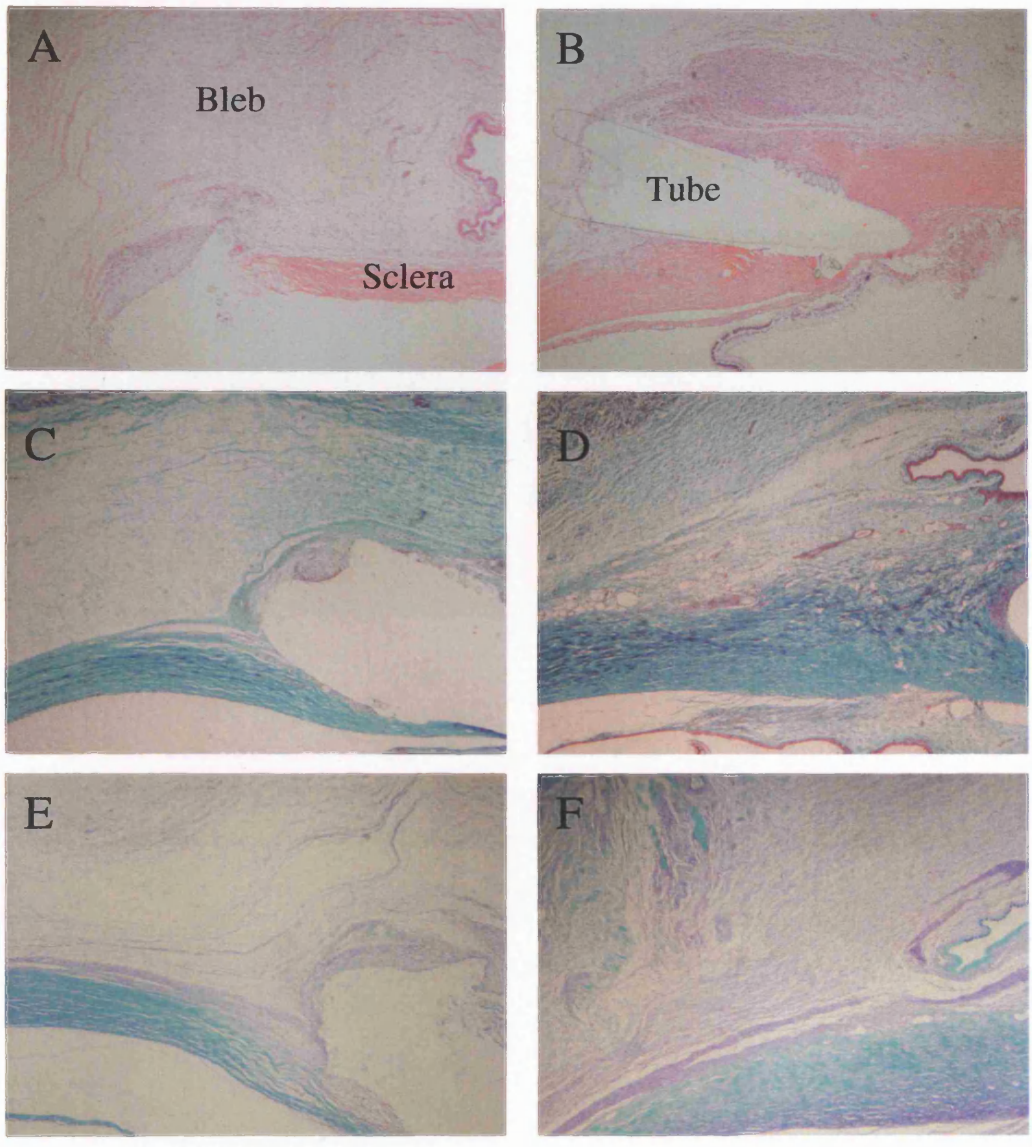

Histological characteristics of filtration blebs on day 21. Hematoxylin and eosin (A-B), Gamoris Trichrome (C-D) and Oxidative aldehyde fuschin (E-F) stained sections are shown of one representative animal per group: TGF β2 antisense OGN treated (A,C,E) and control group (B,D,F). TGF β2 antisense OGN treatment reduced subconjunctival scarring at the microscopic level. The gamoris trichrome staining demonstrated a reduction in the density of subconjunctival collagen deposition (green) with an improvement in the orientation of collagen fibres in TGF β2 antisense OGN treated animals. The oxidative aldehyde fuschin staining showed a reduction in elastic fibre formation (purple) after TGF β2 antisense OGN.

Figure 87 Effect of intra-operative antisense OGN treatment on collagen deposition on day 21 after glaucoma filtration surgery

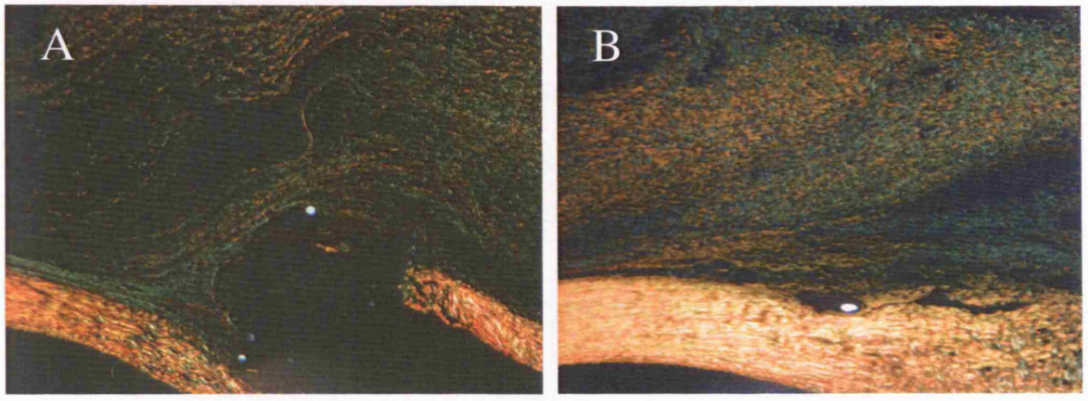

Picrosirius red stained sections of the operative wound site from animals treated with TGF β2 antisense OGN (A) and PBS (B). There was a trend for TGF β2 antisense OGN to reduce collagen density which is stained in green and yellow.

CHAPTER 4. DISCUSSION

4.1 MODULATION OF TGF β AND CONJUNCTIVAL SCARRING IN VITRO

4.1.1 ECM production in human Tenon's fibroblasts

TGF β2 stimulates collagen production in human Tenon's fibroblasts in vitro. Two different assays were performed to investigate collagen production in this study. The Sircol dye method detects all acid soluble collagens. The ELISA for C-terminus propeptide of collagen I (CICP), a marker of newly formed mature type 1 collagen was also used to assess collagen formation. Total collagen and collagen I production by ocular conjunctival fibroblasts was enhanced by TGF β2. The CICP assay was selected to study the effect of CAT-152 on fibroblast collagen generation as this assay could be performed using multiple replicates of the treatment condition with fewer cells whilst maintaining accuracy.

CAT-152 caused a concentration-dependent inhibition of collagen I production; full inhibition of this response was observed with 30nM CAT-152. These findings are consistent with the fact that CAT-152 has also been shown to significantly inhibit TGF β2–mediated collagen contraction by human Tenon's fibroblasts in vitro with an IC50 of 0.12mg/ml or 1nM (Cordeiro et al., 1999a).

Basal stimulation in the CICP assay investigating the effect of TGF β2 on Tenon's fibroblasts induced approximately 1500ng/ml collagen I secretion (Figure 35). Maximal TGF β stimulation induced more than a doubling of this response (264% increase over basal levels). However, when the experiment was repeated to investigate the effect of CAT-152, basal collagen I levels were higher at 2000ng/ml and stimulation with 100pM TGF β consequently only resulted in a 34% increase over basal levels. This between

assay variation in basal collagen I production is difficult to explain given that the experiments were performed using the same cell lines. However, the final set of 4 CICP CAT-152 were set up in 24 well plates with a cell density of 1x 10^5, compared to 6 well plates with a cell density of 7 x 10^5 which may have influenced the results. The same stock TGF β2 was used in this set of experiments.

Inhibition by CAT-152 reduced collagen I secretion to below basal levels at concentrations of 10 nM and above (Figure 41). At high concentrations CAT-152 may have induced a degree of cell death which has been demonstrated before in neutralisation assays. The concentration range tested was from 0.1nM to 1000nM. PBS was the vehicle used to dilute CAT-152. In order to achieve this concentration range a large PBS component containing stock CAT-152 1mg/ml was added to the TGF β2 stimulation media (e.g. 1700μl 117.6pM TGF β2 and 300μl 1mg/ml CAT-152 gave 2000μl of a solution of 100pM TGF β2 and 1000nM CAT-152). The PBS component may have had detrimental effects. Finally, the presence of anti-human antibody in the media may have interfered with the antibodies in the CICP elisa and affected the final reading.

4.1.2 Cytoskeleton and cell morphology

It is apparent from the results that ocular fibroblasts transform into myofibroblasts that express α SMA on treatment with TGF β2. Concomitant treatment with CAT-152 can fully inhibit fibroblast differentiation to the myofibroblast phenotype in this human in vitro model of fibrosis.

Fibroblast differentiation to the myofibroblast phenotype is known to be modulated by cytokines (Darby et al., 1990). Transformation into myofibroblasts is regulated by the environment and is thought to be a two step process in which both mechanical tension

and the presence of TGF β are required. The formation of stress fibres requires an initial up regulation and accumulation of intracellular proteins followed by assembly of these into stress fibres. The stress fibres form a terminal fibronexus adhesion complex which acts as mechano-transduction unit to functionally generate contractile force.

In the present, study TGF β resulted in concentration dependent increase in α SMA expression with maximum TGF β stimulation resulting in a 200% increase over basal levels. Under phase contrast light microscopy changes in cell morphology were clearly identified after stimulation with 10pM TGF β. Cells became less spindle shaped and linear fibres could be defined with greater degree of cell contact. Immunofluorescent microscopy confirmed that the α SMA had been incorporated into stress fibres. No other cytoplasmic α SMA staining was detected. TGF β therefore appears to increase expression and assembly of α SMA stress fibres in these ocular fibroblasts.

Cells at higher passage were found to have increased expression of α SMA under serum free conditions. TGF β2 still upregulated α SMA production; however, this was less marked. Higher passage cells induced a 190% increase over basal levels compared to 374.9% by low passage cells. It is generally accepted that low passage cells behave in a more reproducible and predictable manner and all cell culture experiments were performed on cells between 2 and 6. In addition, it has been shown that fibroblast cell populations can be directed into either the fibroblast or myofibroblast phenotype by the density at which they are cultured. It is hypothesized that low density culture increases the population of myofibroblasts by reducing the degree of cell contact and subsequently increasing the number of TGF β receptors. All cells in this experiment were seeded at a density of $7x\ 10^3$ which resulted in approximately 80% confluence. The same cell line may vary from passage to passage and higher passage cells are more likely at some stage

to have been plated at high density. Finally, great care had to be taken when washing the monolayers with PBS after seeding in the presence of 1% FCS serum. Occasionally, cell loss was detected. This may have affected cell density, the response to TGF β and the level of α SMA expression.

Treatment with CAT-152 completely prevented myofibroblast transformation with an IC50 value of 1.5nM. This was comparable to CAT-152 inhibition of collagen formation in which the IC50 was 1.3nM. Phase contrast microscopy demonstrated that at concentrations of 10nM and above CAT-152 cells became more linear and no intracellular fibres could be seen. Immunofluorescent imaging of the CAT-152 treated fibroblasts showed complete absence of stress fibres staining with α SMA. At high power (x 60) faint granular cytoplasmic staining for α SMA was detected. A similar degree of staining was also detected on the negative control suggesting that related to background staining rather than the presence of cytoplasmic α SMA. CAT-152 appears to inhibit both expression and assembly of α SMA stress fibres.

In summary, it is known that bleb failure is associated with collagen production and conjunctival tissue contraction secondary to myofibroblast activity. We have shown that CAT-152 reduces collagen production and prevents myofibroblast transformation in isolated Tenon's fibroblasts. The IC50 values for CAT-152 were comparable for inhibition of collagen formation and myofibroblast transformation.

This highlights one of the mechanisms by which CAT-152 may act to improve the outcome of glaucoma filtration surgery in vivo.

4.2 MODULATION OF TGF β AND CONJUNCTIVAL SCARRING IN VIVO

4.2.1 Temporal and spatial expression of TGF β and ECM molecules in subconjunctival rabbit tissue after glaucoma filtration surgery

Aqueous flow bathes the wound and provides a unique and changeable concentration of inflammatory mediators. In humans latent TGF-β2 is thought to be produced by tissues within the eye (ciliary body and trabecular meshwork) prior to activation by plasmin and thrombospondin released from blood components after breakdown of the blood aqueous barrier (Grainger et al., 1995; Knisely et al., 1991; Schultz-Cherry et al., 1995; Tripathi et al., 1994a). After glaucoma surgery it is assumed that elevated levels of activated TGF β2 at the wound site are therefore likely to be related to aqueous concentration, the flow of aqueous and breakdown of the blood aqueous barrier. TGF β is also derived locally from degranulating platelets and inflammatory cells at the wound site. In addition TGF β displays the ability to auto induce its own production thereby initiating a perpetuating cascade of activation (Kelley et al., 1993; Li et al., 1999). This working hypothesis of TGF β secretion in GFS has not been experimentally demonstrated to date in the rabbit model.

The aims of this study were to identify the ocular source of TGF β in the rabbit, the effect of GFS on TGF β levels and how CAT-152 influences ocular TGF β2 mRNA and protein expression. In addition we analysed the mRNA and protein expression of ECM in the subconjunctival bleb tissue.

The rank order of relative TGFβ2 mRNA expression in control eye tissues was ciliary body>>iris>cornea>conjunctiva>sclera.Variation in TGFβ1 mRNA expression across the tissues analysed was small, with greatest expression observed in the iris (rank order of

expression; iris > ciliary body > conjunctiva > cornea > sclera). The relative levels of TGF β2 were higher than that of TGF β1 and although this data has to be interpreted carefully as they are not absolute values, it does indicate that the overall levels of TGF β2 are higher that those of TGF β1 in the rabbit eye. In addition, the internal ocular structures (ciliary body and iris) had the highest relative expression of TGF β2 mRNA. These findings are consistent with our current hypothesis of ocular TGF β2 secretion as based on the research by Tripathi and others (Tripathi et al., 1994a; Tripathi et al., 1993).

Relative TGFβ2 mRNA expression was significantly upregulated after GFS in the cornea (day 14; $P<0.05$), iris (day 3; $P<0.01$) and ciliary body (day 3, $P<0.001$ and day 14, $P<0.05$). These increases were modest and mean relative mRNA expression did not exceed >four-fold control levels for any tissue The most striking changes in relative mRNA expression were observed for the TGF β1 gene, which was more than 10 fold greater than control levels at day 3 in both conjunctiva and sclera, possibly representing a delayed local tissue response to the trauma of the GFS procedure.

TGF β mRNA expression appeared to follow a similar temporal pattern reaching a peak on day 3 and gradually returning to pre-operative levels by day 14. This was most clearly seen in the conjunctival tissue. This represents an interesting finding and correlates well the temporal changes in cellularity, collagen and α SMA demonstrated histologically in the rabbit tissue after GFS, which reached a peak at day 10 and gradually reduced by day 30 (Section 3.2.4.8). The levels of total TGF β2 observed in the aqueous humour of control eyes in this study are consistent with values previously reported for the New Zealand White rabbit (i.e. 2.7-4.1ng/mL; Liu, 2002 and 1.4-3.5ng/mL; Cousins et al., 1991) (Cousins et al., 1991; Liu, 2002). However, active TGF β2 levels in control

samples were higher in the present results than those published by Liu (2002) who highlighted a circadian variation in total and active TGF β2 levels in rabbit aqueous humour. This factor was not specifically taken into account when sampling aqueous humour in this study and it is not clear to what extent the apparent difference in active TGF β2 levels is due to such circadian changes. All samples were taken in the morning over a two hour time period.

Total TGF β2 levels were significantly higher in rabbit aqueous humour on the first day after GFS and again displayed a stepwise reduction over time. The day 1 result was not matched with increased relative TGF β2 mRNA expression in any of the ocular tissues assayed until day 3. This may indicate that the initial source of TGF β2 is related to the BAB breakdown rather than local production.

The post-GFS aqueous levels of active TGF β2 described in this report are constant at approximately 600-700pg/mL and appear to more closely reflect the previously reported values derived from normal eyes (i.e. 120-450pg/mL; Liu, 2002 and 320-610pg/mL; Cousins et al., 1991). It would be logical to predict that active TGF β2 levels would also become elevated after GFS. However, at face value, the data presented here indicates that there is a sustained reduction in aqueous levels of active TGF β2. A number of expanantions can be given to account for this. Firstly, the results may demonstrate a spuriously high level of active TGFβ2 in control samples, with post-GFS levels that are reduced or otherwise unchanged from 'normal'. Secondly, active TGF β is a very labile molecule which is difficult to assay. Finally, and most importantly, it is known that on conversion to the active molecule, TGF β becomes bound and sequestered in the tissues. Total active TGF β may well have become elevated after GFS, however, free unbound TGF β2 available for assay would go down.

Treatment with CAT-152 did not result in a clear pattern of changes in the expression of TGFβ mRNA or protein in any of the tissues studied. It was interesting to note and hypothesize on the biological significance of the isolated inhibitory effects seen for relative mRNA expression for TGF β1 (ciliary body; day 3) and TGF β2 (iris; day 3) In this model a tube is positioned in the eye and provides a communication between the anterior chamber and the conjunctival bleb tissue. Thorectically, it may be possible for some of the drug admninistered adjacent to the bleb to enter the eye and act on the internal tissues such as the iris and ciliary body. This would help to explain how subconjunctival CAT-152 can reduce iris and ciliary body TGF β mRNA expression.

Overall, the TGF β data presented suggests that normal rabbit eyes contain high levels of TGF β2 protein, which is the most predominant ocular isotype in the rabbit. The source of TGF β2 in aqueous humour has not been completely elucidated in this study, however, TGF β2 mRNA expression was considerably greater in the ciliary body. This supports the theory that TGF β2 is predominantly produced from internal ocular tissues in the unoperated eye. After GFS early increases in aqueous TGF β2 may result from BAB breakdown. Conjunctival TGF β mRNA demonstrates a temporal expression profile with highest levels detected on day 3 and stepwise reduction by day 14.

Following GFS conjunctival α SMA and collagen III mRNA expression was markedly increased over 100-fold increase compared to controls. Expression was greatest on day 3 and reduced with time. A less marked but similar pattern was also demonstrated in the sclera expression of α SMA and collagen III. Collagen deposition and α-SMA expression are known features of the fibrotic bleb seen after GFS in the rabbit and human (Hitchings et al., 1983). In this model bleb failure occurs on approximately day 14 without any anti-scarring agents. It can be postulated that the increase in conjunctival collagen and α SMA

expression on day 3 would mediate the increase in the deposition of these proteins with in the bleb within this time scale.

After wounding, a fibrin scaffold is formed at the wound site, which is initially replaced by collagen type III and then by collagen type I. In comparison to collagen III, lower levels of collagen I were detected within the time course of the experiment. However, collagen I expression was also highest on day 3 and decreased with time. From this it can be inferred that predominantly collagen III may account for early bleb failure, which may then be replaced with collagen I as the scar is organized with time.

Interesting results were seen in the cornea with strong up regulation of α SMA and collagen III seen up to a maximum of around 100-fold increase on day 14. At this time point expression of collagen I ($p<0.01$) and collagen III ($p<0.001$) reached significance over controls. During the procedure the tube is inserted into the clear cornea beyond the limbus before entering the eye. This is the most likely trigger to the wound healing response in the cornea and the up regulation of both collagen and α SMA. The rabbit appears to exhibit a very pronounced corneal wound healing response clinically with stromal opacification and neovascularisation.

In the iris and cilliary body collagen III was weakly upregulated from day 3 onwards after GFS. During the initial post-operative period the anterior chamber is very flat with close apposition of the tube to the iris. One explanation for the results is that the physical presence of tube in the eye may have initiated injury and a subsequent localised wound healing cascade. However, these tissues were also shown to upregulate the expression TGF β2. High local levels of TGF β2 may have resulted in a subsequent increase in the expression of collagen and α SMA.

CAT-152 was only shown to inhibit the expression of collagen III mRNA in the cornea but did not affect the genes tested in the other ocular tissues.

The data has displayed a relationship between GFS and the ECM deposition associated with bleb failure. However, again it failed to reveal a convincing relationship between changes in ECM expression and the application CAT-152 treatment.

Overall, it seems reasonable to assume that scleral and conjunctival tissue at the site of the drainage bleb would be continuously exposed to the high concentration of TGF β2 in aqueous humour. Total TGF β2 levels are considerably higher in bleb tissue at day 3 post surgery and this may represent accumulation of TGF β2 protein at the site of aqueous humour filtration or *de novo* protein synthesis in the bleb tissue in response to tissue injury. Based on the data presented here, accumulation from filtered aqueous humour seems the more likely explanation given that total TGF β2 levels were transiently increased in aqueous humour at day i) post-GFS, and ii) conjunctival TGF β2 mRNA expression is not significantly upregulated after GFS (although there is a trend to increased expression at day 3 post GFS). Whatever the origin of the conjunctival bleb TGF β2, exposure of the tissues to TGF β2 in this way is likely to contribute to the rapid fibrosis and failure of drainage blebs characteristic of the rabbit model. The concentration of TGF β2 present in aqueous humour in this study (~ 10-100pM) has been shown *in vitro* to promote collagen production in human conjunctival fibroblasts and their transdifferentiation to a myofibroblast phenotype expressing α SMA (As discussed in section 4.1). Both TGF β2-evoked effects can be inhibited by CAT-152. The available evidence suggests that bleb failure in the rabbit experimental GFS model is mediated by fibrotic changes in conjunctival tissue that is exposed to persistently high concentrations

of TGF β2 present in aqueous humour. Prevention of the fibrotic response can be achieved by repeated subconjunctival administration of CAT-152, which neutralises the excess TGF β2 within the bleb tissue leading to a reduction in TGF β2 protein levels, removal of the drive for the fibrotic response and thereby promotes drainage bleb survival.

4.2.2 Modulating effect of Anti-TGF β2 antibody (CAT-152) on the outcome of experimental glaucoma filtration surgery

4.2.2.1 Effect of intra-operative CAT-152 The ideal anti-scarring agent would be administered at the time of surgery as a single treatment. We therefore investigated if intra-operative treatment of CAT-152 given immediately before and after surgery could reduce scarring after glaucoma filtration surgery.

Unfortunately, this study did not show any benefit of a single dose regimen. The main outcome variable was bleb survival. All blebs failed by day 21. Median bleb failure was 14 days after treatment with CAT-152, PBS and with no treatment. These findings were consistent with previous studies using this model, in which untreated control animals most commonly fail around day 14. In addition, the fact that the PBS group displayed similar rates of failure to the no treatment group suggests that the physical act of the subconjunctival injection does not influence bleb outcome.

This finding that is not totally unexpected given knowledge of the timing of peak Tenon's capsule fibroblast activity following injury. Reichel introduced a new model of conjunctival scarring in the mouse eye (Reichel et al., 1998). The inflammatory cell profile following conjunctival injury was demonstrated by sequential histological

analysis. The fibroblast population, the third wave of cellular activity, was shown to increase during the first three days to reach a peak at day 3. Thereafter, it was found to decrease but never quite returned to the control eye activity level. Fibroblast activity was closely associated with the deposition of newly laid extracellular matrix. With TGF β driving this fibroblast proliferation, inhibitory effects induced by its neutralising antibody, CAT-152, are likely to be most demonstrable by administration at times of greatest cytokine activity in the immediate post-operative period.

Rabbit models exhibit an exaggerated healing response compared to human tissue. Demonstration of efficacy in such models is therefore likely to be reproduced in the clinical setting. Conversely, potential clinical benefit may be overlooked when a treatment fails to show efficacy in such as aggressive model.

The technique of glaucoma surgery used in this study localises scarring to the level of the conjunctiva. This is achieved by maintaining a permanent fistula to drain aqueous into the subconjunctival wound site. Previous experience has shown that intraocular pressure is not a reliable indicator of filtration in this model of glaucoma surgery. Furthermore, in this study no significant differences were detected in IOP between groups. This can be explained by the fact that basal pre-operative intraocular pressure in this model of glaucoma filtration surgery is within the normal range (this is a model of subconjunctival scarring not of glaucoma). Given this, bleb failure rather than intraocular pressure has always been defined as the primary outcome variable to represent failure of surgery in this model.

Anterior chamber depth was included in the observations as an indirect indicator of the drainage of fluid through the tube into the subconjunctival space. The rabbit anterior segment is very crowded with a very large lens and small anterior chamber. Therefore in practice, this measurement was fairly difficult to grade. In most of the animals the

anterior chamber was flat on day one and gradually deepened over the next 7 days. No significant difference was found between the treatments in the time taken for the anterior chamber to deepen. Overall, this observation may not be as true a representation of anterior fluid dynamics as had been originally anticipated.

Despite the lack of demonstrable efficacy all the treatments were well tolerated.

4.2.2.2 Effect of prolonged post-operative application of CAT-152: Comparison with 5-Fluorouracil Continued scarring leading to late failure of glaucoma filtration surgery remains a major barrier to long-term intraocular pressure control and arrest of the glaucomatous progression. This experiment was designed to see if post-operative neutralisation of TGF β alone, could prevent bleb failure and provide a means of rescuing failing blebs. 5-FU has been given subconjunctival in the post-operative period to treat failing and encysted blebs so CAT-152 was also compared to the gold standard post-operative anti-scarring agent.

The results of this study demonstrated that neutralising the effects of TGF-β2 in the post-operative period, by subconjunctival administration of CAT-152 can improve the outcome of glaucoma surgery in this model. In addition, the effect of post-operative CAT-152 appears more efficacious than 5-FU and without some of the side effects associated with anti-proliferative use.

As with previous experience no significant differences were detected in IOP between groups in this study.

We found that isolated post-operative 5-FU had the same bleb survival end point as control in this experiment. This model exhibits an extremely aggressive scarring response which may explain this finding. However, conversely, all the treatments that have improved bleb survival in this model have worked in a subsequent clinical setting. Only a

limited number of studies have looked at efficacy of 5-FU as an isolated post-operative agent in animal experiments. Doyle et al compared the effect of 5 post-operative injections of 5-FU with single intra-operative 5-FU, and combined intra and post-operative 5-FU in rabbit filtration surgery. Control animals received intra-operative distilled water only. No significant difference was shown in bleb survival between post-operative 5-FU treatment and control in this study. However, what can be seen in the survival curve from Doyle's study and our data is that post-operative injections of 5-FU appear to shift the survival curve to the right of the control in the early time points, without affecting the final endpoint (Doyle et al., 1993b).

The landmark study of the 5-Fluorouracil Filtration surgery Study Group represents the only definitive report in which post-operative injections of 5-FU were shown to improve surgical outcome (Group, 1989). In this study a total of 21 subconjunctival injections were given: 2 injections per day on days 1-7 after surgery and 1 injection per day on day 7-14 after surgery. If this number of injections had been used we may well have shown efficacy of post-operative 5-FU in this model. When designing the protocol we chose a post-operative regimen that more closely reflected current clinical subconjunctival 5-FU use.

Anterior chamber measurements did not reveal any significant differences between the groups. This again highlights that this observation has not proved itself to be a reliable indicator of transconjunctival drainage.

Ideally all subconjunctival injections would have been given at the same site. In all the pre-clinical and clinical studies of CAT-152 in glaucoma filtration surgery the drug has been administered by subconjunctival injection in the superior nasal quadrant adjacent to the drainage bleb. The same injection site was therefore selected in this study. Clinically, the site of subconjunctival 5-FU administration varies depending on clinical preference.

Some clinicians favour injections adjacent to the bleb, some 90 degrees and some 180 degrees from the operation site. The main concern with injecting 5-FU adjacent to the bleb relates to the possibility of intraocular penetration as the pH of 5-FU is 9. We decided to base our study protocol on the pioneering studies of 5-FU in glaucoma surgery performed by The Fluorouracil Filtering Surgery Study Group. In this study 5-FU was injected 180 degrees from the site of surgery. Given the different injection sites for the CAT-152 and 5-FU groups a universal injection site for a control vehicle was not possible so the no treatment control group was introduced.

Aqueous flow bathes the wound and provides a unique and changeable environment which influences post-operative healing. Of all the growth factors in the aqueous TGF β is the most potent stimulator of human Tenon's fibroblast activity (Khaw et al., 1994b). Latent TGF β2 is produced by tissues within the eye (ciliary body and trabecular meshwork) prior to activation by plasmin and thrombospondin released from blood components (Tripathi et al., 1994a) (Grainger et al., 1995; Knisely et al., 1991; Schultz-Cherry et al., 1995). Aqueous humour in glaucomatous eyes contains increased level of TGF-β2 (Tripathi et al., 1994a). After glaucoma surgery elevated levels of activated TGF β2 at the wound site are therefore likely to be related to aqueous concentration, the flow of aqueous and breakdown of the blood aqueous barrier. In addition, TGF β also displays the ability to auto induce its own production thereby initiating a perpetuating cascade of activation (Kelley et al., 1993; Li et al., 1999). In a mouse model of conjunctival scarring peak levels of TGF β2 have been shown at the wound site at day 7 (Reichel et al., 1998). Without treatment the rabbit model fails by day 14. We propose that isolated post-operative administration of CAT-152, between days 2-14 in this model, can still

neutralise subconjunctival TGF β2 levels at the wound site below a threshold required to mediate downstream effects on the extracellular matrix.

Histological analysis of the rabbit tissues showed that CAT-152 significantly reduced subconjunctival collagen deposition compared to both the 5-FU and control groups.

CAT-152 also significantly reduced the population of cells expressing α smooth muscle actin, indicating an inhibition of fibroblast differentiation into the myofibroblast phenotype. These histological observations taken together with the effects of CAT-152 in isolated Tenon's fibroblasts suggest that the beneficial effects of CAT-152 in glaucoma filtration surgery are mediated by a reduction in collagen production and prevention of myofibroblast transformation resulting in reduced contraction of the drainage bleb tissue

Repeated injections of subconjunctival 5-FU in clinical practice are known to cause corneal epitheliopathy. Similar findings were associated with the use of 5-FU in this study. The more serious complications of avascular bleb formation, bleb related infection and chronic hypotony reflect the cytotoxic mechanism of action of anti-proliferative agents. CAT-152 treatment provides a more physiological alternative.

This represents a potentially useful development in the prevention of late surgical failure and may provide us with a safer therapy to maintain maximal IOP control.

4.2.2.3 Long term effects of combining intra-operative and prolonged post-operative CAT-152 treatment So far the effect of CAT-152 has only been investigated over a 30 day post-operative period. This experiment was designed to identify if maximum dosing with CAT-152 could prevent bleb failure occurring for 45 days. In addition, during the project the cell line used to expand the production CAT-152 was modified. The original batch of CAT-152 had been used in all the previous in vivo experiments. The new antibody was used in this experiment.

The data clearly shows that administration of CAT-152 at the time of surgery and continued post-surgical dosing prevents bleb failure (33% survival at day 45). Survival until 45 days in this model is highly significant. By combining the intra-operative with the prolonged post-operative regimen maximal efficacy appears to have been achieved.

Two control groups were included in the study. In half the animals the PBS was given by superior subconjunctival injection and in the remaining animals by inferior injection. Bleb survival was not significantly different between these groups. The physical effect of the subconjunctival injection, therefore, does not appear to influence conjunctival bleb scarring. This is an important finding and confirms that the efficacy over 5-FU is not related to injection site. This is supported by the finding that there is a similar degree of bleb failure in PBS treated animals (median bleb survival 17 days; present study) and untreated control animals (median bleb survival 14 days in intra-operative study as discussed in section 4.2.21).

No significant differences in IOP survival were detected. However a trend for higher mean post-operative pressure was seen in the 5-FU treated group. Significantly higher pressures in the 5-FU animals compared to CAT-152 were seen on day 14 ($p=0.069$), day 28 ($p=0.096$) and day 31 $p=0.068$) and also compared to PBS on day 28 ($p=0.075$). Mean IOP with CAT-152 was similar to control mean IOP. Care must be taken not to place too much value on this data as it is generally accepted that intraocular pressure is not a reliable indicator of filtration in this model of glaucoma surgery.

In clinical practice 5-FU is associated with corneal epitheliopathy and avascularity. Side effects from administration of 5-Flurouracil were demonstrated in this study. 5-FU prolonged the duration of superficial punctate keratitis and the duration of the nasal avascular segment. These findings relate to the cytotoxic method by which the drug acts. Treatment with CAT-152 did not increase these variables over the control animals.

CAT-152 was also well tolerated as assessed by anterior chamber activity and conjunctival vascularity. However, a new finding of conjunctival chemosis was detected. Transient self limiting chemosis is seen in this model in the first 24 hours after surgery and is thought to be related to tissue trauma. Early chemosis was seen in all treatment groups. However, late chemosis 14 days after GFS has not been seen before and was only observed in the CAT-152 treatment group. Chemosis occurred in one third of animals treated with CAT-152 but did not appear to influence bleb survival. This response may be explained by the administration of multiple injections of a human antibody into the rabbit generating an immune response. It must be highlighted that this frequency of injections is in excess of any regimen that would be translated into the clinical setting. In addition, human administration of a human antibody will not be complicated by such a response. However, given this finding it will be important to understand the mechanism driving this response.

In summary maximal dosing of CAT-152 can maintain long term bleb function and the modifications made in the production of the antibody do not seem to influence efficacy.

4.2.2.4 Effects of a combined course of intra-operative and prolonged treatment with the CAT-152 on the immune response in the rabbit Prolonged dosing of CAT-152 after GFS caused chemosis in a proportion (33%) of treated rabbits. This study was designed to confirm this observation and to investigate the mechanism of CAT-152-induced chemosis.

The incidence of chemosis was evaluated in the rabbit model of GFS following treatment with CAT-152 and a null control human IgG4, CAT-001 according to the prolonged dosing schedule used in 2.7.3 (18 subconjunctival injections of 100μg over 42 days).

Vehicle control (PBS) was administered to a third treatment group using the same injection schedule.

As previously shown, PBS treatment did not cause late chemosis demonstrating that the late response is related to antibody treatment. Early chemosis was seen in the PBS treatment group as well as the CAT-152 and CAT-001 groups. Early chemosis is a response to GFS and is not treatment related. Furthermore, there is no correlation between the incidence of early (induced by GFS) and late (induced by antibody treatment) chemosis.

CAT-152 and CAT-001 induced chemosis in a proportion of the rabbits treated (1 of 6 and 3 of 6 rabbits, respectively). The severity of the chemosis induced by CAT-152 was similar to that induced by CAT-001, although the incidence of chemosis was greater in the CAT-001 treatment group. The ability of CAT-001, a null control human IgG4, to induce chemosis suggests that this response is a consequence of an immune reaction to this human protein. The chemosis induced by CAT-152 is therefore likely to be an immune reaction to the human IgG4 and appears unrelated to neutralisation of TGF β2. It has previously been demonstrated that CAT-001 does not neutralise TGF β2.

Evidence for involvement of immune system is demonstrated by the presence of rabbit antibodies directed against CAT-001 or CAT-152. The majority of human antibody treated rabbits produced an anti-human antibody response (4 of 6 or 5 of 6 for rabbits treated with CAT-152 or CAT-001, respectively). Only those rabbits with anti-CAT-152 or anti-CAT-001 antibodies (detected within the serum) mounted a chemotic response on injection of the human antibodies. However, not all rabbits with serum antibodies to CAT-001 or CAT-152 responded to antibody injection with chemosis. Therefore, the anti-CAT-152 or anti-CAT-001 response, although essential for generation of chemosis,

is not the only factor required to elicit this response. The additional factors in the chemosis response other than the anti-human antibody response are unknown.

The serum level of the anti-CAT-152 or anti-CAT-001 antibody response does not appear to be related to the incidence of chemosis. However, it is important to note that the presence of CAT-152 or CAT-001 in the serum can interfere with the anti-CAT-152 or anti-CAT-001 detection assay, respectively. The presence of CAT-152 in serum 70 days after initiation of CAT-152 treatment (rabbits 5 and 6; see Table 16) may result in an underestimate of the anti-CAT-152 antibody response. CAT-001 was not detected at the 70 day time point; interference is therefore unlikely and so the serum anti-CAT-001 level is a true estimate of the immune response. Within the CAT-001 treatment group chemosis can clearly be dissociated from the anti-CAT-001 serum level (see rabbit 9, Table 16).

Subconjunctival injection of CAT-001 and CAT-152 resulted in systemic exposure of the rabbits to these human antibodies. This has been observed previously with CAT-152. Maximum exposure was observed four days after initiation of treatment (and GFS) and serum levels of CAT-001 and CAT-152 were similar at this time point (999 and 1095ng/ml, respectively). The serum level of CAT-001 declined over time and was not detected at the 70 day time point. A similar pharmacokinetic profile was observed for CAT-152 in the majority of rabbits. However, in two animals the serum concentration of CAT-152 increased between day 24 and 44 and appreciable levels of CAT-152 were observed in serum 70 days after the first injection (28 days after the last injection). The reason for this profile is unknown.

The chemosis induced by CAT-152 in rabbits is unlikely to be manifest in human patients undergoing GFS. The main reason is that the human subjects would not be expected to mount a marked anti-human antibody response (since CAT-152 is a human IgG4 protein). Moreover, application of a regimen (six doses of 100μg of CAT-152 given over 7 days)

in the rabbit model that approximates the clinical regimen (four doses of 100μg of CAT-152 given over 8 days) does not induce chemosis (Cordeiro et al., 1999a).

4.2.2.5 Development and application of CAT-152 as an anti-scarring agent in glaucoma filtration surgery Figure 88 summarises the survival curves of the CAT-152 studies using this model, three of which have been performed in this research project. A dose-regimen response is evident. Administration of CAT-152 at the time of surgery appears to be important but CAT-152 is only effective when surgical dosing is accompanied with post-surgical administration. Post-operative dosing is more important than surgical as isolated post-operative CAT-152 can still improve bleb survival. Maximum efficacy is achieved by the combination of intra-operative and prolonged post-operative CAT-152. CAT-152 from the new cell line was used for this combined experiment (Section 2.7.3: labelled 4 on the graph) and thus it is clear that this batch is also effective in vivo as in vitro testing had indicated. Histologically, CAT-152 reduces collagen deposition and myofibroblast transformation in vitro and in vivo, two essential elements of bleb failure.

Important considerations can be drawn from this preclinical data in the development of this drug as a new anti-scarring agent in clinical glaucoma surgery. Two clinical trials have been performed and a multicentre European trial is reporting. The dose regimen used in the clinic consists of four subconjunctival injections (100μl of 1mg/ml CAT-152). Subconjunctival injections are given at the time of surgery (Immediately before and after the procedure), on day 1 and day 7. Experience with this model indicates that 1 day in the rabbit equates to approximately 1-2 weeks in human scarring. So the clinical dose approximately translates to experimental intra-operative treatment combined with post-operative treatment on day 1 and day 2 in the rabbit. The clinical dose is kept to the

Figure 88 CAT-152 Dose Regimen-Response

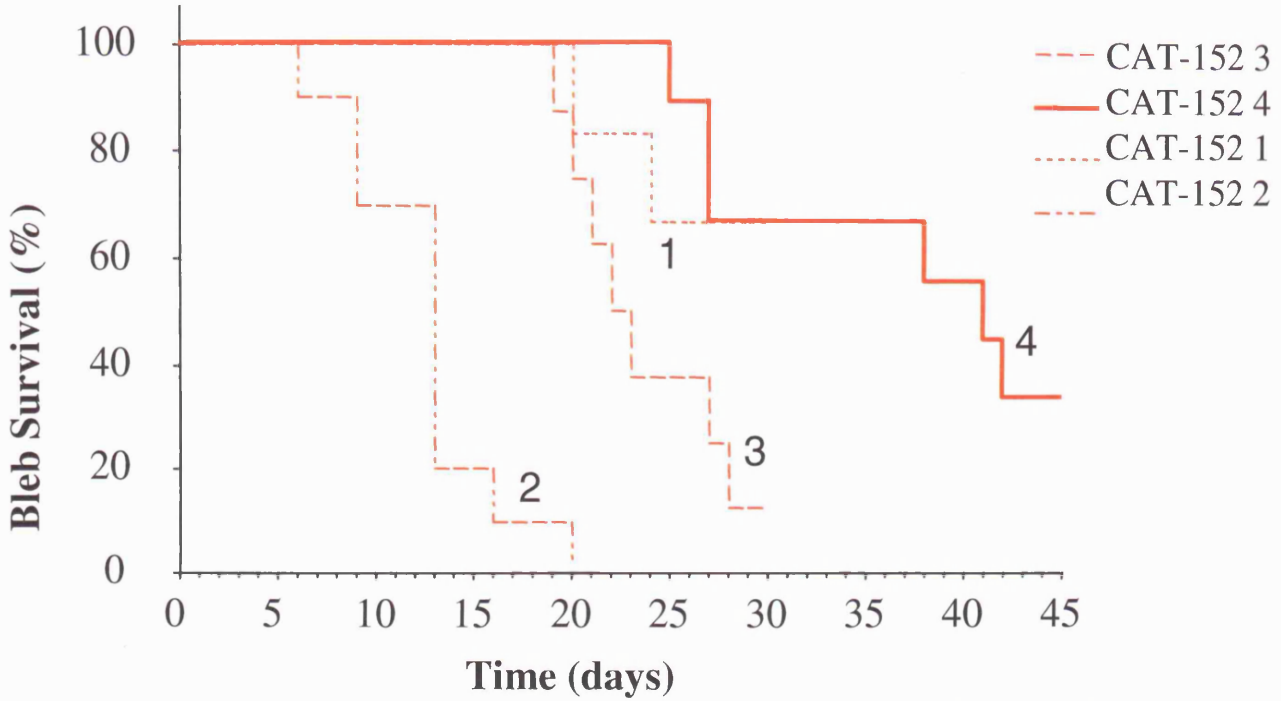

Exp.	Treatment Regimen	Dose (µg)	No. of Injection	Time of Dose (days) [Study end (day)]
2	Surgical alone	100	2	0,0 [30]
1	Surgical+Acute post-surgical	100	6	0,0,1,2,3,7 [30]
3	Prolonged Post-surgical	100	7	2,3,4,7,9,11,14 [30]
4	Surgical+Prolonged Post-surgical	100	18	0,0,1,2,3,4,7,9,11,14,17,21,24,28,31,35,38,42 [45]

Figure 88 summarises the survival curves of the CAT-152 studies using this model, three of which have been performed in this research project. A dose-regimen response is evident.

minimum to aid acceptance and ease of application. This is balanced with the obvious need for the selected regimen to provide efficacy.

The information provided by these experimental studies confirms that this dose regimen is close to optimal from the preclinical standpoint. The data also suggests that post-operative dosing with CAT-152 commenced 2 weeks after surgery and continued at 2 weekly intervals up to three months may provide a means of rescuing failing blebs. A further clinical trial is being planned to test this hypothesis.

CAT-152 has always been shown to be more effective than 5-FU (post-operative or maximal dose regimen) as shown in Figure 89. The dose regimen of 5-FU in the landmark study performed by the fluorouracil filtering study group included 14 post-operative injections. Clinically, 5-FU is now given as a single intra-operative dose or by subconjunctival injection in the post-operative period on an ad hoc basis. The demonstration of enhanced efficacy over 5-FU is extremely important for potential acceptance of CAT-152 as a new scarring agent. In addition the development of the optimal clinical dose regimen has been extensively investigated before licensing of the drug unlike 5-FU.

Finally, in all these experimental studies CAT-152 has been well tolerated. The observation of chemosis in the rabbit model was an interesting finding. This response was investigated in experiment 2.7.4 and the mechanism driving it identified. No chemotic response has been seen clinically and should not be mediated as it was driven by the anti-human antibody response of the rabbit.

Figure 89 Comparison of the effect of CAT-152 with 5FU

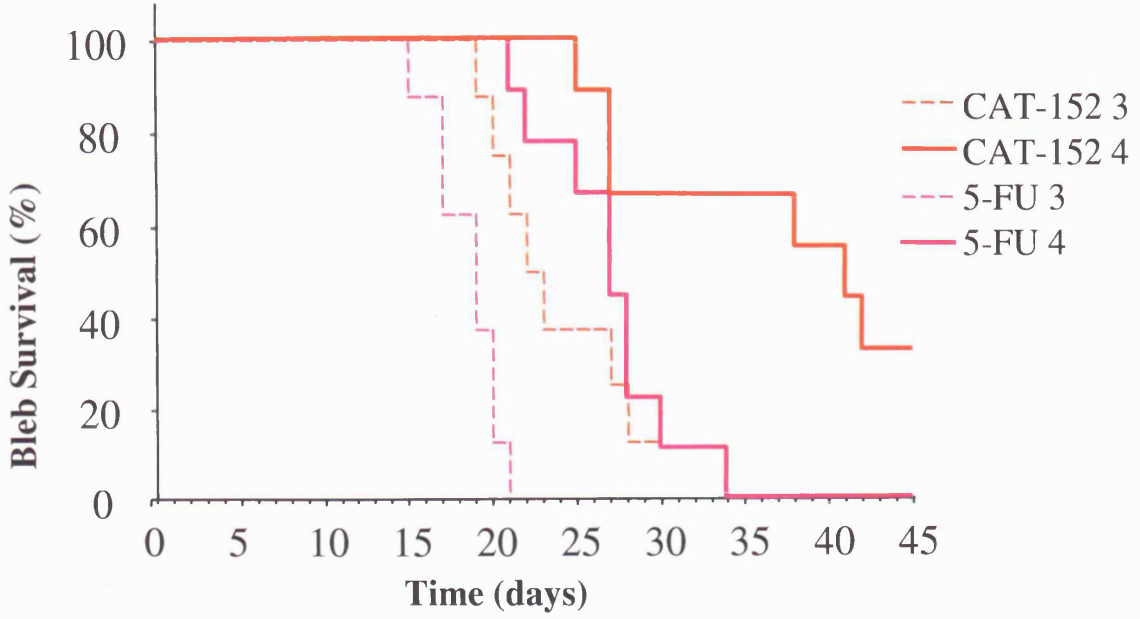

Exp.	Treatment Regimen CAT-152 0.1mg or 5-FU 5mg	Dose (mg)	No. of Injection	Time of Dose (days) [Study end (day)]
3	Prolonged Post-surgical	0.1 or 5	7	2,3,4,7,9,11,14 [30]
4	Surgical+Prolonged Post-surgical	0.1 or 5	18	0,0,1,2,3,4,7,9,11,14,17,21,24,28,31,35,38,42 [45]

CAT-152 has always been shown to be more effective than 5-FU (post-operative or maximal dose regimen)

4.2.3 Modulation effect of antisense oligonucleotides targeting TGF β on the outcome of experimental glaucoma filtration surgery

4.2.3.1 Tolerance to TGF β antisense oligonucleotides

The response of the rabbit to application subconjunctival TGF β1 antisense OGN was investigated in this study. All three doses of antisense 25 μg, 50 μg and 100 μg were well tolerated. This was not unexpected given the similar antisense molecules had been previous tested in the mouse model of conjunctival scarring without adverse effects (Cordeiro et al., 2000a).

4.2.3.2 Efficacy of TGF β antisense oligonucleotides

This study showed that antisense OGN directed against TGF β2 significantly prolonged bleb survival after glaucoma filtration surgery. All animals failed surgery by day 23. The effect of TGF β2 was to extend survival from a median of 14 days in the PBS treated group to 17 days in the treated group.

Previous studies have shown that TGF β2 is the most important isoform involved in conjunctival scarring (Cordeiro et al., 1999b). The reasons why three homologous TGF β isoforms exist in humans is still not fully understood. One possible explanation might be that the differential patterns of expression rely on co-ordination of each of the three isoforms as mediators of mesenchymal–epithelial interactions; hence in the skin, TGF β2 and TGF β3 affect epithelialization and keratocyte migration, while the effects of TGF β1 are predominantly dermal and involve fibroblast functions (Lutty et al., 1993). The conjunctival scarring model used in this project does not involve a breach in the epithelium. Hence the conjunctival stroma is the target tissue, which appears, from this

work and that of Pasquale et al, to primarily involve the TGF β2 isoform (Pasquale et al., 1993). Given that inhibiting TGF β2 appears to be so important in reducing the conjunctival scarring response, it is perhaps not surprising that the antisense OGN to TGF β2 that was most successful in prolonging bleb survival in this model.

However, antisense OGN would be expected to have maximal effects on the local cellular production of TGF β at the wound site and not in the aqueous. Evidence suggests that TGF β1 is secreted in the conjunctiva by local inflammatory cells including fibroblasts and platelets. The expression of TGF β1 mRNA from our study in the rabbit eye is consistent with this. In general most of the TGF β2 is thought to originate from inside the eye with high concentration in the aqueous humour. It was therefore hypothesised that antisense OGN towards TGF β1 would have showed efficacy in this experiment rather than TGF β2. As application of the TGF β antisense OGN is external to the eye it should not directly suppress the intraocular production of TGF β2, so we can only postulate that it may reduce aqueous TGF β2 by interfering the auto induction pathway from the cells within the eye. Alternatively, antisense may infact be able to enter the eye through reverse flow down the tube.

Bleb failure was defined as the presence of a flat scarred bleb in association with a deep anterior chamber. Mean bleb area and bleb height were not significantly increased by any of the treatments. However in animals treated with antisense OGN against TGF β2 the time for the AC to deepen was increased, which subsequently influenced and prolonged the time to bleb failure. The depth of the AC is thought to reflect the speed and degree of transconjunctival drainage of aqueous fluid. As we have gained in experience with this model it is becoming apparent that this is a difficult parameter to measure. In the previous experiments neutralising TGF β2 with CAT-152 the time taken for the AC to deepen has

been consistent across the treatment groups. It is difficult to explain why it took longer for the AC to deepen in this particular experiment, but it is clear that this clinical observation was one of the contributing factors associated with the increase in bleb survival.

Median bleb survival in the TBR II treated group was 17 days and this almost gained significance over treatment with PBS (p=0.0729). Most cell types simultaneously express the main TGF β receptors, TBR I, II and III, which are all present in the conjunctiva. A recent finding has been that TBR IIB an alternatively spliced variant of the TBR-II receptor, is a TGF β2 binding receptor, which mediates signalling via the smad pathway in the absence of TBR III (Rotzer et al., 2001). The expression of TBR IIB is restricted to cells originating from the mesenchymal tissues such as bone where the isoform TGF β2 has the predominant role. It would be interesting to investigate an antisense OGN designed against this spliced variant, as it may be more specific in inhibiting TGF β2 mediated activity.

Histological findings on day 21 correlated with the clinical observations of bleb failure. On day 21 TGF β2 antisense OGN a significantly reduced collagen density and improved collagen orientation and reduced the deposition of elastic fibres. Reduction in TGF β2 protein expression inhibited the downstream TGF β mediated effects on extracellular matrix deposition thereby preventing bleb failure.

It can be concluded that TGF β2 antisense OGN treatment is effective in reducing the scarring response after glaucoma filtration surgery and it appears to be more potent than TBR II and TGF β1 antisense OGN. In addition it appears to be well tolerated in vivo. However, these findings have to be interpreted with care. The mechanism by which TGF β2 was down regulated and the influence of the AC depth measurements on bleb survival must be considered when interpreting the data. In vitro assays of fibroblast function will

need to be carried out using these novel agents before further in vivo testing is performed. However, these results are encouraging and help to confirm both that modulation of TGF β is a very effective way of reducing post-operative subconjunctival scarring and TGF β antisense OGN might represent a novel way of achieving this.

4.3 CONCLUSIONS

In conclusion this project has continued to establish the role of TGF β modulation as a new anti-scarring strategy in glaucoma surgery.

In vitro, I have demonstrated that CAT-152 inhibits TGF β2 induced human Tenon's fibroblast collagen production and myofibroblast transformation at physiological concentrations.

In vivo, this research has added further evidence to suggest that TGF β2 is the most predominant ocular isoform and has identified changes in the expression of TGF β and ECM molecules associated with glaucoma surgery and TGF β modulation in the rabbit eye. Histologically, it appears that collagen deposition and myofibroblast transformation are key elements of bleb failure in the rabbit.

I have demonstrated, in vivo, that subconjunctival administration of CAT-152, given at the time of glaucoma surgery and in the immediate post-operative period, successfully improves surgical outcome, reduces subconjunctival fibrosis and is safe and well tolerated. Isolated post-operative administration of subconjunctival CAT-152 can prevent late bleb failure and prolonged dosing with CAT-152 appears to modulate the long-term scarring response after filtration surgery. Finally, I have shown that the anti-scarring effects of CAT-152 compare favourably to one of the gold standard anti-scarring agents in clinical use. These results have helped in establishing the potential clinical dose

regimen and have influenced the design of clinical trials. Overall, these findings have helped to move the novel antibody CAT-152 nearer to the clinical arena.

In addition, I have shown for the first time that antisense oligonucleotides directed against TGF β may also have a role in the prevention of conjunctival scarring.

New developments and the future The anti-proliferative agents are currently the most effective tool available to suppress conjunctival scarring after glaucoma surgery. Basic research has provided a greater understanding of how these agents work, which has lead to modifications in their use to improve efficacy and safety. This thesis and other research have demonstrated that exciting new physiological anti-scarring agents are now on the horizon. In the future, a multi-therapy approach may offer the best combination of efficacy with minimal side effects analogous to chemotherapy. Continued research and further understanding of the molecular events driving the wound healing response are essential. Ultimately, this will enable us to achieve optimal long-term intraocular pressure control after glaucoma surgery and prevent glaucomatous progression in the majority of patients.

.

Finally, the demonstration that TGF β2 modulation represents a successful anti-scarring strategy in the conjunctiva after GFS, may lead to its application in other scarring conditions in the eye and potentially throughout the body.

REFERENCES

Adams J. C., Lawler J. (2004). The thrombospondins. Int J Biochem Cell Biol 36, 961-968.

AGIS Investigators (2001). The Advanced Glaucoma Intervention Study (AGIS): 9. Comparison of glaucoma outcomes in black and white patients within treatment groups. Am J Ophthalmol 132, 311-320.

Akman A., Bilezikci B., Kucukerdonmez C., Demirhan B., Aydin P. (2003). Suramin modulates wound healing of rabbit conjunctiva after trabeculectomy: comparison with mitomycin C. Curr Eye Res 26, 37-43.

Allen L. E., Manuchehri K., Corridan P. G. (1998). The treatment of encapsulated trabeculectomy blebs in an out-patient setting using a needling technique and subconjunctival 5-fluorouracil injection. Eye 12, 119-123.

Altmann K. H., Dean N. M., Fabbro D., Freier S. M., Geiger T., Haner R., Husken D., Martin P., Monia B. P., Muller M., *et al.* (1996). Second generation of antisense oligonucleotides: From nuclease resistance to biological efficacy in animals. Chimia 50, 168-176.

Anderson D. H., Guerin C. J., Hageman G. S., Pfeffer B. A., Flanders K. C. (1995). Distribution of transforming growth factor-beta isoforms in the mammalian retina. J Neurosci Res 42, 63-79.

Araie M., Shoji N., Shirato S., Nakano Y. (1992). Post-operative subconjunctival 5-fluorouracil injections and success probability in japanese: results of 5 year follow up. Jpn J Ophthalmogy 36, 158-168.

Armaly M. F., Krueger D. E., Maunder L., Becker B., Hetherington J., Jr., Kolker A. E., Levene R. Z., Maumenee A. E., Pollack I. P., Shaffer R. N. (1980). Biostatistical analysis of the collaborative glaucoma study. I. Summary report of the risk factors for glaucomatous visual-field defects. Arch Ophthalmol 98, 2163-2171.

Armstrong D. J., Hiscott P., Batterbury M., Kaye S. (2003). Keratocyte matrix interactions and thrombospondin 2. Mol Vis 17, 74-79.

Asaria R. H., Kon C. H., Bunce C., Charteris D. G., Wong D., Khaw P. T., Aylward G. W. (2001). Adjuvant 5-fluorouracil and heparin prevents proliferative vitreoretinopathy : Results from a randomized, double-blind, controlled clinical trial. Ophthalmology 108, 1179-1183.

Ashcroft G. S., Dodsworth J., van Boxtel E., Tarnuzzer R. W., Horan M. A., Schultz G. S., Ferguson M. W. (1997). Estrogen accelerates cutaneous wound healing associated with an increase in TGF-beta1 levels. Nat Med 3, 1209-1215.

Assoian R. K., Komoriya A., Meyers C. A., Miller D. M., Sporn M. B. (1983). Transforming growth factor-beta in human platelets. J Biol Chem 258, 7155-7160.

Baramova E., Foidart J. M. (1995). Matrix Metalloproteinase family. Cell Biol Internat 19, 239-242.

Bartel D. P., Szostak J. W. (1993). Isolation of new ribozymes from a large pool of random sequences. Science 261, 1411-1418.

Bartram U., Speer C. P. (2004). The role of transforming growth factor beta in lung development and disease. Chest 125, 754-765.

Bassols A M. J. (1988). Transforming growth factor beta regulates the expression and structure of extracellular matrix chondroitin/dermatan sulfate proteoglycans. J Biol Chem 263, 3039-3045.

Bell E., Ivarsson B., Merill (1979). Production of a tissue-like structure by contraction of collagen lattice by human fibroblasts of different proliferative potential in vitro. Proc Natl Acad Sci USA 76, 1274-1278.

Benedikt. O (1975). The mode of action of trabeculectomy. Klin Monatsbl Augenheilkd 167, 679-685.

Berry D. P., Harding K. D., Stanton M. R., Jasani B.,Ehrlich H. P. (1998). Human wound contraction: collagen organisation, fibroblasts and myofibroblasts. Plast Reconstr Surg 102, 124-131.

Belyea D. A., Dan J. A., Stamper R. L., Lieberman M. F.,Spencer W. H. (1997). Late onset of sequential multifocal bleb leaks after glaucoma filtration surgery with 5-fluorouracil and mitomycin C. Am J Ophthalmol 124, 40-45.

Blakytny R., Ludlow A., Martin G. E., Ireland G., Lund L. R., Ferguson M. W., Brunner G. (2004). Latent TGF-beta1 activation by platelets. J Cell Physiol 199, 67-76.

Blalock T. D., Yuan R., Lewin A. S., Schultz G. S. (2004). Hammerhead ribozyme targeting connective tissue growth factor mRNA blocks transforming growth factor-beta mediated cell proliferation. Exp Eye Res 78, 1127-1136.

Blease K., Schuh J. M., Jakubzick C., Lukacs N. W., Krunkel S. L., Joshi B. H., Puri R. K., Kaplan M. H., Hogaboam C. M. (2002). Stat6-deficient mice develop airway hyperesponsiveness and peribronchial fibrosis during chronic fungal asthma. Am J Path 160, 481-490.

Blobe G. C., Schiemann W. P., Lodish H. F. (2000). Role of transforming growth factor beta in human disease. N Engl J Med 342, 1350-1358.

Blobe G. C., Schiemann W. P., Pepin M. C., Beauchemin M., Moustakas A., Lodish H. F., O'Connor-McCourt M. D. (2001). Functional roles for the cytoplasmic domain of the type III transforming growth factor beta receptor in regulating transforming growth factor beta signaling. J Biol Chem 276, 24627-24637.

Bloom P. A., Tsai J. C., Sharma K., Miller M. H., Rice N. S., Hitchings R. A., Khaw P. T. (1997). "Cyclodiode". Trans-scleral diode laser cyclophotocoagulation in the treatment of advanced refractory glaucoma. Ophthalmology 104, 1508-1519.

Blumenkranz M. S., Claflin A., Hajek A. S. (1984). Selection of therapeutic agents for intraocular proliferative disease. Cell culture evaluation. Arch Ophthalmol 102, 598-604.

Blumenkranz M. S., Hartzer M. K., Hajek A. S. (1987). Selection of therapeutic agents for intraocular proliferative disease.II : differing antiproliferative activity of the fluoropyrimidines. Arch Ophthalmol 105, 369-399.

Blumenkranz M. S., Ophir A., Claflin A., Hajek A. S. (1982). Fluorouracil for the treatment of massive periretinal proliferation. Am J Ophthalmol 94, 458-467.

Bornstein P., Agah A., Kyriakides T. R. (2004). The role of thrombospondins 1 and 2 in the regulation of cell-matrix interactions, collagen fibril formation, and the response to injury. Int J Biochem Cell Biol 36, 1115-1125.

Broadway D. C., Grierson I., Hitchings R. A. (1993a). Adverse effects of topical anti-glaucomatous medications on the conjunctiva. Br J Ophthalmol 77, 590-596.

Broadway D. C., Grierson I., Hitchings R. A. (1993b). The effect of topical anti-glaucomatous medications on the cell profile of the conjunctiva. Curr Opin Ophthalmol 4, 51-57.

Broadway D. C., Grierson I., Hitchings R. A. (1994a). Adverse effects of topical anti-glaucoma medication regimens: Part II. The outcome of filtration surgery. Arch Ophthalmol 112, 1446-1454.

Broadway D. C., Grierson I., O'Brien C., Hitchings R. A. (1994b). Adverse effects of topical antiglaucoma medication. Part I. Effect on the conjunctival cell profile. Arch Ophthalmol 112, 1437-1445.

Broadway D. C., Grierson I., Sturmer J., Hitchings R. A. (1996). Reversal of topical antiglaucoma medication effects on the conjunctiva. Arch Ophthalmol 114, 262-267.

Broadway D. C., Migdal C., Salmon M., Franks W. A., Barton K., Khaw P. T. (2002). Adjunctive Anti-TGFß2 Human Monoclonal Antibody as a Novel Agent to Prevent Scarring Following Phacotrabeculectomy. Invest Ophthalmol Vis Sci 43, ARVO E-abstract 3331.

Cairns J. E. (1968). Trabeculectomy: Preliminary report of a new method. Am J Ophthalmol 66, 673-679.

Campochiaro P. A., Hackett S. F., Vinores S. A., Freund J., Csaky C., LaRochelle W., Henderer J., Johnson M., Rodriguez I. R., Friedman Z. (1994). Platelet-derived growth factor is an autocrine growth stimulator in retianl pigmented epithelial cells. 1994 107, 2459-2469.

Carrington L. M., McLeod D. S., Boulton M. E. (2000). IL-10 and antibodies to TGF-beta2 and PDGF inhibit RPE mediated retinal contraction. Invest Ophthalmol Vis Sci 41, 1210-1216.

Chamberlain J., Shah M., Ferguson M. W. (1995). The effect of suramin on healing adult rodent dermal wounds. J Anat 186, 87-96.

Chang L., Crowston J. G., Sabin C. A., Khaw P. T., Akbar A. N. (2001). Human tenon's fibroblast-produced IFN beta and the prevention of t-cell apoptosis. Invest Ophthalmol Vis Sci 42, 1531-1538.

Cheifetz S., Bassols A., Stanley K., Ohta M., Greenberger J., Massague J. (1988). Heterodimeric transforming growth factor beta. Biological properties and interaction with three types of cell surface receptors. J Biol Chem 263, 10783-10789.

Cheifetz S., Weatherbee J. A., Tsang M. L., Anderson J. K., Mole J. E., Lucas R., Massague J. (1987). The transforming growth factor-beta system, a complex pattern of cross-reactive ligands and receptors. Cell 48, 409-415.

Chen C., Michelini-Norris B., Stevens S., Rowsey J., Ren X., Goldstein M., Schultz G. (2000). Measurement of mRNAs for TGFss and extracellular matrix proteins in corneas of rats after PRK. Invest Ophthalmol Vis Sci 41, 4108-4116.

Chen C. W. (1983). Enhanced intraocular pressure controlling effectiveness by local application of mitomycin C. Trans Asia Pacif Acad Ophthalmol, 172-177.

Chen C. W., Huang H.-T., Blair J. S., Lee C. C. (1990). Trabeculectomy with simultaneous topical application of MMC in refractory glaucoma. J Ocul Pharm 6, 175-182.

Chen P. P., Yamamoto T., Sawada A., Parrish R. K., 2nd, Kitazawa Y. (1997). Use of antifibrosis agents and glaucoma drainage devices in the American and Japanese Glaucoma Societies. J Glaucoma 6, 192-196.

Chen S., Jim B., Ziyadeh F. N. (2003). Diabetic nephropathy and transforming growth factor-beta: transforming our view of glomerulosclerosis and fibrosis build-up. Semin Nephrol 23, 532-543.

Cheung J. C., Wright M. M., Murali S., Pedersen J. E. (1997). Intermediate-term outcome of variable dose mitomycin C filtering surgery. Ophthalmology 104, 143-149.

Clark R. A. F., Henson P. M. (1988). The molecular and cell biology of wound repair (New York, Plenum Press).

Coffey R. J. J., Kost L. J., Lyons R. M., Moses H. L., LaRusso N. F. (1987). Hepatic processing of transforming growth factor beta in the rat. Uptake, metabolism, and biliary excretion. J Clin Invest 80, 750-757.

Cohen J. S., Greff L. J., Novack G. D., Wind B. E. (1996). A placebo controlled, double masked evaluation of mitomycin C in combined glaucoma and cataract procedures. Ophthalmology 103, 1934-1942.

Connor T. B., Roberts A. B., Sporn M. B., Danielpour D., Dart L. L., Michels R. G., de Bustros S., Enger C., Kato H., Lansing M., et al. (1989). Correlation of fibrosis and transforming growth factor-beta type 2 levels in the eye. J Clin Invest 83, 1661-1666.

Constable P. H., Crowston J. G., Occleston N. L., Cordeiro M. F.,Khaw P. T. (1998). Long term growth arrest of human Tenon's fibroblasts following single applications of beta radiation. Br J Ophthalmol 82, 448-452.

Cordeiro M. F., Balasubramaniam L, Ali R. R., Alexander R. A., Stecker K., Dean N. M., Khaw P. T. (2000a). Effect and localization of a TGF-β1 Antisense Oligonucleotide in conjunctival scarring-A Potential New Anti-Scarring Strategy in Glaucoma surgery. Invest Ophthalmol Vis Sci 41, 3950(s).

Cordeiro M. F., Bhattacharya S. S., Schultz G. S., Khaw P. T. (2000b). TGF-beta1, -beta2, and -beta3 in vitro: biphasic effects on Tenon's fibroblast contraction, proliferation, and migration. Invest Ophthalmol Vis Sci 41, 756-763.

Cordeiro M. F., Constable P. H., Alexander R. A., Bhattacharya S. S., Khaw P. T. (1997). Effect of varying the mitomycin-C treatment area in glaucoma filtration surgery in the rabbit. Invest Ophthalmol Vis Sci 38, 1639-1646.

Cordeiro M. F., Gay J. A., Khaw P. T. (1999a). Human anti-transforming growth factor-beta2 antibody: a new glaucoma anti-scarring agent. Invest Ophthalmol Vis Sci 40, 2225-2234.

Cordeiro M. F., Mead A. L., Ali R. R., Alexander R. A., Murphy S., Chen C., Dean N., Schultz G., Khaw P. T. (2003). Novel antisense oligonucleotides targeting TGF-beta inhibit in vivo scarring and improve surgical outcome. Gene Therapy 10, 59-71.

Cordeiro M. F., Reichel M. B., Gay J. A., D'Esposita F., Alexander R. A., Khaw P. T. (1999b). Transforming growth factor-beta1, -beta2, and -beta3 in vivo: effects on normal and mitomycin C-modulated conjunctival scarring. Invest Ophthalmol Vis Sci 40, 1975-1982.

Cousins S. W., McCabe M. M., Danielpour D., Streilein J. W. (1991). Identification of transforming growth factor-beta as an immunosuppressive factor in aqueous humor. Invest Ophthalmol Vis Sci 32, 2201-2211.

Cox D. A. (1995). Transforming growth factor beta 3. Cell Biol Internat 19, 357-371.

Critchlow M. A., Bland Y. S., Ashhurst D., E, (1995). The effect of exogenous transforming growth factor-beta 2 on healing fractures in the rabbit. Bone 16, 521-527.

Crowston J. G., Akbar A. N., Constable P. H., Occleston N. L., Daniels J. T., Khaw P. T. (1998). Antimetabolite-induced apoptosis in Tenon's capsule fibroblasts. Invest Ophthalmol Vis Sci 39, 449-454.

Daniels J. T., Cambrey A. D., Occleston N. L., Qian G., Tarnuzzer R. W., Schultz G. S., Khaw P. T. (2003a). Matrix Metalloproteinase Inhibition Modulates Fibroblast-Mediated Matrix Contraction and Collagen Production In Vitro. Invest Ophthalmol Vis Sci 40, 1104-1110.

Daniels J. T., Geerling G., Alexander R. A., Murphy G, Khaw P. T., Saarialho-Kere U. (2003b). Temporal and spatial expression of matrix metalloproteinases during wound healing of human corneal tissue. Exp Eye Res 77, 653-664.
Daniels J. T., Occleston N. L., Crowston J. G., Khaw P. T. (1999). Effects of antimetabolite induced cellular growth arrest on fibroblast-fibroblast interactions. Exp Eye Res 69, 117-127.

Dean D. C., Newby R. F., Bourgeois S. (1988). Regulation of fibronectin biosynthesis by dexamethasone, transforming growth factor beta, and cAMP in human cell lines. J Cell Biol 106, 2159-2170.

Dean N., McKay R., Miraglia L., Geiger T., Muller M., Fabbro D., Bennett C. F. (1996). Antisense oligonucleotides as inhibitors of signal transduction: development from research tools to therapeutic agents. Biochem Soc Trans 24, 623-629.

Dean N.,Griffey R. G. (1997). Identification and characterisation of second generation antisense oligonucleotides. Antisense Nucleic Acid Drug Develop 7, 229-233.

Denk P. O., Hoppe J., Hoppe V., Knorr M. (2003). Effect of growth factors on the activation of human Tenon's capsule fibroblasts. Curr Eye Res 27, 35-44.

Dennis P. A., Rifkin D. B. (1991). Cellular activation of latent transforming growth factor beta requires binding to the cation-independent mannose 6-phosphate/insulin-like growth factor type II receptor. Proc Natl Acad Sci U S A 88, 580-584.

Derynck R., Jarrett J. A., Chen E. Y., Eaton D. H., Bell J. R., Assoian R. K., Roberts A. B., Sporn M. B., Goeddel D. V. (1985). Human transforming growth factor-beta complementary DNA sequence and expression in normal and transformed cells. Nature 316, 701-705.

Derynck R., Zhang Y. E. (2003). Smad-dependent and Smad-independent pathways in TGF-beta family signalling. Nature 2003 Oct 9;425(6958):577-84 Related Ar 425, 577-584.

Desjardins D. C., Parrish R. K., Follberg R., Nevarez J. A., Heuer D. K., Gressel M. G. (1986). Wound healing after filtering surgery in owl monkeys. Arch Ophthalmol 104, 1835-1839.

Desmouliere A., Geinoz A., Gabbiani F., Gabbiani G. (1993). Transforming growth factor-beta 1 induces alpha-smooth muscle actin expression in granulation tissue

myofibroblasts and in quiescent and growing cultured fibroblasts. J Cell Biol 122, 103-111.

Desmouliere A., Redard M., Darby I., Gabbiani G. A. (1995). Apoptosis mediates the decrease in cellularity during the transition between granulation tissue and scar. Am J Path 146, 56-66.

Di Girolamo N., McCluskey P., Lloyd A., Coroneo M. T., Wakefield D. (2000). Expression of MMPs and TIMPs in human pterygia and cultured pterygium epithelial cells. Invest Ophthalmol Vis Sci 41.

Diggory P., Franks W. A. (1996). Medical treatment of glaucoma- a reappraisal of the risks. Br J Ophthalmol 80, 85-89.

Doyle J. W., Sherwood M. B., Khaw P. T., McGrory S., Smith M. F. (1993a). Effects of different regimens of 5-fluorouracil on experimental filtration surgery in the rabbit. Invest Ophthalmol Vis Sci 34, 3313-3319.

Doyle J. W., Sherwood M. B., Khaw P. T., McGrory S., Smith M. F. (1993b). Intraoperative 5-fluorouracil for filtration surgery in the rabbit. Invest Ophthalmol Vis Sci 34, 3313-3319.

Dugina V., Fontao L., Chaponnier C., Vasiliev j., Gabbiani G. A. (2001). Focal adhesions features during myofibroblastic differentiation are controlled by intracellular and extracellular factors. J Cell Sci 114, 3285-3296.

Ebner R., Chen R. H., Shum L., Lawler S., Zioncheck T. F., Lee A., Lopez A. R., Derynck R. (1993). Cloning of a type I TGF-beta receptor and its effect on TGF-beta binding to the type II receptor. Science 260, 1344-1348.

Edwards D. R., Murphy G., Reynolds J. J., Whitham S. E., Docherty A. J., Angel P., Heath J. K. (1987). Transforming growth factor beta modulates the expression of collagenase and metalloproteinase inhibitor. EMBO J 6, 1899-1904.

Ehrlich H. P., Rajaratnam J. B. (1990). Cell locomotion forces versus cell contraction forces for collagen lattice contraction: an in vitro model of wound contraction. Tissue cell 22, 407-417.

Esson D. W., Popp M. P., Liu L., Schultz G. S., Sherwood M. B. (2004). Microarray analysis of the failure of filtering blebs in a rat model of glaucoma filtering surgery. Invest Ophthalmol Vis Sci 45, 4450-62.

Faktorovich E. G., Badawi D. Y., Maloney R. K., Ariyasu R. G. (1999). Growth factor expression in corneal wound healing after excimer laser keratectomy. Cornea 18, 580-588.

Falck F. Y., Skuta G. L., Klein T. B. (1992). Mitomycin versus 5-Fluorouracil antimetabolite therapy for glaucoma filtration surgery. Seminars in Ophthalmology 7, 97.

Foster A., Johnson G. J. (1990). Magnitude and causes of blindness in the developing world. Int Ophthalmol 14, 135-140.

Fuchshofer R., Birke M., Welge-Lussen U., Kook D., Lutjen-Drecoll E. (2005). Transforming growth factor-beta 2 modulated extracellular matrix component expression in cultured human optic nerve head astrocytes. Invest Ophthalmol Vis Sci 46, 568-578.

Gabbiani G. (1998). Evolution and clinical implications of the myofibroblast concept. Cardiovascular Research, 545-548.

Gallenga P. E., Mastropasqua L., Carpineto P., Ciancaglini M.,Zuppardi E. (1997). Delayed post-operative use of 5-fluorouracil in primary open angle glaucoma. Acta Ophthalmol Scand Suppl 224, 45-46.

Gillies M., Su T., Sarossy M., Hollows F. (1993). Interferon-alpha 2b inhibits proliferation of human Tenons fibroblasts. Graefes Arch Clin Exp Ophthalmol 231, 118-121.

Glaser B. M., Michels R. G., Kuppermann B. D., Sjaarda R. N., Pena R. A. (1992). Transforming growth factor-β2 for the treatment of full-thickness macular holes. Ophthalmology 99, 1162-1173.

Goldenfeld M., Krupin T., Ruderman J. M., Wong P. C., Rosenberg L. F., Ritch R., Liebmann J. M., Gieser D. K. (1994). 5-Fluorouracil in initial trabeculectomy. A prospective, randomized, multicenter study. Ophthalmology 101, 1024-1029.

Gordon-Thomson C., de Iongh R. U., Hales A. M., Chamberlain C. G., McAvoy J. W. (1998). Differential cataractogenic potency of TGF-beta1, -beta2, and -beta3 and their expression in the postnatal rat eye. Invest Ophthalmol Vis Sci 39, 1399-1409.

Grainger D. J., Wakefield L., Bethell H. W., Farndale R. W., Metcalf J. C. (1995). Release and activation of platelet latent TGF-beta in blood clots during dissolution with plasmin. Nat Med, 932-937.

Grant W. M., Burke J. F. (1982). Why do some people go blind from glaucoma? Ophthalmology 89, 991-998.

Greenfield D. S., Liebmann J. M., Jee J., Ritch R. (1998). Late-onset bleb leaks after glaucoma filtering surgery. Arch Ophthalmol 116, 443-447.

Griffiths A. D., Williams G. A., Hartley O., Tomlinson I. M., Waterhouse P., Crosby W. L., Kontermann R. E., Jones P. T., Low N. M., Allison T. J. (1994). Isolation of high affinity human antibodies directly from large synthetic repertoires. EMBO J 13, 3245-3260.

Grinnell F. (1994). Mini-review on the mechansims of disease: Fibroblasts, myofibroblasts and wound contraction. J Cell Biol 124, 401-404.

The Fluorouracil Filtering Surgery Study Group. (1989). Fluorouracil Filtering Surgery Study one-year follow-up. Am J Ophthalmol 108, 625-635.

The Fluorouracil Filtering Surgery Study Group. (1996). Five-year follow-up of the Fluorouracil Filtering Surgery Study. Am J Ophthalmol 121, 349-366.

Grinnell F. (1994). Mini-review on the mechansims of disease: Fibroblasts, myofibroblasts and wound contraction. J Cell Biol 124, 401-404.

Gruschwitz M., Muller P. U., Sepp N., Hofer E., Fontana A., Wick G. (1990). Transcription and expression of transforming growth factor type beta in the skin of progressive systemic sclerosis: a mediator of fibrosis? J Invest Dermatol 94, 197-203.

Guidry C. (1993). Fibroblast contraction of collagen gels requires activation of protein kinase C. J cell Physiol 155, 358-367.

Hales A. M., Chamberlain C. G., McAvoy J. W. (1995). Cataract induction in lenses cultured with Transforming Growth Factor -beta. Invest Ophthalmol Vis Sci 36, 1709-1713.

Hales A. M., Chamberlain C. G., McAvoy J. W. (2000). Susceptibility to TGFbeta2-induced cataract increases with aging in the rat. Invest Ophthalmol Vis Sci 41, 3544-3551.

Harris A. K., Stopak D., Wild P. (1981). Fibroblast traction as a mechanism for collagen morphogenesis. Nature 290, 249-251.

Hayashi K., Frangieh G., Wolf G., Kenyon K. R. (1989). Expression of transforming growth factor-beta in wound healing of vitamin A-deficient rat corneas. Invest Ophthalmol Vis Sci 30, 239-247.

Heimark R.L., Twardzik D.R., Schwartz S. M. (1986). Inhibition of endothelial regeneration by type-beta transforming growth factor from platelets. Science 233, 1078-1080.

Heino J., Massague J. (1989). Transforming growth factor-beta switches the pattern of integrins expressed in MG-63 human osteosarcoma cells and causes a selective loss of cell adhesion to laminin. J Biol Chem 1989, 21806-21811.

Hernandez. M R., Pena. J D. (1997). The optic nerve head in glaucomatous optic neuropathy. Arch Ophthalmol 115, 389-395.

Herschler J. (1990). The inhibitory factor in aqueous humour. Vision Research 21, 163.

Heuer D. K., Parrish R. K., 2nd, Gressel M. G., Hodapp E., Desjardins D. C., Skuta G. L., Palmberg P. F., Nevarez J. A., Rockwood E. J. (1986). 5-Fluorouracil and glaucoma filtering surgery. III. Intermediate follow-up of a pilot study. Ophthalmology 93, 1537-1546.

Hinz B., Mastrangelo D., Iselin C. E., Chaponnier C.,Gabbiani G. A. (2001). Mechanical tension controls granulation tissue contractile activity and myofibroblast differentiation. Am J Path 159, 1009-1020.

Hitchings R. A., Grierson I. (1983). Clinico pathological correlation in eyes with failed fistulizing surgery. Trans Ophthalmol Soc U K 103, 84-88.

Hitchings R. A., Migdal C. S., Wormald R., Poinooswamy D., Fitzke F. (1994). The primary treatment trial: changes in the visual field analysis by computer-assisted perimetry. Eye 8, 117-120.

Ho S. L., Dogar G. F., Wang J., Crean J., Wu Q. D., Oliver N., Weitz S., Murra A., Cleary P. E., O'Brien C. (2005). Elevated aqueous humour tissue inhibitor of matrix metalloproteinase-1 and connective tissue growth factor in pseudoexfoliation syndrome. Br J Ophthalmol 89, 169-173.

Huang M., Sharma S., Zhu L. X., Keane M. P., Luo J., Zhang L., Burdick M. D., Lin Y. K., Dohadwala M., Gardner B., *et al.* (2002). IL-7 inhibits fibroblast TGF-β production and signalling in pulmonary fibrosis. J Clin Invest 109, 931-937.

Hunt R. C., Pakalnis V. A., Choudhury P., Black E. P. (1994). Cytokines and serum cause alpha2beta1 integrin mediated contraction of collagen gels by cultured retinal pigment epithelial celss. Invest Ophthalmol Vis Sci 35, 955-963.

Ignotz R. A., Massague J. (1985). Type beta transforming growth factor controls the adipogenic differentiation of 3T3 fibroblasts. Proc Natl Acad Sci U S A 82, 8530-8534.

Ignotz R. A., Massague J. (1986). Transforming growth factor-beta stimulates the expression of fibronectin and collagen and their incorporation into the extracellular matrix. J Biol Chem 261, 4337-4345.

Ignotz R. A., Endo T., Massague J. (1987). Regulation of fibronectin and type I collagen mRNA levels by transforming growth factor-beta. J Biol Chem 262, 6443-6446.

Jakobovits A. (1995). Production of fully human antibodies by transgenic mice. Curr Opin Biotech 6, 561-566.

Jampel H. D., Leong K. W., Dunkelburger G. R., Quigley H. A. (1990a). Glaucoma filtering surgery in Monkeys using 5-fluoruradine in polyanhydride discs. Arch Ophthalmol 108, 430-435.

Jampel H. D., Roche N., Stark W. J.,Roberts A. B. (1990b). Transforming growth factor-beta in human aqueous humor. Curr Eye Res 9, 963-969.

Jampel H. D., Pasquale L. R., Dibernardo C. (1992). Hypotony maculopathy following trabeculectomy with mitomycin C. Arch Ophthalmol 110, 1049-1050.

Jay J. L. (1989). The benefit of early trabeculectomy vs conventional management in POAG relative to the severity of the disease. Eye.

Jay J. L. (1992). Rational choice of therapy in primary open angle glaucoma. Eye 6, 243-247.

Jefferies L. W., Alexander R. A. (1995). Connective tissue fibre production in Keratoconus. Br J Biomed Sci 52, 14-18.

Jester J. V., Barry Lane P. A., Petroll W. M., Olsen D. R., Cavanagh H. D. (1997). Inhibition of corneal fibrosis by topical application of blocking antibodies to TGF beta in the rabbit. Cornea 16, 177-187.

Jester J. V., Petroll W. M., Cavanagh H. D. (1999). Corneal stromal wound healing in refractive surgery: the role of myofibroblasts. Prog Retin Eye Res 18.

Joseph J. P., Grierson I., Hitchings R. A. (1987). Normal rabbit aqueous humour, fibronectin, and fibroblast conditioned media are chemoattractant to Tenon's capsule fibroblasts. Eye 1, 585-592.

Joseph J. P., Grierson I., Hitchings R. A. (1989). Chemotactic activity of aqueous humour: a cause of failure of trabeculectomies. Arch Ophthalmol 1989, 69-74.

Juinquera L. C. U., Cossermelli W., Bretani R. (1978). Differential staining of collagen type I, II and III by sirius red and polarisation microscopy. Archives of Histology of Japan 41, 267-274.

Kaartinen V., Voncken J. W., Shuler C., Warburton D., Bu D., Heisterkamp N., Groffen J. (1995). Abnormal lung development and cleft palate in mice lacking TGF-beta 3 indicates defects of epithelial-mesenchymal interaction. Nat Genet 11, 415-421.

Kaiura T. L., Itoh H., Kubaska S. M. r., McCaffrey T. A., Liu B., Kent K. C. (2000). The effect of growth factors, cytokines, and extracellular matrix proteins on fibronectin production in human vascular smooth muscle cells. J Vasc Surg 31, 577-584.

Kaji Y., Soya K., Amano S., Oshika T., Yamashita H. (2001). Relation between corneal haze and transforming growth factor-beta1 after photorefractive keratectomy and laser in situ keratomileusis. J Cataract Refract Surg 27, 1840-46

Kangas T. A., Greenfield D. S., Flynn H. W., Parrish R. K.,Palmberg P. (1997). Delayed-onset endophthalmitis associated with conjunctival filtering blebs. Ophthalmology 104, 746-752.

Kanzaki T., Olofsson A., Moren A., Wernstedt C., Hellman U., Miyazono K., Claesson-Welsh L., Heldin C. H. (1990). TGF-beta 1 binding protein: a component of the large latent complex of TGF-beta 1 with multiple repeat sequences. Cell 15, 1051-1061.

Katz G. J., Higginbotham E. J., Lichter P. R., Skuta G. L., Musch D. C., Bergstrom T. J., Johnson A. T. (1995). Mitomycin C versus 5-fluorouracil in high-risk glaucoma filtering surgery. Extended follow-up. Ophthalmology 102, 1263-1269.

Kay J. S., Litin B. S., Jones M. A., Fryczkowski A. W., Chvapil M., Herschler J. (1986). Delivery of antifibroblast agents as adjuncts to fitration surgery II Delivery of 5fu and bleomycin in a collagen implant:pilot study in the rabbit. Ophthalmic Surg 17, 796-801.

Kelley J., Shull S., Walsh J. J., Cutroneo K. R., Absher M. (1993). Auto-induction of transforming growth factor-beta in human lung fibroblasts. Am J Respir Cell Mol Biol 8, 417-424.

Kent A. R., Dubiner H. B., Whitaker R., Mundorf T. K., Stewart J. A., Cate E. A., Stewart W. C. (1998). The efficacy and safety of diclofenac 0.1% versus prednisolone acetate 1% following trabeculectomy with adjunctive mitomycin-C. Ophthalmic Surg Lasers 29, 562-569.

Kerr L.D., Miller D.B., Matrisian L.M. (1990). TGF-beta 1 inhibition of transin/stromelysin gene expression is mediated through a Fos binding sequence. Cell 61, 267-278.

Khaw P. T. (1994). The effects of growth factors and anti-proliferative agents on ocular fibroblasts and wound healing after glaucoma filtration surgery (PhD Thesis, University of London), pp. 69-70.

Khaw P. T., Ward S., Grierson I., Rice N. S. (1991). Effect of beta radiation on proliferating human Tenon's capsule fibroblasts. Br J Ophthalmol 75, 580-583.

Khaw P. T., Grierson I., Miller M. H., Joseph J. P., Hitchings R. A. (1992a). Experimental models of wound healing after glaucoma filtration surgery. In Applied Pharmacology of the Glaucomas, S. M. Drance, and A. H. Neufeld, eds. (Baltimore).

Khaw P. T., Sherwood M. B., Doyle J. W., Smith M. F., Grierson I., McGorray S., Schultz G. S. (1992b). Intraoperative and post operative treatment with 5-fluorouracil and mitomycin-c: long term effects in vivo on subconjunctival and scleral fibroblasts. Int Ophthalmol 16, 381-385.

Khaw P. T., Sherwood M. B., MacKay S. L., Rossi M. J., Schultz G. (1992c). Five-minute treatments with fluorouracil, floxuridine, and mitomycin have long-term effects on human Tenon's capsule fibroblasts. Arch Ophthalmol 110, 1150-1154.

Khaw P. T., Ward S., Porter A., Grierson I., Hitchings R. A., Rice N. S. (1992d). The long-term effects of 5-fluorouracil and sodium butyrate on human Tenon's fibroblasts. Invest Ophthalmol Vis Sci 33, 2043-2052.

Khaw P. T., Doyle J. W., Sherwood M. B., Grierson I., Schultz G., McGorray S. (1993a). Prolonged localized tissue effects from 5-minute exposures to fluorouracil and mitomycin C. Arch Ophthalmol 111, 263-267.

Khaw P. T., Doyle J. W., Sherwood M. B., Smith M. F., McGorray S. (1993b). Effects of intraoperative 5-fluorouracil or mitomycin C on glaucoma filtration surgery in the rabbit. Ophthalmology 100, 367-372.

Khaw P. T., Mannan M., Vyas W., Alexander R., Jefferies L. W., Sherwood M. B. (1993c). Single intraoperative exposures to mitomycin c: long term effects on scleral cellularity. Invest Ophthalmol Vis Sci (Suppl) 34, 726.

Khaw P. T., Occleston N. L., Larkin G., Shad H., Schultz G. S., Grierson I., Grant M. B. (1994a). The effects of growth factors on human ocular fibroblast proliferation, migration and collagen production. Invest Ophthalmol Vis Sci (Suppl) 35, 1898.

Khaw P. T., Occleston N. L., Schultz G., Grierson I., Sherwood M. B., Larkin G. (1994b). Activation and suppression of fibroblast function. Eye 8, 188-195.

Khaw P. T., Chang L., Wong T. T. L., Mead A. L., Daniels J. T., Cordeiro M. F. (2001). Modulation of wound healing after glaucoma filtration surgery. Current Opinion in Ophthalmology 12, 143-148.

Khaw P. T., Wells A. P., Green C., Clarke J. C. K., Alteri M., Overton B., Migdal C. S. (2003). Three Year Follow-Up of an Early Phase Clinical Trial of CAT-152 Anti-TGFß2 Human Monoclonal Antibody as an Adjunct to First Time Trabeculectomy. Invest Ophthalmol Vis Sci 44, ARVO E-abstract 1198.

Kim S. J., Angel P., Lafyatis R., Hattori K., Kim K. Y., Sporn M. B., Karin M., Roberts A. B. (1990). Autoinduction of transforming growth factor beta 1 is mediated by the AP-1 complex. Mol Cell Biol 10, 1492-1497.

Kim S. J., Jeang K. T., Glick A., Sporn M. B., Roberts A. B. (1989). Promotor sequences of the human transforming growth factor β1 gene responsive to transforming growth factor β1 autoinduction. J Biol Chem 263, 7041-7045.

Kim S. J., Lee H. D., Robbins P. D., Busam K., Sporn M. B., Roberts A. B. (1991). Regulation of transforming growth factor beta 1 gene expression by the product of the retinoblastoma-susceptibility gene. Proc Natl Acad Sci USA 88, 3052-3056.

Kingsey D. M. (1994). The TGF-beta superfamily: new members, new receptors, and new genetic tests of function in different organisms. Genes Dev 8.

Kitazawa Y., Kawase K., Matsushita H., Minobe M. (1991). Trabeculectomy with mitomycin. A comparative study with fluorouracil. Arch Ophthalmol 109, 1693-1698.

Knisely T. L., Bleicher P. A., Vibbard C. A., Granstein R. D. (1991). Production of latent transforming growth factor-beta and other inhibitory factors by cultured murine iris and ciliary body cells. Curr Eye Res 10, 761-771.

Kohler G., Milstein C. (1975). Continuous cultures of fused cells secreting antibody of predefined specificity. Nature 256, 495-497.

Kokawa N., Sotozono C., Nishida K., Kinoshita S. (1996). High total TGF-b2 vels in normal human tears. Curr Eye Res 15, 341-343.

Kon C. H., Occleston N. L., Aylward G. W., Khaw P. T. (1999). Expression of vitreous cytokines in proliferative vitreoretinopathy: a prospective study. Invest Ophthalmol Vis Sci 40, 705-712.

Kottler U. B., Schloetzer-Schrehardt U. M., Pfeffer N., Naumann G. O. H., Juenemann A. G. M. (2003). Expression of TGF-ß1 and TGF-ß2 in Failed Filtering Blebs of Patients with Pseudoexfoliation and Primary Open-angle Glaucoma. Invest Ophthalmol Vis Sci 43, ARVO E-abstract 1214.

Krause U., Neimi A., Raunio A. (1971). Effect of paracentesis on the protein content of the aqueous humour. Ophthalmologica 163, 136-149.

Lamping K. A., Belkin J. K. (1995). 5-Fluorouracil and mitomycin C in pseudophakic patients. Ophthalmology 102, 70-75.

Lavin M. J., Wormald R. P. L., Migdal C. S., Hitchings R. A. (1990). The influence on prior therapy on the success of trabeculectomy. Arch Ophthalmol 108, 1543-1549.

Lee D. A., Flores R. A., Anderson P. J., Leong K. W., Teekhasaenee C., De Kater A. W., Hertzmark E. (1987). Glaucoma filtration surgery in rabbits using bioerodible polymers and 5 fluorouracil. Ophthalmology 94, 1523-1530.

Lee D. A., Lee T. C., Cortes A. E., Kitada S.(1990a). Effects of Mitramycin, mitomycin, duanorubicin and bleomycin on human subconjunctival fibroblast attachment and proliferation. Invest Ophthalmol Vis Sci 31, 2136-2144.

Lee D. A., Shapourifar-Tehrani D., Kitada S. (1990b). The effect of 5FU and cytarabine on humans fibroblasts from tenons capsule. Invest Ophthalmol Vis Sci 31, 1848-1855.

Lee D. A., Shapourifar-Tehrani D., Stephenson T. R., Kitada S. (1991). The effect of fluorinated FUR, FUdR,FUMP and FdUMP on human Tenon's fibroblasts. Invest Ophthalmol Vis Sci 31.

Lee E. H., Seomum Y., Hwang K. H., Kim J. E., Kim I. S., Kim J. H., Joo C. K. (2000). Overexpression of the transforming beta inducible gene betaig-h3 in anterior polar cataracts. Invest Ophthalmol Vis Sci 41, 1840-1845.

Lee T. Y., Chin G. S., Kim W. J., Chau D., Gittes G. K., Longaker M. T. (1999). Expression of transforming growth factor beta 1, 2, and 3 proteins in keloids. Ann Plast Surg 43, 179-184.

Leske C. M., Connell A. M., Wu S. Y., Hyman L. G., Schachat A. P. (1995). Risk factors for early glaucoma. The Barbados Eye Study. Arch Ophthalmol 113.

Leske C. M., Heijl A., Hussein M., Bengtsson B., Hyman L. G., Komaroff E. (2003). Factors for glaucoma progression and the effect of treatment: the early manifest glaucoma trial. Arch Ophthalmol 121, 48-56.

Levine J. H., Moses H. L., Gold L. I., Nanney L. B. (1993).Spatial and temporal patterns of immunoreactive transforming growth factor beta 1, beta 2, and beta 3 during excisional wound repair. Am J Path 143, 368-380.

Li D. Q., Lee S. B., Tseng S. (1999). Differential expression and regulation of TGF-beta1, TGF-beta2, TGF-beta3, TGF-betaRI, TGF-betaRII and TGF-betaRIII in cultured human corneal, limbal, and conjunctival fibroblasts. Curr Eye Res 19, 154-161.

Li J., Tripathi B. J., Tripathi R. C. (2000). Modulation of pre-mRNA splicing and protein production of fibronectin by TGF-beta2 in porcine trabecular cells. Invest Ophthalmol Vis Sci 41, 3437-3443.

Lillie R. D., Tracy P., Pizzolata P., Donaldson P. T., Reynolds C. (1980). Diffential staining of collagen subtypes in paraffin sections: a colour change in degraded forms. Virchows Archives 386, 153-159.

Liu C. J., Huang Y. L., Chiu A. W., Ju J. P. (2004). Transcript expression of matrix metalloproteinases in the conjunctiva following glaucoma filtration surgery in rabbits. Ophthalmic Res 36, 114-119.

Liu J. H. K. (2002). Circadian variations of transforming growth factor- 2 and basic fibroblast growth factor in the rabbit aqueous humor. Curr Eye Res 2002;24:75-80. Curr Eye Res 24, 75-80.

Longaker M. T., Whitby D. J., Adzick N. S., Crombleholme T. M., Langer J. C., Duncan B. W., Bradley S. M., Stern R., Ferguson M. W., Harrison M. R. (1990). Studies in fetal wound healing, VI. Second and early third trimester fetal wounds demonstrate rapid collagen deposition without scar formation. J Pediatr Surg 25, 63-68.

Lorena D., Uchio K., Costa A. M. A., Desmouliere A. (2002). Normal scarring: importance of myofibroblasts. Wound Repair Regen 10, 86-92.

Lund L. R., Riccio A., Andreasen P. A., Nielsen L. S., Kristensen P., Laiho M., Saksela O., Blasi F., Dano K. (1987). Transforming growth factor-beta is a strong and fast acting positive regulator of the level of type-1 plasminogen activator inhibitor mRNA in WI-38 human lung fibroblasts. EMBO J 6, 1281-1286.

Lutty G. A., Merges C., Threlkeld A. B., Crone S., McLeod D. S. (1993). Heterogeneity in localization of isoforms of TGF-beta in human retina, vitreous, and choroid. Invest Ophthalmol Vis Sci 34, 477-487.

Lyons R. M., Keski-Oja J., Moses H. L. (1988). Proteolytic activation of latent transforming growth factor-beta from fibroblast-conditioned medium. J Cell Biol 106, 1659-1665.

Mamiya K., Ohguro H., Ohguro I., Metoki T., Ishikawa F., Yamazaki H., Takano Y., Ito T., Nakazawa M. (2004). Effects of matrix metalloproteinase-3 gene transfer by electroporation in glaucoma filter surgery. Exp Eye Res 79, 405-410.

Mao L. K., Stewart W. C., Shields M. B. (1991). Correlation between intraocular pressure and progressive glaucomatous damage in primary open angle glaucoma. Am J Ophthalmol 111, 51-55.

Marcusson E. G., Bhat B., Manharan M., Bennett C. F., Dean N. M. (1998). Phosphorothiote oligoribonucleotides dissociate from cationic lipids before entering the nucleus. Nuclei Acids Research 26, 2016-2023.

Massague J., Cheifetz S., Endo T., Nadal-Ginard B. (1986). Type beta transforming growth factor is an inhibitor of myogenic differentiation. Proc Natl Acad Sci U S A 83, 8206-8210.

Massague J., Chen Y. G. (2000). Controlling TGF-beta signaling. Genes Dev 14, 627-644.

Mastropasqua L., Carpineto P., Ciancaglini M., Zuppardi E., Lobefalo L., Gallenga P. E. (1998). Delayed post-operative use of 5-fluorouracil as an adjunct in medically uncontrolled open angle glaucoma. Eye 12, 701-706.

Masui T., Wakefield L. M., Lechner J. F., LaVeck M. A., Sporn M. B., Harris C. C. (1986). Type beta transforming growth factor is the primary differentiation-inducing serum factor for normal human bronchial epithelial cells. Proc Natl Acad Sci U S A 83, 2438-2442.

McCafferty J., Griffiths A. D., Winter G. F., Chiswell D. W. (1990). Phage antibodies: Filamentous phage displaying antibody variable domains. Nature 348, 552-554.

McCaffrey T. A. (2000). TGF-betas and TGF-beta receptors in atherosclerosis. Cytokine Growth Factor Rev 11, 103-114.
McMahon G. A., Dignam J. D., Gentry L. E. (1996). Structural characterization of the latent complex between transforming growth factor beta 1 and beta 1-latency-associated peptide. Biochem J 313, 343-351.

Meshel A. S., Wei Q., Adelstein R. S., Sheetz M. P. (2005). Basic mechanism of three-dimensional collagen fibre transport by fibroblasts. Nat Cell Biol 7, 157-164.

Mietz H., Chevez-Barrios P., Feldman R. M., Lieberman M. W. (1998a). Suramin inhibits wound healing following filtering procedures for glaucoma. Br J Ophthalmol 82, 816-820.

Mietz H., Chevez-Barrios P., Lieberman M. W. (1998b). A mouse model to study the wound healing response following filtration surgery. Graefes Arch Clin Exp Ophthalmol 236, 467-475.

Migdal C. (1995). What is the appropriate treatment for patients with primary open-angle glaucoma: medicine, laser, or primary surgery? Ophthalmic Surg 26, 108-109.

Migdal C., Gregory W., Hitchings R. (1994). Long-term functional outcome after early surgery compared with laser and medicine in open-angle glaucoma. Ophthalmology 101, 1651-1656.

Migdal C., Hitchings R. A. (1983). The developing bleb: Effect of topical anti-prostoglandins on the outcome of fistulizing surgery. Br J Ophthalmol 67, 655-660.

Miller M. H., Grierson I., Unger W. I., Hitchings R. A. (1989). Wound Healing in an animal model of glaucoma fistulizing surgery in the rabbit. Ophthalmic Surgery 20, 350-357.

Miller M. H., Joseph N. H., Ennis K. W., Grierson I., Hitchings R. A. (1985). An animal model of filtration surgery. Trans Ophthalmol Soc U K 104, 893-897.

Miller M. H., Rice N. S. C. (1991). Trabeculectomy combined with beta irradiation for congenital glaucoma. Br J Ophthalmol 75, 580-583.

Mohan R., Chintala S. K., Jung J. C., Villar W. V., McCabe F., Russo L. A., Lee Y., McCarthy B. E., Wollenberg K. R., Jester J. V., *et al.* (2002). Matrix metalloproteinase gelatinase B (MMP-9) coordinates and effects epithelial regeneration. J Biol Chem 277, 2065-2072.

Moller-pedersen T., Cavanagh H. D., Petroll W. M., Jester J. V. (1998). Neutralizing antibody to TGFbeta modulates stromal fibrosis but not regression of photoablative effect following PRK. Curr Eye Res 17, 736-747.

Molteno A., Straughan J., Ancker E. (1976). Long tube implants in the mangement of glaucoma. Afr Med J 50, 1062-1066.

Montes G. S. (1996). Structural biology of the fibres of the collagenous and elastic systems. Cell Biol Internat 20, 15-27.

Moodley Y., Rigby P., Bundell C., Bunt S., Hayashi H., Misso N., McAnulty R., Laurent G., Scaffidi A., Thompson P., Knight D. (2003). Macrophage recognition and phagocytosis of apoptotic fibroblasts is critically dependent on fibroblast-derived thrombospondin 1 and CD36. Am J Pathol 162, 771-779.

Mora J. S., Nguyen N., Iwach A. G., Gaffney M. M., Hetherington J. J., Hoskins H. D. J., Wong P. C., Tran H., Dickens C. J. (1996). Trabeculectomy with intraoperative sponge 5-fluorouracil. Ophthalmology 103, 963-970.

Mussener A., Funa K., Kleinau S., Klareskog L. (1997). Dynamic expression of transforming growth factor-betas (TGF-beta) and their type I and type II receptors in the synovial tissue of arthritic rats. Clin Exp Immunol 107, 112-119.

Myers J. S., Gomes J. A., Siepser S. B., Rapuano C. J., Eagle R. C. J., Thom S. B. (1997). Effect of transforming growth factor beta 1 on stromal haze following excimer laser photorefractive keratectomy in rabbits. J Cataract Refract Surg 13, 356-361.

Nakamura H., Siddiqui S. S., Shen X., Malik A. B., Pulido J. S., Kumar N. M., Yue B. Y. (2004). RNA interference targeting transforming growth factor-beta type II receptor suppresses ocular inflammation and fibrosis. Mol Vis 10, 703-711.

Nakao A., Imamura T., Souchelnytskyi S., Kawabata M., Ishisaki A., Oeda E., Tamaki K., Hanai J., Heldin C. H., Miyazono K., ten Dijke P. (1997). TGF-beta receptor-mediated signalling through Smad2, Smad3 and Smad4. EMBO J 16, 5353-5362.

Nishi O., Nishi K., Wada K., Ohmoto Y. (1995). Expression of transforming growth factor (TGF) alpha, TGF-beta(2) and interleukin 8 messenger RNA in post surgical and cultured lens epithelial cells obtained from patients with senile cataracts. Graefes Arch Clin Exp Ophthalmol 237, 806-811.

Nishida K., Sotozono C., Adachi W., Yamamoto S., Yokoi N., Kinoshita S. (1995). Transforming growth factor-beta 1, -beta 2 and -beta 3 mRNA expression in human cornea. Curr Eye Res 14, 235-241.

Nishiyama T., Tominaga N., Nakajima K., Hayashi T. (1988). Quantitative evaluation of the factors affecting the process of fibroblast-mediated collagen gel contraction by separating the process into three pahses. Coll Relat Res 8, 259-273.

Noda K., Ishida S., Inoue M., Obata K., Oguchi Y., Okada Y., Ikeda E. (2003). Production and activation of matrix metalloproteinase-2 in proliferative diabetic retinopathy. 44, 2163-2170.

Obata H., Kaji Y., Yamada H., Kato M., Tsuru T.,Yamashita H. (1999). Expression of transforming growth factor-beta superfamily receptors in rat eyes. Acta Ophthalmol Scand 77, 151-156.

Occleston N. L., Alexander R. A., Mazure A., Larkin G., Khaw P. T. (1994). Effects of single exposures to antiproliferative agents on ocular fibroblast-mediated collagen contraction. Invest Ophthalmol Vis Sci 35, 3681-3690.

Occleston N. L., Daniels J. T., Tarnuzzer R. W., Sethi K. K., Alexander R. A., Bhattacharya S. S., Schultz G. S., Khaw P. T. (1997). Single exposures to antiproliferatives: long-term effects on ocular fibroblast wound-healing behavior. Invest Ophthalmol Vis Sci 38, 1998-2007.

Odberg T. (1987). Visual field prognosis in advanced glaucoma. Acta Ophthalmol Scand Suppl 65, 27-29.

Ohta M., Greenberger J. S., Anklesaria P., Bassols A., Massague J. (1987). Two forms of transforming growth factor-beta distinguished by multipotential haematopoietic progenitor cells. Nature 329, 539-541.

Ophir A., Porges Y. (2000). Needling with intra-bleb 5 fluorouracil for intractable neovascular glaucoma. Ophthalmic Surg Lasers 31, 38-42.

Ophir A., Ticho U. (1992). A randomized study of trabeculectomy and subconjunctival administration of fluorouracil in primary glaucomas. Arch Ophthalmol 110, 1072-1075.

Overall C. M., Wrana J. L., Sodek J. (1988). Independent regulation of collagenase, 72-kDa progelatinase, and metalloendoproteinase inhibitor expression in human fibroblasts by transforming growth factor-beta. J Biol Chem 264, 1860-1869.

Parrish R., Minckler D. (1996). "Late endophthalmitis"--filtering surgery time bomb? Ophthalmology 103, 1167-1168.

Pasquale L. R., Dorman Pease M. E., Lutty G. A., Quigley H. A., Jampel H. D. (1993). Immunolocalization of TGF-beta 1, TGF-beta 2, and TGF-beta 3 in the anterior segment of the human eye. Invest Ophthalmol Vis Sci 34, 23-30.

Peacock E. (1984). Wound Repair (Philadelphia, Saunders).

Penttinen R. P., Kobayashi S., Bornstein P. (1988). Transforming growth factor beta increases mRNA for matrix proteins both in the presence and in the absence of changes in mRNA stability. Proc Natl Acad Sci U S A 85, 1105-1108.

Perkins T., W,, Gangnon R., Ladd W., Kaufman P. L., Heatley G. A. (1998). Trabeculectomy with mitomycin C: intermediate-term results. J Glaucoma 7, 230-236.

Pflugfelder S. C., Farley W., Luo L., Chen L. Z., de Paiva C. S., Olmos L. C., Li D. Q., Fini M. E. (2005). Matrix metalloproteinase-9 knockout confers resistance to corneal epithelial barrier disruption in experimental dry eye. Am J Pathol 166, 61-71.

Pitaru S., Soldinger M., Madgar D., Metzger Z. (1987). Bacterial endotoxin inhibits migration, attachment, and orientation of human gingival fibroblasts in vitro and delays collagen gel contraction. J Dent Res 66, 1449-1455.

Postlethwaite A. E., Kang A. H. (1976). Collagen and collagen peptide induced chemotaxis of human blood monocytes. J Exp Med 143, 1299-1307.

Postlethwaite A. E., Keski-oja J., Balian G. (1981). Induction of fibroblast chemotaxis by fibronectin: localisation of the chemotactic region to a 140 000 molecular weight non gelatin binding fragment. J Exp Med 153, 494-499.

Postlethwaite A. E., Keski-oja J., Moses H. L., Kang A. H. (1987). Stimulation of the chemotactic migration of human fibroblasts by transforming growth factor beta. J Exp Med 165, 251-256.

Postlethwaite A. E., Seyer J. M., Kang A. H. (1978). Chemoattractic attraction of human fibroblasts to type I II and III collagens and collagen derived peptides. Proc Natl Acad Sci USA 75, 871-875.

Postlethwaite A. E., Synderman R. K., Kang A. H. (1979). Generation of a fibroblast chemotactic factor in serum by activation of complement. J Clin Invest 64, 1379-1385.

Prince J. H. (1964). The rabbit in eye research, Springfield).

Quigley H. A. (1996). Number of people with glaucoma worldwide. Br J Ophthalmol 80, 389-393.

Radius R. L., Herschler J., Claflin A., Fiorentino G. (1980). Aqueous humor changes after experimental filtering surgery. Am J Ophthalmol 89, 250-254.

Ravitz M. J., Wenner C. E. (1997). Cyclin-dependent kinase regulation during G1 phase and cell cycle regulation by TGF-beta. Adv Cancer Res 71, 165-207.

Reddan J. R., Weinsieder A., Wilson D. (1979). Aqueous humour from traumatised eyes triggers cell division in the epithelia of cultured cells. Exp Eye Res 1979, 267-176.

Reichel M. B., Cordeiro M. F., Alexander R. A., Cree I. A., Bhattacharya S. S., Khaw P. T. (1998). New model of conjunctival scarring in the mouse eye. Br J Ophthalmol 82, 1072-1077.

Richter A., Puddicombe S. M., Lordan J. L., Bucchieri F., Wilson S. J., Djukanovic R., Dent G., Holgate S. T., Davies D. E. (2001). The contribution of interleukin (IL)-4 and IL-13 to the epithelial-mesenchymal trophic unit in asthma. Am J Respir Cell Mol Biol 25, 385-391.

Roberts A. B., Anzano M. A., Lamb L. C., Smith L. C., Sporn M. B. (1981). New class of transforming growth factors potentiated by epidermal growth factor. Proc Natl Acad Sci USA 78.

Roberts A. B., Anzano M. A., Wakefield L. A., Roche N. S., Stern D. F., Sporn M. B. (1985). Type beta transforming growth factor: A bifunctional regulator if cellular growth. Proc Natl Acad Sci USA 82, 119-123.

Roberts A. B., Lamb L. C., Newton D., Sporn M. B., De Larco J. E., Todaro G. J. (1980). Transforming growth factors: Isolation of polypeptides from virally and chemically transformed cells by acid/ethanol extraction. Proc Natl Acad Sci USA 77, 3494-3498.

Roberts A. B., Sporn M. B. (1990). The transforming growth factor-betas. In Handbook of experimental pharmacologypolypeptide growth factors and their receptors, M. B. Sporn, and A. B. Roberts, eds. (Berlin, Springer-Verlag).

Roberts A. B., Sporn M. B., Assoian R. K., Smith J. M., Roche N. S. (1986). Transforming growth factor beta: Rapid induction of fibrosis and angiogenesis in vivo and stimulation of collagen formation in vitro. Proc Natl Acad Sci USA 83, 4167-4171.

Robin A. L., Pollack I. P. (1983). Argon laser trabeculoplasty in secondary forms of open-angle glaucoma. Arch Ophthalmol 101, 328-324.

Ronnov-Jessen L.,Petersen O. W. (1993). Induction of alpha-smooth muscle actin by transforming growth factor-beta 1 in quiescent human breast gland fibroblasts. Implications for myofibroblast generation in breast neoplasia. Lab Invest 68, 696-707.

Ross R., Odland G. (1968). Human wound repair. II. Inflammatory cells, epithelial-mesenchymal interrelations and fibrogenesis. J Cell Biol 39, 152-168.

Roth S. M., Spaeth G. L., Starita R. J., Birbillis E. M., Steinmann W. C. (1991). The effects of postoperative corticosteroids on trabeculectomy and the clinical course of glaucoma: five-year follow-up study. Ophthalmic Surg 22, 724-729.

Rothman R. F., Liebmann J. M., Ritch R. (2000). Low-dose 5-fluorouracil trabeculectomy as initial surgery in uncomplicated glaucoma: long-term followup. Ophthalmology 107, 1184-1190.

Rotzer D R. M., Lutz M, Lindemann D, Sebald W, Knaus P. (2001). Type III TGF-beta receptor-independent signalling of TGF-beta2 via TGFbetaRII-B, an alternatively spliced TGF-beta type II receptor. EMBO J 20, 480-490.

Ruderman J. M., Welch D. B., Smith M. F., Shoch D. E. (1987). A randomized study of 5-fluorouracil and filtration surgery. Ophthalmology 104, 1184-1190.

Sachdev S., Zou X., Higginbotham E. J. (1990). The effect of 5FU impregnated shield implants in filtration surgery in rabbits. Invest Ophthalmol Vis Sci (suppl) 31, 3.

Saika S., Ohmi S., Tanaka S., Ohnishi Y., Yamanaka A., Ooshima A. (1997). Light and scanning electron microscopy of rabbit lens capsules with intraocular lenses. J Cataract Refract Surg 23, 787-794.

Sakai K., Sumi Y., Muramatsu H., Hata K., Muramatsu T., Ueda M. (2003). Thrombospondin-1 promotes fibroblast-mediated collagen gel contraction caused by activation of latent transforming growth factor beta-1. J Dermatol Sci 31, 99-109.

Sakamoto T., Ueno H., Sonoda K., Hisatomi T., Shimizu K., Ohashi H., Inomata H. (2000). Blockade of TGF-beta by in vivo gene transfer of a soluble TGF-beta type II receptor in the muscle inhibits corneal opacification, edema and angiogenesis. Gene Thearpy 7, 1915-1924.

Sanderson N., Factor V., Nagy P., Kopp J., Kondaiah P., Wakefield L., Roberts A. B., Sporn M. B., Thorgeirsson S. S. (1995). Hepatic expression of matureTransforming growth factor beta1 in transgenic mice results in multiple tissue lesions. Proc Natl Acad Sci USA 92.

Sanford L. P., Ormsby I., A.C. G.-d. G., Sariola H., Friedman R., Boivin G. P., Cardell E. L., Doetschman T. (1997). TGFbeta2 knockout mice have multiple developmental defects that are non-overlapping with other TGFbeta knockout phenotypes. Development 124, 2659-2670.

Schlunegger M. P., Grutter M. G. (1992). An unusual feature revealed by the crystal structure at 2.2 A resolution of human transforming growth factor-beta 2. Nature 358.

Schmidt J. A., Mizel S. B., Cohen D., Green I. (1982). Interleukin-1, a potential regulator of fibroblast proliferation. J Immunol 128, 2177.

Schultz-Cherry S., Chen H., Mosher D. F. (1995). Regulation of transforming growth factor beta activation by discrete sequences of thrombospondin. J Biol Chem 270, 932-937.

Senderoff R. I. (1990). Evaluation of anti-proliferative agents using a cell culture model. Invest Ophthalmol Vis Sci 31, 2572-2578.

Serini G. (1998). The fibronectin domain ED-A is crucial for myofibroblastic phenotype induction by transforming growth factor-b1. J Cell Biol 109, 873-881.

Serini G., Gabbiani G. A. (1996). Modulation of α smooth muscle actin expression in fibroblasts by transforming growth factor β isoforms: an in vivo and in vitro study. Wound Repair Regen 4, 278-287.

Shah M., Foreman D. M., Ferguson M. W. J. (1992). Control of scarring in adult wounds by neutralising antibody to transforming growth factor beta. Lancet 339, 231-234.

Shah M., Foreman D. M., Ferguson M. W. J. (1994). Neutralising antibody to TGF-beta 1,2 reduces cutaneous scarring in adult rodents. Journal of cell science 107, 1137-1157.

Shah M., Foreman D. M., Ferguson M. W. J. (1995). Neutralisation of TGF-beta 1 and TGF-beta 2 or exogenous addition of TGF-beta 3 to cutaneous rat wounds reduces scarring. J Cell Sci 108, 985-1002.

Shaunak S., Thomas S., Gianasi E., Godwin A., Jones E., Teo I., Mireskandari K., Luthert P. J., Duncan R., Patterson S., *et al.* (2004). Polyvalent dendrimer glucosamine conjugates prevent scar tissue formation. Nat Biotechnol 22, 977-984.

Shaw L. C., Afzal A., Lewin A. S., Timmers A. M., Spoerri P. E., Grant M. B. (2003). Decreased expression of the insulin-like growth factor 1 receptor by ribozyme cleavage. Invest Ophthalmol Vis Sci 44, 4105-4113.

Sheridan C. M., Occleston N. L., Hiscott P., Kon C. H., Khaw P. T., Grierson I. (2001). Matrix metalloproteinases: a role in the contraction of vitreo-retinal scar tissue. Am J Path 159, 1555-1566.

Sherwood M. B., Garcia-Siekavizza A., Meltzer M. I., Hebert A., Burns A. F., McGorray S. (1998). Glaucoma's impact on quality of life and its relation to clinical indicators. A pilot study. Ophthalmology 105, 561-566.

Shin D. H., Juzych M. S., Khatana A. K., Swendris R. P., Parrow K. A. (1993). Needling revision of failed filtering blebs with adjunctive 5-fluorouracil. Ophthalmic Surg 24, 242-248.

Shipley G. D., Pittelkow M. R., Wille J. J. J., Scott R. E., Moses H. L. (1986). Reversible inhibition of normal human prokeratinocyte proliferation by type beta transforming growth factor-growth inhibitor in serum-free medium. Cancer Res 46, 2068-2071.

Shipley G. D., Tucker R. F., Moses H. L. (1985). Type beta transforming growth factor/growth inhibitor stimulates entry of monolayer cultures of AKR-2B cells into S phase after a prolonged prereplicative interval. Proc Natl Acad Sci U S A 82, 4147-4151.

Sidoti P. A., Choi J. C., Morinelli E. N., Lee P. P., Baerveldt G., Minckler D. S., Heuer D., K, (1998). Trabeculectomy with intraoperative 5-fluorouracil. Ophthalmic Surg Lasers 29, 552-561.

Sime P.J., O'Reilly K. M. (2001). Fibrosis of the lung and other tissues: new concepts in pathogenesis and treatment. Clin Immunol 99, 308-319.

Siriwardena D., Khaw P. T., King A. J., Donaldson M. L., Migdal C., Cordeiro M. F. (2002). Human Anti-transforming growth factor b2 Monoclonal Antibody-A new modulator of wound healing in trabeculectomy. A randomised placebo controlled clinical study. Ophthalmology 109.

Siriwardena D., Kotecha A., Minassian D., Dart J. K., Khaw P. T. (2000). Anterior chamber flare after trabeculectomy and after phacoemulsification. Br J Ophthalmol 84, 1056-1057.

Sivak J. M., Fini M. E. (2002). MMPs in the eye: emerging roles for matrix metalloproteinases in ocular physiology. Prog Retin Eye Res 21, 1-14.

Skuta G. L., Assil K., Parrish R. K. I., Follberg R., Weinreb R. N. (1987). Filtering surgery in owl monkeys treated with anti-metabolite 5-fluorouradine 5 monophosphate entrapped in multivesicular liposomes [Letter]. Am J Ophthalmol, 714-715.

Smiddy W. E., Glaser B. M., Green W. R., Connor T. B., Roberts A. B., Lucas R., Sporn M. B. (1989). Transforming growth factor beta. A biologic chorioretinal glue. Arch Ophthalmol 107, 577-580.

Smith M. F., Sherwood M. B., Doyle J. W., Khaw P. T. (1992). Results of intraoperative 5-fluorouracil supplementation on trabeculectomy for open-angle glaucoma. Am J Ophthalmol 114, 737-741.

Snaders D. R., Kraff M. C., Leiberman H. L. (1982). Breakdown and re-establishement of the blood aqueous barrier with implant surgery. Arch Ophthalmol 100, 588-592.
Snyder R. W., Lambrou F. H., Williams G. A. (1987). Intraocular fibrinolysis with recombinant human tissue plasminogen activator. Experimental treatment in a rabbit model. Arch Ophthalmol 105, 1277-1280.

Soltau J. B., Rothman R. F., Budenz D. L., Greenfield D. S., Feuer W., Lieberman M. F. (2000). Risk factors for filtering bleb infections. Arch Ophthalmol 118, 338-342.

Sommer A., Tielsch J. M., Katz J. (1991). Relationship between intraocular pressure and primary open angle glaucoma among white and black Americans. The Baltimore Eye Survey. Arch Ophthalmol 109, 1090-1095.

Sporn M. B., Roberts A. B., Wakefield L. M., Assoian R. K. (1986). Transforming growth factor-β:Biological function and chemical structure. Science 233.

Stamper R. L., McMenemy M. G., Lieberman M. F. (1992). Hypotonous maculopathy after trabeculectomy with subconjunctival 5-fluorouracil. Am J Ophthalmol 114, 544-553.

Starita R. J., Fellman R. L., Spaeth G. L., Poryzees E. M., Greenidge K. C., Traverso C. E. (1985). Short- and long-term effects of postoperative corticosteroids on trabeculectomy. Ophthalmology 92, 938-946.

Stephenson M. L., Zamecnik P. C. (1978). Inhibition of rous sarcoma viral RNA translation by a specific oligodeoxyribonucleotide. Proc Natl Acad Sci USA 75, 285-288.

Sullivan K. M., Lorenz H. P., Meuli M., Lin R. Y., Adzick N. S. (1995). A model of scarless human fetal wound repair is deficient in transforming growth factor beta. J Pediatr Surg 30, 198-202.

Tahery M. M., Lee D.A. (1989). Pharmalogical control of wound healing in glaucoma surgery. Journal of Ocular Pharmacology 5, 155-179.

Taipale J., Miyazono K., Heldin C. H., Keski-Oja J. (1994). Latent transforming growth factor-beta 1 associates to fibroblast extracellular matrix via latent TGF-beta binding protein. J Cell Biol 124, 171-181.

Tamm I., Dorken B., Hartmann G. (2001). Antisense therapy in oncology: new hope for an old idea? Lancet 358, 489-497.

Thom S. B., Myers J. S., Rapuano C. J., Eagle R. C. J., Siepser S. B., Gomes J. A. (1997). Effect of topical anti-transforming growth factor-beta on corneal stromal haze after photorefractive keratectomy in rabbits. J Cataract Refract Surg 23, 1324-1330.

Thomas D. W., O'Neill I. D., Harding K. D., Shepherd J. P. (1995). Cutanoeus wound healing: A current perpective. J Oral Maxillofacial Surg 53, 443-447.

Thompson J. E., Vaughan T. J., Williams A. J., Wilton J., Johnson K. S., Bacon L., Green J. A., Field R., Ruddock S., Martins M., *et al.* (1999). A fully human antibody neutralising biologically active human TGFβ2 for use in therapy. J immunol methods 227, 17-29.

Thylefors B., Negrel A. D. (1994). The global impact of glaucoma. Bull World Health Organ 72, 323-326.

Towler H. M., McCluskey P., Shaer B., Lightman S. (2000). Long-term follow-up of trabeculectomy with intr-operative 5-fluorouracil for uveitis related glaucoma. Ophthalmology 107, 1882-1888.

Tripathi B. J., Tripathi R. C., Chen J., Gotsis S., Li J. (2004). Trabecular cell expression of fibronectin and MMP-3 is modulated by aqueous humor growth factors. Exp Cell Res 78, 653-660.

Tripathi R. C., Chan W. F., Li J., Tripathi B. J. (1994a). Trabecular cells express the TGF-beta 2 gene and secrete the cytokine. Exp Eye Res 58, 523-528.

Tripathi R. C., Li J., Borisuth N. S., Tripathi B. J. (1993). Trabecular cells of the eye express messenger RNA for transforming growth factor-beta 1 and secrete this cytokine. Invest Ophthalmol Vis Sci 34, 2562-2569.

Tripathi R. C., Li J., Chan W. F., Tripathi B. J. (1994b). Aqueous humor in glaucomatous eyes contains an increased level of TGF-beta 2. Exp Eye Res 59, 723-727.

Tsai J. C., Feuer W., Parrish R. K., Grajewski A. L. (1995). 5-fluorouracil filtering surgery and neovascular glaucoma. Long term follow-up of the original pilot study. Ophthalmology 102, 887-892; discussion 892-883.

Tucker R. F., Shipley G. D., Moses H. L., Holley R. W. (1984). Growth inhibitor from BSC-1 cells closely related to platelet type beta transforming growth factor. Science 226, 705-707.

Vaalamo M., Weckroth M., Puolakkainen P. (1996). Patterns of matrix metalloproteinase and TIMP-1 expression in chronic and normally healing cutanoeus wounds. Br J Dermatol 135, 52-59.

Van Obberghen-Schilling E., Roche N. S., Flanders K. C., Sporn M. B., Roberts A. B. (1988). Transforming growth factor beta 1 positively regulates its own expression in normal and transformed cells. J Biol Chem 263, 7741-7746.

Vaughan M. B., Howard E. W., Tomasek J. J. (2000). Transforming growth factor b1 promotes morphological and functional differentiation of the myofibroblast. Exp Cell Res 257, 180-189.

Vaughan T. J., Williams A. J., Pritchard K., Osbourn J. K., Pope A. P., Earnshaw J. C., McCafferty J., Hodits R. A., Wilton J., Johnson K. S. (1996). Human antibodies with sub-nanomolar affinities isolated from a large non-immunised phage display library. Nature Biotechnology 14, 309-314.

Wahl S. M. (1989). Glucocorticoids and wound healing. In Anti-inflammatory steroid action: Basic and clinical aspects, R. P. Scleimer, and Claman, eds. (New York, Academic Press), pp. 280-302.

Wakefield L. M., Smith D. M., Flanders K. C., Sporn M. B. (1988). Latent transforming growth factor-beta from human platelets. A high molecular weight complex containing precursor sequences. J Biol Chem 263, 7646-7654.

Wakefield L. M., Smith D. M., Masui T., Harris C. C., Sporn M. B. (1987). Distribution and modulation of the cellular receptor for transforming growth factor-beta. J Cell Biol 105, 965-975.

Watson P. G. (1972). Surgery of the glaucomas. Br J Ophthalmol 56, 299-318.

Watson P. G., Grierson I. (1981). The place of trabeculectomy in the treatment of glaucoma. Ophthalmology 88, 175-196.

Webb N. R., Madisen L., Rose T. M., Purchio A. F. (1988). Structural and sequence analysis of TGF-beta 2 cDNA clones predicts two different precursor proteins produced by alternative mRNA splicing. DNA 7, 493-497.

Weinreb R. N. (1987). Adjusting the dose of 5FU after filtration surgery to minimise side effects. Ophthalmology 94, 564-570.

Wells A. P., Cordeiro M. F., Bunce C., Khaw P. T. (2003). Cystic Bleb Formation and Related Complications in Limbus Versus Fornix Based Conjunctival Flaps in Paediatric and Young Adult Trabeculectomy with Mitomycin-C. Ophthalmology.

Whitby D. J., Ferguson M. W. (1991). Immunohistochemical localization of growth factors in fetal wound healing. Dev Biol 147, 207-215.

Wilson C., Szostak J. W. (1995). In vitro evolution of a self alkylating ribozyme. Nature 374, 777-782.

Wimmer I., Welge-Luessen U., Picht G., Grehn F. (2003). Influence of argon laser trabeculoplasty on transforming growth factor-beta 2 concentration and bleb scarring following trabeculectomy. Graefes Arch Clin Exp Ophthalmol 241, 631-636.

Winter D. F., Jones M. A., Simmons S. T., Smith R. S. (1987). A histological analysis of 5fu liposomal delivery system following subconjunctival injections in rabbits. Invest Ophthalmol Vis Sci (Suppl) 28, 271.

Winter G., Griffiths A. D., Hawkins R. E., Hoogenboom H. R. (1994). Making antibodies by phage dispaly technology. Annu Rev Immunol 12, 433-455

Wong T. L. L., Sethi C., Daniels J. T., Limb G. A., Murphy G.,Khaw P. T. (2002). Matrix metalloproteases in disease and repair processes in the anterior segment. Surv Ophthalmol 47, 239-256.

Wong T. T. L., Daniels J. T., Crowston J. G., Khaw P. T. (2004). MMP inhibition prevents human lens epithelial cell migration and contraction of the lens capsule. Br J Ophthalmol 88.

Wong T. T. L., Mead A. L., Khaw P. T. (2003). Matrix Metalloproteinase Inhibition Modulates Post operative scarring after Experimental Glaucoma Surgery. Invest Ophthalmol Vis Sci 44, 1097-1103.

Wong T. T. L., Mead A. L., Khaw P. T. (2005). Long Term Modulation of Ocular Scarring by Matrix Metalloproteinase Inhibition - Comparison with Mitomycin-C Treatment following Experimental Glaucoma Filtration. Invest Ophthalmol Vis Sci *In press.*

Wormstone I. M., Tamiya S., Anderson I. K., Duncan G. (2002). TGF-beta2-induced matrix modification and cell transdifferentiation in the human lens capsular bag. Invest Ophthalmol Vis Sci 43, 2301-2308.

Wrana J. L., Attisano L., Wieser R., Ventura F., Massague J. (1994). Mechanism of activation of the TGF-beta receptor. Nature 370, 341-347.

Zhang K., Rekhter M. D., Gordon D., Phan S. H. (1994). Myofibroblasts and their role in lung collagen gene expression during pulmonary fibrosis. A combined immunohistochemical and in situ hybridization study. Am J Pathol *145, 114-125.*

Zieske J. D., Hutcheon A. E., Guo X., Chung E. H., Joyce N. C. (2001). TGF-beta receptor types I and II are differentially expressed during corneal epithelial wound repair. Invest Ophthalmol Vis Sci 42, 1465.

Zumkeller W., Schofield P. N. (1995). Growth factors, cytokines and soluble forms of receptor molecules in cancer patients. Anticancer Res 15, 344-348.